AN ABSTRACT OF THE DISSERTATION OF

Gaylen Sinclair for the degree of Doctor of Philosophy in Geology presented on April 1, 2019.

Title: North Atlantic Climate and Cryosphere Variability Over the Past 20,000 Years

Abstract approved: _____

Eric Kirby

Reconstructing the sensitivity of past climate to forcings, and of ancient glaciers and ice sheets to this climate, can allow us to better understand the range of climate and cryosphere behavior we may see in the coming centuries. The Arctic is a region of particular importance due to its well-documented amplification of climate change, the presence of the Greenland Ice Sheet, and the acceleration of climate and cryosphere change in the past two decades. In this dissertation, I investigate the past 20,000 years in the area, focusing specifically on the last deglacial period and the late Holocene to answer the overarching question: what magnitude of forcing is required to exceed regional variability in the climate system? I address this through three sub-questions: (1) was there regional variability in retreat of the Greenland Ice Sheet during the last deglaciation, and if so what drove this variability? (2) does Arctic regional climate match the average climate history of the region during the Common Era, and (3) is ice sheet and glacier behavior in southernmost Greenland during the late Holocene synchronous across different glacier types? I use a combination of geostatistical and geochemical techniques to answer these questions, and throughout stress the power of large datasets to reveal significant climate signal within proxy noise.

To answer the first question, I present a database of all surface exposure ages and radiocarbon ages published for Greenland. I recalculate all ages using consistent production rates and scaling schemes to allow all ages to be directly compared with each other and to ice sheet models. Factor analysis of surface exposure ages reveals diachronous retreat of the ice sheet, with east Greenland deglaciating during and

immediately following the end of the Younger Dryas cold period (~12.9-11.7 ka), with peaks in retreat ~13.0-11.5 ka. In contrast, terrestrial retreat of south Greenland occurs between 11.0 and 10.0 ka, and west Greenland retreats between 10.5 and 7.5 ka. This spatial variability is not present in either minimum-limiting radiocarbon ages or an ice-sheet model reconstruction, and is likely due to ocean warming forcing an early retreat in east Greenland. The model reconstruction we compare to does not include realistic ice-ocean interactions which likely account for the model-data misfit.

To answer the second two questions, I investigate climate and cryosphere interactions in the late Holocene (~4 ka to present) in the Arctic. Temperature changes in the latest Holocene are less dramatic than the deglacial temperature increase, but occur at centennial timescales relevant to human societies. To address the second question, I use a climate field reconstruction to merge geochemical climate proxies that cover the Common Era (2 ka to present) with a spatially-resolved reanalysis dataset. This approach allows me to build gridded maps of Arctic temperatures at five-year resolution covering the period 10-2010 C.E., then use these maps to investigate spatial patterns in climate, potential forcings of this climate, and timings of significant temperature shifts in individual gridcells.

Throughout the Common Era prior to recent warming, we observe significant spatial variability, particularly between the eastern and western Arctic, which are uncorrelated through most of the period. Continental areas in general show more variability than ocean regions. A preliminary variance attribution study reveals that a combination of five proposed forcings of Arctic climate (volcanic eruptions, the North Atlantic Oscillation, Atlantic meridional ocean circulation, CO_2, and total solar irradiance) explain at most ~20% of climate variance during this period. Onset of Little Ice Age cooling is also spatially variable, with a range of ~600 years, and is very sensitive to the reference period used to calculate the transition to significantly colder temperatures. By contrast, recent emergence into significantly warmer temperatures is less sensitive to reference period, and shows warming significantly above background temperatures across most of the Arctic between 1850 and 1950 C.E., suggesting

relatively early emergence throughout the Arctic, except in parts of the North Atlantic, Arctic Europe, and Siberia.

To answer question 3, I present a set of 51 ^{10}Be cosmogenic surface exposure ages from six sites in southernmost Greenland. Each site records the late Holocene maxima of the adjacent glacier, so the exposure dates indicate timing of retreat from the late Holocene maximum extent of the ice sheet. Here, I find substantial variability in the response of the south Greenland Ice Sheet and its surrounding glaciers and ice caps to climate. Smaller mountain glaciers and ice caps, as well as glaciers draining the piedmont-like Qassimiut lobe of the ice sheet show a potential response to a localized warming event between ~1.0-0.4 ka. However, those glaciers draining the high altitude alpine-like Julianhåb Ice Cap show greater variability, with retreat ages between 3.7 and 0.4 ka, This suggests the magnitude and duration of climate changes in the late-Holocene (before the most recent warming) were too small to force a widespread response of south Greenland's terrestrial cryosphere.

North Atlantic Climate and Cryosphere Variability Over the Past 20,000 Years

by
Gaylen Sinclair

A DISSERTATION

submitted to

Oregon State University

in partial fulfillment of
the requirements for the
degree of

Doctor of Philosophy

Presented April 1 2019
Commencement June 2019

Doctor of Philosophy dissertation of Gaylen Sinclair presented on April 1, 2019

APPROVED:

Major Professor, representing Geology

Dean of the College of Earth, Ocean, and Atmospheric Sciences

---

Dean of the Graduate School

I understand that my dissertation will become part of the permanent collection of Oregon State University libraries. My signature below authorizes release of my dissertation to any reader upon request.

Gaylen Sinclair, Author

ACKNOWLEDGEMENTS

It takes a village to raise a dissertation, and I would like to thank the entire OSU and Corvallis community for all the support I have received throughout this process. First and foremost, I would like to thank my committee and advisors. Ed Brook and Joe Stoner have been consistently supportive—in the most challenging times during this process they have stood up for me, reassured me that I belong in the program, and asked the right questions when they needed to be asked to improve my science greatly. Dominique Bachelet has been the best GCR possible since the first year of my PhD.

I especially want to thank Alan Mix and Peter Clark, who shepherded my final two chapters, gave encouragement when I needed it most, and gave the most fulfilling discussions about science I have ever had. They are the two most generous scientists I know and I am honored to have worked with them. Alan strengthened my first chapter enormously, and his advice on my second chapter made it what it is today. When all I could see was random noise Alan saw potential for a gridded climate reconstruction. And he never gave up on Arctic Common Era climate. I am astounded by what we put together for that chapter—it grew beyond what I thought was possible, took on a life of its own, and taught me more than I thought I could possibly learn about statistics and Matlab. And Peter Clark's guidance on cosmogenic exposure dating and glacial geology were invaluable to my third chapter. Peter has a way of looking at data and immediately knowing the right questions to ask and the full potential of a data set. His patience and compassion were a constant source of encouragement for me, and I am so happy to have had his support throughout my dissertation.

I met Eric Kirby in my very first graduate class, which was also the first class he taught at Oregon State. His patience with my complete bafflement by both tectonics and geomorphology made a lasting impression, and I am so happy to have had him as an advisor and champion at OSU. Eric always made time for me even when there was no time, and stepped in when he had no obligation to, to guide me through the completion of this endeavor—I cannot thank him enough.

I have had the honor of working with the best coauthors in the world, and all of them have made critical contributions to these papers. I want to thank Anders Carlson in particular for his unflinching support and guidance for the last six years. Dylan Rood's endless good cheer and geochemical wizardry made work in Svalbard and New South Wales a delight. And Yarrow Axford and her team at Northwestern made fieldwork in South Greenland more successful than I could have imagined.

Fieldwork is never easy, and fieldwork in the Arctic carries its own set of challenges. Brenden Reilly kept me sane during the insanity that was the 12 days in the wilderness of our 2014 Greenland field trip. Anders Carlson and Dylan Rood made our Svalbard field work in 2015 the most fun I've ever had in the field, and Jamie McFarlin, Everett Lasher, and Aaron Hartz made our trip to Greenland in 2016 the fieldwork of a lifetime. And back at Oregon States, all of my lab assistants were invaluable: thank you to Fritz Freudenberger, Alisa Kotash, Alder Cromwell, and Aspen Mathias for pouring days of your life into crushing rocks, frantzing, and fighting with Microsoft Excel to build a massive database of radiocarbon ages.

All of the CEOAS graduate students, past and present have built an incredible support system. Aaron Barth, Nilo Bill, Dave Leydet, and Jeremy Hoffman were always there for whatever I needed whether you were in Corvallis or far away, from a set of calculations or instructions on how to order geochemical supplies to a full-blown 2-hour mock oral exam. Heather Bervid and Anna Glüder—you were the best of labmates and a constant source of support and inspiration.

I wouldn't have made it through this process without the Corvallis community and all of the friends who have supported me since 2013—you all know who you are and everything you have done for me. I want to thank everyone at the Majestic Theatre who welcomed me with open arms and let me pretend to be a Victorian London Society lady. Thank you especially to all the teammates I've had at the Corvallis Sports Park—Tuesday evenings at the park were often the bright spots in long weeks, and my teammates gave me the perspective I often needed about what is most important in life (blocking shots on goal).

Finally, I would like to thank my family both near and far. My parents are the strongest people I know—my mom taught me that coding is cool and nobody can tell you otherwise, and my dad gave me the best advice of anyone on navigating graduate school. My brother is always just a phone call away, and he and his family are a constant source of inspiration. Lindsay—you are my rock. You always know how to cheer me up, bring me perspective, and constantly amaze me with your strength and perseverance.

CONTRIBUTIONS OF AUTHORS

Chapter 2—G. Sinclair and A. Carlson co-wrote the manuscript. G. Sinclair, A. Carlson, and A.C. Mix co-conceived the project. G. Sinclair and A. Mathias compiled the databases and performed geochemical calculations. G. Sinclair performed the statistical analyses. B.S. Lecavalier, G. Milne, C. Buizert, and R. DeConto contributed model results and interpretation of ice sheet models.

Chapter 3—G. Sinclair and A.C. Mix co-wrote the manuscript. G. Sinclair, A.C. Mix, and A. Carlson co-conceived the project.

Chapter 4—A.E. Carlson, A. Reyes, and Y. Axford co-conceived the project. G. Sinclair wrote the manuscript and performed geochemical procedures to extract ^{10}Be. D.H. Rood and K. Wilcken assisted with geochemical procedures to prepare samples and run the accelerator mass spectrometer. M. Walczak performed geochemical procedures to prepare and run radiocarbon samples.

TABLE OF CONTENTS

TABLE OF CONTENTS (Continued)

TABLE OF CONTENTS (Continued)

LIST OF FIGURES

LIST OF FIGURES (Continued)

LIST OF TABLES

LIST OF APPENDIX FIGURES

LIST OF APPENDIX FIGURES (Continued)

LIST OF APPENDIX TABLES

DEDICATION

For Li Guo. A scholar, lover of learning, and great teacher.

North Atlantic Climate and Cryosphere Variability Over the Past 20,000 Years

Chapter 1

Introduction

1.1 Forward

Using traditional estimates of glacier response time to climate forcing, the polar ice sheets should have too much thermal intertia to respond to climate forcing on decadal timescales. For this reason, in early IPCC reports, the Greenland and Antarctic ice sheets were estimated to be fairly stable, with limited potential contributions to global sea-level rise in the coming century (Warrick et al., 1991). However, several studies at the beginning of the 21st Century began to challenge this assumption. Jakobshavn Isbræ, the fastest non-surging glacier on the planet, which drains ~6% of the Greenland Ice Sheet, began to collapse in the late 1990s, thinning up to 15 m/yr and doubling in speed (Joughin et al., 2004; Thomas et al., 2003). Many other outlet glaciers around the ice sheet accelerated dramatically at this time and soon after (e.g. Howat et al., 2005; Rignot and Kanagaratnam 2006) Researchers proposed new processes contributing to dynamical thinning and retreat of the glaciers (e.g. Schoof, 2005; Schoof, 2007). Catastrophic draining of surface lakes through moulins can lubricate the bed, leading to ice acceleration (e.g. Zwally et al., 2002; Shannon et al., 2013;). At the ice margin, hydraulic fracturing and cliff destabilization can contribute to very rapid retreat of calving glaciers (Pollard et al., 2015). This can be exacerbated by intrusion of warm subsurface water from the open ocean through troughs in the continental shelf into fjords and the calving front, and by reverse bed slopes at the grounding line, which can enhance ice retreat (e.g. Jamieson et al., 2012; Pollard et al., 2015).

This research was accompanied by advances in both direct and remote observation of the polar ice sheets, revealing rapid and accelerating retreat of the Greenland Ice Sheet in particular (e.g. Bevis et al., 2019; Chen et al., 2017). However, with only 15-20 years of

direct and satellite observations of the ice sheet, we must look to the historical and geologic record to understand the extent to which these observations are unprecendented in Earth's history. Paleoclimate and paleoglaciological research uses Earth's geologic record as a natural laboratory, with various times in the past when the climate was changing naturally as experiments to test hypotheses about the magnitude, rate, and spatial expression of climate change. So, by investigating Greenland's past response to climate forcing, we can begin to understand how it might respond to anthropogenic climate change into the 21st and 22nd centuries.

The period between the last Glacial Maximum (LGM, ~26-19 ka) and present is an ideal target for investigations of the Greenland Ice Sheet. Sequential ice advances tend to obliterate all evidence of previous advances, so the best record of glacier or ice sheet behavior always comes from its most recent advance and retreat. In addition, the proportion of precise and high-resolution climate proxy records increases dramatically closer to the present. This high data density allows us to use spatial statistics to extract new information from the large amount of existing data, and gives ample opportunity for comparing new data to better reconstruct spatio-temporal variability of the climate and cryosphere.

Finally, this time period has a variety of rates and magnitudes of climate change. Most notable are the two events which bookend this period: the deglacial (~19-8 ka), characterized by dramatic climate warming (~3°C, Shakun et al 2012) and collapse of Northern Hemisphere ice sheets, and anthropogenic climate warming in the 20th and 21st Centuries. The latest Holocene (~4 ka-present), also contains several 100-500 year climate fluctuations, which are ideal for reconstructing the rate and magnitude of climate changes, as well as glacier and ice sheet response to these climate changes.

1.2 Project Objectives

The last deglaciation (~19-8 ka) is the most recent period of large scale climate warming accompanied by ice sheet collapse. Eustatic sea level increased ~125 m (Carlson and Clark, 2012) over this time period, due mainly to the collapse of the Laurentide,

Cordilleran, Scandinavian, and British-Irish Ice Sheets. The Greenland Ice Sheet contributed only ~5m to sea-level rise (Lecavalier et al., 2014), but this retreat was expressed in Greenland as retreat from at or near the shelf break to within its current boundaries (e.g. Funder et al., 2011; Lecavalier et al., 2014).

In *Chapter 2*, I compile all existing ice margin ages from around the Greenland Ice Sheet, and apply factor analysis to investigate possible forcings of ice retreat over the deglacial. Unlike previous radiocarbon-based investigations, our study finds spatially diachronous retreat. East Greenland appears to deglaciate first, followed by south and finally west Greenland. We attribute this spatial variability, and the fact that it is not captured by a state-of-the-science ice sheet model, to variable forcings. The early retreat of eastern Greenland is likely forced by earlier ocean warming than western Greenland. This chapter highlights the importance of including the effect of direct ocean warming in ice sheet models.

The late Holocene (~4 ka to present) and its associated Neoglacial ice advance (Solomina et al., 2015), presents a slightly different natural experiment. Instead of a dramatic climate shift from a glacial to a non-glacial state, the background climate conditions of the late Holocene are similar to their pre-industrial (before 1750 C.E.) levels. Greenhouse gasses did not change dramatically over the last 4 ka (until the advent of the industrial revolution). Earth's orbital configuration has changed slightly over this period, but the late Holocene is much more similar to present than its LGM or deglacial conditions. There are only two major ice sheets through this period, and eustatic sea level fluctuations over this period are within 1m (Kopp et al. 2016). This does not mean that climate was static over this period however. Proxy records from around the world point to centennial-scale climate fluctuations, most notably the Little Ice Age, a period of generally cooler temperatures and ice expansion sometime in the last millennium. These centennial-scale fluctuations are important to investigate to establish background climate and glacier variability. In other words, if we can reconstruct the late Holocene climate

and glacier variability in more detail, we can begin to better understand exactly how unprecendented anthropogenic climate change and its consequences are.

In *Chapter 3*, I investigate the climate proxy side of this question. We use climate field reconstructions to extract the common variability within geochemical proxy records and the Hadley reanalysis dataset. This allows us to extend the gridded reanalysis dataset throughout the Common Era and investigate both the drivers of climate change and the timings of the most prominent climatic events during the Common Era: the Little Ice Age and 20th-21st century emergence from background variability. We find surprisingly low explanatory power of five proposed drivers of Common Era climate (total solar irradiance, Atlantic Ocean circulation, the North Atlantic Oscillation, atmospheric carbon dioxide, and global sulfate loading). The five combined forcings explain ~20% of the reconstructed temperature record, suggesting either a significant portion of noise or other forcings not included in this variance attribution study. Possibly related to this, we map the Little Ice Age (defined as the most recent sustained cold period) in the record as a spatially-variable event, with most gridcells entering their coldest period in the 15th-18th centuries. By contrast, warming out of Common Era variability occurs across the Arctic in the late 19th to early 20th centuries, suggesting timing of emergence studies using only the instrumental era may miss the early emergence of climate from background variability in the Arctic.

This regional variability in Common Era climate helps us explain the cosmogenic exposure ages I present in *Chapter 4*. Here, I target southernmost Greenland, an area with a wide variety of glaciological regimes and a climate different from western Greenland. I target six moraines outboard of the most recent drift limit. Most glaciers leave their late Holocene maxima between 1.0 and 0.4 ka, overlapping with other surface exposure ages in Greenland as well as an initial advance of ice into lake catchments recorded by threshold lakes and implying that this early advance may have been the most extensive of the post-deglacial Holocene. However, glaciers draining the alpine-like Julianhåb ice cap

show more stochastic behavior, implying glacier size and geometry has an important impact on glacier sensitivity to climate change at centennial timescales.

1.3 References

Bevis, M., Harig, C., Khan S.A., Brown, A., Simons, F.J., Willis, M., Fettweis, X., van den Broeke, M.R., Madsen, F.B., Kendrick, E., Cacamise, D.J., van Dam, T., Knudsen, P., Nylen, T., 2019. Accelerating changes in ice mass within Greenland, and the ice sheet's sensitivity to atmospheric forcing. *Proceedings of the National Academy of Sciences* 116, 1934-1939.

Carlson, A.E., Clark, P.U., 2012. Ice sheet sources of sea level rise and freshwater discharge during the last deglaciation. *Reviews of Geophysics* 50, RG4007.

Chen, X., Zhang, X., Church, J.A., Watson, C.S., King, M.A., Monselesan, D., Legresy, B., Harig, C., 2017. The increasing rate of global mean sea-level rise during 1993-2014. *Nature Climate Change* 7, 492-495.

Funder, S., Kjeldsen, K.K., Kjær, K.H., Ó Cofaigh, C., 2011. The Greenland Ice Sheet during the past 300,000 years: a review. In Ehlers, J., Gibbard, P.L., and Hughes, P.D., eds. *Quaternary Glaciations—extent and chronology*. Amsterdam: Elsevier.

Howat, I. M., Joughin, I., Tulaczyk, S. Gogineni, S. 2005. Rapid retreat and acceleration of Helheim Glacier, east Greenland. *Geophysical Research Letters* 32, L22502, doi:10.1029/2005GL024737.

Jamieson, S.R., Vieli, A., Livingstone, S.J., Ó Cofaigh, C., Stokes, C., Hillenbrand, C.-D., Dowdeswell J.A., 2012; Ice-stream stability on a reverse bed slope. *Nature Geoscience* 5, 799-802

Joughin, I., Abdalati, W., Fahnestock, M., 2004, Large fluctuations in speed on Greenland's Jakobshavn Isbrae Glacier. *Nature* 432, 608 – 610.

Kopp, R.E., Kemp, A.C., Bittermann, K., Horton, B.P., Donnelly, J.P., Roland Gehrels, W., Hay, C.C., Mitrovica, J.X., Morrow, E.D., Rahmstorf, S., 2016. Temperature-driven global sea-level variability in the Common Era. *Proceedings of the National Academy of Sciences* 113. dx.doi.org://10.1073/pnas.1517056113

Lecavalier, B.S., Milne, G.A.. Simpson, M.J.R., Wake, L., Huybrechts, P., Tarasov, L., Kjeldsen, K.K., Funder, S., Long, A.J., Woodroffe, S., Dyke, A.S., Larsen, N.K., 2014 A model of Greenland Ice Sheet Deglaciation Constrained by Observations of Relative Sea Level and Ice Extent. *Quaternary Science Reviews* 102, 54-84

Pollard, D., DeConto, R., Alley, R.B., 2015. Potential Antarctic Ice Sheet retreat driven by hydrofracturing and ice cliff failure. *Earth and Planetary Science Letters* 412, 112-121.

Rignot, E., Kanagaratnam, P., 2006. Changes in the velocity structure of the Greenland Ice Sheet. *Science*, 311 986 – 990.

Schoof, C., 2005. The effect of cavitation on glacier sliding, *Proceedings of the Royal Society of London Series A* 461, 609-627

Schoof, C., 2007. Ice sheet grounding line dynamics: Steady states, stability, and hysteresis, *Journal of Geophysical Research*, 112, F03S28, doi:10.1029/ 2006JF000664.

Shannon, S.R., Payne, A.J., Bartholomew, I.D., van den Broeke, M.R., Edwards, T.L., Fettweis, X., Gagliardini, O., Gillet-Chaulet, F., Goelzer, H., Hoffman, M.J., Huybrechts, P., Mair, D.W.F., Nienow, P.W., Perego, M., Price, S.F., Smeets, C.J.P.P., Sole, A.J., van de Wal, R.S.W., Zwinger, T., 2013. Enhanced basal lubrication and the contribution of

the Greenland ice sheet to future sea-level rise. *Proceedings of the National Academy of Sciences* 110, 14156-14161.

Shakun, J.D., Clark, P.U., He, F., Marcott, S.A., Mix, A.C., Liu, Z., Otto-Bliesner, B., Schmittner, A., Bard, E., 2012. Global warming preceded by increasing carbon dioxide concentrations during the last deglaciation. *Nature* 484, 49-53.

Solomina, O.N., Bradley, R.S., Hodgson, D.A., Ivy-Ochs, S., Jomelli, V., Mackintosh, A.N., Nesje, A., Owen, L.A., Wanner, H., Wiles, G.C., Young, N.E., 2015. Holocene glacier fluctuations. *Quaternary Science Reviews* 111, 9-34.

Thomas, R. H., W. Abdalati, E. Frederick, W. B. Krabill, S. Manizade, and K. Steffen (2003), Investigation of surface melting and dynamic thinning on Jakobshavn Isbrae, Greenland, J. Glaciol., 49(165), 231 – 239, doi:10.3189/172756503781830764.

Warrick, R., Oerlemans, J., Beaumont, P., Braithwaite, R.J., Drewery, D.J., Gornitz, V., Grove, J.M., Haeberli, W., Higashi, A., Leiva, J.C., Lingle, C.S., Lorius, C., Raper, S.C.B., Wold, B., Woodworth, P.L., 1991. 9. Sea Level Rise. In Houghton, J.T., Jenkins, G.J., Ephraums, J.J., 1991. *Climate Change: The IPCC Scientific Assessment*.

Zwally, H.J., Abdalati, W., Herring, T., Larson, K., Saba, J., Steffen., K., 2002. Surface melt-induced acceleration of Greenland Ice-Sheet flow. *Science* 12, 218-222.

Chapter 2

Diachronous retreat of the Greenland ice sheet during the last deglaciation

Gaylen Sinclair[1], Anders E. Carlson[1], Alan C. Mix[1], Benoit S. Lecavalier[2], Glen Milne[3], Aspen Mathias[1], Christo Buizert[1], Robert DeConto[4]

[1]College of Earth, Ocean, and Atmospheric Sciences, Oregon State University, USA

[2]Department of Physics and Physical Oceanography, Memorial University, Canada

[3]Department of Earth and Environmental Sciences, University of Ottawa, Canada

[4]Department of Geosciences, University of Massachusetts, Amherst, USA

Quaternary Science Reviews
Volume 145, May 2016

2.1 Abstract

The last deglaciation is the most recent interval of large-scale climate change and drove the Greenland ice sheet margin from the continental shelf to within its present extent. Here, we use a database of 645 published ^{10}Be ages from Greenland to document the spatial and temporal patterns of retreat of the Greenland ice sheet during the last deglaciation. Following initial retreat of its marine margins, most land-based deglaciation occurred in Greenland following the end of the Younger Dryas cold period (12.9–11.7 ka). However, deglaciation in east Greenland peaked significantly earlier (13.0–11.5 ka) than that in south Greenland (11.0–10 ka) or west Greenland (10.5–7.0 ka). The terrestrial deglaciation of east and south Greenland coincide with adjacent ocean warming. ^{14}C ages and a recent ice-sheet model reconstruction do not capture this progression of terrestrial deglacial ages from east to west Greenland, showing deglaciation occurring later than observed in ^{10}Be ages. This model-data misfit likely reflects the absence of realistic ice-ocean interactions. We suggest that oceanic changes may have played an important role in driving the spatial-temporal ice-retreat pattern evident in the ^{10}Be data.

2.2 Introduction

During the global Last Glacial Maximum (LGM, 19–26 ka; Clark et al., 2009), the Greenland ice sheet (GrIS) covered ~65% more area than its present extent and in many places extended to the continental shelf-slope break (Funder et al., 2011). Over the next ~15 ka as temperatures increased, the GrIS retreated, reaching a smaller-than-present extent in the early to middle Holocene (e.g., Carlson et al., 2014, Larsen et al., 2015, Young and Briner, 2015). Several rapid climate fluctuations in the North Atlantic region are superimposed on the general warming trend from the LGM to the middle Holocene. Abrupt warming initiated the Bølling Interstadial period at ~14.6 ka. Regional cooling initiated the Younger Dryas Stadial at ~12.9 ka, and abrupt warming defines the onset of the Holocene at ~11.7 ka (Shakun and Carlson, 2010, Clark et al., 2012, Buizert

et al., 2014). While the GrIS retreated in response to this most recent interval of large-scale climate change, whether retreat was synchronous across the island is unknown.

Several studies have examined regional to continental-scale deglaciation of Greenland, using both proxy data and model results (e.g., Bennike and Björck, 2002, Dyke, 2004, Simpson et al., 2009, Funder et al., 2011, Lecavalier et al., 2014, Young and Briner, 2015); the emergence of ^{10}Be surface exposure dating enables increasingly detailed and precise geochronological studies. Thirty-seven studies using ^{10}Be ages to date ice-marginal systems around Greenland have been published since 2007, addressing land-based retreat from the outer coast to the present margin (Figure 2.1). This rapidly growing data set documents spatial and temporal information about GrIS responses to deglacial climate change, and can be used to independently validate ice-sheet models.

Here, we assemble a complete database of all published ^{10}Be ages from Greenland. All ages are recalculated with the most up-to-date production rate (Young et al., 2013a) and scaling schemes, and are therefore internally consistent. We use this compilation and factor analysis to investigate the spatial-temporal patterns of GrIS margin retreat. We also compare our results against an updated ^{14}C database and a recent ice-sheet model simulation of the last deglaciation (Lecavalier et al., 2014) to test whether the simulated GrIS response to deglacial climate change agrees with observations, building on recent model-data comparisons for the Holocene when the GrIS was smaller than its present extent (Larsen et al., 2015, Young and Briner, 2015).

2.3 Methods

2.3.1 The ^{10}Be database

An extensive literature review revealed 36 publications (as of May 2016) that include ^{10}Be exposure ages in Greenland (Figure 2.1, Table 2.1). A total of 645 ages have been published, with between two and 47 ages per publication. Most studies focused on constructing a local to regional ice-retreat chronology, although some use ^{10}Be ages to evaluate response of parts of the GrIS to climatic events like the Younger Dryas, 9.3 ka

and 8.2 ka events (Young et al., 2013b, Larsen et al., 2016) or to constrain the thickness and extent of the GrIS during the LGM (e.g., Håkansson et al., 2007a). Several papers also investigated the behavior of local ice caps and mountain glaciers separate from the main ice sheet (e.g., Kelly et al., 2008, Möller et al., 2010, Levy et al., 2014, Lowell et al., 2013, Young et al., 2015, Larsen et al., 2016). All ages are included in our database.

All the data necessary to calculate ^{10}Be ages using the CRONUS-Earth online calculator (Balco et al., 2008; hereafter the CRONUS calculator) were extracted from the original publications. In case of ambiguity or missing data, corresponding authors were contacted to provide original data. If ^{26}Al measurements were performed in the original study, ^{26}Al concentrations, uncertainties, and standards were included in the database to facilitate calculation of ^{26}Al exposure ages. However, ^{26}Al ages were excluded from the data-model comparison presented below, because only 90 samples included ^{26}Al ages in addition to ^{10}Be ages, and ^{26}Al ages were used in the original studies primarily to supplement ^{10}Be ages and test for inheritance.

In the original publications, slightly different standards were used for several fields in the CRONUS calculator. To account for this, the following minor modifications were performed with the original data to ensure the dataset is internally consistent. All granitic and gneissic samples were assigned a density of 2.65 g cm^{-3}, and all sandstone samples were assigned a density of 2.38 g cm^{-3}. Densities of granite/gneissic samples, where reported, ranged between 2.56 and 2.81 g cm^{-3}; however, these were generally inferred instead of directly measured, so a constant density assigned here is equally plausible and is internally consistent. In addition, all samples were assigned zero post-exposure erosion. Some evidence of erosion was observed in original studies, particularly in east Greenland (Levy et al., 2014, Håkansson et al., 2007b). However, in most regions little to no post-exposure erosion was observed, and small-scale glacial erosional features, such as polish and striae, were often observed, indicating the surfaces are well preserved since deglaciation. The database includes both the assigned densities and erosion rates and the original reported values for reference, although they are not included in our analyses.

No correction for isostatic uplift was included in the re-calculated ages for two reasons. First, only three of the original studies included an isostatic uplift correction for ^{10}Be ages (Kelly et al., 2008, Young et al., 2011a, Rinterknecht et al., 2014). Including isostatic uplift in these two studies changed ages by 2–9%. Second, estimating the precise amount of isostatic uplift is difficult, because local relative sea-level change near ice sheets is influenced by isostatic adjustment of the solid Earth as well as changes in ocean surface height due to global meltwater influx and local gravity changes associated with surface (ice-ocean) and internal (Earth deformation) mass redistribution (Farrell and Clark, 1976, Milne and Shennan, 2013). Therefore, estimating the amount of atmospheric depth change requires the use of an isostatic sea-level model, which in turn requires estimating the position of the glacier margin, leading to somewhat circular reasoning and calculations.

Once the database of published information was compiled, all ^{10}Be ages were re-calculated using the CRONUS calculator, version 2.2 (http://hess.ess.washington.edu/). Calculations using both the Northeast North American (Balco et al., 2009) and Arctic (Young et al., 2013a) production rates were performed. Results from all five scaling schemes calculated on the CRONUS calculator are reported in the database, along with information from the publications necessary to reproduce these calculations or re-calculate ages with any future changes to regional production rates and/or scaling schemes. In our analysis, we use ^{10}Be ages calculated using the Arctic production rate (Young et al., 2013a) and the Lal/Stone time-varying scaling scheme, with internal uncertainties. Use of alternate scaling schemes does not significantly impact results; the internal uncertainty calculated with CRONUS for a given sample is on average 6.1 times greater than the difference between the oldest and youngest ages calculated from the different scaling schemes. The difference between re-calculated ages and reported ages is negligible for most recent publications (from 2011 to 2015), but is significant for the 148 ages published between 2007 and 2010, where the median difference between reported and re-calculated ages is 1.7 ka. The database is available in .xls, .kmz, and .shp form from the U.S. National Climate Data Center. No published samples are excluded from this database; even where ^{10}Be ages were excluded from analysis in the original

publications they have been included here to ensure the dataset is complete for future investigations, which may have different research goals from those of the original publications.

A subset of ^{10}Be ages (n = 443 samples) was compiled to investigate the main phase of GrIS retreat from the LGM to the middle Holocene. The deglacial interval is defined here as occurring between 21 ka and the onset of Neoglacial cooling around 4 ka (Clark et al., 2009, Lecavalier et al., 2014, Larsen et al., 2015). This data set contains the same information as the main database, but all 141 samples older than 21 ka and all 39 samples younger than 4 ka were excluded from the comparison *a priori*. Seven further samples were excluded from the dataset because while they are older than 4 ka, they are 'old' outliers from late-Holocene moraines (Levy et al., 2014, Winsor et al., 2014), likely due to inheritance from earlier exposure histories. All ^{10}Be ages from pebbles on moraines were excluded, to avoid anomalously young ages due to exhumation of small clasts. The only ^{10}Be study in Greenland to rely heavily on amalgamated pebble samples due to a lack of suitable bedrock or boulder samples had widely scattered ages spanning ~8 ka (Alexanderson and Håkansson, 2014). This suggests that the oldest ages could be minimum limiting (i.e., constraining the younger limit of the potential age range of the moraine), because the pebbles have likely experienced significant exhumation since deglaciation (Alexanderson and Håkansson, 2014).

2.3.2 ^{14}C Database

In addition to the ^{10}Be database, a deglacial database of ^{14}C ages was constructed that builds on the existing database of Dyke (2004) (Figure 2.2, Table 2.2). The ^{14}C database was used to check ^{10}Be ages, testing the hypothesis that ^{10}Be ages are on average older than ^{14}C ages; ^{14}C ages are by definition minimum limiting because they date death of organic material which grows sometime after retreat of the ice sheet. While this ^{14}C database can also be used to test ice-sheet model simulations, the comparison was not done here. The ice-sheet model was tuned in part to the ^{14}C records (Lecavalier et al., 2014), so validating it with the ^{14}C database would introduce an element of circularity. Like the ^{10}Be database, the ^{14}C database was constructed through a detailed literature

review. 791 ^{14}C dates and metadata were pulled from the original publications, and re-calibrated using the IntCal13 calibration dataset in Calib14 (Reimer et al., 2013; http://calib.qub.ac.uk). To maintain consistency across calculations from different research groups, all marine ages were corrected for a constant 400-year ^{14}C reservoir age (i.e., $\Delta R = 0$), which is commonly used around Greenland (Dyke, 2004, Carlson et al., 2008, Jennings et al., 2006, Jennings et al., 2014). Radiocarbon ages were then calculated as the median between the upper and lower limits of all age distributions for both 1- and 2-sigma uncertainties. The ^{14}C database is available in .xls, .kmz, and .shp form from the U.S. National Climate Data Center.

2.3.3 Factor analysis of cosmogenic and radiocarbon data

Q-mode factor analysis (e.g., Imbrie and van Andel, 1964) and associated transfer functions have traditionally been applied to ocean sediment data in paleoceanography and paleoclimate. This method is most commonly used with marine biological assemblages to determine past ocean temperatures (e.g., Imbrie and Kipp, 1971, Mix et al., 1999). Imbrie and van Andel (1964)established the method for applying Q-mode factor analysis to geochemical data. This method takes a set of samples characterized by multiple variables, and extracts a set of factors representing theoretical end member assemblages that can be combined in different proportions to recreate the sample set. Q-mode analysis should be used with most geochemical data, as opposed to R-mode analysis, because its factors represent end-member samples instead of variables (ibid, Pisias et al., 2013). Q-mode factor analysis weights the relationships between all variables and all samples equally, and therefore does not rely on *a priori* assignment of groups based on perceived similarities and/or geographic location. This analysis will therefore provide objective estimates of (1) the number of end-member assemblages explaining the majority of variance within the samples; (2) the composition of these assemblages; and (3) the contributions of these end members to each individual sample (Imbrie and van Andel, 1964). Here, ^{10}Be and ^{14}C ages are evaluated using factor analysis to determine if a spatial pattern can be objectively identified, and if this pattern can be related to paleoclimate records.

We performed the Q-mode analysis on normalized grid cell probability density functions (PDFs). Figure 2.3 shows a schematic illustration of the process for assigning samples to grid cells and building PDFs for the ^{10}Be factor analysis. First, ^{10}Be samples are sorted into grid cells. For simplicity and to facilitate later data-model comparison, we have used the Huy3 20 km model grid cell to sort the samples (Lecavalier et al., 2014). We assigned ^{10}Be samples to their grid cells by calculating the distance from the sample to the midpoint of each grid cell. The sample was then placed into the nearest grid cell (1). Between 1 and 27 samples were located in each grid cell. Next, a Gaussian distribution was calculated at 10-year intervals from 0 ka to the maximum possible age of the sample (4-sigma greater than the re-calculated age, using the internal analytical uncertainty as the 1-sigma uncertainty) (2). The Gaussians for all samples in a grid cell are then summed to create a grid cell PDF (3). To avoid weighting the analysis to those grid cells with many samples, each grid cell PDF is normalized to an area under the curve of 1 (4). These normalized grid cell PDFs are then used for Q-mode factor analysis following Pisias et al. (2013). A final varimax factor matrix is achieved by rotating a preliminary matrix calculated with the retained significant orthogonal factors to maximize positive loadings of all factors. This results in the retained factors explaining approximately equal amounts of variance (Imbrie and van Andel, 1964).

The process for calculating factors for the ^{14}C database is identical to that for the ^{10}Be database, with the exception that instead of using all data points in a given grid cell, we calculate the normalized PDF for only the oldest ^{14}C age in a grid cell. This controls for the fact that many of the ^{14}C ages come from lake or marine cores, where only the oldest age is relevant for determining minimum ice-retreat ages, and is also a way to identify the oldest minimum-limiting ^{14}C age in a given 20 km area.

2.3.4 Data-model comparison

Our ^{10}Be database represents the most complete record of terrestrial GrIS retreat currently available and can therefore be used as an independent validation tool for ice-sheet models. This data set provides a framework to test the Huy3 reconstruction of GrIS retreat from ~19 ka to the present (Lecavalier et al., 2014). The ice-sheet reconstruction

is based on a thermodynamic ice-sheet model used in series with a glacial isostatic adjustment model of sea-level change. The ice model was run at 20 km grid resolution. For this analysis, we considered model output of ice extent at 1 ka intervals. The model was forced from 19 ka to the late Holocene using atmospheric temperatures extrapolated from the GRIP $\delta^{18}O$ temperature reconstruction. Certain model aspects and parameters were varied to seek an optimal fit to both ice-extent data from the LGM through to the present as well as a regional relative sea-level database (see Lecavalier et al. (2014)for detailed descriptions of model forcing and physics).

To facilitate comparison with the ice-sheet model reconstruction, each ^{10}Be sample from the deglacial dataset was associated with a model grid cell as described in Section 2.2. Where more than three samples were present in an individual grid cell, Chauvenet's criterion was used to test for outliers (Balco, 2011). This is a gentle test for anomalous data, which compares each ^{10}Be age to the mean and standard deviation of the samples in a grid cell. If the sample deviation exceeds the maximum assigned for a given number of samples, the sample is excluded from the analysis. This method led to the exclusion of ten ^{10}Be ages. In an effort to maintain objectivity in the data-model comparison, no further ^{10}Be ages were excluded from the comparison, even when they were excluded from analysis in the original publications.

After removal of samples with Chauvenet's criterion, 443 samples remained for comparison within 102 model grid cells. To compare these ages with the model grid cells, all the normalized grid cell PDFs in each of the 14 regions around the island were summed (Figure 2.3, Figure 2.4), and the resulting PDF was compared to a histogram of model ice-retreat ages from that region (Figure 2.4).

2.4 Results

2.4.1 Factor Analysis

Results of the factor analysis are shown in Figure 2.5, Figure 2.6c. Note that 39 ages from Upernavik, Thule, Johannes V. Jensen Land, and Store Koldewey were excluded from the analysis. We excluded these ages from the factor analysis because

these areas have a very high proportion of inherited ^{10}Be, and have widely scattered ages (Larsen et al., 2016, Corbett et al., 2013, Corbett et al., 2015, Möller et al., 2010, Håkansson et al., 2007b). Factor analysis including all ages is not significantly different from that presented here, but the factors explain a smaller proportion of the total variance. Six factors were required to explain ~82% of the variance in the data, but only four were retained to calculate orthogonal factors. These explain ~72% of total variance (Table 2.3) and simplify the final analysis. The final factors are named from the age of maximum probability, although it is important to note that each factor plot has significant structure beyond the peak. In particular, the 12 ka factor includes elevated values from ~20 ka to 11.5 ka. The 12 ka factor has its highest loadings in east Greenland (Figure 2.5a), with scattered grid cells in south and west Greenland, most notably a cluster of grid cells on the west coast of the Sisimiut-Kangerlussuaq region. In contrast, the 7.5 ka grid cell is almost exclusively concentrated in west Greenland, particularly in the eastern part of Sisimiut-Kangerlussuaq, Disko Bugt, and Uummannaq. Both the 10 ka and 11 ka factors are relatively high across the island, although the 10 ka factor is notably diminished in east Greenland.

The map of dominant factors shows a similar spatial pattern to the maps of individual factors (Figure 2.5b). The dominant factor is defined here as the factor that explains the plurality of variance in a grid cell. In east Greenland, the 12 ka and 11 ka factors dominate. West Greenland is the only place where the 7.5 ka factor is dominant. The 10 ka factor is dominant in south Greenland, in addition to scattered grid cells where the 11 ka and 12 ka ages are dominant. The average communality of factors in all gridcells is 0.72; Figure 2.5c shows how this is distributed around the island.

In contrast to the ^{10}Be ages, factor analysis of ^{14}C ages does not reveal a significant spatial pattern. Figure 2.7, Figure 2.8 show the results of the factor analysis of ^{14}C ages. Ten factors were required to explain ~80% of the variance in the data (Table 2.4); we retained four factors for the final analysis, which explain ~62% of the total variance in the ^{14}C ages. The four factors each have sharply defined peaks at 11.2 ka, 10.2 ka, 9.5 ka, and 8.3 ka (Figure 2.7). However, none of the factors are heavily concentrated in any given region (Figure 2.8a), and there are no distinctive patterns in the

map of dominant factors (Figure 2.8b). In addition, communality in the factors is significantly lower in the ^{14}C analysis (Figure 2.8c), with average communality of 0.61.

2.4.2 Model-data comparisons

Figure 2.4 shows that model-data fits vary between different regions in Greenland. The closest match between the Huy3 model and ^{10}Be ages is in west Greenland, where model retreat ages overlap with ^{10}Be PDFs in Upernavik, Uummannaq, Disko Bugt, Sisimiut-Kangerlussuaq, and Nuuk. In contrast, ^{10}Be PDFs consistently peak between 1 and 4 ka before modeled ice retreat occurs in north, east, and south Greenland, including Scoresby Sund, Kangerdlussuaq, Sermilik, and Paamiut. In Bernstorffs and Narsarsuaq, the majority of modeled ice retreat occurs after the main peak in the ^{10}Be ages, although the lead in ^{10}Be ages is less pronounced than in the rest of east and south Greenland.

2.5 Discussion

The ^{10}Be factor analysis results differ significantly from the deglacial GrIS retreat scenario outlined by Funder et al. (2011), which shows deglaciation from the outer coast after ~11.7 ka in all locations except Scoresby Sund (deglaciated before ~12.4 ka) and Kap Farvel at the southern tip of Greenland (deglaciated by ~14 ka). In our analysis, significant terrestrial ice retreat occurred before ~11.7 ka at Scoresby Sund, Kangerdlussuaq, Sermilik, Nuuk, and Sisimiut-Kangerlussuaq (Figure 2.5, Figure 2.6c) (also further north at Johannes V. Jensen Land, and Store Koldewey; Figure 2.4). Several studies from east Greenland investigated the behavior of local glaciers and ice caps after the retreat of the ice sheet (Kelly et al., 2008, Levy et al., 2014, Lowell et al., 2013); these minimum-limiting ages may suggest even earlier ice retreat of the GrIS from the region, consistent with the overall spatial pattern observed here. This difference is expected as the Funder et al. (2011) reconstruction relied largely on minimum-limiting ^{14}C ages that reflect the first establishment of soils, marine life and vegetation, which has an unknown lag time behind ice-margin retreat.

In our factor analysis of ^{14}C ages, there is no evidence of the spatial pattern clearly expressed in the ^{10}Be data. A direct comparison of the average ^{10}Be age and the oldest ^{14}C age in the 27 grid cells containing both types of data shows that in most cases ^{14}C ages lag ^{10}Be ages, but that the offset is not constant (Figure 2.9). ^{10}Be ages should directly date ice-margin retreat in most cases (if inheritance, erosion, or later exhumation are not an issue), so the offset is likely explained by the minimum-limiting nature of ^{14}C ages and an unknown time between ice retreat and migration of vegetation to the site.

In contrast to the spatial Greenland deglaciation pattern identified by factor analysis, the Huy3 model shows homogenous terrestrial ice-margin retreat. At a local scale, ^{10}Be ages generally lead the Huy3 model results (Figure 2.4), with the exceptions of Uummannaq, Disko Bugt, Nuuk and Sisimiut-Kangerlussuaq regions. This pattern is particularly pronounced in east Greenland, where there is generally little to no overlap of ^{10}Be PDFs and model histograms. The majority of data used to calibrate the Huy3 model comes from west Greenland, particularly from near Disko Bugt, so it is perhaps not surprising that this region shows the best data-model fit. Discrepancies in other regions suggest some combination of model limitations (e.g., inaccurate or missing forcings), a young bias in the data used to tune the model (e.g., use of ^{14}C ages), or systematic biases in the ^{10}Be database. We note that the Huy3 model does have periods of GrIS retreat as early as ~16 ka (Lecavalier et al., 2014), but this retreat is on the continental shelf and not in regions constrained by ^{10}Be data. In the following sub-sections, we discuss three hypotheses that could explain the spatial variability of terrestrial deglaciation and the data-model misfit.

2.5.1 Elevation Signal in ^{10}Be ages

It is possible that the asynchronous retreat of the GrIS observed here is due to different elevations of samples. East Greenland has higher mountains in general than south and west Greenland, so the earlier deglaciation observed there could be a result of ice thinning, if the samples were taken at higher elevations. However, there is no relationship between elevation and ^{10}Be ages in most parts of the ice sheet (Table 2.5);

the only two regions with an age-elevation relationship significant at $p < 0.05$ are Disko Bugt and Johannes V. Jensen Land. The correlation coefficient for Disko Bugt is negative, suggesting older ages are at lower elevations, and therefore do not represent thinning of the ice sheet. There may be some thinning of the ice recorded in cosmogenic ages in Johannes V. Jensen Land, however these were excluded from the factor analysis and therefore cannot bias the analysis to thinning of the ice. We therefore believe that most to all of the cosmogenic ages from the island record retreat of the ice margin, not the GrIS thinning history.

2.5.2 ^{10}Be inheritance and post-exposure erosion

Systematic inheritance of ^{10}Be may account for the older ^{10}Be ages in some regions. Fast-flowing, warm-based ice may remove at least 2 m of bedrock over a glacial cycle, removing most inherited nuclides, but glacial erosivity is highly variable (e.g., Koppes and Montgomery, 2009), and surfaces beneath cold-based ice may be preserved for several glacial cycles (e.g., Davis et al., 2006, Stroeven et al., 2002, Corbett et al., 2011, Corbett et al., 2013). Inheritance of ^{10}Be can be identified in individual studies if sufficient samples are analyzed. Ideally, anomalous ^{10}Be ages would be identified at the landform scale (e.g., at individual moraines), using quantitative statistics with more than seven samples per landform collected (Putkonen and Swanson, 2003). Unfortunately, in most Greenland locations where ^{10}Be ages have been collected, too few samples were collected to quantitatively identify outliers. Only 31 grid cells (30%) have five or more ^{10}Be samples, and only 11 grid cells (11%) have 10 or more samples (Figure 2.10). This presents a significant limitation for objectively identifying outliers. However, our *a priori* exclusion should remove most old outliers; in the original literature, 47 samples (out of 645) were identified as old outliers younger than 21 ka, while 141 samples are older than 21 ka. In this study, Chauvenet's criterion was applied at the model grid-cell scale where three or more samples are present, which led to the exclusion of ten ages. This approach therefore leads to the inclusion of ages that may have been excluded from original publications as outliers, but it also represents an objective method for excluding outliers and forcing ^{10}Be data to match model outputs.

One method for testing inheritance in ^{10}Be ages is to compare boulder and bedrock ^{10}Be ages, because erratic boulders are less likely to show significant inheritance (e.g., Briner et al., 2006). Figure 2.11 shows that the majority of regions with both boulder and bedrock ages have older bedrock ages than boulder ages. However, the Wilcoxon signed rank test for different distributions shows significantly different ages ($p < 0.05$) for only three regions: Sermilik, Sisimiut-Kangerlussuaq, and Scoresby Sund (Table 2.6). All of the coastal ages from Sermilik are from bedrock with no adjacent boulder samples; the boulder samples come from further inland. The "outliers" in the Sisimiut-Kangerlussuaq boulder distribution overlapping the bedrock ages come from the coast. It is therefore difficult to ascertain if the older bedrock ages are a result of systematic inheritance or geographic location in these cases. In the case of Scoresby Sund, it is possible that the bedrock samples are influenced by inheritance. However, these bedrock ages compose only 15% of all deglacial samples from Scoresby Sund, and therefore cannot account for the trends observed across the island.

Post-exposure erosion removes ^{10}Be-rich surface layers, thereby biasing the samples towards younger ages. There is some evidence of erosion in east Greenland (Håkansson et al., 2011), although it has not been directly measured. If significant post-exposure erosion indeed occurred in east Greenland, it could not account for the older exposure ages found there; on the contrary, it would make the lead of east GrIS deglaciation even more pronounced

2.5.3 Model resolution and approximations

A third hypothesis for the ^{10}Be data-model mismatch is that the ice-sheet model in its present form is unable to capture high-resolution changes in the ice-margin reconstructed by ^{10}Be studies. Young and Briner (2015)noted such deficiencies in their review of Disko Bugt deglaciation relative to the simulated deglaciation. ^{10}Be ages in Greenland are largely collected from within and near fjord systems. These fjords are generally 3–5 km wide and rarely wider than 10 km, and therefore cannot be fully resolved in a model that runs at 20 km resolution. So, while small-scale topographical features may significantly impact ice-margin behavior and be recorded in the ^{10}Be record

(e.g., Lane et al., 2013), this behavior will not be captured in a model that does not resolve these topographic features.

The Huy3 model uses the shallow-ice approximation (Hutter, 1983, Simpson et al., 2009, Lecavalier et al., 2014). This means that longitudinal stresses are ignored in the model, and basal traction provides the only resistance to ice flow. This approximation works well for ice-sheet interiors where longitudinal stresses are minimal, but breaks down at ice-sheet margins. In particular, the approximation does not simulate marine-terminating outlet glaciers well (e.g., Dupont and Alley, 2005). ^{10}Be ages may therefore detect more rapid and earlier deglaciation in fjords, while the model will reconstruct slower and therefore later deglaciation.

Disko Bugt, Sisimiut-Kangerlussuaq and Nuuk are the only regions where ^{10}Be ages do not significantly lead model deglaciation ages (Figure 2.4). The Sisimiut-Kangerlussuaq and Nuuk ^{10}Be ages mostly measure terrestrial deglaciation in regions with more limited fjord systems, so model resolution is less of an issue (Larsen et al., 2013, Winsor et al., 2015a). For Disko Bugt, the data-model agreement likely also reflects the wealth of high precision relative sea-level data from this locality (Simpson et al., 2009, Lecavalier et al., 2014).

Several further model limitations may explain the model-data discrepancies. When comparing the modelled and observed present-day ice thickness distribution, the model over-predicts ice thickness at the margin, which is also likely true for past GrIS geometries. Due to the steep horizontal gradient in ice thickness at the margin, a small change in extent quickly propagates to large ice thickness changes. Additionally, the adopted grid spacing poorly resolves ice streams and outlet glaciers, which leads to an under-estimated discharge of ice at the margins, thereby overestimating ice thickness at the margins. This highlights the need to improve the model resolution, particularly in marginal areas with more complex topography. The Huy3 model is at present the highest resolution model reconstruction of the last Greenland deglaciation, but the comparison discussed above indicates that there are still limitations within this model that should be addressed in the future.

2.5.4 Climatic forcing

The largest source of uncertainty in the modeled ice-retreat reconstruction is the climate forcing (e.g., Zweck and Huybrechts, 2005). The Huy3 model uses a climate forcing based on the GRIP $\delta^{18}O$ record scaled to temperature, which differs significantly from more accurate recent temperature reconstructions of the deglacial interval using nitrogen isotopes (Figure 2.6b) (Buizert et al., 2014). Such differences between the estimated and actual climate forcing could contribute to the data-model mismatch.

In addition, the ice-sheet model was not forced with regionally constrained temperatures, which are especially necessary given the significance of surface mass balance in governing ice-sheet extent. Marginal lakes have been recently used for climate reconstructions, which could constrain the climate forcing at the ice margin (e.g., D'Andrea et al., 2011, Young et al., 2011a, Axford et al., 2013, Carlson et al., 2014, Larsen et al., 2015), but these records do not extend back into the deglacial period. These model weaknesses are outstanding issues in most standard glacial cycle simulations (Huybrechts, 2002, Tarasov and Peltier, 2002, Simpson et al., 2009, Tarasov et al., 2012) and have ramifications on the ice-sheet model reconstruction and on the quality of the fit to the ^{10}Be ages.

The model does not explicitly incorporate the direct effects of ocean temperatures on ice-sheet mass loss (Rignot et al., 2010). Where the glacier terminus is grounded below sea level, enhanced melting by warmer oceans can undercut the ice cliff, accelerating calving and ice retreat (Kirkbride and Warren, 1997, Van der Veen, 2002), in addition to direct melting. If a floating ice shelf is present, warming ocean waters can lead to enhanced basal melting of the shelf, reducing buttressing effects and permitting faster flow and thinning of the ice (Schoof, 2007, Dupont and Alley, 2005, Shepherd et al., 2004). In addition, collapse of floating ice shelves can cause rapid acceleration and retreat of outlet glaciers feeding into the former ice shelf (e.g., Scambos et al., 2004, Marcott et al., 2011).

The lack of an ocean forcing can explain the discrepancy in areas such as southeast and south Greenland, where marine records show a general warming trend from ~15 ka to peak warmth ~10 ka (Figure 2.6a) (Williams, 1993, Solignac et al.,

2004, Jennings et al., 2006, Winsor et al., 2012). This warming continues through the Younger Dryas cold period, and is concurrent with increased sediment discharge from southeast Greenland (Carlson et al., 2008, Colville et al., 2011) and southern Greenland (Winsor et al., 2015b). The warming trend is also concurrent with the increase in the varimax factor scores for the 12 ka factor, which is most concentrated in east Greenland and northern southeast Greenland (Figure 2.6b). Peak ocean warmth occurs between approximately 12 ka and 9.5 ka, encompassing the maximum values of all factors except the 7.5 ka factor (Figure 2.6c). We therefore hypothesize that south and east GrIS margin retreat from the shelf and into fjords prior to modeled margin retreat could reflect this additional climate forcing that was excluded in the Huy3 model. Marine records from west Greenland show cold glacial conditions persisting until 7–8 ka near the end of west GrIS retreat and the peak in the 7.5 ka factor (Figure 2.6a–c) (Jennings et al., 2014), possibly explaining the agreement between ice-sheet-modeled deglaciation and ^{10}Be-observed deglaciation as the main climate forcing would be atmospheric changes that were included in the ice-sheet model.

2.6 Conclusions

Our analyses of the ^{10}Be database highlights several important deglacial features of the GrIS. While the majority of terrestrial ice retreat likely occurred following the Younger Dryas in the early Holocene, it was spatially variable, with factor analysis indicating it can be explained by the combination of 4 orthogonal factors. In general, east Greenland is best explained by the 12 ka and 11 ka factors, south Greenland is best explained by the 11 ka and 10 ka factors, and west Greenland is best explained by the 10 ka and 7.5 ka factors. These factors define a progression of GrIS retreat from east to south to west Greenland. This pattern is not observed in a similar analysis of ^{14}C ages, and the Huy3 ice sheet model reconstruction does not simulate the earlier onset of GrIS retreat in east and south Greenland, where it lags the ^{10}Be ages. This could be partly due to the minimum-limiting nature of ^{14}C ages and the resolution of the model, which is too coarse to resolve the many fjord systems in these regions, limiting ice-ocean interactions. Also, the Huy3 model does not include any direct influence of ocean warming on mass

loss, and east to south GrIS retreat is concurrent with general surface and subsurface ocean warming suggesting a potential causal linkage. Conversely, the model captures the deglacial pattern of west GrIS retreat, where fjord systems are more limited (with the exception of Disko Bugt) and where ocean temperatures did not begin to warm until near the end of the deglaciation. As such, the simpler atmospheric model forcing and ice-sheet model resolution were sufficient to simulate deglaciation in this region.

Future ice-sheet modeling efforts should focus on improving model resolution to resolve the complex topography of Greenland and include interaction with ocean waters. Specifically, the model would benefit from increased resolution, dynamics derived from geophysical processes, and the inclusion of ice-ocean interactions using ocean temperature forcing informed by ocean proxy records. As advances in modeling techniques and resolution continue, the ^{10}Be database presented here will continue to be a useful tool for developing and validating models, particularly as new data continue to be collected and published.

2.7 Acknowledgements

Funding for this research was provided by the National Science Foundation (PLR-1418074 to AEC and PLR-1417886 to RD), and an Oregon State University Provost Fellowship and a National Science Foundation Graduate Fellowship to GS. Inspiring discussions from the PAGES/INQUA working group PALeo constraints on SEA level rise 2 (PALSEA2) are acknowledged. Two anonymous reviewers, Vincent Rinterknecht and Nicolaj Larsen helped improve earlier versions of this paper.

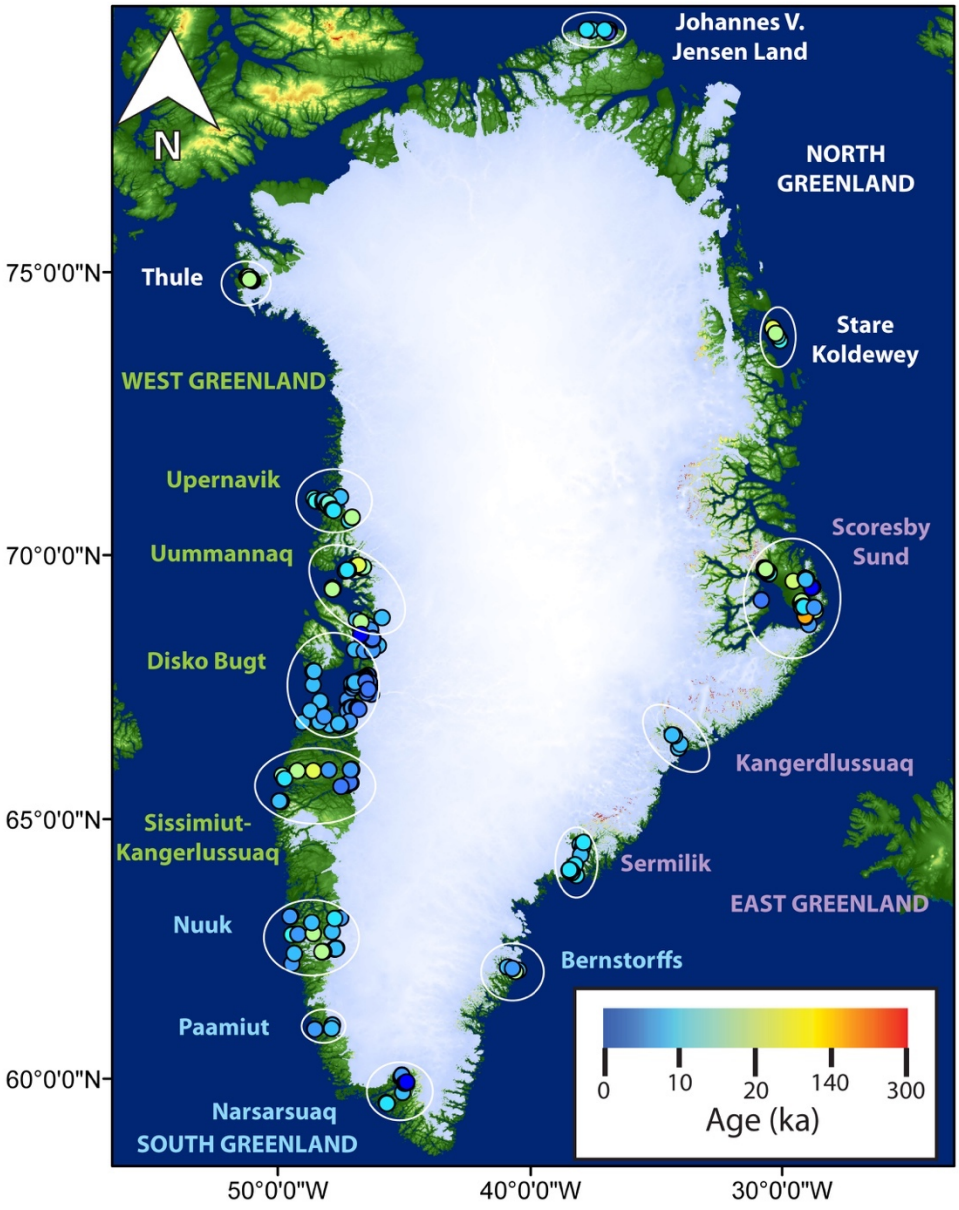

Figure 2.1: Map of all published ^{10}Be ages from Greenland. Individual ^{10}Be ages are represented by dots, with colors corresponding to the age of the sample. Text colors correspond to the broader region (identified in all capitals) each individual location is assigned to by factor analysis.

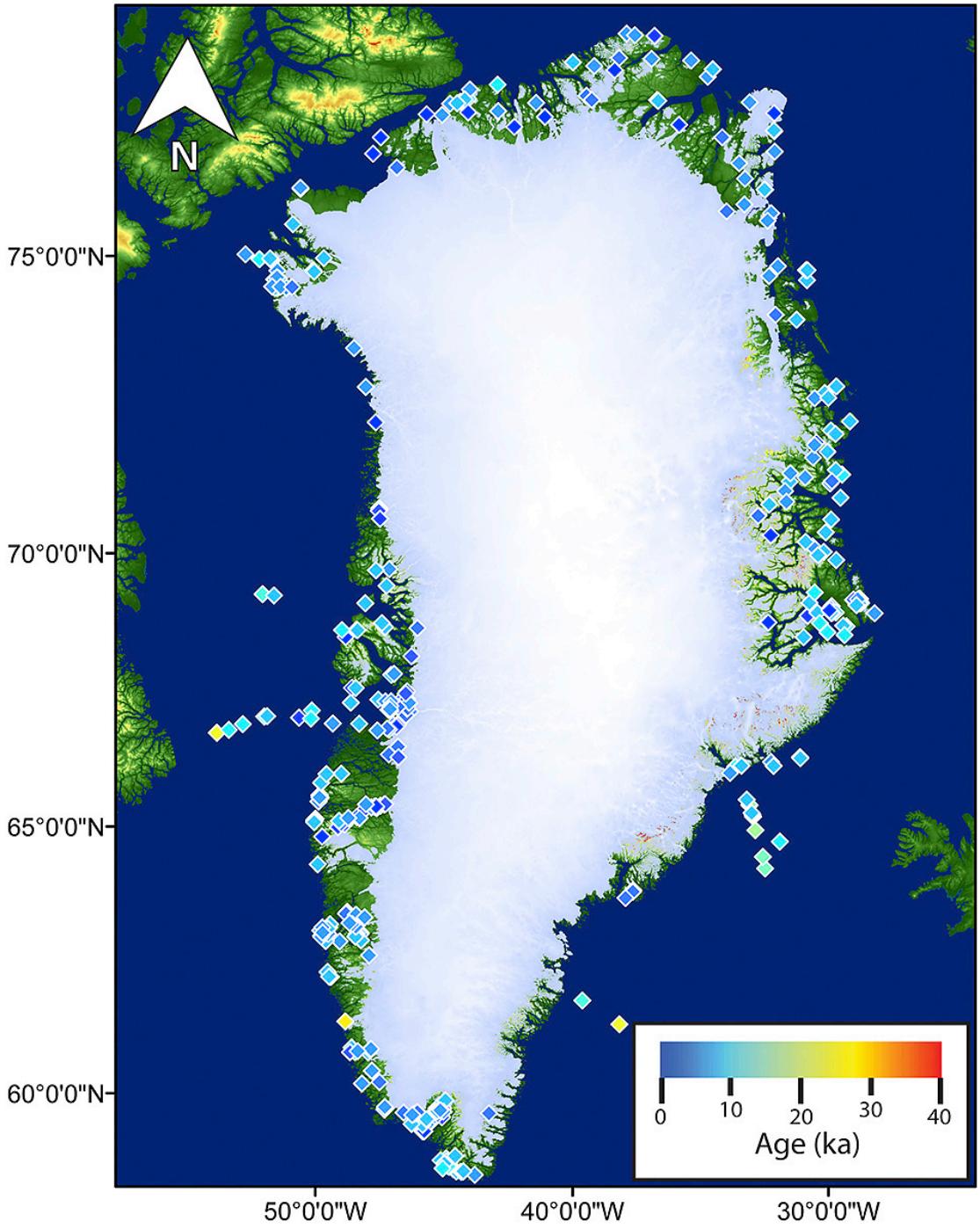

Figure 2.2: Map of all published ^{14}C ages from Greenland. Individual ^{14}C ages are represented by diamonds, with colors corresponding to the age of the sample (note the scale in this color bar is different from Figure 1).

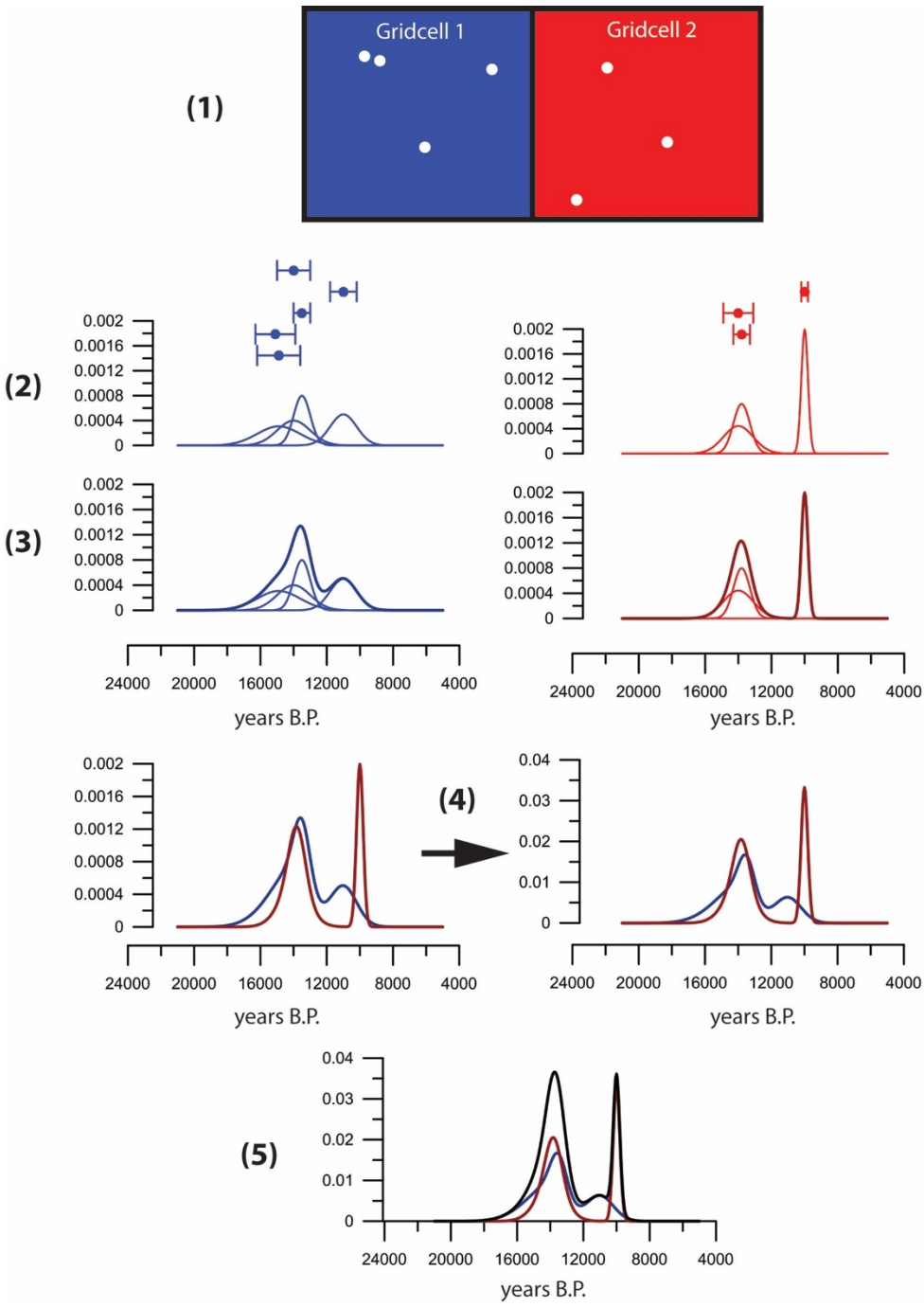

Figure 2.3: Schematic diagram showing method for calculating normalized grid cell PDFs for factor analysis, and regional PDFs for comparison with the Huy3 ice sheet model reconstruction. The reader is referred to the text for a full description of the Figure.

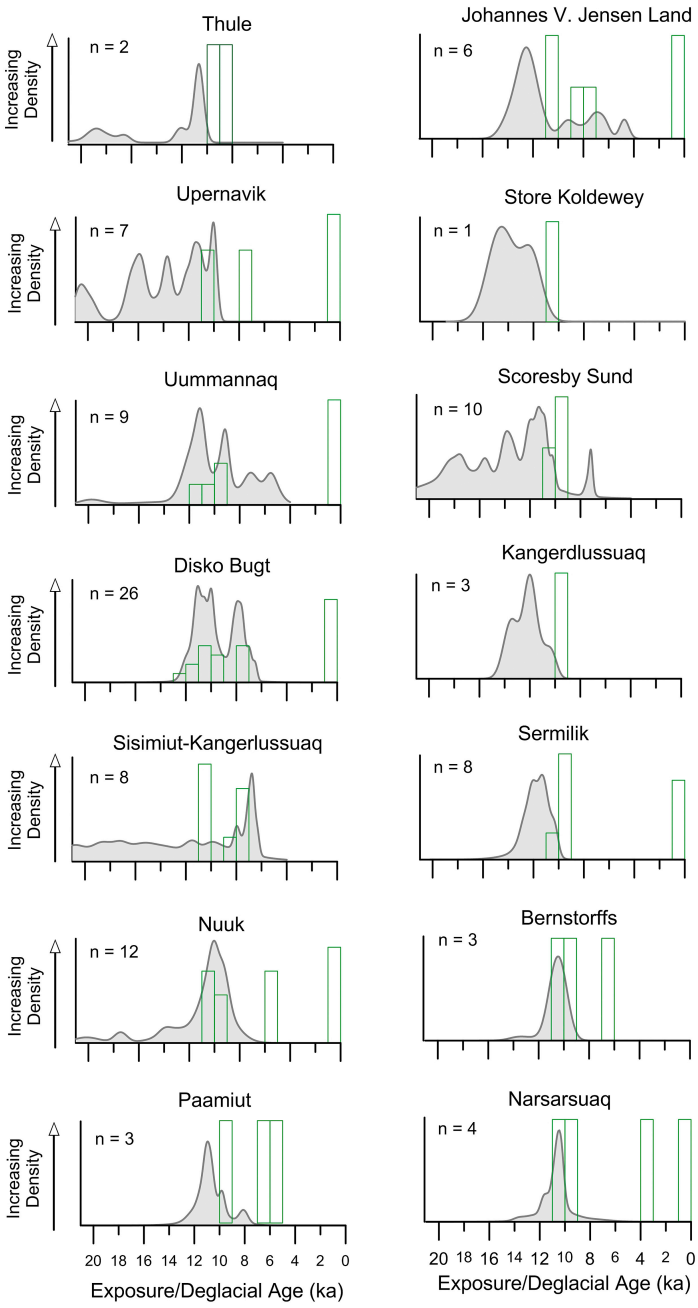

Figure 2.4: Summed grid cell PDFs of deglacial ^{10}Be ages in Greenland, compared with deglacial ages in the Huy3 model. Each region is labeled with the number of samples indicated. Gray shading is the PDF while the green bars are the model results.

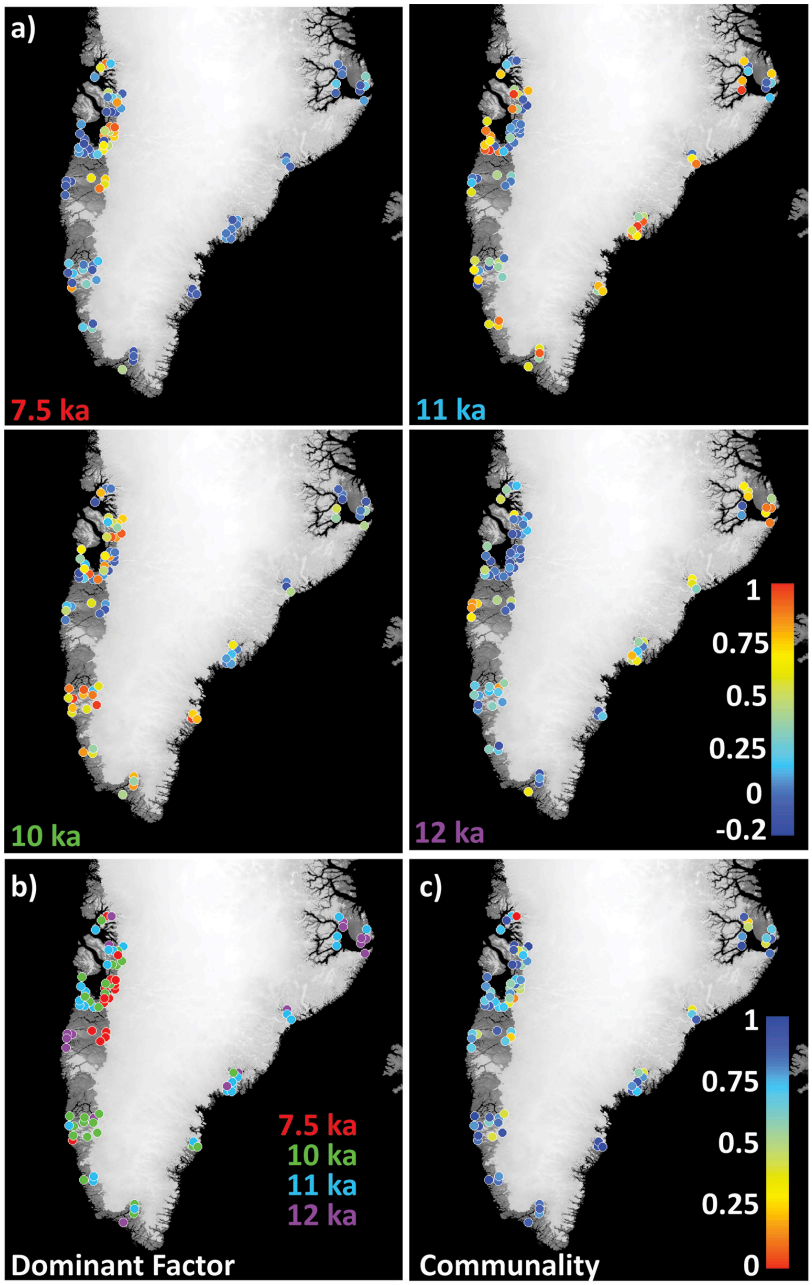

Figure 2.5 ^{10}Be Factor Analysis (a) Factor loadings in individual grid cells with the factors noted by the peak of that factor; height of the bar denotes the strength of each factor in that cell. (b) Dominant factor in each grid cell, defined as the factor with the highest loading in that cell; colors correspond to (a). (c) Communality of factors for each grid cell, which indicates how much of the variance of each grid cell is explained by the sum of the four factors.

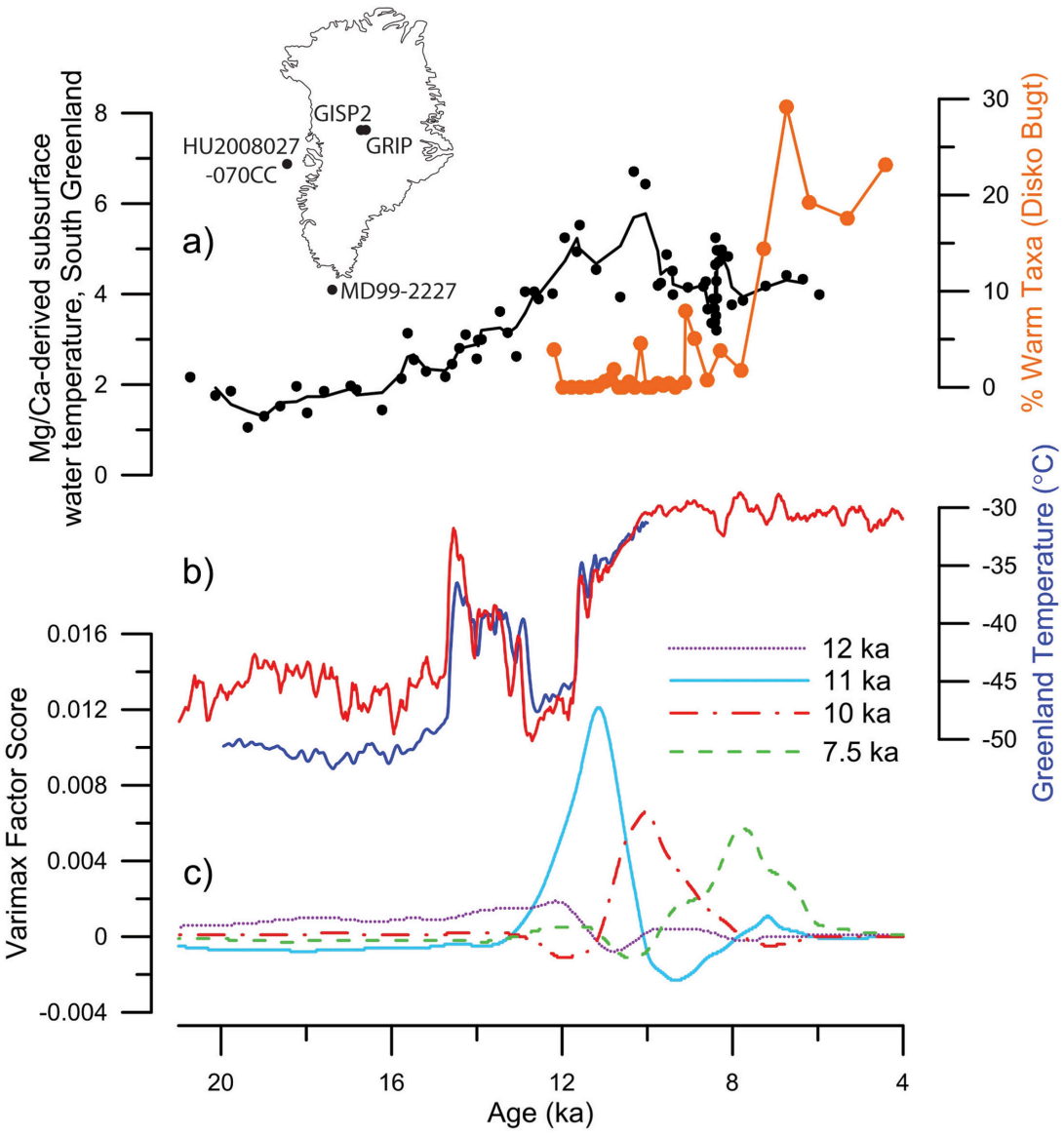

Figure 2.6: Comparison of ^{10}Be factors with climatic forcings. (a) Mg/Ca-derived subsurface water temperatures at Eirik Drift, south Greenland (points), with 3-point running average (line) (MD99-2227, Winsor et al., 2012) and percentage of warm-water foraminifera in Disko Bugt (orange) (HU2008029-070CC, Jennings et al., 2014); (b) Huy3 temperature forcing (red; GRIP ice core, Lecavalier et al., 2014) and reconstructed central Greenland air surface temperatures (blue; GISP2 ice core, Buizert et al., 2014); (c) ^{10}Be varimax factor loadings (this study), with colors representing different factors labeled by their peak value. Inset map shows approximate locations of ice and ocean core records.

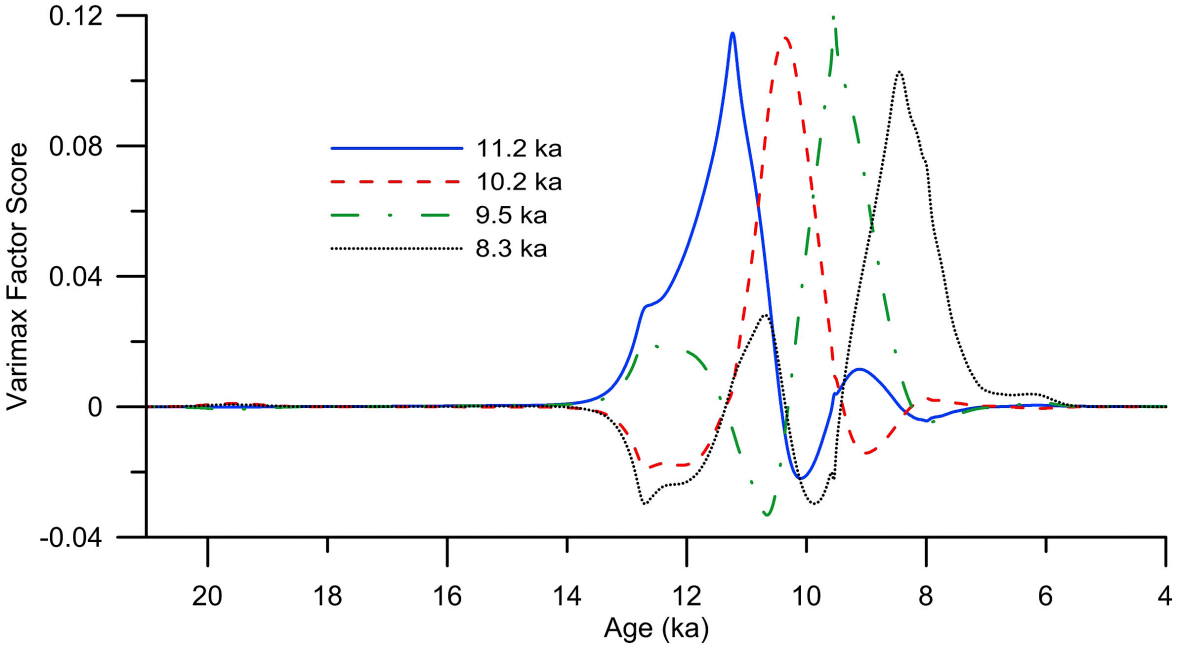

Figure 2.7: ^{14}C varimax factor loadings, with colors representing different factors labeled by their peak value.

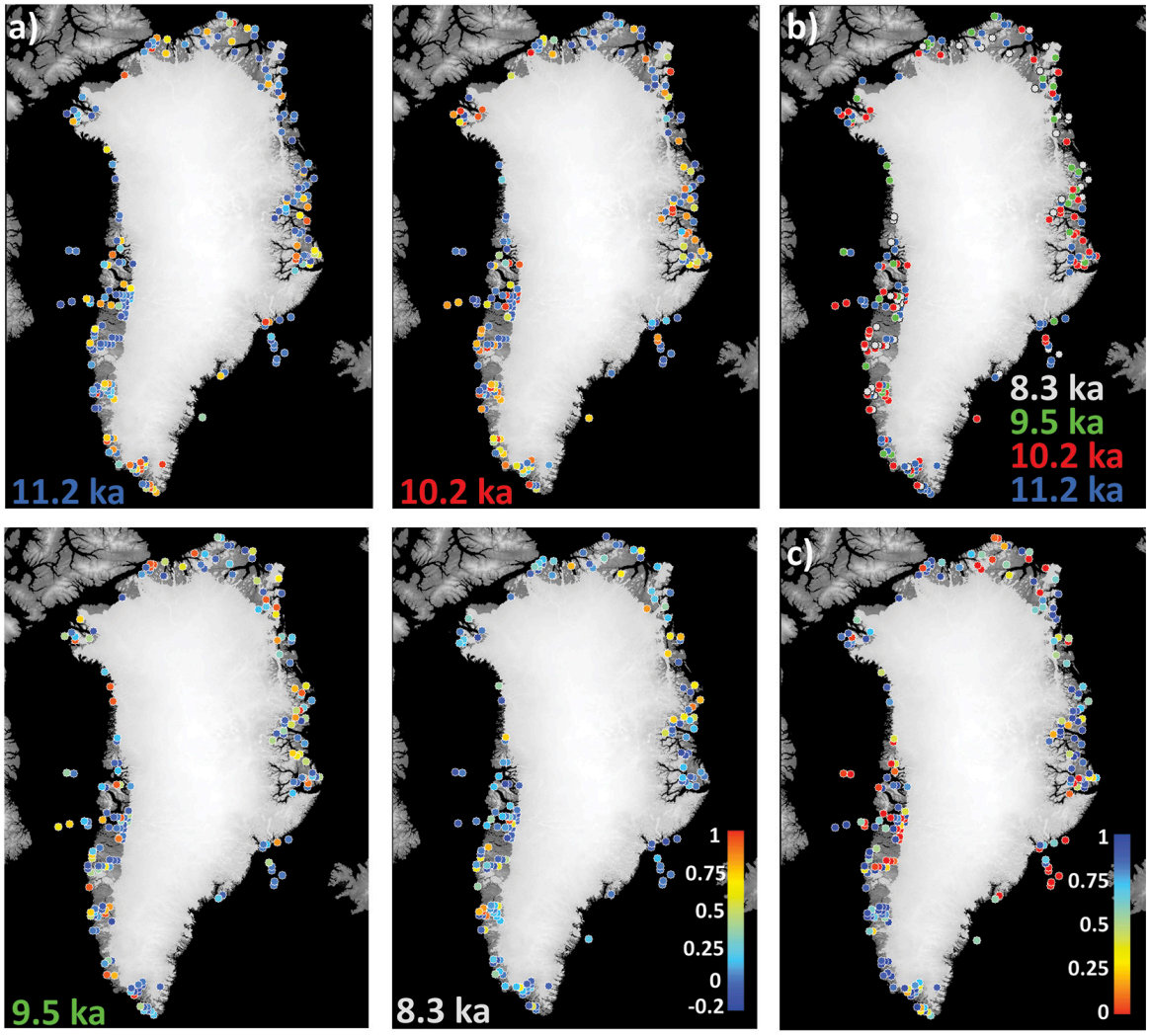

Figure 2.8: ^{14}C Factor Analysis (a) Factor loadings in individual grid cells with the factors noted by the peak of that factor; height of the bar denotes the strength of each factor in that cell. (b) Dominant factor in each grid cell, defined as the factor with the highest loading in that cell; colors correspond to (a). (c) Communality of factors for each grid cell, which indicates how much of the variance of each grid cell is explained by the sum of the four factors.

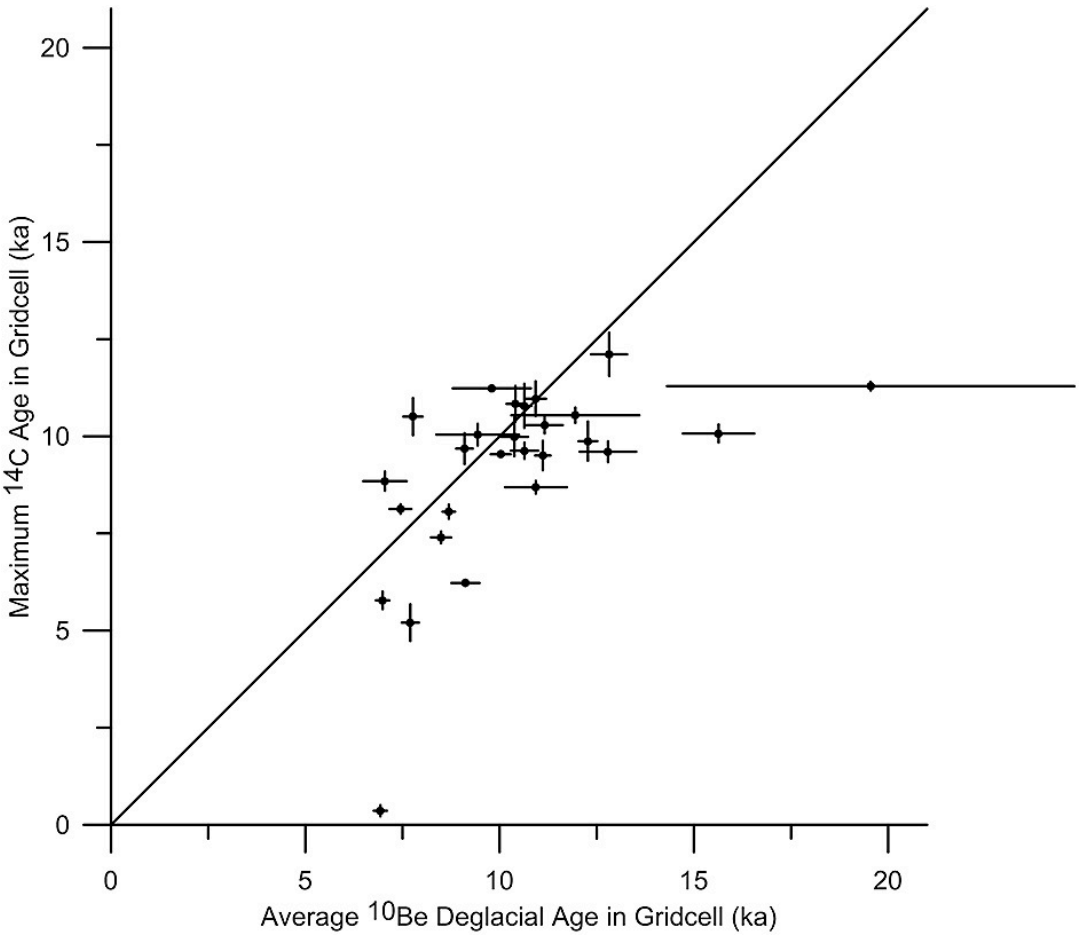

Figure 2.9: Comparison of average ^{10}Be and oldest ^{14}C ages in the same grid cell. Uncertainty bars for ^{14}C ages reflect 1-sigma uncertainty for the sample; uncertainty bars for ^{10}Be ages reflect standard error of ^{10}Be ages in the grid cell (if 3 or more samples are present) or average analytical uncertainty of ages (if fewer than 3 samples are present).

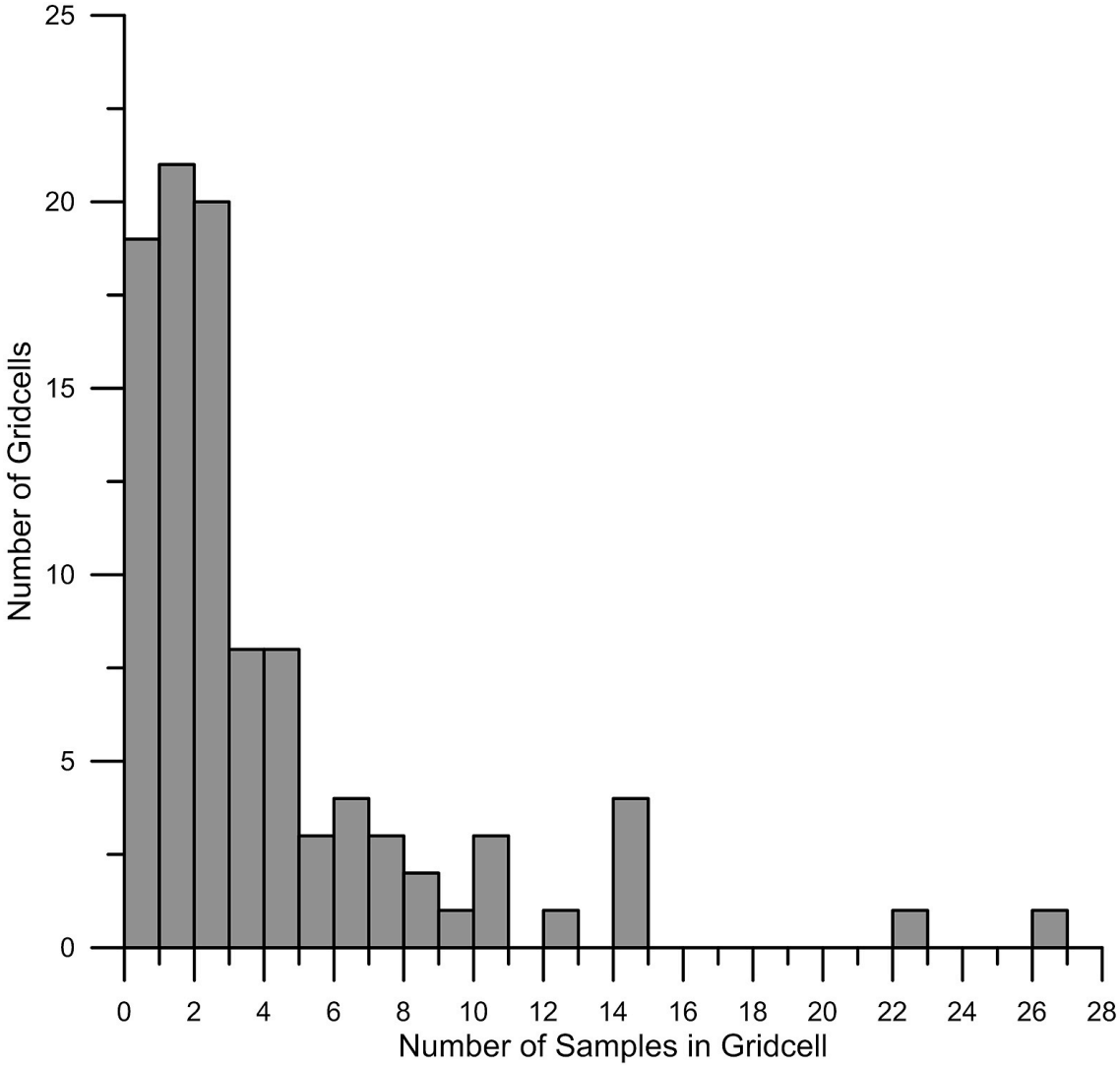

Figure 2.10: Histogram showing the number of model grid cells with a given number of ^{10}Be samples.

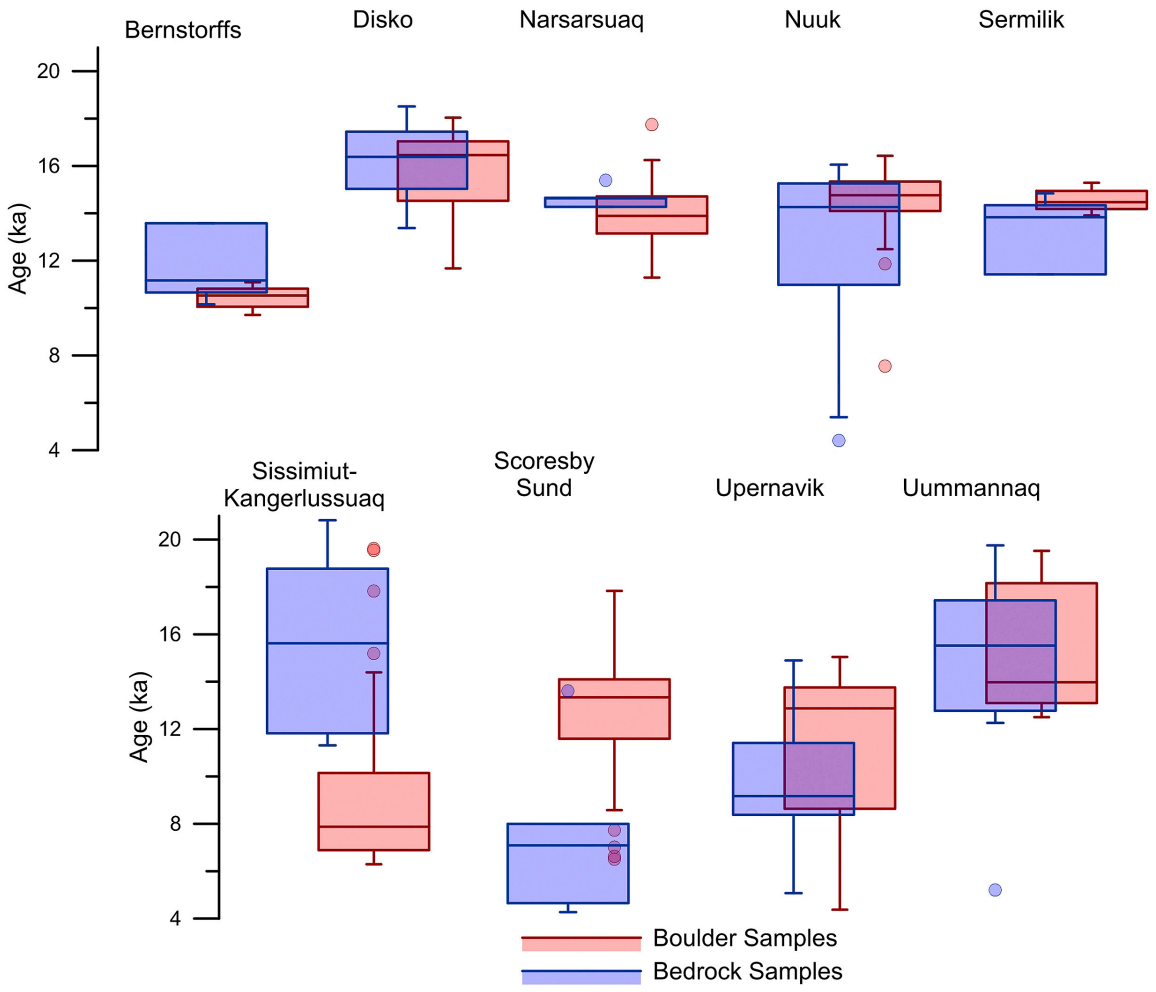

Figure 2.11: Comparison via whisker plots of bedrock (blue) and boulder (red) ages for all regions in Greenland (labeled) with both bedrock and boulder ages. The box shows the one sigma range with the bar in the middle being the median age while the lines (whiskers) denote the two sigma range of the samples.

Study Title	Region	Number of Samples
Håkanson et al. 2007a	Scoresby Sund	4
Håkanson et al. 2007b	Store Koldewey	7
Kelly et al. 2008	Scoresby Sund	38
Roberts et al. 2008	Sermilik	12
Håkanson et al. 2009	Scoresby Sund	43
Rinterknecht et al. 2009	Sissimiut-Kangerlussuaq	12
Roberts et al. 2009	Sissimiut-Kangerlussuaq	16
Moller et al. 2010	Johannes V. Jensen Land	16
Corbett et al. 2011	Disko Bugt	30
Håkanson et al. 2011	Scoresby Sund	14
Young et al. 2011a	Disko Bugt	18
Young et al. 2011b	Disko Bugt	8
Hughes et al. 2012	Sermilik	12
Levy et al. 2012	Sissimiut-Kangerlussuaq	9
Briner et al. 2013	Disko Bugt	2
Corbett et al. 2013	Upernavik	33
Kelley et al. 2013	Disko Bugt	12
Lane et al. 2013	Uummannaq	15
Larsen et al. 2013	Nuuk	47
Levy et al. 2014	Scoresby Sund	12
Lowell et al. 2013	Scoresby Sund	6
Roberts et al. 2013	Uummannaq	17
Young et al. 2013	Disko Bugt	21
Alexanderson and Håkansson 2014	Scoresby Sund	8
Carlson et al. 2014	Disko Bugt, Paamiut, Sissimiut-Kangerlussuaq, Narsarsuaq	29
Dyke et al. 2014	Sermilik	23
Nelson et al. 2014	Narsarsuaq	11
Rinterknecht et al. 2014	Disko Bugt	7
Winsor et al. 2014	Narsarsuaq	17
Corbett et al. 2015	Thule	28
Winsor et al. 2015	Narsarsuaq, Paamiut, Sissimiut-Kangerlussuaq, Nuuk	47
Kelley et al. 2015	Disko Bugt	18
Cronauer et al. 2015	Disko Bugt	11
Young et al. 2015	Disko Bugt	9
Larsen et al. 2016	Johannes V. Jensen	6
Corbett et al. 2016	Thule	28
Levy et al. 2016	Scoresby Sund	27

Table 2.1: Description of all published papers with ^{10}Be ages in Greenland, with region of publication and number of ^{10}Be samples. Full references in reference list.

Study	Number of Samples
Fredskild 1973	2
Kelly 1974	1
Kelly 1975	1
Weidick 1975	2
Funder 1979	1
Bennike et al. 2002	6
Kuijpers et al. 2003	16
Weidick et al. 2004	12
Dyke 2004 (and references therein)	235
Lloyd et al. 2005	7
Jennings et al. 2006	41
Sparrenbom et al. 2006a	30
Sparrenbom et al. 2006b	38
Bennike and Sparrenbom 2007	3
Bennike 2007	1
Long et al. 2008	6
Long et al. 2009	9
Nørgaard-Pedersen and Mikkelsen 2009	8
Briner et al. 2010	18
Bennike et al. 2011	9
Jennings et al. 2011	9
Larsen et al. 2011	10
Lloyd et al. 2011	1
Olsen et al. 2011	24
Young et al. 2011a	3
Young et al. 2011b	7
Bennike and Wagner 2012	5
Kelley et al. 2012	6
Massa et al. 2012	28
Storms et al. 2012	17
Briner et al. 2013	15
Lane et al. 2013	2
Lowell et al. 2013	55
Ó Cofaigh et al. 2013	19
Perner et al. 2013	16
Sparrenbom et al. 2013	15
Young et al. 2013	3
Briner et al. 2014	22
Ha°kansson et al. 2014	11
Levy et al. 2014	20
Larsen et al. 2015	15
Corbett et al. 2015	4
Cronauer et al. 2015	6
Sheldon et al. 2016	2
Hogan et al. 2016	6

Table 2.2: Description of all published papers with ^{14}C ages in Greenland, with number of ^{14}C samples. Full references in reference list.

Factor number	Eigenvalues	Percent variance explained	Cumulative percent varience explained
1	33.8	39.3	39.3
2	11.9	13.8	53.1
3	9.5	11.0	64.1
4	7.0	8.1	72.3
5	4.6	5.4	77.6
6	4.3	5.0	82.7

Table 2.3: Eigenvalues for initial factors in ^{10}Be Q-mode analysis.

Factor number	Eigenvalues	Percent variance explained	Cumulative percent varience explained
1	60.6801	28.6227	28.6227
2	33.562	15.8311	44.4538
3	20.9421	9.8783	54.3322
4	14.6875	6.9281	61.2602
5	12.1803	5.7454	67.0057
6	8.7107	4.1088	71.1145
7	6.6403	3.1322	74.2467
8	5.3779	2.5367	76.7834
9	4.4372	2.093	78.8764
10	3.9669	1.8712	80.7476

Table 2.4: Eigenvalues for initial factors in ^{14}C Q-mode analysis.

Region	Pearson's Correlation Coefficient	P-value
Thule	-0.323	0.177
Upernavik	0.108	0.643
Uummannaq	-0.323	0.177
Disko Bugt	-0.202	0.022
Sissimiut-Kangerlussuaq	0.103	0.529
Nuuk	0.160	0.310
Paamiut	0.057	0.806
Narsarsuaq	0.155	0.441
Bernstorffs	-0.105	0.720
Sermilik	0.095	0.660
Kangerdlussuaq	-0.596	0.158
Scoresby Sund	-0.014	0.912
Store Koldewey	0.224	0.857
Johannes V. Jensen Land	0.576	0.008

Table 2.5: Pearson's correlation coefficient and p-values for ^{10}Be age-elevation relationships for the different regions of Greenland.

Region	Number of Bedrock Samples	Number of Boulder Samples	p-value in Wilcoxon Test
Bernstorffs	5	9	0.082
Disko Bugt	57	71	0.075
Narsarsuaq	5	22	0.21
Nuuk	12	30	0.3
Sermilik	18	6	0.00065
Sissimiut-Kangerlussuaq	7	33	0.0011
Scoresby Sund	9	58	0.028
Upernavik	8	13	0.21
Uummannaq	13	7	0.94

Table 2.6: Results of Wilcoxon signed-rank test for bedrock and boulder ages.

2.8 References

Alexanderson, H., Håkansson, L., 2014. Coastal glaciers advanced onto Jameson Land, East Greenland during the late glacial-early Holocene Milne Land Stade. *Polar Research,* 33. http://dx.doi.org/10.3402/polar.v33.20313.

Axford, Y., Losee, S., Briner, J.P., Francis, D.R., Langdon, P.G., Walker, I.R., 2013. Holocene temperature history at the western Greenland Ice Sheet margin reconstructed from lake sediments. *Quaternary Science Reviews* 59, 87-100.

Balco, G., Stone, J.O., Lifton, N.A., Dunai, T.J., 2008. A complete and easily accessible means of calculating surface exposure ages or erosion rates from Be-10 and Al-26 measurements. *Quaternary Geochronology* 3, 174-195.

Balco, G., Briner, J., Finkel, R.C., Rayburn, J.A., Ridge, J.C., Schaefer, J.M., 2009. Regional beryllium-10 production rate calibration for northeastern North America. *Quaternary Geochronology* 4, 93-107.

Balco, G., 2011. Contributions and unrealized potential contributions of cosmogenic-nuclide exposure dating to glacier chronology, 1990-2010. *Quaternary Science Reviews* 30, 3-27.

Bennike, O., 2008. An early Holocene Greenland whale from Melville Bugt, Greenland. *Quaternary Research* 69, 72-76.

Bennike, O., Björck, S., 2002. Chronology of the last recession of the Greenland Ice Sheet. *Journal of Quaternary Science* 17, 211-219.

Bennike, O., Sparrrenbom, C.J., 2007. Dating of the Narssarssuaq stade in southern Greenland. Holocene 17, 279-282.

Bennike, O., Björck, S., Lambeck, K., 2002. Estimates of South Greenland late-glacial ice limits from a new relative sea level curve. *Earth and Planetary Science Letters* 197, 171-186.

Bennike, O., Wagner, B., 2012. Deglaciation chronology, sea-level changes and environmental changes from Holocene lake sediments of Germania Havn Sø, Sabine Ø, northeast Greenland. *Quaternary Research* 78, 103-109.

Bennike, O., Wagner, B., Righter, A., 2011. Relative sea level changes during the Holocene in the Sisimiut area, south-western Greenland. *Journal of Quaternary Science,* 26, 353-361.

Briner, J.P., Håkansson, L., Bennike, O., 2013. The deglaciation and neoglaciation of Upernavik Isstrøm, Greenland. *Quaternary Research* 80, 459-467.

Briner, J.P., Kaufman, D.S., Bennike, O., Kosnik, M.A., 2014. Amino acid ratios in reworked marine bivalve shells constrain Greenland Ice Sheet history during the Holocene. *Geology*. http://dx.doi.org/10.1130/G34843.1

Briner, J.P., Miller, G.H., Davis, P.T., Finkel, R.C., 2006. Cosmogenic radionuclides from fiord landscapes support differential erosion by overriding ice sheets. *Geological Society of America Bulletin* 118, 406-420.

Briner, J.P., Stewart, H.A.M., Young, N.E., Phillipps, W., Losee, S., 2010 Using proglacial-threshold lakes to constrain fluctuations of the Jakobshavn Isbrae ice margin, western Greenland, during the Holocene. *Quaternary Science Reviews* 29, 3861-3874.

Buizert, C., Gkinis, V., Severinghaus, J.P., He, F., Lecavalier, B.S., Kindler, P., Leuenberger, M., Carlson, A.E., Vinther, B., Masson-Delmotte, V., White, J.W.C., Liu,

Z., Otto-Bleisner, B., Brook, E.J., 2014. Greenland temperature responses to climate forcing during the last deglaciation. *Science* 345, 1177-1180.

Carlson, A.E., Stoner, J.S., Donnelly, J.P., Hillaire-Marcel, C., 2008. Response of the southern Greenland Ice Sheet during the last two deglaciations. *Geology* 36, 359-362.

Carlson, A.E., Winsor, K., Ullman, D.J., Brook, E.J., Rood, D.H., Axford, Y., LeGrande, A.N., Anslow, F.S., Sinclair, G., 2014. Earliest Holocene south Greenland ice sheet retreat within its late Holocene extent. *Geophysical Research Letters* 41, 5514-5521.

Clark, P.U., Dyke, A.S., Shakun, J.D., Carlson, A.E., Clark, J., Wohlfarth, B., Hostetler, S.W., Mitrovica, J.X., McCabe, A.M., 2009. The Last Glacial Maximum. *Science* 325, 710-714.

Clark, P.U., Shakun, J.D., Baker, P.A., Bartlein, P.J., Brewer, S., Brook, E., Carlson, A.E., Cheng, H., Kaufman, D.S., Liu, Z., Marchitto, T.M., Mix, A.C., Morrill, C., Otto-Bleisner, B.L., Pahnke, K., Russell, J.M., Whitlock, C., Adkins, J.F., Blois, J.L., Clark, J., Colman, S.M., Curry, W.B., Flower, B.P., He, F., Johnson, T.C., Lynch-Stieglitz, J., Markgraf, V., McManus, J., Mitrovica, J.X., Moreno, P.I., Williams, J.W., 2012. Global climate evolution during the last deglaciation. *Proc. Natl. Acad. Sciences* 109, http://dx.doi.org/10.1073/pnas.1116619109.

Colville, E.J., Carlson, A.E., Beard, B.L., Hatfield, R.G., Stoner, J.S., Reyes, A.V., Ullman, D.J., 2011. Sr-Nd-Pb isotope evidence for ice-sheet presence on Southern Greenland during the last interglacial. *Science* 333, 620-623.

Corbett, L.B., Bierman, P.R., Graly, J.A., Neumann, T.A., Rood, D.H. 2013. Constraining landscape history and glacial erosivity using paired cosmogenic nuclides in Upernavik, northwest Greenland. *Geological Society of America Bulletin* 125, 1539-1553.

Corbett, L.B., Young, N.E., Bierman, P.R. Briner, J.P., Neumann, T.A., Rood, D.H., Graly, J.A., 2011. Paired bedrock and boulder ^{10}Be concentrations resulting from early Holocene ice retreat near Jakobshavn Isfjord, western Greenland. *Quaternary Science Reviews* 30, 1739-1747.

Corbett, L.B., Bierman, P.R., Everett Lasher, G., Rood, D.H., 2015. Landscape chronology and glacial history in Thule, northwest Greenland. *Quaternary Science Reviews* 109, 57-67.

Cronauer, S.L., Briner, J.P., Kelley, S.E., Zimmerman, S.R.H., Morlighem, M., 2015. ^{10}Be dating reveals early-middle Holocene age of the Drygalski Moraines in central West Greenland. *Quaternary Science Reviews*, in press.

D'Andrea, W.J., Huang, Y., Fritz, S.C., Anderson, N.J., 2011. Abrupt Holocene climate change as an important factor for human migration in West Greenland. *Proceedings of the National Academy of Sciences,* doi: 10.1073/pnas.1101708108.

Davis, P.T., Briner, J.P., Coulthard, R.D., Finkel, R.W., Miller, G.H., 2006. Preservation of Arctic landscapes overridden by cold-based ice sheets. *Quaternary Research* 65, 156-163.

Dupont, T.K., Alley, R.B., 2005. Assessment of the importance of ice-shelf buttressing to ice sheet flow. *Geophysical Research Letters.* doi: 10.1029/2004GL022024.

Dyke, A.S., 2004. An outline of North American deglaciation with emphasis on central and northern Canada. In Ehlers, J., and Gibbard, P.L. (eds), *Quaternary Glaciations—Extent and chronology*. *Part II: North America.* Amsterdam: Elsevier.

Dyke, L.M., Hughes, A.L.C., Murray, T., Heimstra, J.F., Andresen, C.S., Rodés, Á., 2014. Evidence for the asynchronous retreat of large outlet glaciers in southeast Greenland at the end of the last glaciation. *Quaternary Science Reviews* 99, 244-259.

Farrell, W.E., Clark, J.A., 1976. On postglacial sea level. *Geophysical Journal of the Royal Astronomical Society* 46, 647-667.

Fredskild, B., 1973. Studies in vegetational history of Greenland. *Meddelelser om Grønland Geoscience* 11, 24 pp.

Funder, S., 1979. The Quaternary geology of the Narssaq area, South Greenland. *Rapport Grønlands Geologiske Undersøgelse* 86, 24 pp.

Funder, S., Kjeldsen, K.K., Kjær, K.H., Ó Cofaigh, C., 2011. The Greenland Ice Sheet during the past 300,000 years: a review. In Ehlers, J., Gibbard, P.L., and Hughes, P.D., eds. *Quaternary Glaciations—extent and chronology*. Amsterdam: Elsevier.

Håkansson, L., Briner, J.P., Aldahan, A., Possnert, G., 2011. ^{10}Be data from meltwater channels suggest that Jameson Land, east Greenland, was ice-covered during the last glacial maximum. *Quaternary Research* 76, 452-459.

Håkansson, L., Briner, J., Alexanderson, H., Aldahan, A., Possnert, G., 2007a. ^{10}Be ages from central east Greenland constrain the extent of the Greenland ice sheet during the Last Glacial Maximum. *Quaternary Science Reviews* 26, 2316-2321.

Håkansson, L., Briner, J.P., Andresen, C.S., Thomas, E.K., Bennike, O., 2014. Slow retreat of a land based sector of the West Greenland Ice Sheet during the Holocene Thermal Maximum: evidence from threshold lakes at Paakitsoq. *Quaternary Science Reviews* 98, 74-83.

Håkansson, L., Graf, A., Strasky, S., Ivy-Ochs, S., Kubik, P.W., Hjort, C., Schlüchter, C., 2007b. Cosmogenic ^{10}Be-ages from the Store Koldewey Island, NE Greenland. *Geografiska Annaler* 89, 195-202.

Håkansson, L., Hjort, H., Möller, P., Briner, J.P., Aldahan, A., Possnert, G. 2009. Late Pleistocene glacial history of Jameson Land, central East Greenland, derived from cosmogenic ^{10}Be and ^{26}Al exposure dating. *Boreas* 38, 244-260.

Hogan, K.A., Ó Cofaigh, C., Jennings, A.E., Dowdeswell, J.A., Heimstra, J.F., 2016. Deglaciation of a major palaeo-ice stream in Disko Trough, West Greenland. *Quaternary Science Reviews,* in press. http://dx.doi.org/ 10.1016/j.quascirev.2016.01.018.

Hughes, A.L.C., Rainsley, E., Murray, T., Fogwill, C.J., Schnabel, C., Xu, S., 2012. Rapid response of Helheim Glacier, southeast Greenland, to early Holocene climate warming. *Geology* 40, 427-430.

Hutter, K., 1983. *Theoretical Glaciology: Material science of ice and the mechanics of glaciers and ice sheets.* Norwell, MA: Kluwer Academic.

Huybrechts, P., 2002. Sea-level changes at the LGM from ice-dynamic reconstructions of the Greenland and Antarctic ice sheets during the glacial cycles. *Quaternary Science Reviews* 21, 203-231.

Imbrie, J., and Kipp, N.G., 1971. A new micropaleontological method for quantitative paleoclimatology: application to a late Pleistocene Caribbean core. In Turekian, K.K., ed. *The Late Cenozoic Glacial Ages*. New Haven: Yale University Press

Imbrie, J., and van Andel, T.H., 1964. Vector analysis of heavy-mineral data. *Geological Soceity of America Bulletin* 75, 1131-1156.

Jennings, A., Andrews, J., Wilson, L., 2011. Holocene environmental evolution of the SE Greenland Shelf North and South of the Denmark Strait: Irminger and East Greenland current interactions. *Quaternary Science Reviews* 30, 980-998.

Jennings, A.E., Hald, M., Smith, M., Andrews, J.T., 2006. Freshwater forcing from the Greenland Ice Sheet during the Younger Dryas: evidence from southeastern Greenland shelf cores. *Quaternary Science Reviews* 25, 282-298.

Jennings, A.E., Walton, M.E., Ó Cofaigh, C., Kilfeather A., Andrews, J.T., Ortiz, J.D., De Vernal, A., Dowdeswell, J.A., 2014. Paleoenvironments during the Younger Dryas-Early Holocene retreat of the Greenland Ice Sheet from outer Disko Trough, central west Greenland. *Journal of Quaternary Science* 29, 27-40.

Kelley, S.E., Briner, J.P., Young, N.E., 2013. Rapid ice retreat in Disko Bugt supported by ^{10}Be dating of the last recession of the western Greenland Ice Sheet. *Quaternary Science Reviews* 82, 13-22.

Kelley, S.E., Briner, J.P., Young, N.E., Babonis, G.S., Csatho, B., 2012. Maximum late Holocene extent of the western Greenland Ice Sheet during the late 20th Century. *Quaternary Science Reviews* 56, 89-98.

Kelley, S.E., Briner, J.P. and Zimmerman, S., 2015. The influence of ice marginal setting on early Holocene retreat rates in central West Greenland. Journal of Quaternary Science, v. 30, p. 271-280

Kelly, M.A., Lowell, T.V., Hall, B.L., Schaefer, J.M., Finkel, R.C., Goehring, B.M., Alley, R.B., Denton, G.H., 2008. A ^{10}Be chronology of late glacial and Holocene mountain glaciation in the Scoresby Sund region, east Greenland: implications for seasonality during lateglacial time. *Quaternary Science Reviews* 27, 2273-2282.

Kelly, M., 1974. The marine limit in Julianhab district, south Greenland, and its isostatic implications. In Blundel, D.J., ed: *Crustal Structure of the Gardar Rift, South Greenland: Report on Fieldwork 1973*. Lancaster: Department of Environmental Sciences

Kelly, M., 1975 A note on the implications of two radiocarbon dated samples from Qaleraglit ima, South Greenland. *Bulletin of the Geological Society of Denmark* 24, 21-26

Kirkbride, M.P., Warren, C.R., 1997. Calving processes at a grounded ice cliff. *Annals of Glaciology* 24, 116-121.

Koppes, M.N., and Montgomery, D.R., 2009. The relative efficacy of fluvial and glacial erosion over modern to orogenic timescales. *Nature Geoscience* 2, 644-647.

Kuijpers, A., Troelstra, S.R., Prins, M.A., Linthout, K., Akhmetzhanov, A., Bouryak, S., Bachmann, M.F., Lassen, S., Rasmussen, S., Jensen, J.B., 2003. Late Quaternary sedimentary processes and ocean circulation changes at the Southeast Greenland margin. *Marine Geology* 195, 109-129.

Lane, T.P., Roberts, D.H., Rea, B.R., Ó Cofaigh, C., Vieli, A., Rodés, A., 2013. Controls upon the Last Glacial Maximum deglaciation of the northern Uummannaq Ice Stream System, West Greenland. *Quaternary Science Reviews* 92, 324-344.

Larsen, N.K., Funder, S., Kjær, K.H., Kjeldsen, K.K., Knudsen, M.F., Linge, H., 2013. Rapid early Holocene ice retreat in West Greenland. *Quaternary Science Reviews* 92, 310-323.

Larsen, N.K., Funder, S., Linge, H., Möller, P., Schomacker, A., Fabel, D., Xu, S., Kjær, K.H., 2016. A Younger Dryas re-advance of local glaciers in north Greenland. *Quaternary Science Reviews,* doi: 10.1016/j.quascirev.2015.10.036.

Larsen, N.K., Kjær, K.H., Lecavalier, B., Bjørk, A.A., Colding, S., Huybrechts, P., Jakobsen, K.E., Kjeldsen, K.K., Knudsen, K.-L., Odgaard, B.V., Olsen, J., 2015. The response of the southern Greenland ice sheet to the Holocene thermal maximum. Geology, doi: 10.1130/G36476.1.

Larsen, N.K., Kjær, K.H., Olsen, J., Funder, S., Kjeldsen, K.K., Nørgaard-Pedersen, N., 2011. Restricted impact of Holocene climate variations on the southern Greenland Ice Sheet. *Quaternary Science Reviews* 3171-3180

Lecavalier, B.S., Milne, G.A.. Simpson, M.J.R., Wake, L., Huybrechts, P., Tarasov, L., Kjeldsen, K.K., Funder, S., Long, A.J., Woodroffe, S., Dyke, A.S., Larsen, N.K., 2014 A model of Greenland Ice Sheet Deglaciation Constrained by Observations of Relative Sea Level and Ice Extent. *Quaternary Science Reviews* 102, 54-84.

Levy, L.B., Kelly, M.A., Howley, J.A., Virginia, R.A., 2012. Age of the Ørkendalen moraines, Kangerlussuaq, Greenland: constraints on the extent of the southwestern margin of the Greenland Ice Sheet during the Holocene. *Quaternary Science Reviews* 52, 1-5.

Levy, L.B., Kelly, M.A., Lowell, T.V., Hall, B.L., Hempel, L.A., Honsaker, W.M., Lusas, A.R., Howley, J.A., Axford, Y.L., 2014. Holocene fluctuations of Bregne ice cap, Scoresby Sund, east Greenland: a proxy for climate along the Greenland Ice Sheet margin. *Quaternary Science Reviews* 92, 356-368.

Levy, L.B., Kelly, M.A., Lowell, T.V., Hall, B.L., Howley, J.A., Smith, C.A., 2016. Coeval fluctuations of the Greenland ice sheet and a local glacier, central East Greenland, during late glacial and early Holocene time. *Geophysical Research Letters* 43, 1623-1631.

Lloyd, J.M., Park, L.A., Kuijpers, A., Moros, M., 2005. Early Holocene palaeoceanography and detailed chronology of Disko Bugt, West Greenland. *Quaternary Science Reviews* 24, 1741-1755.

Lloyd, J., M. Moros, K. Perner, R. J. Telford, A. Kuijpers, E. Jansen, McCarthy, D., 2011. A 100 yr record of ocean temperature control on the stability of Jakobshavn Isbrae, West Greenland. *Geology* 39, 867–870.

Long, A.J., Roberts, D.H., Simpson, M.J.R., Dawson, S., Milne, G.A., Huybrechts, P., 2008. Late Weichselian relative sea-level changes and ice sheet history in southeast Greenland. *Earth and Planetary Science Letters* 272, 8-18.

Long, A.J., Woodroffe, S.A., Dawson, S., Roberts, D.H., Bryant, C.L., 2009. Late Holocene relative sea level rise and the Neoglacial history of the Greenland ice sheet. *Journal of Quaternary Science* 24, 345-359.

Lowell, T.V., Hall, B.L., Kelly, M.A., Bennike, O., Lusas, A.R., Honsaker, W., Smith, C.A., Levy, L.B., Travis, S., Denton, G.H., 2013. Late Holocene expansion of Istorvet ice cap, Liverpool Land, east Greenland. *Quaternary Science Reviews* 63, 128-140.

Marcott, S.A., Clark, P.U., Padman, L., Klinkhammer, G.P., Springer, S., Liu, Z., Otto-Bliesner, B.L., Carlson, A.E., Ungerer, A., Padman, J., He, F., Cheng, J., Schmittner, A., 2011. Ice-shelf collapse from subsurface warming as a trigger for Heinrich events. *Proceedings of the National Academy of Sciences*, doi: 10.1073/pnas.1104772108.

Massa, C., Perren, B.B., Gauthier, É, Bichet, V., Petit, C., Richard, H., 2012. A multiproxy evaluation of Holocene environmental change from Lake Igaliku, South Greenland. *Journal of Paleolimnology* 48, 241-258.

Milne, G.A., Shennan, I., 2013. Isostasy: glaciation induced sea-level change. *Encyclopedia of Quaternary Science* 3, 452-459.

Mix, A.C., et al., 1999. Foraminiferal faunal estimates of paleotemperature: Circumventing the no-analog problem yields cool ice age tropics. *Paleoceanography* 14, 350-359

Möller, P., Larsen, N.K., Kjær, K.H., Funder, S., Schomacker, A., Linge, H., Fabel, D., 2010. Early to middle Holocene valley glaciations on northernmost Greenland. *Quaternary Science Reviews* 29, 3379-3398.

Nelson, A., Bierman, P.R., Shakun, J.D., Rood, D.H., 2014. Using *in situ* cosmogenic ^{10}Be to identify the source of sediment leaving Greenland. *Earth Surface Processes and Landforms*. 39, 1087-1100.

Nøgaard-Pedersen, N., and Mikkelsen, N., 2009. 8000 year marine record of climate variability and fjord dynamics from Southern Greenland. *Marine Geology* 264, 177-189.

Ó Cofaigh, C., Dowdeswell, J.A., Jennings, A.E., Hogan, K.A., Kilfeather, A., Heimstra, J.F., Noormets, R., Evans, J., McCarthy, D.J., Andrews, J.T., Lloyd, J.M., Moros, M., An extensive and dynamic ice sheet on the West Greenland shelf during the last glacial cycle. *Geology.* http://dx.doi.org/10.1130/G33759.1

Olsen, J., Kjær, K.H., Funder, S., Larsen, N.K., Ludikova, A., 2011. High-Arctic climate conditions for the last 7000 years inferred from multi-proxy analysis of the Bliss Lake record, North Greenland. *Journal of Quaternary Science.* http://dx.doi.org/10.1002/jqs.1548

Perner, K., Moros, M., Jennings, A., Lloyd, J.M., Knudsen, K.L., 2013. Holocene palaeoceanographic evolution off West Greenland. *The Holocene* 23, 374-387.

Pisias, N.G., Murray, R.W., Scudder, R.P., 2013. Multivariate statistical analysis and partitioning of sedimentary geochemical data sets : General principles and specific MATLAB scripts. *Geochemistry Geophysics Geosystems* 14, 4015-4020

Putkonen, J., Swanson, T., 2003. Accuracy of cosmogenic ages for moraines. *Quaternary Research* 59, http://dx.doi.org/10.1016/S0033-5894(03)00006-1.

Reimer, P.J., Bard, E., Bayliss, A., Beck, J.W., Blackwell, P.G., Ramsey, C.B., Buck, C.E., Haflidason, H., Hajdas, I., Hatté, C., Heaton, T.J., Hoffmann, D.L., Hogg, A.G., Hughen, K.A., Kaiser, K.F., Kromer, B., Manning, S.W., Niu, M., Reimer, R.W., Richards, D.A., Scott, E.M., Southon, J.R., Staff, R.A., Turney, C.S.M., van der Plicht, J., 2013. IntCal13 and Marine13 radiocarbon age calibration curves 0-50,000 BP. Radiocarbon 55, 1869-1887.

Rignot, E., Koppes, M., Velicogna, I., 2010. Rapid submarine melting of the calving faces of West Greenland glaciers. *Nature Geoscience* 3, 187-191.
Cheng, H., Edwards, R.L., Friedrich, M., Grootes, P.M., Guilderson, T.P.,

Rinterknecht, V., Gorokhovich, Y., Schaefer, J., Caffee, M., 2009. Preliminary ^{10}Be chronology for the last deglaciation of the western margin of the Greenland Ice Sheet. *Journal of Quaternary Science* 24, 270-278.

Rinterknecht, V., Jomelli, V., Brunstein, D., Favier, V., Masson-Delmotte, V., Bourlès, D., Leanni, L., Schläppy, R., 2014. Unstable ice stream in Greenland during the Younger Dryas cold event. *Geology,* http://dx.doi.org/10.1130/G35929.1.

Roberts, D.H., Long, A.J., Schnabel, C., Davies, B.J., Xu, S., Simpson, M.J.R., Huybrechts, P., 2009. Ice sheet extent and early deglacial history of the southwestern sector of the Greenland Ice Sheet. *Quaternary Science Reviews* 28, 2760-2773.

Roberts, D.H., Long, A.J., Schnabel, C., Freeman, S., Simpson, M.J.R., 2008. The deglacial history of southeast sector of the Greenland Ice Sheet during the Last Glacial Maximum. *Quaternary Science Reviews* 27, 1505-1516.

Roberts, D.H., Rea, B.R., Lane, T.P., Schnabel, C., Rodès, A., 2013. New constraints on Greenland ice sheet dynamics during the last glacial cycle: evidence from the Uummannaq ice stream system. *Journal of Geophysical Research: Earth Surface* 118, 1-23.

Scambos, T.A., Bohlander, J.A., Shuman, C.A., Skvarca, P., 2004. Glacier acceleration and thinning after ice shelf collapse in the Larsen B embayment, Antarctica. *Geophysical Research Letters* 31, http://dx.doi.org/10.1029/2004GL020670.

Schoof, C., 2007. Ice sheet grounding line dynamics: steady states, stability, and hysteresis. *Journal of Geophysical Research* 112, doi: 10.1029/2006JF000664.

Shakun, J., Carlson, A.E., 2010. A global perspective on Last Glacial Maximum to Holocene climate change. *Quaternary Science Reviews* 29, 1801-1816.

Sheldon, C., Jennings, A., Andrews, J.T., Ó Cofaigh, C., Hogan, K., Dowdeswell, J.A., Seidenkrantz, M.-S., 2016. Ice stream retreat following the LGM and onset of the west Greenland current in Uummannaq Trough, west Greenland. *Quaternary Science Reviews,* in press. http://dx.doi.org /10.1016/j.quascirev.2016.01.019.

Shepherd, A., Wingham, D., Rignot, E., 2004. Warm ocean is eroding West Antarctic Ice Sheet. *Geophysical Research Letters* 31, http://dx.doi.org/10.1029/2004GL021106.

Simpson, M.J.R., Milne, G.A., Huybrechts, P., Long, A.J., 2009. Calibrating a glaciological model of the Greenland ice sheet from the Last Glacial Maximum to

present-day using field observations of relative sea level and ice extent. *Quaternary Science Reviews* 29, 1631-1657.

Solignac, S., de Vernal, A., Hillaire-Marcel, C., 2004. Holocene sea-surface conditions in the North Atlantic—contrasting trends and regimes in the western and eastern sectors (Labrador Sea vs. Iceland Basin). *Quaternary Science Reviews* 23, 319-334.

Sparrenbom, C.J., Bennike, O., Björck, Lambeck, K., 2006a. Holocene relative sea-level changes in the Qaqortoq area, southern Greenland. *Boreas* 35, 171-187

Sparrenbom, C.J., Bennike, O., Björck, Lambeck, K., 2006b. Relative sea-level changes since 15000 cal. Yr BP in the Nanortalik area, southern Greenland. *Journal of Quaternary Science* 21, 29-48.

Sparrenbom, C.J., Bennike, O., Fredh, D., Randsalu-Wendrup, L., Zwartz, D., Ljung, K., Björck, S., Lambeck, K., 2013. Holocene relative sea-level changes in the inner Bredefjord area, southern Greenland, *Quaternary Science Reviews*, 69, 107-124.

Storms, J.E.A., de Winter, I.L., Overeem, I., Drijkoningen, G.G., Lykke-Andersen, H., 2012. The Holocene sedimentary history of the Kangerlussuaq Fjord-valley fill, West Greenland. *Quaternary Science Reviews* 35, 29-50

Stroeven, A.P., Fabel, D., Hättestrand, C., Harbor, J., 2002. A relict landscape in the centre of Fennoscandian glaciation: cosmogenic radionuclide evidence of tors preserved through multiple glacial cycles. *Geomorphology* 44, 145-154.

Tarasov, L., Dyke, A.S., Neal, R.M., Peltier, W.R., 2012. A data-calibrated distribution of deglacial chronologies for the North American ice complex from glaciological modeling. *Earth and Planetary Science Letters* 315-316, 30-40.

Tarasov, L., Peltier, W.R., 2002. Greenland glacial history and local geodynamic consequences. *Geophysics Journal International* 150, 198-229.

Van der Veen, C.J., 2002. Calving glaciers. *Progress in Physical Geography* 26, 96-122.
Weidick, A., 1975. Holocene shorelines and glacial stages in Greenland—an attempt at correlation. *Rapport Grønlands Geologiske Undersøgelse* 41, 39 pp.

Weidick, A., 1975. Holocene shorelines and glacial stages in Greenland—an attempt at correlation. Rapp. Grønl. Geol. Unders. 41, 39.

Weidick, A., Kelly, M., Bennike, O., 2004. Late Quaternary development of the southern sector of the Greenland Ice Sheet, with particular reference to the Qassimiut lobe. Boreas 33, 284-299

Williams, K.M., 1993. Ice sheet and ocean interactions, margin of the East Greenland Ice Sheet (14 ka to present): diatom evidence. *Paleoceanography* 8, 69-83.

Winsor, K., Carlson, A.E., Klinkhammer, G.P., Stoner, J.S., Hatfield, R.G., 2012. Evolution of the northeast Labrador Sea during the last interglaciation. *Geochemistry, Geophysics, Geosystems* 13, http://dx.doi.org/10.1029/2012GC004263.

Winsor, K., Carlson, A.E., Rood, D.H., 2014. ^{10}Be dating of the Narsarsuaq moraine in southernmost Greenland: evidence for a late-Holocene ice advance exceeding the Little Ice Age maximum. *Quaternary Science Reviews* 98, 135-143.

Winsor, K., Carlson, A.E., Caffee, M., Rood, D.H., 2015a. Rapid last-deglacial thinning and retreat of the marine-terminating southwestern Greenland ice sheet. *Earth and Planetary Science Letters* 426, 1-12.

Winsor, K., Carlson, A.E., Welke, B., Reilly, B., 2015b. Early deglacial onset of southwestern Greenland ice-sheet retreat on the continental shelf. *Quaternary Science Reviews* 128, 117-126.

Young, N.E., Briner, J.P., 2015. Holocene evolution of the western Greenland Ice Sheet: assessing geophysical ice-sheet models with geological reconstructions of ice-margin change. *Quaternary Science Reviews* 114, 1-17.

Young, N.E., Briner, J.P., Stewart, H.A.M., Axford, Y., Csatho, B., Rood, D.H., Finkel, R.C., 2011a. Response of Jakobshavn Isbrae, Greenland, to Holocene climate change. *Geology* 39, 131-134.

Young, N.E., Briner, J.P., Axford, Y., Csatho, B., Babonis, G.S., Rood, D.H., Finkel, R.C., 2011b. Response of a marine-terminating Greenland outlet glacier to abrupt cooling 8200 and 9300 years ago. *Geophysical Research Letters* 38, http://dx.doi.org/10.1029/2011GL049639.

Young, N.E., Schaefer, J.M., Briner, J.P., Goehring, B.M., 2013a. A Be-10 production rate calibration for the Arctic. *Journal of Quaternary Science* 28, 515-526.

Young, N.E., Briner, J.P., Rood, D.H., Finkel, R.C., Corbett, L.B., Bierman, P.R., 2013b. Age of the Fjord Stade moraines in the Disko Bugt region, western Greenland, and the 9.3 and 8.2 ka cooling events. *Quaternary Science Reviews* 60, 76-90.

Young, N.E., Schweinsberg, A.D., Briner, J.P., Schaefer, J.M., 2015. Glacier maxima in Baffin Bay during the Medieval Warm Period coeval with Norse settlement. *Sci. Adv.*, e1500806.

Zweck, C., Huybrechts, P., 2005. Modeling of the northern hemisphere ice sheets during the last glacial cycle and glaciological sensitivity. *Journal of Geophysical Research: Atmospheres* 110. http://dx.doi.org/10.1029/2004JD005489.

Chapter 3

Paleo-reanalysis of spatially- and temporally-resolved Arctic climate 10-2010 C.E.

Gaylen Sinclair[1], Alan C. Mix[1], Anders E. Carlson[1]

[1]College of Earth, Ocean, and Atmospheric Sciences, Oregon State University, USA

To be submitted to *Proceedings of the National Academy of Sciences*

3.1 Abstract

Understanding the spatial pattern of climate variability in the Arctic is critical for better understanding both the climate forcings and the magnitude of 20th and 21st century climate change relative to baseline variability. Here, climate field reconstruction yields a gridded spatial-temporal reanalysis product throughout the Common Era. Continental regions generally have more variability than ocean regions, and the eastern and western Arctic frequently show uncorrelated temperatures prior to recent warming. Five proposed Common Era climate forcings (total solar irradiance, Atlantic meridional overturning circulation, North Atlantic Oscillation, sulfate loading, and CO_2) combined explain at most ~20 % of the temperature variability present in both reanalysis and proxy data. The onset of significant cooling into the Little Ice Age varies spatially by nearly 600 years, suggesting a rough coincidence of several regional cooling events, rather than a single global event. Persistent warming, (emergence from background variability of the Common Era) started by the early 19th century in Arctic North America and Europe, but was delayed to the end of the 19th century the Greenland-Norwegian Sea and Arctic Ocean.

3.2 Introduction

Arctic amplification of anthropogenic climate change carries risks in a warming world (Overland et al. 2011; Serreze & Barry 2011; Cohen et al., 2014; Clark et al., 2016). Understanding these risks demands knowledge of baseline variability and regional sensitivity to forcing, but instrumental records of Arctic variability are limited by logistical challenges. Paleoclimate data helps to fill this knowledge gap (Kaufmann et al., 2009). The Common Era (0-2000 CE) is an ideal target for investigating the baseline variability of Arctic climate. Over this time frame, excepting anthropogenic changes in atmospheric CO_2 levels and ongoing insolation changes, boundary conditions are similar to today (Mann et al 2008) and a relatively high density of high-resolution paleoclimate data exists (e.g., PAGES 2k, 2017). The Common Era exhibits several centennial-scale climate fluctuations, which can be used to address the rate and spatial character of climate changes at timescales relevant to humanity, to assess whether recent changes

have emerged from background variability into an unprecedented state, and to better understand the regional impacts of changing climate in the Arctic.

Individual paleotemperature proxy records do not necessarily record a simple signal of local temperature; they instead may reflect a combination of local temperature, non-temperature climate-related signal, local temperature noise not representative of the region, analytical proxy noise, and calibration errors. Nevertheless, meaningful spatio-temporal climate reconstructions can be developed from sparse observational data based on statistical climate field reconstruction (CFR) methods (e.g. Fritts et al., 1971; Pisias 1978; Evans et al, 2001; Evans et al., 2002; Mann et al. 2009), or data assimilation modeling (e.g. Hakim et al., 2016; Perkins and Hakim 2017). Here we employ elements of both strategies, applying CFR methods to extend paleo-proxy data arrays into spatial reconstructions of Artic climate over the Common Era, calibrated in an overlapping interval based on regression to reanalysis products.

Climate field reconstructions (CFRs) take advantage of the fact that multiple proxy records share common patterns of variability; combining records can therefore suppress variations (noise or local signals) that are not common to multiple records and preserve shared variance. Here, we combine the most comprehensive database of proxy data from the Common Era (PAGES 2k Consortium 2017) with a reanalysis dataset for the interval 1850-1970 (Morice et al., 2012), to create a temporally calibrated, spatially resolved reanalysis product throughout the Common Era. We then use this data product to assess correspondence to potential external forcings, and consider whether and when regional climates have emerged from this longer record of baseline variability under anthropogenic change. This analysis extends that of previous studies that were limited to stacking and averaging (e.g. Kaufman et al., 2009, McKay and Kaufman 2014), to resolve spatio-temporal variability in a more complete regional grid.

3.3 Data synthesis and analysis

We include 17 highly resolved paleoclimate proxy records (PAGES 2k Consortium 2017) in the latitude bands 60-90N that have average temporal resolution of <15 years, and cover the time period 10-1970 C.E. After converting raw proxy data to z-

scores and linearly interpolating to a 5-year intervals, we decompose the data array via R-mode factor analysis and retain four significant orthogonal factors. We exclude five records with no discernable influence on our final temperature reconstructions (Appendix B.4).

We use the HadCRUT4.2 reanalysis dataset to build the spatial regression. This dataset covers the period from 1850-2010 C.E., so provides a long enough time series to regress against the proxy factors over the period 1850-1970 C.E. We regress the four factors against HadCRUT4.2 annual-average and seasonal (winter, DJF and summer, JJA) temperatures at each HadCRUT4.2 grid cell (Morice et al., 2012 as modifed by PAGES2k, 2017) over their overlapping range (1850-1970 C.E.) to calibrate and predict reanalysis temperatures from paleo factor timeseries, at each grid cell from 10-2010 CE. One thousand Monte Carlo simulations at each grid cell address uncertainties in calibration of factors and provide uncertainty estimates for time-slice maps, time series, and animations. Our paleo-reanalysis provides a spatially resolved gridded time series, assuming stationarity relative to the calibration interval. We examine spatial fingerprints of relationships between several proposed climate forcings and the gridded temperature time series (Lindeman et al., 1980; Grömping 2007).

We estimate the timing of the Little Ice Age (LIA) and the emergence of sustained warmth in the Anthropogenic era in each gridcell as the final year at the end of a 50-yr overlapping block that is significantly warmer or colder, relative to all previous timesteps (Welch's T test, p=0.05).

3.4 Results and discussion

Our final set of proxy records includes three tree ring compilations, two high-resolution marine sediment cores, seven ice cores, four lake sediment cores, and one speleothem. These proxies are broadly similar to the entire Arctic portion of the PAGES database in terms of spatial and temporal resolution and proxy type, although this subset is notably missing the last millennium North American tree ring records that comprise ~32% of the PAGES 2k record (Appendix B.3). Four orthogonal factors explain ~48% of the variance in the paleoclimate proxies (Figure 3.1). Retaining additional factors does

not significantly improve the regressions to reanalysis data (Appendix B.5). Factor 1 (15.7% of paleo variance) closely resembles previous estimates of Arctic temperature changes in the Common Era based on stacking and averaging (PAGES 2k Consortium, 2017), and is significant in most of the reanalysis gridcells. However, communality values below 0.4 indicate that many of the proxies have a significant uncorrelated component within the available sampling arrray.

Factor 2 (13.6% of paleo variance) displays a long-term warming trend (cooling where loadings are negative, such as in Scandinavia). This factor lacks strong correlation to recent reanalyses, so may represent a non-temperature aspects of climate or longer-term trend not expressed in the calibration period of 1850-1970.

Factor 3 (10.1% of paleo variance) is significant in regressions against reanalysis temperatures in central Siberia, while Factor 4 (8.9% of paleo variance) is inversely related to annual temperatures in western Greenland and Arctic North America, and positively related to temperatures in Arctic Europe, indicating that these two factors capture meaningful regional variations in climate. Factors 3 and 4 have stronger correlations with winter temperatures, and weaker correlations with summer temperatures (Figures B.13 and B.14).

The multiple regression of the four empirical paleo factors onto gridcell reanalysis temperatures explains 50% of observed temperature variance. By comparison, direct factor analysis of the reanalysis temperature data alone explains ~80% of observed variance at all gridcell. This implies that the paleo-reconstructions here likely underestimate true paleotemperature variance relative to what would be observed in a more complete observational array.

Averaged across all Arctic grid points, the warmest (pre-20th century) period was between 350 and 455 C.E., overlapping with the end of the so-called Roman Warm Period (RWP, approximately -500 BCE to 400 CE (Wang et al., 2012)), with an average temperature ~0.44°C warmer than the pre-industrial (1850-1900 C.E.) average (Figure 3.2a). The Mediaeval Climate Anomaly (MCA, 950-1400 CE (Diaz et al., 2011)) is contains the warmest part of the second millennium in this arctic average (Figure 3.2b), but here is characterized more by high variability, with multidecadal temperatures swings

greater than 1°C. While such variability is not commonly noted as a feature of the MCA in other regions, similar variability is observed in Scots Pine reconstructions from Lapland (Helama et al., 2009). The coldest average interval is 1660-1750 C.E., with temperatures on average 0.8°C colder than the 1850-1900 C.E. average at each gridpoint (Figure 3.2d). A second notable feature is the 20th century, which in most areas is warmer than the previous two millennia (Figure 3.2c). An exception to this pattern is the North Atlantic, which has no significant warming relative to the average of the previous two millennia.

Continental regions are generally more variable than ocean regions (Figure 3.3). Much of the variability in the Arctic Ocean comes from Winter temperatures, suggestive of variability in sea-ice production (Sup. Fig.). The eastern Arctic (including Arctic Europe and Siberia) lacks the characteristic second millennium cooling that distinguishes the western Arctic. Running correlations between the eastern and western Arctic annual averages are only significant for brief periods over the Common Era, whereas correlations between regions within the eastern and western Arctic are significant throughout. This is evident in the maps of Common Era climate, in which the eastern continental Arctic frequently has a different temperature or trajectory from most of the rest of the Arctic (sup. Movie).

When calibrated separately for seasons, reconstructed Arctic average temperature anomalies have more variance in winter than summer; for example, the temperature changes during the MCA and LIA events are more pronounced in winter. The regional expressions of Factors 3 and 4 are also mostly a winter feature (sup fig).

To assess possible causes of Arctic variability in the Common Era, we regress five proposed climate forcings against our temperature reconstructions in all grid cells (Figure 3.3). Total solar irradiance (TSI) and CO_2 are significant predictors of temperature over the interval in which all forcing reconstructions overlap (450-1680 CE). Reconstructions of the oceanic Atlantic meridional Overturning circulation (AMOC) and the atmospheric North Atlantic Oscillation (NAO) index do not significantly predict whole-Arctic temperature variability. In contrast, sulfate loading related to explosive volcanic eruptions are significantly correlated with whole-Arctic temperature variations

(p=0.05). In combination, a linear response to these five potential forcing variables can explain ~20% of pooled proxy-derived temperature variability, suggesting other factors must be invoked to explain the observations.

Regional expression of variance explained by known forcings (Figure 3.4) shows that combined forcings are more highly correlated to temperature in the Atlantic and Arctic Ocean sectors, whereas climate in Arctic North America is only weakly linked to hypothesized forcings. NAO and AMOC may play a role in Siberian variability, but are mostly insignificant elsewhere. For comparison, models indicate warming in Arctic Europe when the North Atlantic cools (Caesar et al., 2018). CO_2 forcing is most prominently correlated to observations in Arctic Europe, while TSI explains at best 9 % of variance in small parts of eastern North America. The appearance of regional temperature variations in the Arctic Ocean, northern Greenland, North Atlantic, and Siberian regions explained by volcanic sulfate loading is tenuous – the variance explained is low (typically less than 2%) and the sign of regression counterintuitively relates warming to volcanic eruptions. Ad hoc explanations could link polar warming with stratospheric dynamics perturbed by explosive volcanism (Wunderlich and Mitchell, 2017; Stenchikov et al., 2002; Ogi et al., 2016, Rigor et al., 2002), and volcanic ash deposition on glacier and sea-ice surfaces could contribute warming via albedo reduction (e.g. Praetorious et al., 2016), but the small amount of variance explained leave these linkages as speculative.

On average, the Little Ice Age begins (relative to preceding baseline) at 1605 ± 185 C.E., and ends at 1740 ± 180 C.E. (Figure 3.5a). Using a fixed reference of 10-1000 C.E. expands these ages, to an average beginning at 1540 ± 205 C.E. and end at 1770 ± 225 C.E. However, these averages mask substantial variability, particularly in LIA onset. In western Siberia, LIA onset is near 1100 C.E., while eastern Siberia cools significantly between 1600 and 1700 C.E. Parts of Europe, the Greenland-Norwegian Sea region, and the Arctic Ocean delay significant cooling until 1700-1800, especially when using a fixed reference. Timing of LIA onset in Baffin Island and eastern Greenland is verified by independent well-dated records. Ice expansion in Baffin Island and eastern Greenland occurred 1430s to 1450s C.E., similar to the timing of the start of the LIA defined here in

both the fixed and floating reference periods (Miller et al. 2012; 2013). The large spatial variability we observe for LIA initiation between approximately 1200 and 1900 C.E., as well as its sensitivity to baseline, suggests that the LIA is not a single forced event, but may be an approximate coincidence of several centennial-scale regional fluctuations, either forced or stochastic, superimposed on a longer-term cooling trend (Marcott et al., 2013). Centennial-scale fluctuations superimposed on this long-term trend may reflect local to regional scale variability. Potential causes for these composite regional events include solar activity, volcanic eruptions, and land-use change (e.g. Owens et al., 2017). If these fluctuations are unforced variance at centennial timescales, there may be an increased probability that the coldest period in a given Arctic record will come during the last millennium, but the actual timing of this may be more stochastic, leading to spatial variability in the onset of the LIA we observe here.

Significant and sustained warming relative to a baseline of all earlier variations starts early (near 1800 CE) in western Siberia and Alaska, in the mid 19th Century in parts of Greenland and eastern North America, but in the mid 20th century in the North Atlantic, parts of the Arctic Ocean, and eastern Siberia. Our analysis suggest that Scandinavia and parts of the Irminger Sea and Southern Greenland have not yet (as of 2010 CE) emerged as significantly warmer than past variability. The middle range of emergent warming in our study is roughly similar to that of Abram et al (2017), 1831-1852 in northern latitudes, based on the timing of sustained, significant climate warming in proxy reconstructions, and a reference period that coincided with the LIA. A change of the baseline interval to exclude the LIA (i.e., a baseline of 10-1000 C.E. makes timing of emergent warming more recent by on average 16 years. The relatively late emergence of ocean warming relative to baseline temperatures may be explained by the higher thermal inertia of the oceans: regions with later emergence tend to have less pronounced cooling over the preceding 2,000 years, so it takes longer for warming these areas to emerge as statistically significant relative to their baseline variability, even though the patterns of recent warming in the early and late regions is basically similar.

3.5 Conclusions

Assuming that relationships between paleo data and recent reanalysis temperatures in the calibration period (1850-1970) apply to longer time intervals (i.e., that the system is stationary), we calibrate and project sparse high-resolution climate proxy records over the past 2000 years to reconstruct spatially-resolved Arctic climate variability through the common Era. This gridded spatial-temporal product helps to fingerprint the influence of various forcing mechanisms on Arctic climate; we find a significant role for solar irradiance and CO_2 variability, and limited influence of NAO and AMOC variability. Sulphate loading is conterintuitively associated with slight warming in the Arctic, suggesting the relationship between sulphate aerosols and Arctic Climate may be very complex. The LIA appears with variable timing, suggesting and approximate coincidence of independent regional events superimposed on a long-term cooling trend, rather than a discrete forced global event. In our reconstruction, early sustained warming emerged from background variability near 1800 CE in Alaska and western Siberia, but in the eastern North Atlantic, parts of the Arctic Ocean, and eastern Siberia, sustained warming became significant later, in the mid 20th century CE, and Scandinavia had not emerged as significantly warmer than its baseline variability as of 2010 CE. Lagging emergence of warmth in regions of maritime climate are consistent with a longer thermal inertia associated with the ocean and implying substantial existing commitment to future changes in the marine regions of the Arctic.

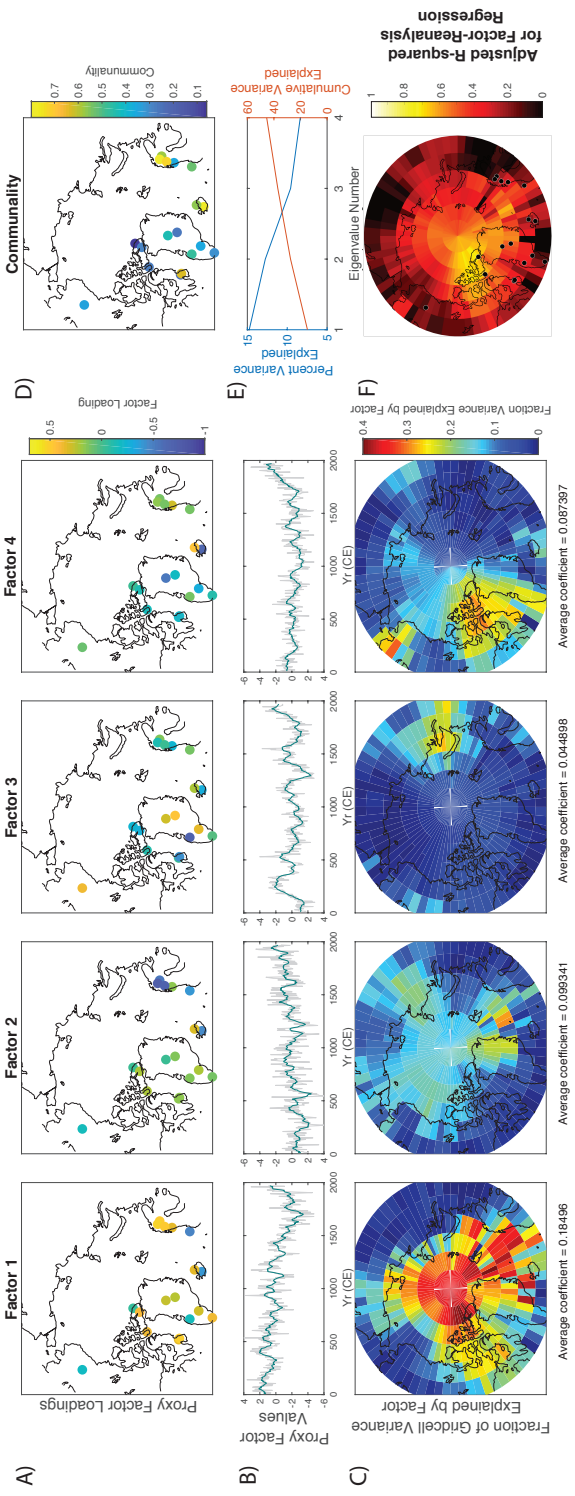

Figure 3.1: Summary of proxy factor analysis and regression to reanalysis data.

Figure 3.1: Summary of proxy factor analysis and regression to reanalysis data. (A) Proxy factor loadings. Color of dot indicates loading of factor. (B) Proxy factor values. Thin grey line is at 5-year resolution, heavy green line is 5-point moving average. (C) Percent variance explained by each factor in multiple regression to HadCRUT reanalysis gridcell temperature over the period 1850-1970. (D) Communality of factor analysis at proxy sites. (E) Eigenvalues summary of factor analysis. (F) Adjusted R-squared for proxy factor/reanalysis regression.

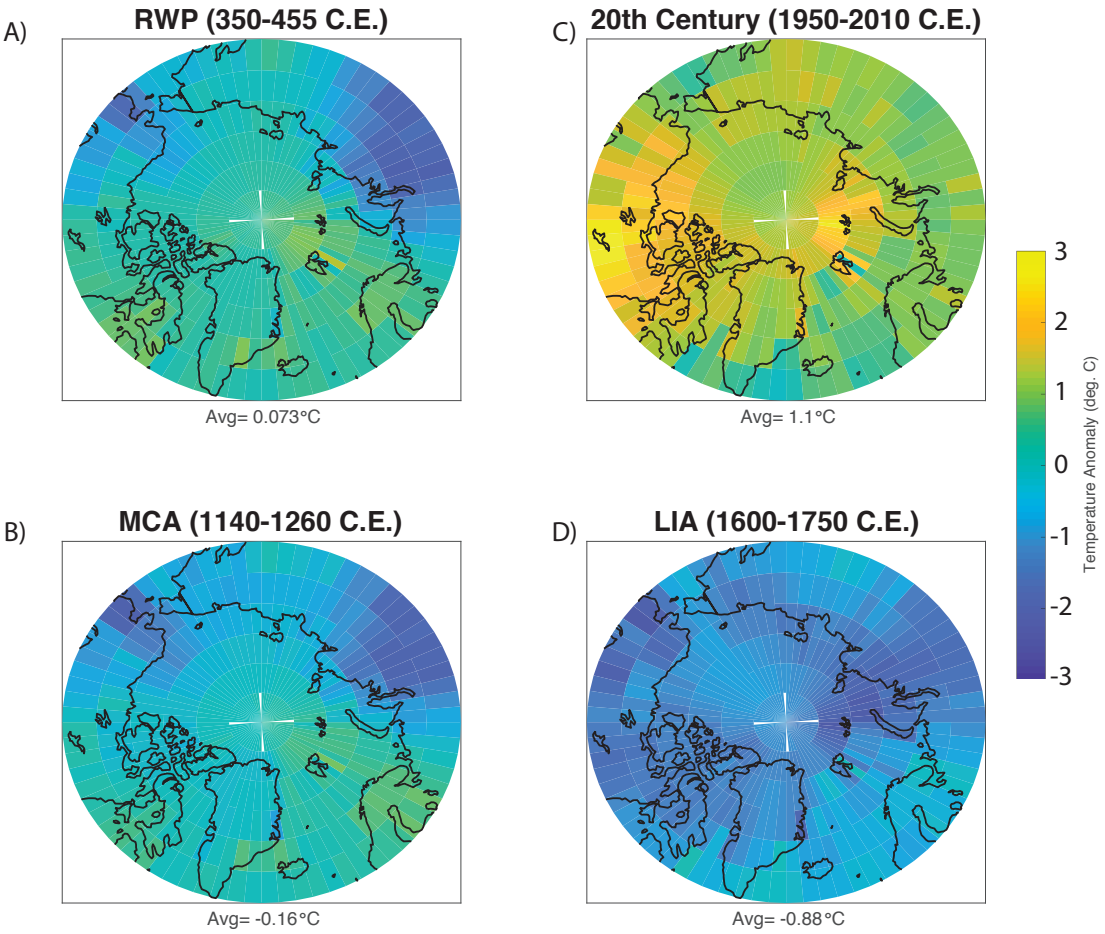

Figure 3.2: Average temperature anomalies for selected time periods, relative to the average of 1850-1900 C.E., with average anomaly noted below each map. (A) Warmest (Arctic average) pre-20th Century period in the Average temperature record, ~350-455 C.E (B) Warmest (Arctic average) part of the Medieval Climate Anomaly, ~1140-1260 C.E.(C) 1950-2010 C.E. (D) The coldest (Arctic average) part of the Little Ice Age, ~1600-1750 C.E.

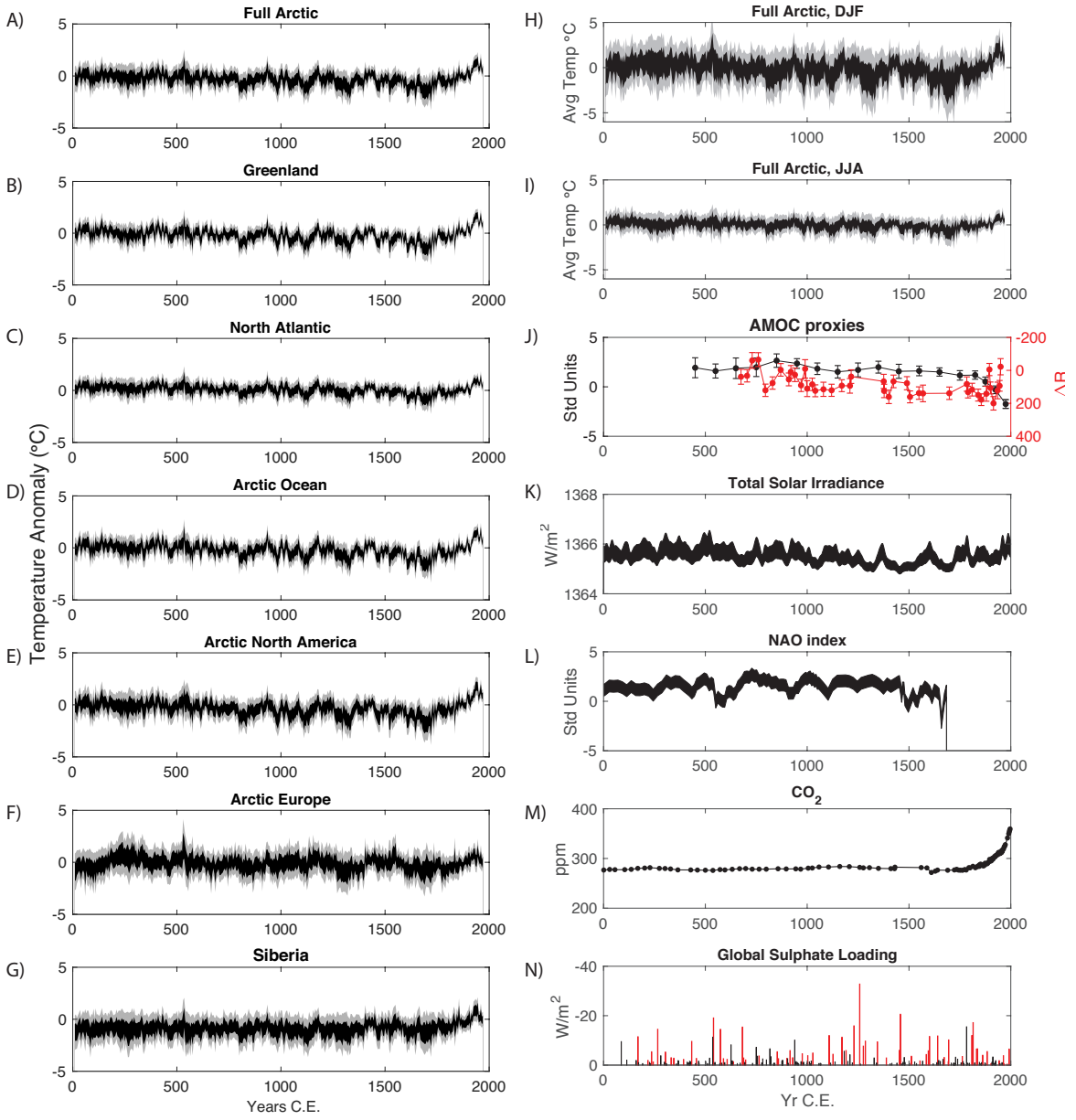

Figure 3.3: Regional and seasonal temperature anomaly reconstructions (relative to 1850-1900), and proposed Common Era forcings.

Figure 3.3: Regional and seasonal temperature anomaly reconstructions, and proposed Common Era forcings. (A) Full Arctic temperature stack, where temperature is referenced to 1850-1900 mean. (B-G) Regional temperature stacks, where temperature is referenced to 1850-1900 mean. (H) Winter (DJF) temperature anomaly. (I) Summer (JJA) temperature anomaly. (J) AMOC proxies from Thornalley et al., 2018 (black) and Wanamaker et al., 2012 (red). (K) Total Solar Irradiance (Roth and Joos 2013). (L) NAO Index (Olsen et al., 2013). (M) CO_2 reconstructed from Law Dome, Antarctica (MM 2006). (N) Global Sulphate loading from Northern Hemisphere (black) and tropical (red) volcanic eruptions (Sigl et al., 2015).

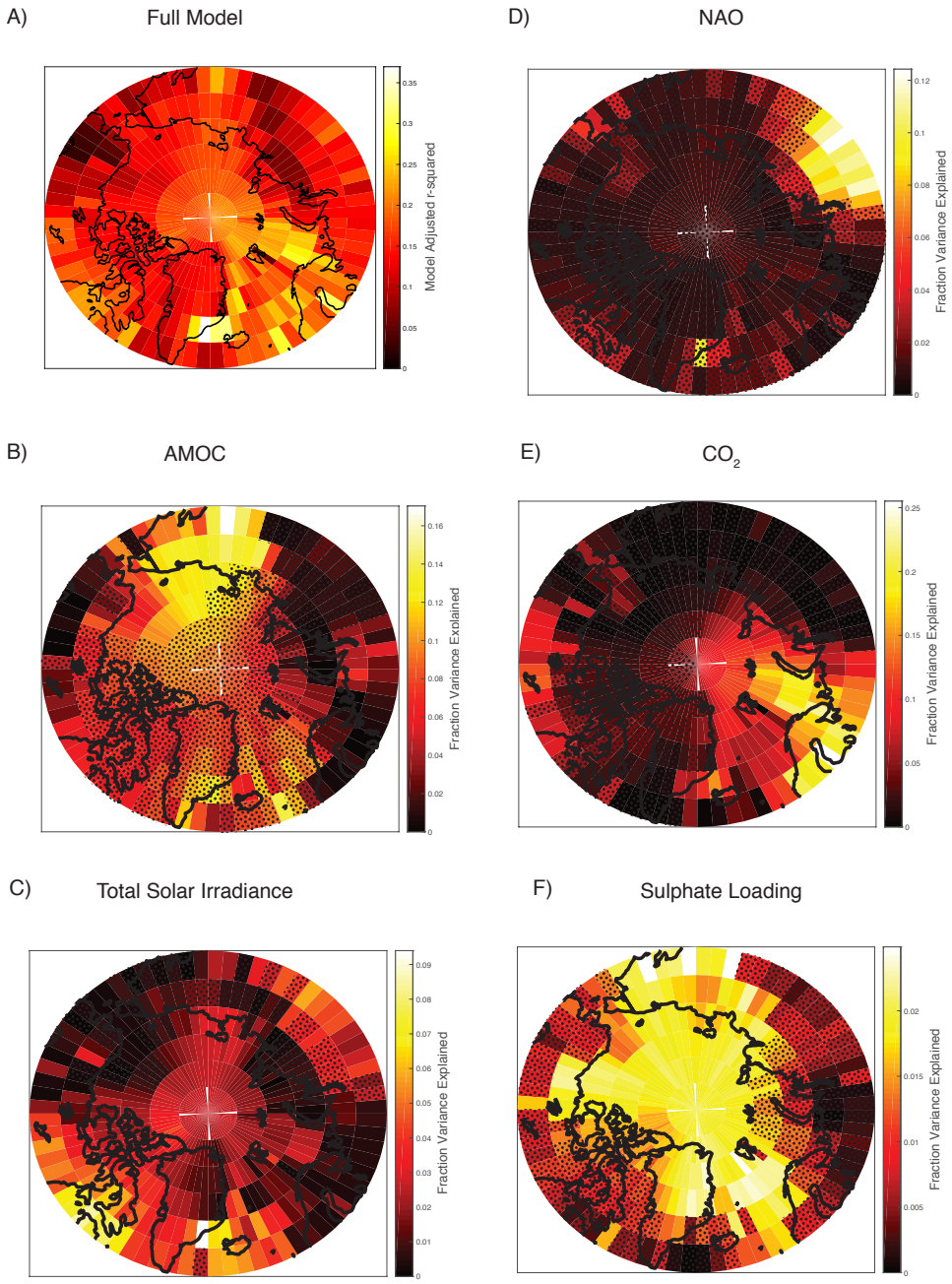

Figure 3.4: Variance decomposition for multiple regression of gridcell temperature records against proposed Common Era climate forcings. Color indicates percent variance explained by the individual forcing, and stippling indicates regions where regression coefficient in a multiple regression is not significant at p=0.05.

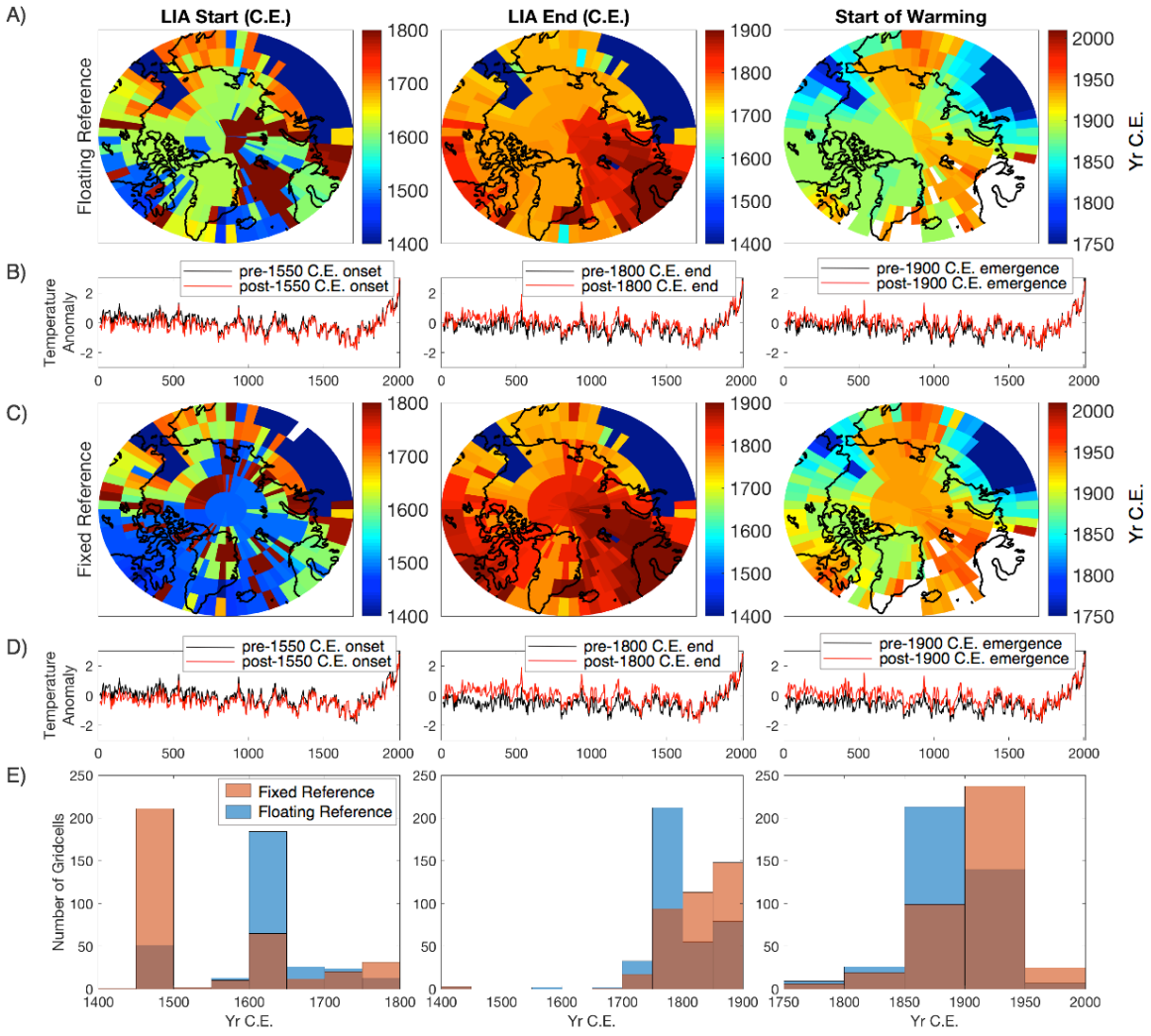

Figure 3.5: Timings of Little Ice Age and Industrial Era warming. (A) Timing of Little Ice Age onset, completion, and Statistically significant emergence of recent warming relative to past variability, using a floating reference period (all 50-year periods preceding the period of interest). (B) Average temperature anomalies (relative to 1850-1900 C.E. mean), split between early (black) and late (red) transition into and out of LIA, and 19th-21st Century warming. (C) and (D) same as (A) and (B) except using a fixed reference period (10-1000 C.E.). (E) Histogram of transition between periods. Blue bars use floating reference, red bars use fixed reference.

3.6 References

Berger, A., Loutre, M.F., 1991. Insolation values for the climate of the last 10 million years. *Quaternary Science Reviews* 10, 291-317

Bindoff, N.L., Stott, P.A., AchutaRao, K.M., Allen, M.R., Gillett, N., Gutzler, D., Hansingo, K., Hegerl, G., Hu, Y., Jain, S., Mokhov, I.I., Overland, J., Perlwitz, J., Sebbari, R., Zhang, X., 2013: Detection and attribution of climate change: From global to regional. In *Climate Change 2013: The Physical Science Basis. Contribution of Working Group I to the Fifth Assessment Report of the Intergovernmental Panel on Climate Change*. T.F. Stocker, D. Qin, G.-K. Plattner, M. Tignor, S.K. Allen, J. Doschung, A. Nauels, Y. Xia, V. Bex, and P.M. Midgley, Eds. Cambridge University Press, pp. 867-952

Caesar, L., Rahmstorf, S., Robinson, A., Feulner, G., Saba, V., 2018. Observed fingerprint of a weakening Atlantic Ocean overturning circulation. *Nature* 556, 191-196.

Clark, P.U., Shakun, J.D., Marcott, S.A., Mix, A.C., Eby, M., Kulp, S., Levermann, A., Milne, G.A., Pfister, P.L., Santer, B.D., Schrag, D.P., Solomon, S., Stocker, T.F., Strauss, B.H., Weaver, A.J., Winkelmann, R., Archer, D., Bard, E., Goldner, A., Lambeck, K., Pierrrehumbert, R.T., Plattner, G., 2016. Consequences of twenty-first-century policy for multi-millenial climate and sea-level change. *Nature Climate Change* 6, 360-369

Cohen, J., Screen, J.A., Furtado, J.C., Barlow, M., Whittleston, D., Coumou, D., Francis, J., Dethloff, K., Entekhabi, D., Overland, J., Jones, J., 2014. Recent Arctic amplification and extreme mid-latitude weather. *Nature Geoscience* 7, 627-637

Diaz, H.F., Trigo, R., Hughes, M.K., Mann, M.E., Xoplaki, E., Barriobedro, D., 2011. Spatial and temporal characteristics of climat in medieval times revisited. *Bulletin of the American Meteorological Society* 92, 1487-1500

Evans, M.N., Kaplan, A., Cane, M.A., 2002. Pacific se asurface temperature field reconstruction from coral $\delta^{18}O$ data using reduced space objective analysis. *Paleoceanography* 17, dx.doi.org://10.1029/2000PA000590

Evans, M.N., Kaplan, A., Cane, M.A., Villalba, R., 2001. Globality and optimality in climate field reconstructions from proxy data. In Markgraf, V., (ed). *Interhemispheric Climate Linkages*. New York: Cambridge University Press.

Fritts, H.C., Blasing, T.J., Hayden, B.P., Kutzbach, J.E., 1971. Multivariate techniques for specifying tree-growth and climate relationships and for reconstructing anomalies in paleoclimate. *Journal of Applied Meteorology* 10, 845-864

Grömping, U., 2007. Estimators of relative importance in linear regression based on variance decomposition. *The American Statistician* 61, 139-147.

Hakim, G.J., Emile-Geay, J., Steig, E.J., Noone, D., Anderson, D.M., Tardif, R., Steiger, N., Perkins, W.A., 2016. The last millennium climate reanalysis project: framework and first results. *Journal of Geophysical Research: Atmospheres* 121, 6745-6764

Hansen, J., Ruedy, R., Sato, M., Lo, K., 2010. Global surface temperature change. *Reviews of Geophysics* 48. Dx.doi.org:// 10.1029/2010RG000345

Helama, S., Meriläinen, J., Tuomenvirta, H., 2009. Multicentennial megadrought in northern Europe coincided with a global El Niño-Southern Oscillation drought pattern during the Medieval Climate Anomaly. *Geology* 37, 175-178.

Indermühle, A., Stocker, T.F., Joos, F., Fischer, H., Smith, H.J., Wahlen, M., Deck, B., Mastroianni, D., Tschumi, J., Blunier, T., Meyer, R., Stauffer, B., 1999. Holocene

carbon-cycle dynamics based on CO_2 trapped in ice at Taylor Dome, Antarctica. *Nature* 298, 121-126

Jiang, H., Eiriksson, J., Schulz, M., Knudsen, K.-L., Seidenkrantz, M.-S., 2005. Evidence for solar forcing of sea-surface temperature on the North Icelandic Shelf during the late Holocene. *Geology* 33, 73-76.

Jones, P.D., Lister, D.H., Osborn, T.J., Harpham, C., Salmon, M., Morice, C.P., 2012. Hemispheric and large-scale land-surface air temperature variations: An extensive revision and update to 2010. *Journal of Geophysical Research: Atmopsheres* 117. dx.doi.org://10.1029/2011JD017139

Kaufman, D.S., Schneider, D.P., McKay, N.P., Ammann, C.M., Bradley, R.S., Briffa, K.R., Miller, G.F., Otto-Bleisner, B.L., Overpeck, J.T., Vinther, B.M., Arctic Lakes 2k Project Members, 2009. Recent warming reverses long-term Arctic cooling. *Science* 325, 1236-1239

Kopp, R.E., Kemp, A.C., Bittermann, K., Horton, B.P., Donnelly, J.P., Roland Gehrels, W., Hay, C.C., Mitrovica, J.X., Morrow, E.D., Rahmstorf, S., 2016. Temperature-driven global sea-level variability in the Common Era. *Proceedings of the National Academy of Sciences* 113. dx.doi.org://10.1073/pnas.1517056113

Larsen, D.J., Miller, G.H., Geirsdóttir, Á, 2011. A 3000-year varved record of glacier activity and climate change from the proglacial lake Hvítárvatn, Iceland. *Quaternary Science Reviews* 30, 2715-2731.

Larsen, N.K., Kjær, K.H., Olsen, J., Funder, S., Kjeldsen, K.K., Nørgaard-Pedersen, N., 2011. Restricted impact of Holocene climate variations on the southern Greenland Ice Sheet. *Quaternary Science Reviews* 3171-3180

Lindeman, R.H., Merenda, P.F., Gold, R.Z., 1980. *Introduction to Bivariate and Multivariate Analysis.* Glenview IL: Scott, Foresman and Company.

Ljungqvist, F.C., 2010. A new reconstruction of temperature variability in the extra-tropical northern hemisphere during the last two millenia. *Geografiska Annaler* 92, 339-351.

Mann, M.E., Bradley, R.S., Hughes, M.K., 1998. Global-scale temperature patterns and climate forcing over the past six centuries. *Nature* 392, 779-787

Mann, M.E., Zhang, Z., Rutherford, S., Bradley, R.S., Hughes, M.K., Shindell, D., Ammann, C., Faluvegi, G., Ni, F., 2009. Global signatures and dynamical origins of the Little Ice Age and Medieval Climate Anomaly. *Science* 326, 1256-1260

Mann, M.E., Zhang, Z., Hughes, M.K., Bradley, R.S., Miller, S.K., Rutherford, S., Ni, F., 2008. Proxy-based reconstructions of hemispheric and global surface temperature variations over the past two millenia. *Proceedings of the National Academy of Sciences* 105, 13252-13257.

Marcott, S.A., Shakun, J.D., Clark, P.U., Mix, A.C., 2013. A reconstruction of regional and global temperature for the past 11,300 years. *Science* 339, 1198-1201

McKay, N.P., Kaufman, D.S., 2014. An extended Arctic proxy temperature database for the past 2,000 years. *Nature Scientific Data* 1, https://doi.org/10.1038/sdata.2014.26

Morice, C.P., Kennedy, J.J., Rayner, N.A., Jones, P.D., 2012. Quantifying uncertainties in global and regional temperature change using an ensemble of observational estimates: The HadCRUT4 data set. *Journal of Geophysical Research: Atmospheres* 117, dx.doi.org://10.1029/2011JD017187

Ogi, M., Barber, D.G., Rysgaard, S., 2016. The relationship between summer sea ice extent in Hudson Bay and the Arctic Ocean via the atmospheric circulation. *Atmospheric Science Letters* 17, 603-609.

Overland, J.E., Wang, M., Walsh, J.E., Stroeve, J.C., 2013. Future Arctic climate changes: Adaptation and mitigation time scales. *Earth's Future* 2, 68-74.

PAGES 2k Consortium, 2017. A global multiproxy database for temperature reconstructions of the Common Era. *Nature Scientific Data* 4, https://doi.org/10.1038/sdata.2017.88

Perkins, W.A., and Hakim, G.J., 2017. Reconstructing paleoclimate fields using online data assimilation with a linear inverse model. *Climate of the Past* 13, 421-436.
Pisias, N.G., 1978. Paleoceanography of the Santa Barbara Basin during the last 8000 years. *Quaternary Research* 10, 366-384

Praetorious, S.K., Mix, A.C., Jensen, B.J.L., Froese, D.G., Milne, G., Wolhowe, M.D., Addison, J., Prahl, F., 2016. Interaction between climate, volcanism, and isostatic rebound in Southeast Alaska during the last deglaciation. *Earth and Planetary Science Letters* 452, 79-89.

Rigor, I.G., Wallace, J.M., Colony, R.L., 2002. Response of sea ice to the Arctic Oscillation. *Journal of Climate* 15, 2648-2663

Serreze, M.C., and Barry, R.G., 2011. Processes and impacts of Arctic amplification: A research synthesis. *Global and Planetary Change* 77, 85-96

Solomina, O.N., Bradley, R.S., Hodgson, D.A., Ivy-Ochs, S., Jomelli, V., Mackintosh, A.N., Nesje, A., Owen, L.A., Wanner, H., Wiles, G.C., Young, N.E., 2015. Holocene glacier fluctuations. *Quaternary Science Reviews* 111, 9-34.

Stenchikov, G., Robock, A., Ramaswamy, V., Schwarzkopf, M.D., Hamilton, K., Ramachandran, S., 2002. Arctic Oscillation response to the 1991 Mount Pinatubo eruption: Effects of volcanic aerosols and ozone depletion. *Journal of Geophysical Research* 107, dx.doi.org://10.1029/2002JD002090

Vose, R.S., Arndt, D., Banzon, V.F., Easterling, D.R., Gleason, B., Huang, B., Kearns, E., Lawrimore, J.H., Menne, M.J., Peterson, T.C., Reynolds, R.W., Smith, T.M., Williams, C.N., Wuertz, D.B., 2012. NOAA's merged land-ocean surface temperature analysis. 2012. *Bulletin of the American Metorological Society* 93, 1677-1685

Wang T., Surge, D., Mithen., S., 2012. Seasonal temperature variability oft he Neoglacial (3300-2500 B.P.), and Roman Warm Period (2500-1600 B.P.) reconstructed from oxygen isotope ratios of limpet shells (*Patella vulgata*), Northwest Scotland. *Palaeogeography, Palaeoclimatology, Palaeoecology* 317-318, 104-113.

Waters, C.N., Zalasiewicz, J., Summerhayes, C., Barnosky, A.D., Poirier, C., Gałuszka, A., 2016. The Anthropocene is functionally and stratigraphically distinct from the Holocene. *Science* 351, dx.doi.org:// 10.1126/science.aad2622

Wunderlich, F., Mitchell, D.M., 2017. Revisiting the observed surface climate response to volcanic eruptions. *Atmospheric Chemistry and Physics* 17, 485-499.

Chapter 4

Late Holocene Glacier and Ice-Sheet Variability in South Greenland

Sinclair, G.[1], Carlson, A.E. [1], Rood, D.H. [2], Reyes, A. [3], Axford, Y.[4], Wilcken, K. [5], Walczak, M. [1]

[1]College of Earth, Ocean, and Atmospheric Sciences, Oregon State University
[2]Department of Earth Science and Engineering, Royal School of Mines, Imperial College London
[3]Department of Earth and Atmospheric Sciences, University of Alberta
[4]Department of Earth and Planetary Sciences, Northwestern University
[5]Australian Nuclear Science and Technology Organization

To be submitted to *Journal of Quaternary Sciences*

4.1 Abstract

The late Holocene is a period characterized by several centennial-scale climate fluctuations superimposed on gradual Northern Hemisphere cooling, and is therefore an ideal time period to test sensitivity of glaciers and ice caps to climate change at timescales relevant to human society. Here, we present 51 ^{10}Be cosmogenic surface exposure ages from southernmost Greenland, targeting late Holocene moraines distal to the most recent drift limit in a variety of glaciological environments. We find that most glaciers retreated from their late-Holocene maxima between 1.0 and 0.4 ka, similar to that suggested from other late Holocene surface exposure ages from western Greenland and overlapping with the timing of ice advance recorded by threshold lakes in Greenland. This may indicate that the late-Holocene advance of ice into lake catchments in the last millennium was its most extensive since the deglaciation. A small retreat from this maximum may have been triggered by a brief warming event 1.0-0.4 ka in south Greenland observed in a nearby lake record. Glaciers draining the Julianhåb Ice Cap do not show this pattern, possibly because this ice cap is less sensitive to climate at centennial to multi-centennial timescales.

4.2 Introduction

The global cryosphere has undergone significant change over the past twenty years, with near global retreat of glaciers and ice sheets (Zwally et al., 2011; Shepherd et al., 2012; Vaughan et al., 2013; Bamber et al., 2018) likely in response to anthropogenic climate warming (Church et al., 2013; Marzeion et al., 2014; Roe et al., 2017). Understanding the future retreat of Earth's terrestrial cryosphere is critical for society to plan for future sea-level rise, but this requires a thorough understanding of the range of its past natural variability and sensitivity to climate forcing. The Arctic is a region of particular concern due to its well-documented amplification of climate change (Overland et al., 2013; Serreze and Barry, 2011; Cohen et al., 2014), and Greenland specifically is important due to its large potential contribution to sea level rise and its recent acceleration of mass loss (e.g. Zwally et al., 2011; Khan et al., 2015).

Cosmogenic surface exposure dating has significantly improved our understanding of the history of the Greenland Ice Sheet and its associated ice caps and mountain glaciers (e.g. Håkansson et al., 2011; Young et al., 2011, 2013b; Larsen et al., 2013; Corbett et al., 2015; Nelson et al., 2014; Schaeffer et al., 2016; Bierman et al., 2016; Sinclair et al., 2016). Surface exposure studies on Greenland have largely focused on its retreat and thinning history from the Last Glacial Maximum (LGM, ~26-19 ka, Clark et al., 2009) to the early Holocene (e.g. Sinclair et al., 2016; Håkansson et al., 2007; Möller et al., 2010; Young et al., 2013b; Levy et al., 2012), ice sheet erosivity and bed temperature (Corbett et al., 2015; Nelson et al., 2014), or ice sheet stability at orbital to tectonic timescales (Schaeffer et al., 2016; Bierman et al., 2016). However, recent advances have permitted increasingly precise dating of centennial-scale glacial variability in the late Holocene (e.g Granger et al, 2013; Balco 2011), in some cases allowing resolution of separate advances to within the last 500 years (Schimmelpfennig et al., 2014). This opens new opportunities for better reconstructing Greenland's glacier variability at shorter and to evaluate responses of the ice system to recent forcings.

The late Holocene (between 4 ka and the present) in Greenland is characterized by a series of centennial-scale climate fluctuations superimposed on a period of gradual cooling (e.g. Perner et al., 2011; D'Andrea et al., 2011; Lasher and Axford, 2019; Sinclair et al., in prep). These climate fluctuations are less pronounced than either the deglacial or recent anthropogenic warming, but occur on centennial timescales relevant to human society. Understanding the background climate and glacial variability will facilitate more accurate comparisons with current retreat rates and provide an important context for assessing the role of natural variability, helping to isolate an anthropogenic signal and determine to what extent the current behavior of the Greenland terrestrial cryosphere is unprecedented.

Southernmost Greenland presents an ideal location to investigate these questions. A number of glaciers of different sizes occur in a region small enough to experience spatially uniform climate change. Both marine- and land-terminating outlet glaciers occur, draining a piedmont-like extension of the south Greenland Ice Sheet (the Qassimiut lobe), the main south Greenland Ice Sheet (sGrIS), and the Julianhåb Ice Cap,

which itself is surrounded by smaller land- and marine-terminating glaciers and ice caps, especially near Kap Farvel.

Existing information about south Greenland's Neoglaciation suggests a complex and variable history. Earlier advances of some glaciers may have been at least as extensive as the most recent, likely Little Ice Age (LIA, ~0.5-0.2 ka) advance, if not more so (e.g. Bennike and Sparrenbom, 2007; Winsor et al. 2014). Weidick (1959, 1975) mapped an extensive series of moraines in front of this most recent, likely LIA, drift limit. He named these the "Narsarsuaq Stade" moraines and proposed they represented a regional advance of the south Greenland Ice Sheet that was more extensive than its LIA extent. Winsor et al. (2014) and Bennike and Sparrenbom (2007) dated a moraine near Narsarsuaq suggesting retreat from this maximum at ~1.5-1.2 ka. However, recent data from a series of threshold lakes near the Qassimiut Lobe suggest a later advance around 0.5 ka (Larsen et al., 2011; 2015), suggesting the maximum advance may have been during the LIA. Here we date Weidick's "Narsarsuaq Stade" moraines with cosmogenic ^{10}Be to test if they mark a synchronous advance of the south Greenland Ice Sheet that was more extensive than its most recent LIA advance.

4.3 Methods

We sampled boulders for ^{10}Be dating from six sites in southernmost Greenland (Figure 4.1). Each site has the following characteristics. (1) There is a clear modern drift limit, usually fronted by a moraine. This feature is characterized by bare rock and diamict and does not have clear soil development. Where we are able to directly observe this youngest drift, there is evidence of active melting of ice-cored moraines resulting in mass movement. (2) There is at least one moraine within 2-5 km of the modern limit. These outer moraines have some soil development, significant lichen growth, and moraine boulders are characterized by visible small erosional features such as polish and striations. Distal to these moraines, the landscape has more fully developed soils and vegetation with occasional large moraines, and no evidence of small-scale erosional features.

We sampled boulders from five locations where the outer moraines occur within 3 km of the youngest drift limit (Figure 4.2): two moraines from a marine-terminating glacier draining the Qassimiut Lobe; two sites with land-terminating glaciers draining the Julianhåb Ice Cap; and two moraines fronting glaciers and ice caps in southernmost Greenland near Kap Farvel (Figure 4.1). At one site near the Nuuk ice margin, there are no prominent moraines immediately distal to the youngest drift limit, so we sampled boulders on bedrock within 200 m of the modern limit.

We sampled the top 2-8 cm of 5-10 boulders from the crest of each moraine. We processed all samples at Oregon State University (OSU) using the standard chemical procedures outlined in Licciardi (2000) and Marcott (2011). $^{10}Be/^{9}Be$ ratios were measured using the Sirius 10 MeV Pelletron Accelerator at the Centre for Accelerator Science at the Australian Nuclear Science and Technology Organization in December, 2018, using the KNSTD07 standard.

We calculate ages with the CRONUS online exposure age calculator, version 3 (hess.ess.washington.edu), using the Arctic production rate (Young et al., 2013a) and the Lal/Stone time-varying scaling scheme. Using another scaling scheme or the Northeast North American production rate (Balco et al., 2011) changes the calculated ages up to 3%. We make no correction for post-depositional erosion of the samples. All moraines dating to the last 4 kyr have boulders with small-scale glacial erosional features such as polish, striations, and chattermarks, indicating negligible post-depositional erosion or weathering. Shielding is calculated from topographical measurements in the field using an inclinometer, and a Brunton compass is used for strike-and-dip measurements. We use the standard density of quartz (2.6 g/cm^3) for all samples, and measured average thickness across the sample.

We use two methods for identifying statistical outliers when calculating landform ages. First we apply Chauvenet's criterion that tests for statistical outliers by comparing each boulder age to the mean and standard deviation of the landform dataset, and removes the age if it exceeds a prescribed number of standard deviations from the mean (e.g. Balco et al., 2011; Sinclair et al., 2016). We also use a more stringent test that only uses those ages which overlap at one standard deviation and form a clear peak in the PDF

of the ages (Figures C.10-C.21), similar to the approach recently employed for Neoglacial landforms on Baffin and Disko Islands (Young et al., 2016). The differences in the mean ages of landforms using these two outlier techniques are within several centuries, but the sizes of error bars are significantly larger using the Chauvenet's only dataset (Appendix C.4). Here we present the datasets using the more stringent test for outliers.

4.4 Results

Table 1 outlines the glacier characteristics and moraine ages for the six sites we sampled in southern Greenland, and Table 2 gives individual sample characteristics. Figure 4.3 shows PDFs of all landform ages in this study. A detailed description of the sites and outlier ages is in Appendix C. Where available, we use the glacier names defined in Bjørk et al. (2015).

The Nuuk ice margin and Tupaussat sites have early Holocene ages. The Tupaussat outer moraine is the oldest (11.5±1.0 ka), similar to surrounding deglacial ages (Carlson et al., 2014, Nelson et al., 2014). The Nuuk ice margin boulders have an average age of 8.3±0.3 ka, and are also similar in age to nearby ages (Larsen et al., 2013, Carlson et al., 2014; Levy et al., 2012, However, the outer Tupaussat moraine has an inner neoglacial moraine (discussed below), whereas the Nuuk boulders come from immediately distal to the most recent drift limit, indicating that the advance depositing the latest drift at the Nuuk ice margin site was the most extensive since the early Holocene.

There is no evidence of moraine abandonment between deposition of the Nuuk ice margin boulders at ~8.3 ka and the mid-Holocene. The first possible Neoglacial moraine (i.e., likely deposited following a mid- to late-Holocene advance) for south Greenland is at Jespersen Bræ, where three boulders have an average age of 3.7±0.4 ka.

Five moraines at four sites have ages that are <1.0 ka. The moraine ages at Naajat Sermiat are in stratigraphic order (0.6±0.2 ka for the outer moraine and 0.5±0.2 for the inner moraine). These ages agree within uncertainty with the age of the oldest macrofossil sampled from the silt/gyttja contact at Lower Nuuluusuaq Lake (informal

name, 0.2-0.5 ka at 2 sigma), a threshold lake immediately adjacent to the outer moraine. Naajat Sermiat was a marine-terminating glacier when these moraines were deposited. Another marine-terminating glacier, Paarlit Sermiat, and a land terminating glacier at Tupaussat have similar ages (0.7±0.1 ka and 0.8±0.2 ka, respectively). Ages on boulders from the Sermeq Kangilleq moraine indicate retreat from a late-Holocene maximum after 0.4±0.1 ka.

4.5 Discussion

4.5.1 Are Greenland's Neoglacial fluctuations synchronous?

Seventeen Neoglacial moraines at eleven sites from Greenland have previously been dated using cosmogenic dating (Winsor et al., 2014, Jomelli et al., 2016, Young et al., 2015, Reusche et al., 2018). Additional information on Holocene ice-sheet variability comes from threshold lakes that record a rapid change in sediment lithology, usually from organic-rich gyttja to glacial silt and clay, when ice advances over a topographic threshold into the lake catchment (Belascio et al., 2015; Briner et al., 2010; Kelley et al., 2012; Larsen et al., 2011; Larsen et al., 2015; Larsen et al., 2016; Levy et al., 2014; Lowell et al., 2013; Young et al., 2011), although determining the extent of these advances beyond the topographic threshold is generally not possible. We combine existing ^{10}Be dates and threshold lake data with our new ^{10}Be dates to further constrain Holocene glacier and GrIS variability from west and south Greenland. There is much less comparable information from east Greenland, with four threshold lake records (Lowell et al, 2013; Levy et al., 2014; Larsen et al., 2015) and two Neoglacial moraines dated with a single cosmogenic age each (Lowell et al., 2013; Levy et al., 2014).

Ages on the moraine we dated immediately distal to Neoglacial moraines at Tupaussat in southernmost Greenland (11.5±1.0 ka) and boulders on bedrock distal to the most recent drift limit near Nuuk in southeastern Greenland (8.3 ± 0.3 ka) are similar to nearby ^{10}Be ages, indicating deglaciation within ~5 km of the modern ice margin by 11.2 ± 0.4 ka in southern Greenland (Carlson et al., 2014; Nelson et al., 2014) and between

10.2 ± 0.1 and 6.9 ± 0.3 ka in southeastern Greenland (Larsen et al., 2013, Carlson et al., 2014; Levy et al., 2012).

Ice-sheet modeling and sea-level investigations indicate that Neoglacial ice advance both in Greenland and elsewhere in the Northern Hemisphere began around 5-4 ka (Solomina et al., 2015; Lecavalier et al 2014; Simpson et al., 2009). Four out of 15 threshold lakes with Neoglacial records suggest ice advance into the lake catchments between 4 and 2 ka (Figure 4.5). These advances are usually relatively short-lived, with all but one of the cores indicating ice retreat from the lake catchment within 1500 years. Only one landform dated with ^{10}Be (Jespersen Bræ) indicates ice retreat from a late-Holocene maximum during this period. Our ages for the moraine at Jespersen Bræ (3.7 ± 0.4) therefore indicate that this glacier reached its late Holocene maximum extent anomalously early when compared with other late-Holocene glacial advances in Greenland. Glacier advances during the earliest part of the Neoglaciation were therefore rarely associated with the post-deglacial maxima in south Greenland.

By contrast, the Common Era (2 ka-present) is a period of widespread glacier and ice-sheet advances throughout west and south Greenland. The Narsarsuaq moraine in south Greenland and the Uigordleq moraine in west Greenland have retreat ages between 2 and 1 ka. Threshold lake records suggest widespread and persistent advances within the last millennium; 13 out of 19 threshold lakes show ice advance into the lake catchment during the last millennium, with glacial sediments persisting in cores until the core-tops. Cosmogenic ages on moraines, however, indicate that retreat from late-Holocene maxima occurred primarily during the first half of the last millennium, overlapping in time with advances recorded by threshold lakes. This likely indicates that the initial ice advance during the last millennium was the largest advance to deposit the moraines. The fact that in most threshold lakes glacial silt persists to the top of the cores then suggests that retreat from this initial advance was limited, so ice remained in lake catchments until at least the late 20th Century. With the exceptions of Jespersen Bræ, where retreat from the late-Holocene maximum occurred at ~0.4 ka, and Humboldt and Petermann glaciers in northwest Greenland, where retreat occurred at ~0.3 ka (Reusche et al., 2018), the cosmogenic ages suggest that glaciers in south and west Greenland began to retreat from

their maximum extent before 0.5 ka. Subsequent advances in each of these glacier systems did not exceed this advance.

There is unavoidable bias in our site selection whereby we only targeted those sites which are reasonably accessible in a field season and have clear evidence from satellite imagery of an advance more extensive than the most recent drift deposits. However, our ages overlap with independently sampled moraines in west Greenland (Jomelli et al., 2016; Young et al., 2015), and a survey of satellite imagery from south Greenland suggests that these moraines may be widespread. In addition to those moraines dated here, we have identified an additional 24 moraines or trimlines between Kap Farvel and Narsarsuaq. These are between 0.5 and 2 km in front of the modern glacier limits, and are clearly distal to or partially overridden by the most recent drift.

4.5.2 Cryosphere response to climate forcing in south Greenland

The majority of glacier systems investigated here and in previous studies began retreating from their late Holocene maximum extents in the first half of the second millennium, and threshold lake records suggest that this retreat likely followed a second millennium advance. Local and regional climate records indicate that the period between ~1,000 and 300 B.P. likely contained the coldest period of the Common Era, although the timing of this cold period varies between records (Figure 4.5). Sinclair et al.'s (in prep) Greenland temperature estimate suggests the coldest period of the Common Era occurred between 400 and 300 B.P., but shows episodic cooling throughout the record, superimposed on a gradual 1,000 year cooling trend in the second millennium. A similar second millennium cooling trend is observed in a west Greenland marine record (Perner et al., 2011) and in a chironomid-based lake temperature record (Axford et al., 2013), although the latter has a less dramatic cooling before ~300 B.P.

However, a west Greenland alkenone-derived temperature record does not show this cooling during the last millennium, with brief cooling events at ~0.8 and 0.25 ka (D'Andrea et al., 2004). A temperature record derived from chironomid $\delta^{18}O$ (Lasher and Axford, 2019) is the closest record to the sites presented here, and the only temperature proxy record south of Kangerlussuaq; it may therefore best approximate regional

temperature at the south Greenland sites. This record shows a cold event between approximately 1.0 and 0.1 ka, interrupted by warming between 1.0 and 0.4 ka. This warming event overlaps within uncertainty with the ages of five moraines at four sites presented here (Naajat Sermiat, Sermeq Kangilleq, Tupaussat, and Paarlit Sermiat), as well as Lyngmarksbreen's distal moraine on Disko Island (Jomelli et al., 2016). These ages do not show any similarity to a record of precipitation based on biogenic silica from southernmost Greenland (Andresen et al., 2004), suggesting that temperature is a more important driver of glaciers in this region than precipitation.

The Jespersen Bræ and the Narsarsuaq moraines from south Greenland (Winsor et al., 2014) have cosmogenic exposure ages older than the 1.0-0.4 ka warming event observed by Lasher and Axford (2019). A third moraine at Sermeq Kangilleq indicates retreat from its Neoglacial maximum after the end of this event, when the $\delta^{18}O$ indicates regional cooling. These three glaciers drain the Julianhåb Ice Cap, and therefore may behave differently than the three glacier systems which more closely overlap with the warmer period in the $\delta^{18}O$ record (Lasher and Axford 2019). Paarlit Sermiat is a marine-terminating outlet of a small unnamed ice cap, and the Tupaussat moraine was deposited by an unnamed glacier. Smaller glaciers generally have shorter response times than larger ice caps like the Julianhåb Ice Cap. Finally, Naajat Sermiat drains the Qassimiut Lobe of the South Greenland Ice Sheet. The Qassimiut Lobe is a low-altitude piedmont-like extension of the Greenland Ice Sheet, so an increase in equilibrium line altitude will lead to a relatively large expansion of the ablation zone when compared to a glacier or ice cap with a greater surface slope. These factors may make these glaciers more sensitive to centennial-scale climate fluctuations than those draining the main ice sheet or the Julianhåb Ice Cap. This pattern is similar to what we observe in western Greenland: two glaciers draining small ice caps have age ranges for their distal moraines overlapping with our ages for the smaller and more climate sensitive glaciers (Young et al., 2015, Jomelli et al., 2016), while a glacier draining the ice sheet retreated from its Neoglacial maximum slightly later, closer to 0.3 ka (Reusche et al., 2018).

On the other hand, we can not rule out the possibility that some of the centennial-to millennial-scale variability identified here originates from inter-annual variability in an

autocorrelated process instead of a regionally-coherent retreat forced by climate trends (e.g. Roe et al., 2009). This effect has been investigated at Mt. Baker in Washington State, USA, where Roe and O'Neal (2009) find that all the observed "Little Ice Age" fluctuations of glaciers can be explained by natural variability of glaciers with memory operating in a stochastic climate. Reichert et al. (2002) find similar results at Nigardsbreen in Norway and Rhonegletscher in the Swiss Alps. If these glaciers do respond to climate, the expression of smaller climate events in the moraine record can be obscured by the stochastic behavior of the system. Especially if the size of the events and glacier responses are similar over time, the chances of any one event depositing the Neoglacial maximum moraine may be significantly decreased, leading to variability in the system (Gibbons et al., 1984). This stochastic behavior may account for some of the variability we observe in the threshold lake and cosmogenic records, but it is also possible that the relative sensitivity to climate fluctuations may drive the different behaviors of glaciers we observe here.

Combining climate and threshold-lake records and our new ^{10}Be ages, we develop a conceptual model of climate and cryosphere fluctuations in the latest Holocene in south Greenland (Figure 4.6). The ice sheet and surrounding glaciers advanced during the late Holocene in response to millennial-scale cooling (Figure 4.6b). A localized warming event in south Greenland (Lasher and Axford 2019) triggered a limited retreat between 1 and 0.5 ka, with abandonment of the moraines sampled here (Figure 4.6c). However, persistence of glacial sedimentation in threshold lakes suggests that the retreat was limited in extent and to smaller and more climate-sensitive glaciers. A more recent retreat was more widespread (Figure 4.6d), as recorded by the very young drift deposit fronting all glaciers and by the observations of widespread 20th-21st Century retreat of the Greenland Ice Sheet (e.g. Gardner et al., 2013; Bjørk et al., 2018). We note that this conceptual model is based only on six moraines systems and a single climate record, so more work should be done to further investigate this hypothesis.

4.6 Conclusions

The ^{10}Be cosmogenic ages presented here represent the first effort to build a detailed record of Neoglacial variability of Greenland glaciers and the SGrIS using ^{10}Be dating. The results indicate advance of the Greenland Ice Sheet and surrounding glaciers and ice caps during the late Holocene, with most glaciers reaching their maxima before or during the last millennium, followed by centennial-scale glacial variability during overall retreat. Smaller glaciers and ice caps in south Greenland may respond to multi-centennial climate fluctuations, especially a possible warming event in the first half of the last millennium, but glaciers draining the larger and higher altitude Julianhåb Ice Cap may not respond to climate variability at these shorter timescales.

4.7 Acknowledgements

This project was funded by a National Science Foundation Graduate Research Fellowship grant to G. Sinclair, a National Science Foundation Division of Spatial Sciences Doctoral Dissertation Research Improvement Grant to G. Sinclair and A. Carlson (award number: 1557541), and two Geological Society of America Research Grants to G. Sinclair. Invaluable field assistance was provided by Brendan Reilly, Jamie McFarlin, G. Everett Lasher, and Aaron Hartz. Logistical support and transportation in Greenland was provided by Jacky Simoud, Air Greenland, Carl Olsen, and Polar Field Services. We thank the people and Government of Greenland (Scientific Expedition Numbers VU-0076 and VU-00104 and Export License Numbers 046/2014 and 046/2016). Alder Cromwell, Fritz Freudenberger, Alisa Kotash, Aaron Barth, Dave Ullman, and David Leydet provided invaluable laboratory assistance. Feedback from Peter Clark greatly improved this manuscript.

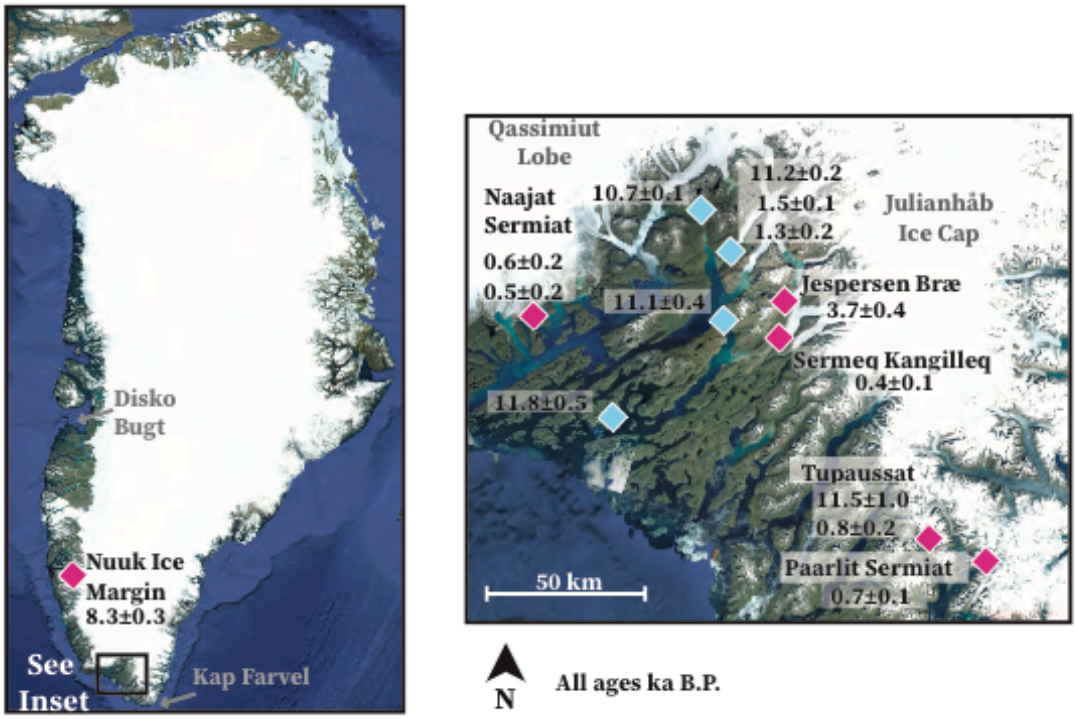

Figure 4.1: Map of sites sampled for this study. Pink diamonds indicate new sites for this study, blue diamonds indicate sites with published data (from Winsor et al., 2014; Winsor et al., 2015; and Nelson et al., 2015). The average age of previously published landforms is noted. Glacier names are derived from Bjørk et al. (2015), where available.

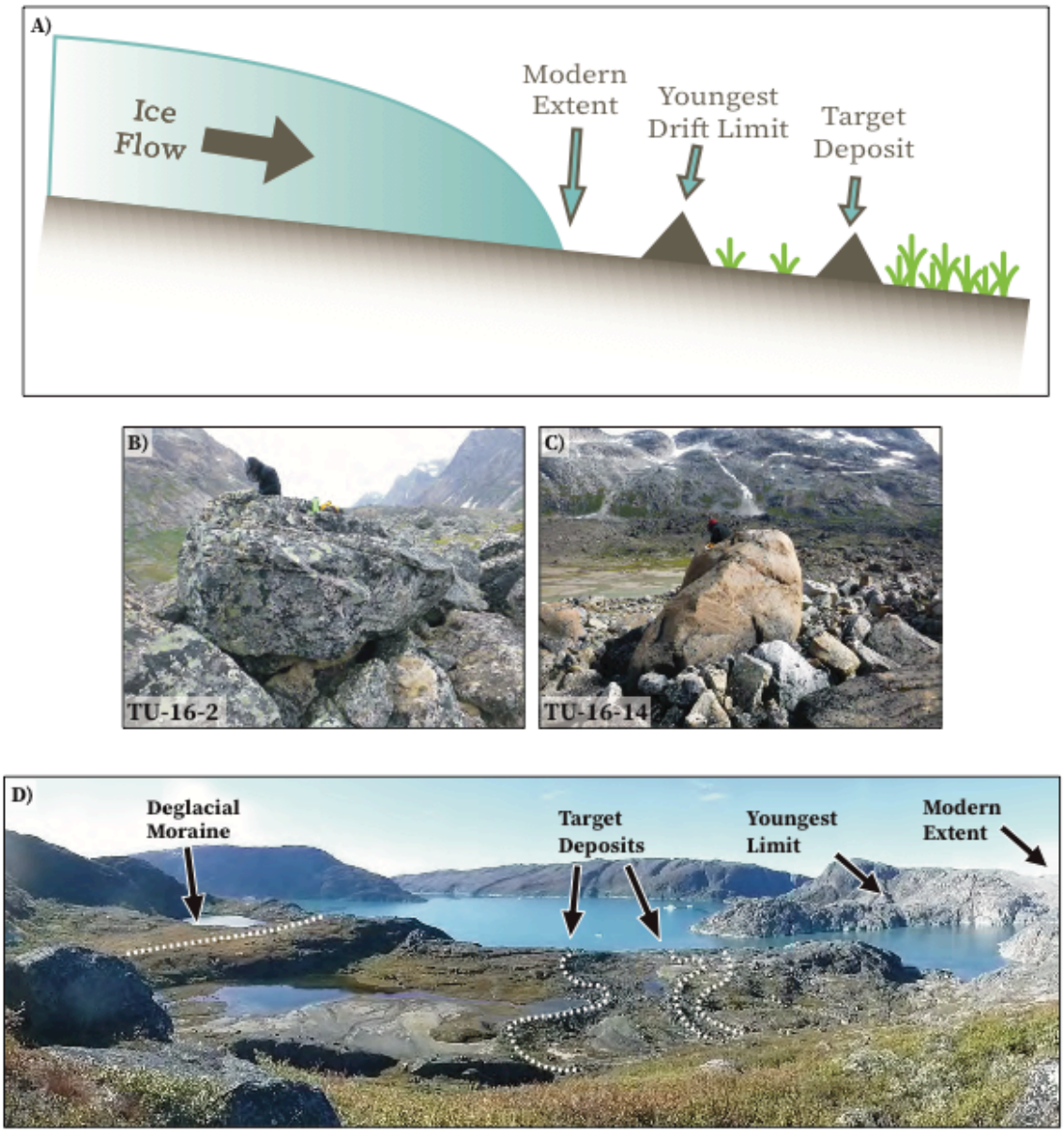

Figure 4.2: (A) Schematic of sampling strategy. We target the first landform outboard of the youngest drift limit. This deposit separates a heavily vegetated landscape from one with fewer plants and more limited soil development. (B) Representative deglacial boulder. (C) Representative boulder from target Neoglacial moraine. (D) Panoramic photograph of Naajat Sermiat moraines, illustrating sampled terrain. Moraines B-D separate oldest terrain from intermediate terrain. Barren rock on far right is most recently deglaciated terrain.

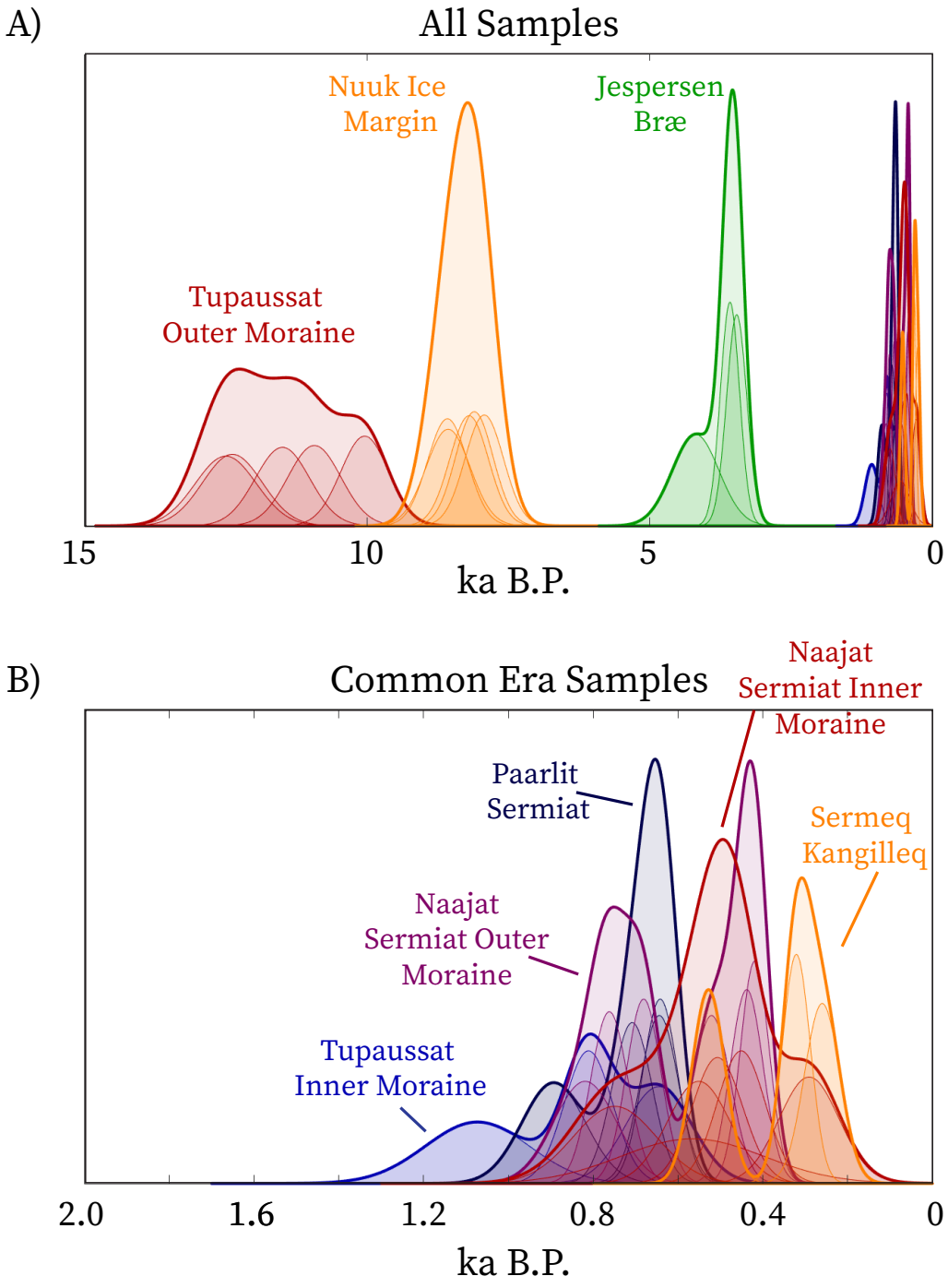

Figure 4.3: PDFs of landforms dated in this study (outliers excluded). Thin lines indicate single samples, thick lines indicate sum of all samples for a moraine or site. (A) All sites. (B) Only sites with samples in the Common Era (2-0 ka).

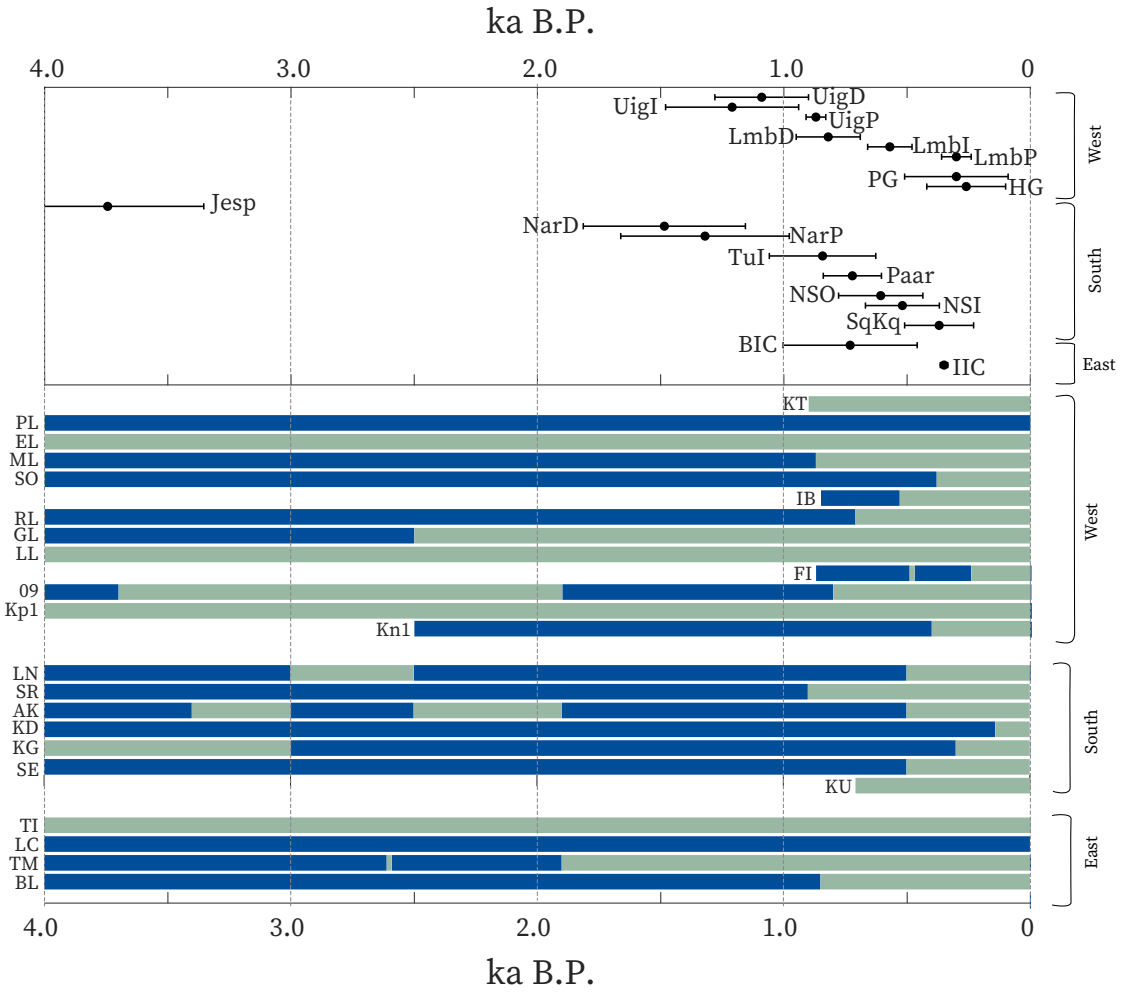

Figure 4.4: Summary of cosmogenic surface exposure ages and threshold lakes from Greenland. Top: average age of landforms dated by surface exposure dating, grouped by region. Bottom: timings of threshold lake records and advance of glacier into lake catchment. Dark blue indicates glaciers are not in the catchments. Light blue indicates glaciers in catchment. See Figure C.22 and table C.6 for locations of records and their references

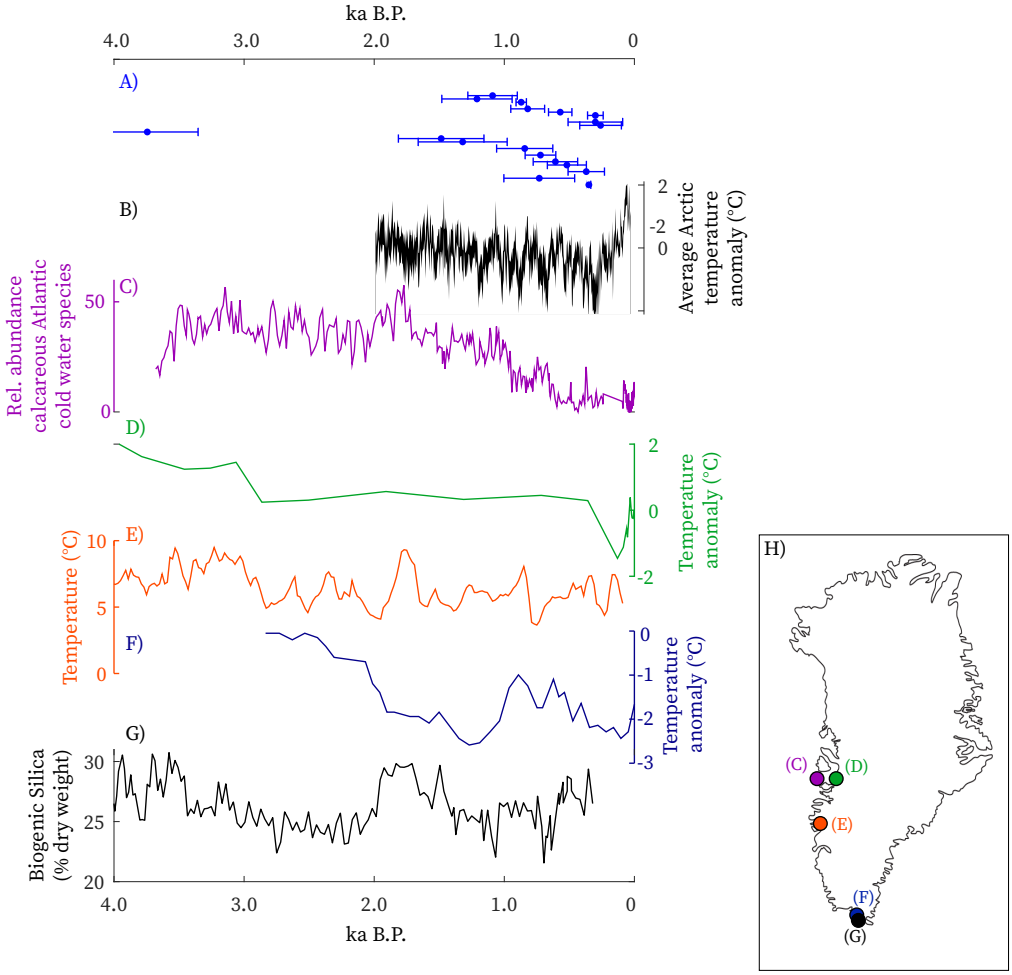

Figure 4.5: Summary of Greenland's late Holocene glacier and climate records. (A) All landforms dated with cosmogenic surface exposure methods during the Neoglacial (this study, Reusche et al., 2017; Winsor et al., 2014; Jomelli et al., 2016; Young et al., 2015; Levy et al., 2014; Lowell et al., 2013). (B) Average Arctic temperature anomaly (referenced to 1850-1900 average) in the Common Era (Sinclair et al., in prep). (C) Relative abundance of calcareous Atlantic cold water foraminifera from a west Greenland ocean core (Perner et al., 2011). (D) Summer temperature calculated from a west Greenland lake record (Axford et al., 2013). (E) Alkenone-derived summer temperatures from southwest Greenland (D'Andrea et al., 2011). (F) (G) Biogenic silica record from southernmost Greenland. Higher percentage of biogenic silica represents more productive conditions (Andresen et al., 2004). (I) Map showing locations of climate records.

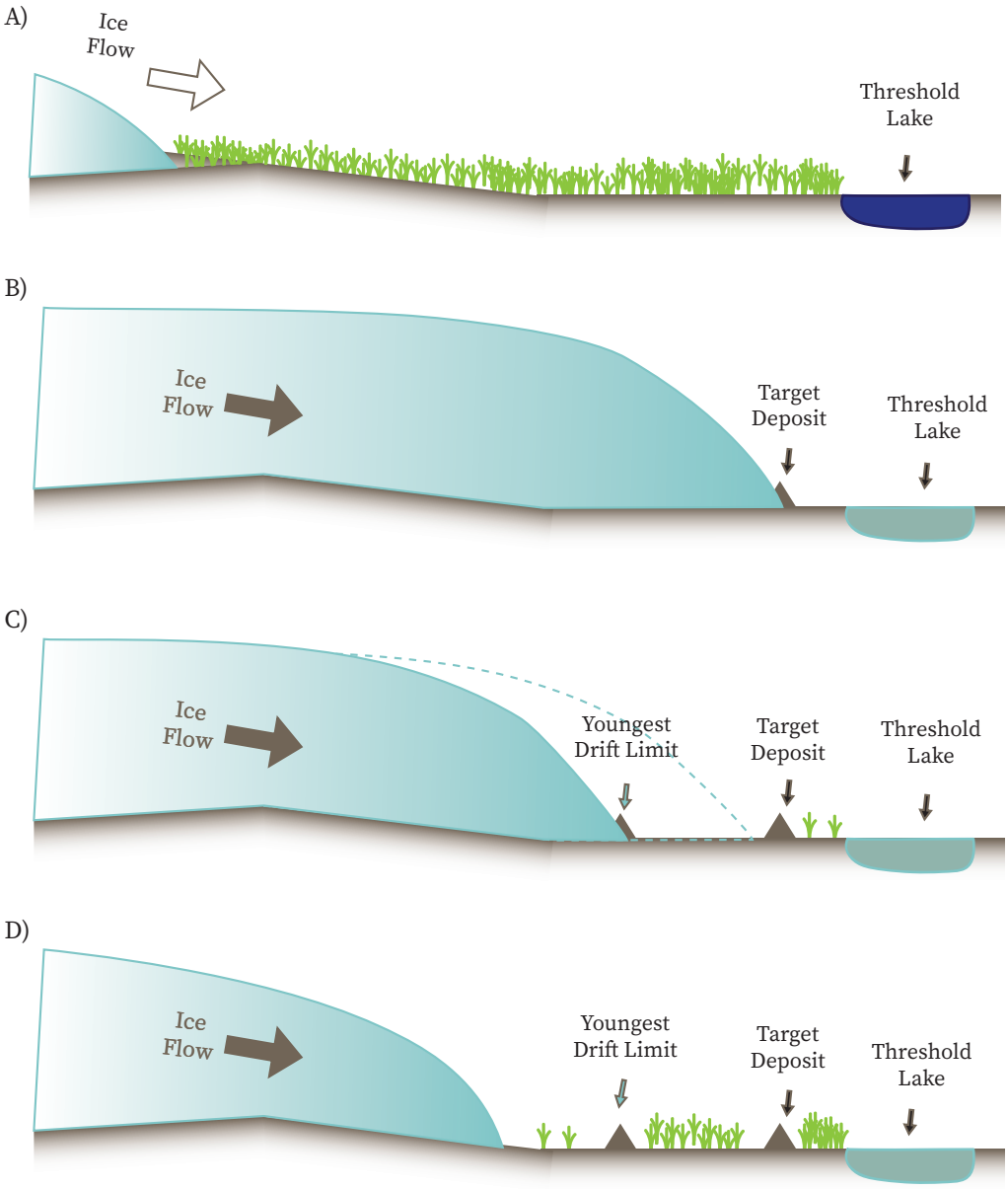

Figure 4.6: Summary of conceptual model. See text for description.

Table 4.1 Site Information

Table 4.1: Site Information				
Site Name (Abbreviation)	**Glacier name**	**Terminus Type**	**Glacier type**	**Landform Age (ka)**
Nuuk Ice Margin (NIM)	Narsap Sermia/unnamed	Land (n=5), marine (n=1)	Outlet of Greenland Ice Sheet	8.3 ± 0.3
Naajat Sermia Outer (NSO)	Naajat Sermiat Outer	Marine	Outlet of Qassimiut Lobe	0.6 ± 0.2
Naajat Sermia Inner (NSI)	Naajat Sermiat Outer	Marine	Outlet of Qassimiut Lobe	0.5 ± 0.2
Jespersen Bræ (Jesp)	Jespersen Bræ	Land	Outlet of Julianhåb Ice Cap	3.7 ± 0.4
Sermeq Kangilleq (SqKq)	Sermeq Kangilleq	Land	Outlet of Julianhåb Ice Cap	0.4 ± 0.1
Tupaussat Outer (TuO)	Mosquito Glacier (inf. name)	Land	Cirque Glacier	11.5 ± 1.0
Tupaussat Inner (TuI)	Mosquito Glacier (inf. name)	Land	Cirque Glacier	0.8 ± 0.2
Paarliit Sermiat (Paar)	Paarliit Sermiat	Marine	Outlet of unnamed ice cap	0.7 ± 0.1

Table 4.2: Sample Information

Sample Name	Latitude (°N)	Longitude (°E)	Elevation (m asl)	Thickness (cm)	Topographic Shielding Factor	^{10}Be Concentration (atoms g^{-1})	^{10}Be Uncertainty (atoms g^{-1})	Sample Age (yrs B.P.)	Internal Error (yrs)	External Error (yrs)
Nuuk ice margin							**Average**	8273 ± 289		
NU-13-1	64.778	-49.514	983	2	0.9756	85608	1383	8102	131	331
NU-13-2	64.778	-49.514	980	3	0.9989	91720	1567	8577	147	353
NU-13-3	64.778	-49.514	980	4	0.9989	86996	1625	8194	153	343
NU-13-4	64.778	-49.514	986	3	0.9989	85252	1793	7926	167	341
NU-13-5	*64.778*	*-49.514*	*980*	*3*	*0.9989*	*99919*	*1861*	*9362*	*175*	*392*
NU-13-18	64.742	-49.583	735	1.5	1.0000	74459	1939	8565	224	391
Naajat Sermiat outer							**Average**	607 ± 171		
NQ-13-12	61.013	-46.525	77	3.5	0.9943	2057	168	438	36	39
NQ-13-15	61.013	-46.525	77	3	0.9943	3933	321	819	67	74
NQ-13-32	61.013	-46.528	67	2	0.9959	3283	158	681	33	41
NQ-13-33	61.013	-46.528	67	2	0.9959	1967	139	419	30	34
NQ-13-36	*61.013*	*-46.528*	*67*	*4*	*0.9959*	*6004*	*202*	*1285*	*43*	*65*
NQ-13-38	61.013	-46.528	62	3	0.9956	3621	161	762	34	44
NQ-13-41	61.014	-46.526	62	2	0.9955	2477	194	521	41	45
Naajat Sermiat inner							**Average**	519 ± 150		
QA-14-1	61.015	-46.525	56	5	0.9620	1251	303	291	70	71
QA-14-5	*61.015*	*-46.525*	*59*	*2.5*	*0.9897*	*10241*	*480*	*2230*	*105*	*134*
QA-14-7	61.015	-46.527	54	4	0.9709	2292	258	507	57	60
QA-14-8	61.014	-46.527	65	5	0.9445	1971	237	451	54	57
QA-14-9	61.015	-46.526	56	1.5	0.9712	3497	440	749	94	98
QA-14-10	*61.015*	*-46.525*	*62*	*6.5*	*0.9779*	*4767*	*538*	*1064*	*120*	*127*
QA-14-11	*61.015*	*-46.525*	*63*	*5*	*0.9799*	*8269*	*642*	*1836*	*143*	*158*
QA-14-12	61.015	-46.525	59	2	0.9671	2612	772	566	167	169
QA-14-13	61.015	-46.527	59	4	0.8782	2273	292	551	71	74
QA-14-14	*61.015*	*-46.526*	*57*	*3*	*0.9927*	*7494*	*717*	*1617*	*155*	*166*
Jespersen Bræ							**Average**	3744 ± 390		
KS-16-3	*61.078*	*-45.027*	*212*	*3*	*0.9515*	*46379*	*2281*	*9269*	*457*	*574*
KS-16-4	*61.078*	*-45.027*	*205*	*2*	*0.9913*	*59808*	*1653*	*11503*	*319*	*536*
KS-16-6	61.076	-45.026	212	3	0.9845	18071	645	3462	124	179
KS-16-8	61.074	-45.025	213	3	0.9180	20196	1838	4189	382	413
KS-16-9	61.074	-45.025	221	3	0.9966	19056	548	3581	103	169
KS-16-10	*61.074*	*-45.025*	*213*	*2.5*	*0.9694*	*40688*	*1414*	*7917*	*276*	*405*
Sermeq Kangilleq							**Average**	370 ± 140		
JB-16-1	*60.916*	*-45.028*	*175*	*2.5*	*0.9615*	*3408*	*427*	*663*	*83*	*87*
JB-16-3	60.917	-45.029	175	2.5	0.9542	2677	173	528	34	39
JB-16-6	60.916	-45.026	169	2.5	0.9858	1624	153	321	30	33
JB-16-9	60.916	-45.024	178	2.5	0.9840	1298	206	260	41	42
Tupaussat outer							**Average**	11486 ± 1026		
TU-16-2	60.381	-44.288	276	3.5	0.9704	62076	1158	11494	215	481
TU-16-3	*60.381*	*-44.288*	*277*	*5*	*0.9638*	*79573*	*1488*	*15010*	*282*	*630*
TU-16-4	60.381	-44.287	289	1.5	0.9727	68923	1400	12379	252	528
TU-16-5	60.381	-44.288	285	4	0.9721	59445	1252	10930	231	470
TU-16-6	60.381	-44.287	284	6	0.9238	63508	1379	12496	272	542
TU-16-8	60.382	-44.286	297	5	0.9694	54760	1023	10041	188	421
Tupaussat inner							**Average**	843 ± 216		
TU-16-11	*60.388*	*-44.274*	*305*	*3*	*0.9283*	*27747*	*764*	*5223*	*144*	*243*
TU-16-13	*60.388*	*-44.274*	*314*	*3*	*0.9530*	*8325*	*739*	*1454*	*129*	*140*
TU-16-14	60.389	-44.273	307	3	0.9549	6121	664	1073	116	123
TU-16-15	60.389	-44.273	307	3	0.9297	3633	417	645	74	78
TU-16-16	*60.389*	*-44.273*	*319*	*4*	*0.9549*	*1539*	*320*	*278*	*58*	*59*
TU-16-17	60.389	-44.273	316	3	0.9548	4727	282	811	48	57
Paarlit Sermiat							**Average**	722 ± 118		
NK-16-1	60.323	-43.932	356	3.5	0.9554	3881	204	642	34	41
NK-16-2	60.323	-43.932	351	3.5	0.9518	3858	229	644	38	45
NK-16-4	*60.322*	*-43.934*	*364*	*3.5*	*0.7296*	*28927*	*711*	*6521*	*161*	*292*
NK-16-5	60.322	-43.933	355	3.5	0.8816	3960	216	708	39	47
NK-16-6	60.323	-43.933	351	3	0.9545	5347	404	893	67	75
NK-16-7	*60.323*	*-43.933*	*359*	*4*	*0.9463*	*8940*	*592*	*1519*	*101*	*116*

Table 4.2 Sample Information

4.8 References

Andresen, C.S., Björck, S., Bennike, O., Bond, G., 2004. Holocene climate changes in southern Greenland: evidence from lake sediments. *Journal of Quaternary Science* 19, 783-795

Axford, Y., Losee, S., Briner, J.P., Francis, D.R., Langdon, P.G., Walker, I.R., 2013. Holocene temperature history at the western Greenland Ice Sheet margin reconstructed from lake sediments. *Quaternary Science Reviews* 59, 87-100.

Bamber J.L., Westaway, R.M., Marzeion, B., Wouters, B., 2018. The land ice contribution to sea level during the satellite era. *Environmental Research Letters*, 13. dx.doi.org:/10.1088/1748-9326/aac2f0

Balco, G., 2011. Contributions and unrealized potential contributions of cosmogenic-nuclide exposure dating to glacier chronology, 1990-2010. *Quaternary Science Reviews* 30, 3-27.

Belascio, N.L., D'Andrea, W.J., Bradley, R.S., 2015. Glacier response to North Atlantic climate variability during the Holocene. *Climate of the Past* 11, 1587-1598

Bennike, O., Sparrrenbom, C.J., 2007. Dating of the Narssarssuaq stade in southern Greenland. *The Holocene* 17, 279-282

Bierman, P.R., Shakun, J.D., Corbett, L.B., Zimmerman, S.R., Rood, D.H., 2016. A persistent and dynamic East Greenland Ice Sheet over the past 7.5 million years. *Nature* 540, 256-260.

Bjørk, A.A., et al., 2015. Brief communication: Getting Greenland's glacier names right—a new data set of all official Greenlandic glacier names. *The Cryosphere* 9, 2215-2218.

Bjørk, A.A., Aagaard, S., Lütt, A., Khan, S.A., Box, J.E., Kjeldsen, K.K., Larsen, N.K., Korsgaard, N.J., Cappelen, J., Colgan, W.T., Machguth, H., Andresen, C.S., Peings, Y., Kjær, K.H., 2018. Changes in Greenland's peripheral glaciers linked to the North Atlantic Oscillation. *Nature Climate Change* 8, 48-52.

Briner, J.P., Stewart, H.A.M., Young, N.E., Phillipps, W., Losee, S., 2010. Using proglacial-threshold lakes to constrain fluctuations of the Jakobshavn Isbrae ice margin, western Greenland, during the Holocene. *Quaternary Science Reviews* 29, 3861-3874

Carlson, A.E., Winsor, K., Ullman, D.J., Brook, E.J., Rood, D.H., Axford, Y., LeGrande, A.N., Anslow, F.S., Sinclair, G., 2014. Earliest Holocene south Greenland ice sheet retreat within its late Holocene extent. *Geophysical Research Letters* 41, 5514-5521

Church, J.A., Clark, P.U., Cazenave, A., Gregory, J.M., Jevrejeva, S., Levermann, A., Merrifeld, M.A., Milne, G.A., Nerem, R.S., Nunn, P.D., Payne, A.J., Pfeffer, W.T., Stammer, D., Unnikrishnan, A.S., 2013. Sea-Level Change. In: Climate Change 2013: The Physical Science Basis. Contribution of Working Group I to the Fifth Assessment Report of the Intergovernmental Panel on Climate Change [Stocker, T.F., D. Qin, G.-K. Plattner, M. Tignor, S.K. Allen, J. Boschung, A. Nauels, Y. Xia, V. Bex and P.M. Midgley (eds.)]. Cambridge University Press, Cambridge, United Kingdom and New York, NY, USA.

Clark, P.U., Dyke, A.S., Shakun, J.D., Carlson, A.E., Clark, J., Wohlfarth, B., Hostetler, S.W., Mitrovica, J.X., McCabe, A.M., 2009. The last glacial maximum. Science 325, 710-714

Cohen, J., Screen, J.A., Furtado, J.C., Barlow, M., Whittleston, D., Coumou, D., Francis, J., Dethloff, K., Entekhabi, D., Overland, J., Jones, J., 2014. Recent Arctic amplification and extreme mid-latitude weather. *Nature Geoscience* 7, 627-637.

Corbett, L.B., Bierman, P.R., Lasher, G.E., Rood, D.H., 2015. Landscape chronology and glacial history in Thule, northwest Greenland. *Quaternary Science Reviews* 109, 57-67.

D'Andrea, W.J., Huang, Y., Fritz, S.C., Anderson, N.J., 2011. Abrupt Holocene climate change as an important factor for human migration in West Greenland. *Proceedings of the National Academy of Sciences* 108, 9765-9769

Gardner, A.S., Moholdt, G., Cogley, J.G., Wouters, B., Arendt, A.A., Wahr, J., Berthier, E., Hock, R., Pfeffer, W.T., Kaser, G., Ligtenberg, S.R.M., Bolch, T., Sharp, M.J., Hagen, J.O., van den Broeke, M.R., Paul, F., 2013. A reconciled estimate of glacier contributions to sea level rise: 2003 to 2009. *Science* 340, 852-857

Gibbons, A.B., Megeath, J.D., Pierce, K.L., 1984. Probability of moraine survival in a succession of glacial advances. *Geology* 12, 327-330

Granger, D.E., Lifton, N.A., Willenbring, J.K., 2013. A cosmic trip: 25 years of cosmogenic nuclides in geology. *Geological Society of Americal Bulletin* 125, 1379-1402.

Håkansson, L., Briner, J.P., Aldahan, A., Possnert, G., 2011. ^{10}Be data from meltwater channels suggest that Jameson Land, east Greenland, was ice-covered during the last glacial maximum. *Quaternary Research* 76, 452-459.

Håkansson, L., Briner, J., Alexanderson, H., Aldahan, A., Possnert, G., 2007. ^{10}Be ages from central east Greenland constrain the extent of the Greenland ice sheet during the Last Glacial Maximum. *Quaternary Science Reviews* 26, 2316-2321

Jomelli, V., Lane, T., Favier, V., Masson-Delmotte, V., Swingedouw, D., Rinterknect, V., Schimmelpfennig, I., Brunstein, D., Verfaillie, D., Adamson, K., Leanni, L., Mokadem, F., ASTER Team, 2016. Paradoxical cold conditions during the medieval climate anomaly in the Western Arctic. *Nature Scientific Reports* 6, dx.doi.org://10.1038/srep32984

Kelley, S.E., Briner, J.P., Young, N.E., Babonis, G.S., Csatho, B., 2012. Maximum late Holocene extent of the western Greenland Ice Sheet during the late 20th Century. *Quaternary Science Reviews* 56, 89-98

Khan, S.A, Aschwanden, A., Bjørk, A.A., Wahr, J., Kjeldsen, K.K., Kjær, K.H., 2015. Greenland ice sheet mass balance: a review. *Reports on Progress in Physics* 79, dx.doi.org://10.1088/0034-4885/78/046801

Larsen, N.K., Find, J., Kristensen, A., Bjørk, A.A., Kjeldsen, K.K.k, Odgaard, B.V., Kjær, K.H., 2016 .Holocene ice marginal fluctuations of the Qassimiut lobe in South Greenland. *Nature Scientific Reports* 6, dx.doi.org://10.1038/srep22362

Larsen, N.K., Funder, S., Kjær, K.H., Kjeldsen, K.K., Knudsen, M.F., Linge, H., 2013. Rapid early Holocene ice retreat in West Greenland. *Quaternary Science Reviews* 92, 310-323

Larsen, N.K., Kjær, K.H., Lecavalier, B., Bjørk, A.A., Colding, S., Huybrechts, P., Jakobsen, K.E., Kjeldsen, K.K., Knudsen, K-L., Odgaard, B.V., Olsen, J., 2015. The response of the southern Greenland ice sheet to the Holocene thermal maximum. *Geology* 43, 291-294

Larsen, N.K., Kjær, K.H., Olsen, J., Funder, S., Kjeldsen, K.K., Nørgaard-Pedersen, N., 2011. Restricted impact of Holocene climate variations on the southern Greenland Ice Sheet. *Quaternary Science Reviews* 3171-3180

Lasher, G.E., Axford, Y., 2019. Medieval warmth confirmed at the Norse Eastern Settlement in Greenland. *Geology* 47, 267-270.

Lecavalier, B.S., Milne, G.A.. Simpson, M.J.R., Wake, L., Huybrechts, P., Tarasov, L., Kjeldsen, K.K., Funder, S., Long, A.J., Woodroffe, S., Dyke, A.S., Larsen, N.K., 2014 A model of Greenland Ice Sheet Deglaciation Constrained by Observations of Relative Sea Level and Ice Extent. *Quaternary Science Reviews* 102, 54-84

Levy, L.B., Kelly, M.A., Howley, J.A., Virginia, R.A., 2012. Age of the Ørkendalen moraines, Kangerlussuaq, Greenland: constraints on the extent of the southwestern margin of the Greenland Ice Sheet during the Holocene. *Quaternary Science Reviews* 52, 1-5

Levy, L.B., Kelly, M.A., Lowell, T.V., Hall, B.L., Hempel, L.A., Honsaker, W.M., Lusas, A.R., Howley, J.A., Axford, Y.L., 2014. Holocene fluctuations of Bregne ice cap, Scoresby Sund, east Greenland: a proxy for climate along the Greenland Ice Sheet margin. *Quaternary Science Reviews* 92, 356-368

Licciardi, J.M., 2000. Alpine glacier and pluvial lake records of late Pleistocene climate variability in the western United States (Ph.D. thesis). Corvallis, Oregon State University, 155p

Lowell, T.V., Hall, B.L., Kelly, M.A., Bennike, O., Lusas, A.R., Honsaker, W., Smith, C.A., Levy, L.B., Travis, S., Denton, G.H., 2013. Late Holocene expansion of Istorvet ice cap, Liverpool Land, east Greenland. *Quaternary Science Reviews* 63, 128-140

Marcott, S.A., 2011. Late Pleistocene and Holocene glacier and climate change (Ph.D. thesis). Corvallis, Oregon State University, 260 p.

Marzeion, B., Cogley, J.G., Richter, K., Parkes, D., 2014. Attribution of global glacier mass loss to anthropogenic and natural causes. *Science* 345, 919-921

Möller, P., Larsen, N.K., Kjær, K.H., Funder, S., Schomacker, A., Linge, H., Fabel, D., 2010. Early to middle Holocene valley glaciations on northernmost Greenland. *Quaternary Science Reviews* 29, 3379-3398.

Nelson, A.H., Bierman, P.R., Shakun, J.D., Rood, D.H., 2014. Using *in situ* cosmogenic ^{10}Be to identify the source of sediment leaving Greenland. *Earth Surface Processes and Landforms* 39, 1087-1100.

Overland, J.E., Wang, M., Walsh, J.E., Stroeve, J.C., 2013. Future Arctic climate changes: Adaptation and mitigation time scales. *Earth's Future* 2, 68-74.

Perner, K., Moros, M., Lloyd, J.M., Kuijpers, A., Telford, R.J., Harff, J., 2011. Centennial scale benthic foraminiferal record of late Holocene oceanography variability in Disko Bugt, West Greenland. *Quaternary Science Reviews* 30, 2815-2826.

Reichert, B.K., Bengtsson, L., Oerlemans, J., 2002. Recent glacier retreat exceeds internal variability. *Journal of Climate* 15, 3069-3081

Reusche, M., Marcott, S., Ceperley, E., Barth, A., Brook, E., Mix, A., Caffe, M., 2018. Early to late Holocene surface exposure ages from two marine-terminating outlet glaciers in northwest Greenland. *Geophysical Research Letters*, dx.doi.org/10.1029/2018GL078266

Roe, G.H., Baker, M.B., Herla, F., 2017. Centennial glacier retreat as categorical evidence of regional climate change. *Nature Geoscience* 10, 95-99

Roe, G.H., and O'Neal, M.A., 2009. The response of glaciers to intrinsic climate variability: Observations and models of late-Holocene variations in the Pacific Northwest: *Journal of Glaciology* 55, 839-854.

Schaefer, J.M., Finkel, R.C., Balco, G., Alley, R.B., Caffee, M.W., Briner, J.P., Young, N.E., Gow, A.J., Schwartz, R., 2016. Greenland was nearly ice-free for extended periods during the Pleistocene. *Nature* 540, 252-255.

Schimmelpfennig, I., Schaefer, J.M., Akçar, N., Koffman, T., Ivy-Ochs, S., Schwartz, R., Finkel, R.C., Zimmerman, S., Schlüchter, C., 2014. A chronology of Holocene and Little Ice Age glacier culminations of the Steingletscher, Central Alps, Switzerland, based on high-sensitivity beryllium-10 moraine dating. *Earth and Planetary Science Letters* 393, 220-230

Serreze, M.C., and Barry, R.G., 2011. Processes and impacts of Arctic amplification: A research synthesis. *Global and Planetary Change* 77, 85-96

Shepherd, A., Ivins, E.R., A, G., Barletta, V.R., Bentley, M.J., Bettadpur, S., Briggs, K.H., Bromwich, D.H., Forsberg, R., Galin, N., Horwath, M., Jacobs, S., Joughin, I., King, M.A., Lenaerts, J.T.M., Li, J., Lightenberg, S.R.M., Luckman, A., Luthcke, S.B., McMillan, M., Meister, R. Milne, G., Mouginot, J., Muir, A., Nicolas, J.P., Paden, J, Payne, A.J., Pritchard, H.,

Simpson, M.J.R., Milne, G.A., Huybrechts, P., Long, A.J., 2009. Calibrating a glaciological model of the Greenland ice sheet from the Last Glacial Maximum to present-day using field observations of relative sea level and ice extent. *Quaternary Science Reviews* 29, 1631-1657

Sinclair, G., Carlson, A.E., Mix, A.C., Lecavalier, B.S., Milne, G.A., Mathias, A., Buizert, C., DeConto, R.M. Diachronous retreat of the Greenland ice sheet during the last deglaciation. *Quaternary Science Reviews* 145, 243-258

Solomina, O.N., Bradley, R.S., Hodgson, D.A., Ivy-Ochs, S., Jomelli, V., Mackintosh, A.N., Nesje, A., Owen, L.A., Wanner, H., Wiles, G.C., Young, N.E., 2015. Holocene glacier fluctuations. *Quaternary Science Reviews* 111, 9-34.

Vaughan, D.G., J.C. Comiso, I. Allison, J. Carrasco, G. Kaser, R. Kwok, P. Mote, T. Murray, F. Paul, J. Ren, E. Rignot, O. Solomina, K. Steffen and T. Zhang, 2013: Observations: Cryosphere. In: Climate Change 2013: The Physical Science Basis. Contribution of Working Group I to the Fifth Assessment Report of the Intergovernmental Panel on Climate Change [Stocker, T.F., D. Qin, G.-K. Plattner, M. Tignor, S.K. Allen, J. Boschung, A. Nauels, Y. Xia, V. Bex and P.M. Midgley (eds.)]. Cambridge University Press, Cambridge, United Kingdom and New York, NY, USA.

Weidick, A., 1959. Glacial variations in West Greenland in historical time, part 1. *Meddelelser om Grønland*, 158, 4

Weidick, A., 1975. Holocene shorelines and glacial stages in Greenland—an attempt at correlation. *Rapport Grønlands Geologiske Undersøgelse* 41, 39 pp.

Winsor, K., Carlson, A.E., Rood, D.H., 2014. ^{10}Be dating of the Narsarsuaq moraine in southernmost Greenland: evidence for a late-Holocene ice advance exceeding the Little Ice Age maximum. *Quaternary Science Reviews* 98, 135-143

Young, N.E., Schaefer, J.M., Briner, J.P., Goehring, B.M., 2013a. A Be-10 production rate calibration for the Arctic. *Journal of Quaternary Science* 28, 515-526

Young, N.E., Briner, J.P., Rood, D.H., Finkel, R.C., Corbett, L.B., Bierman, P.R., 2013b. Age of the Fjord Stade moraines in the Disko Bugt region, western Greenland, and the 9.3 and 8.2 ka cooling events. *Quaternary Science Reviews* 60, 76-90

Young, N.E., Briner, J.P., Sterwart, H.A.M., Axford, Y., Csatho, B., Rood, D.H., Finkel, R.C., 2011. Response of Jakobshavn Isbrae, Greenland, to Holocene climate change. *Geology* 39, 131-134

Young, N.E., Schweinsburg, A.D., Briner, J.P., Schaeffer, J.M., 2015. Glacier maxima in Baffin Bay during the Medieval Warm Period coeval with Norse settlement. *Science Advances* 1, dx.doi.org://10.1126/sciadv.1500806

Zwally, H.J., Li, J., Brenner, A.C., Beckley, M., Cornejo, H.G., DiMarzio, J., Giovinetto, M.B., Neumann, T.A., Robbins, J., Saba, J.L., Yi, D., Wang, W., 2011. Greenland ice sheet mass balance: distribution of increased mass loss with climate warming; 2003-07 versus 1992-2002., *Journal of Glaciology* 25, 88-102

Chapter 5

Conclusions

The past 20,000 years give us several time periods to perform natural experiments to investigate the sensitivity of Earth systems to external forcings. Here, we present three studies investigating Arctic climate and the response of Greenland's cryosphere to climate forcing. Chapter 2 shows the importance of ocean warming in forcing diachronous retreat of the Greenland ice sheet, a result that was not captured by an ice sheet model that does not include spatially-variable ocean forcings.

Chapters 3 and 4 focus on the latest Holocene, revealing spatial variability in both climate and cryosphere behavior over this period. Chapter 3 demonstrates how using a network of proxy records statistically combined with reanalysis data reveal a map of Common era climate with prominent spatial variability, particularly between the eastern and western Arctic. Commonly proposed forcings for Common Era climate explain ~20% of the temperature variability, suggesting that either significant noise or unresolved forcings may drive much of Arctic climate over this period. Chapter 4 demonstrates the importance of glacier size for determining its sensitivity to local climate forcing. Glaciers draining the alpine-like Julianhåb Ice Cap have a wide range of retreat dates from their late Holocene maxima (~3.7, 1.5, and 0.4 ka). In contrast, glaciers draining the piedmont-like Qassimiut Lobe of the Greenland ice sheet and the small mountain glaciers and ice caps surrounding the ice sheet have a smaller range of ages (~0.8 to 0.5 ka), which may indicate response to a local warming event.

Overall, these studies each demonstrate the dynamic spatial and temporal variability of Arctic climate and cryosphere behavior over the past 20,000 years. They each also demonstrate the power of large datasets to parse true signals from proxy and climate noise, revealing patterns and behavior that cannot be resolved from single spatially-disparate records.

Appendices

Appendix A. Diachronous retreat of the Greenland ice sheet during the last deglaciation

A.1 Supplementary data

Supplementary data related to this article can be found at hhtp://dx.doi.org/10.1016/j.quascirev.2016.05.040

Appendix B. Paleo-reanalysis of spatially- and temporally-resolved Arctic climate 10-2010 C.E.

B.1 Detailed methods

Here we extend the spatially resolved reanalysis of Arctic climate, currently available from the interval 1850-1970 CE, through the entire Common Era of 10-2010 CE, adapting a CFR approach (Pisias 1978; Fritts et al., 1971; Evans et al.; 2001, 2002). Drivers of climate may have changed due to anthropogenic activities in the 20th and 21st centuries (e.g Waters et al., 2016; Bindoff et al., 2013), and therefore the following process should be viewed as a method to statistically extend a reanalysis dataset, rather than a pure reconstruction of Arctic Common Era climate.

1. We assemble 17 highly resolved paleoclimate proxy records (from the PAGES 2K database; PAGES 2k Consortium 2017) in the latitude bands 60-90N that have average temporal resolution of 15 years, and cover the time period 10-1970 C.E. We convert the proxy records to z-scores and linearly interpolate to each record to a 5-year interval.

2. We characterize orthogonal components of variability in this data array via R-mode factor analysis and retain four significant factors. We iterate, excluding five records with a communality less than 0.2. Removing these records has no discernable influence on our final temperature reconstructions (Appendix B.5).

3. We regress the four factors against HadCRUT4.2 annual-average and seasonal (winter, DJF and summer, JJA) temperatures at each HadCRUT4.2 grid cell (Morice et al., 2012 with modifications outlined in PAGES2k (2017) over their overlapping range (1850-1970 C.E.). This yields a set of four coefficients, an intercept, and an uncertainty) to predict reanalysis temperatures from paleo factor timeseries, at each grid cell.

4. At each gridcell, we apply the temperature calibration coefficients from Step 3 to predict gridcell temperatures over the full paleo time range, 10-1970 C.E. Errors are assessed by Monte Carlo simulation of 1,000 realizations based on the 95% confidence interval of the original regression. Results are expressed as averages and standard deviations at each 5-year time step and each grid cell, and illustrated as time-slice maps or animations, or regional average timeseries stacks.

5. We assess random and systematic biases between reanalysis temperatures and the proxy reconstruction temperatures, and find no evidence of persistent regional biases.

6. We compare our paleo-reanalysis to previously published Arctic, regional, and global climate reconstructions, including the Arctic2k temperature stack (McKay and Kaufman 2014) and the PAGES2k temperature stack, and with a larger dataset spanning the last 1,000 years.

7. We examine the potential relationships between several proposed forcings of Common Era change and the paleo-reanalysis based on multiple regression and variance decomposition (Lindeman et al., 1980) controlling for potential correlation between regressors (Grömping 2007).

8. We define the timing of emergence in the Anthropogenic era in each gridcell as the end of a 50-year period that is significantly warmer than the rest of the Common Era leading up to that point, provided all succeeding timesteps are also greater than all preceeding temperatures. We use a two-sample t-test without assuming equal variances, and p=0.05 for the analysis, and include reanalysis data for the period 1970-2010.

9. We identify the “Little Ice Age” (LIA) onset for each gridcell as the end of the most recent period with at least five consecutive timesteps significantly cold (at

p=0.05) than the preceding timeseries, and the end of the LIA as the end of the first timestep that is no longer significantly colder than everything previous.

B.2 Caveats and assumptions

Caveats and assumptions include: (1) that variability in the paleoproxies adequately explains the reanalysis, and (2) relationships between paleo data and reanalysis temperatures in the calibration period (1850-1970) apply to longer time intervals (i.e., the system is stationary). The first assumption is partially true - the proxy regression analysis explains 50% of the reanalysis temperatures, this lack of fit is propagated into the uncertainties in the Monte Carlo. The second assumption is presently difficult to test, but could be assessed in the future based on systematic divergence of our reconstructed paleotemperatures over time relative to independently calibrated high-resolution records.

B.3 Proxy records used in analysis

We use 17 records from the PAGES 2k database in this study (Table B.1). The initial criteria we use is based on the length of the record. Our goal is to reconstruct climate across the Common Era, so we select those records which cover almost the entirety of the Common Era. Input to the R-mode factor analysis requires the records to be of equal length, so we use the period 10-1970 C.E. to maximize the number of records to include while still covering the majority of the Common Era and keeping enough records in the 20th century for adequate comparison with the Hadley reanalysis. Figure B.1 outlines this: eight records begin between 0 and 10 C.E., then no new records begin until 110 C.E. In the 20th Century, the number of records ending in a given decade increases dramatically after 1970. A total of 23 records remain after we restrict the records to this time period. We then exclude those remaining records with communalities less than 0.2 in an initial R-mode analysis, leaving 17 records. The characteristics of the proxies have similar distributions in terms of proxy type, location, and temporal resolution to the PAGES 2k records (Figure B.2). The main exception to this is the lower percentage of tree-ring records in our subset, mainly because most tree ring records in the

PAGES database begin during the second millennium C.E. We note that the proxies included in this study have major data gaps, principally in the Arctic Ocean and eastern Russia, where records in the PAGES 2k database are least densely distributed (Figure B.1)

B.4 Including all records vs. high-communality only records

There is very little difference between a temperature stack produced using all proxy records and one using only those with communalities greater than 0.2 in the R-mode analysis. Those records that have the least communality will by definition contribute least to the proxy-derived factors. Figure B.4 illustrates this—the average temperature records using both methods are virtually indistinguishable, and overlap within 1-sigma uncertainty. The record compiled using all records is on average 0.15K warmer than that using the higher-communality records, and the Pearson's correlation coefficient is 0.96, significant at p=0.01.

B.5 Effect of retaining six factors from R-mode investigation

Similar to the investigation using all proxies, there is little change in the final temperature stack from retaining six factors in the initial proxy R-mode analysis instead of the four we retain in the stack used in the main body of the manuscript. Including six factors increases variance of proxy data explained in the factor analysis from 48% to 62%. However, the corresponding increases in explanatory power of the factor regressions onto Hadley temperature records is relatively small: the average ordinary r-squared value for the regression increases from 0.49 to 0.53. Factors 5 and 6 may therefore represent non-temperature related variance in the proxy data. The final temperature stacks overlap within uncertainty (Figure B.5) with a correlation coefficient of 0.87 (significant at p=0.01). The stack built with 6 factors has substantially greater uncertainty than that built with four factors, again suggesting the final two factors have little relationship to Arctic temperatures.

B.6 Spatial correlations

Figure B.6 shows the correlations between each gridcell's estimated gridcell temperature record and each regional temperature stack. In general, we observe high correlations in the Arctic ocean and western Arctic both with regional stacks and the Arctic Average. However, Europe and Siberia show a different pattern, with the European stack in particular showing near-zero to negative correlations to much of the Arctic. This is supported by running correlations between regional averages (Figure B.7), which show statistically significant correlations throughout the Common Era for all regions except Europe, which frequently shows non-significant correlations to all regions, including Siberia.

B.7 Comparison of R-mode analysis of Hadley data and last 2 ka paleo-reanalysis

One measure of the extent to which this analysis captures the spatial variability of Arctic climate is to compare the spatial factors in the reanalysis data with those on the full grid temperature reconstruction for the last 2 ka. The results of these two analyses are are presented in Figure B.8 and Figure B.9. Three factors explain 97% of the temperature reconstruction, while the first three factors in the R-mode analysis on the Hadley reanalysis data explain 77% of the temperature variance. We are therefore missing some variance. However, the first three factors in both analyses are similar to each other in spatial pattern. Factor one in both analyses shows the least pronounced spatial patterns, although in both cases it is closer to zero in the North Atlantic, Europe, and Siberia and further from zero (more positive in the temperature reconstruction and more negative in the Hadley analyses). Pearson's correlation coefficient between the two sets of factor loadings is -0.85. The factor two maps for each analysis are positively correlated across much of the Arctic, with the eastern Arctic showing more negative loadings and the western Arctic showing more positive loadings. The maps diverge significantly in eastern Siberia, but still have an overall significant correlation coefficient of 0.72. Finally, factor 3 in both analyses show a divergence in loadings between the region from Arctic Canada to Europe and Arctic Russia to Alaska, with a correlation coefficient of -0.69.

B.8 Comparison to 1 ka and Arc2k stacks

Figure B.10 shows the results of a comparison between the temperature stack presented here, a stack using an entirely different set of proxies covering only the last 1 ka, and the Arc2k stack presented by McKay and Kaufman (2014). All three stacks overlap within uncertainty and are significantly correlated to each other, although the 1 ka stack is warmer than the 2 ka and Arc2k stacks until 1800 C.E.

B.9 Comparison to Hadley reanalysis product

Comparing the proxy reconstruction with the HadCRUT4.2 reanalysis product shows no evidence of systematic bias in the proxy reconstruction (Figure B.11). The reconstructed temperature stack has a correlation coefficient of 0.85 with the Hadley temperature stack where they overlap, significant at p=0.05. There are also no regions where we see a consistent offset between proxy and reanalysis data (Figure B.12), although at individual time slices we observe temperature differences of up to 3 K in individual regions in individual years when comparing the proxy and reanalysis data (Movie B.1).

B.10 Description of movie

Movie B.2 shows our reconstruction of average Arctic temperatures for the Common Era .The top left panel shows gridcell temperature, where each gridcell is the average of 1,000 iteratiions of the regression equation. The top right panel is the cell standard deviation of the 1,000 iterations, and the bottom panel shows the average Arctic temperature with 1-sigma uncertainty range in black and the 2-sigma uncertainty range in grey. The red dot tacks average Arctic temperature over the records. Movie B.3 shows the same gridcell and Arctic average as Movie B.2, but in 1970 C.E. the record switches from our reconstruction to the Hadley reanalysis reconstruction. We note the temperatures in the 20th century are often greater than the temperature scale allows.

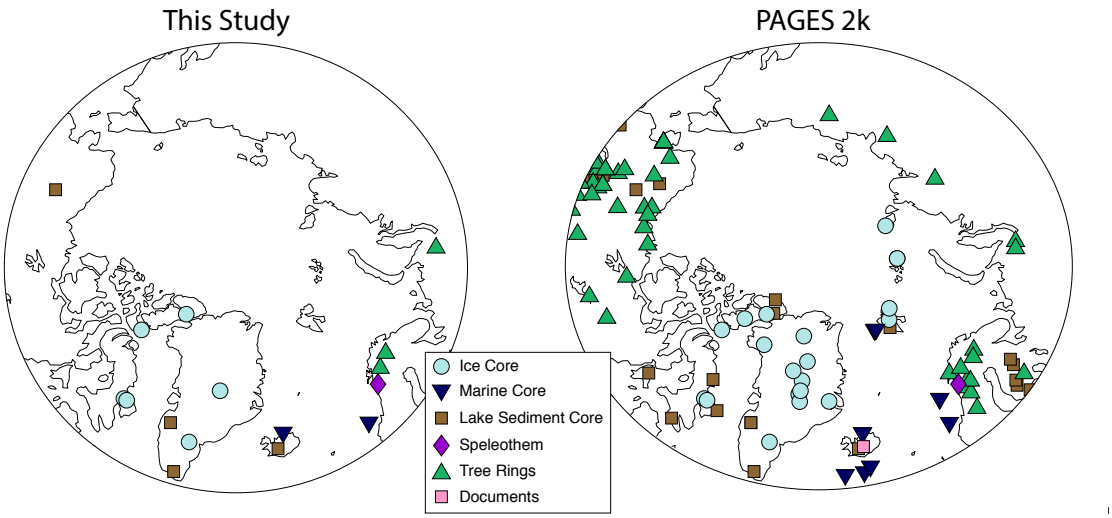

Figure B.1 Map of proxy records used in this study (left) and the PAGES 2k database (right).

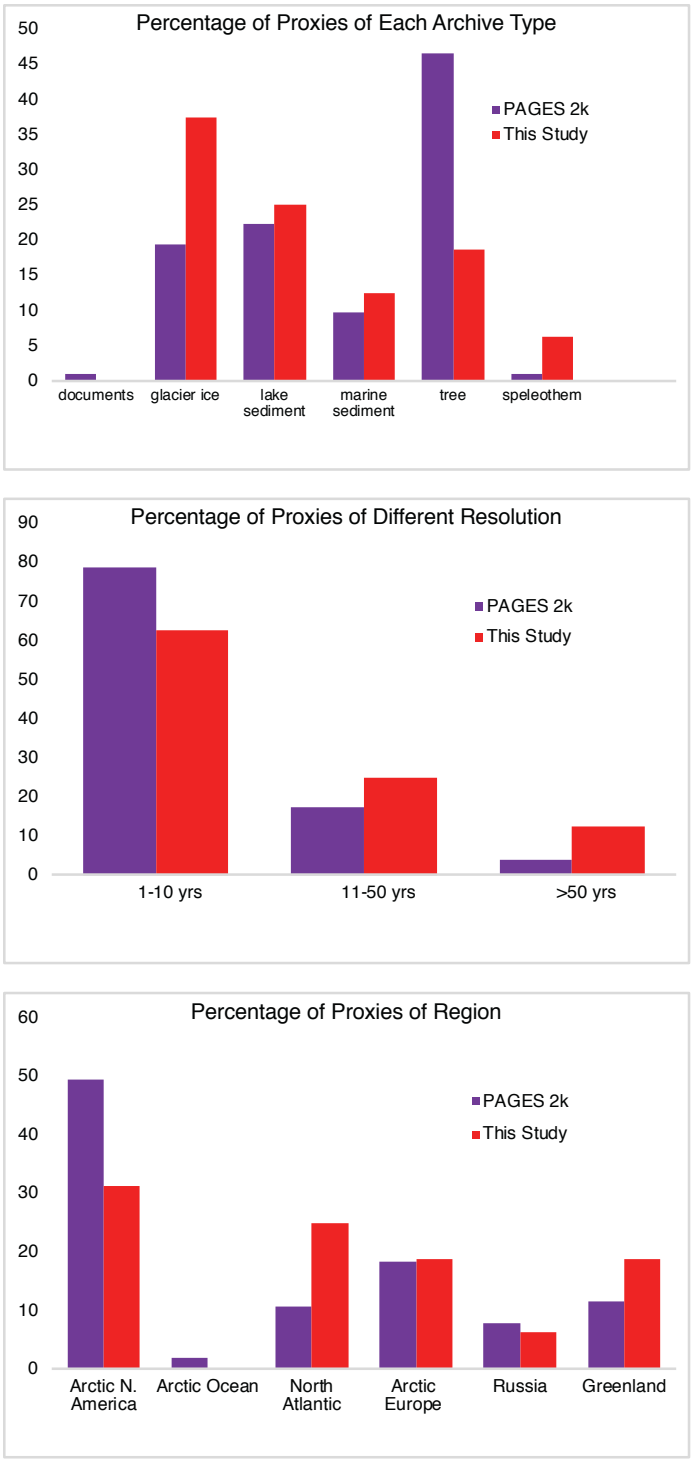

Figure B.2 Comparison of proxy characteristics in Arctic section of PAGES 2k database and those used in this study

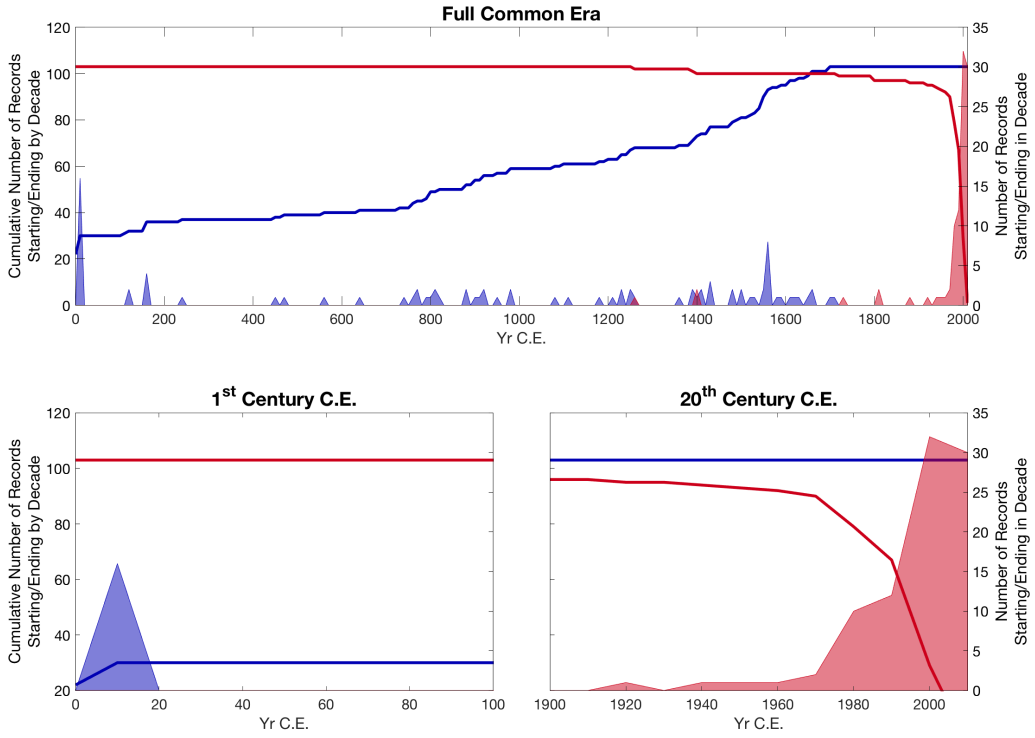

Figure B.3 Number of Records added per decade. Blue line indicates cumulative number of records started by given decade. Red line indicates number of records completed by a given decade. Blue shaded lines indicate number of records added in a given decade, red shaded lines indicate number of records completed during a given decade.

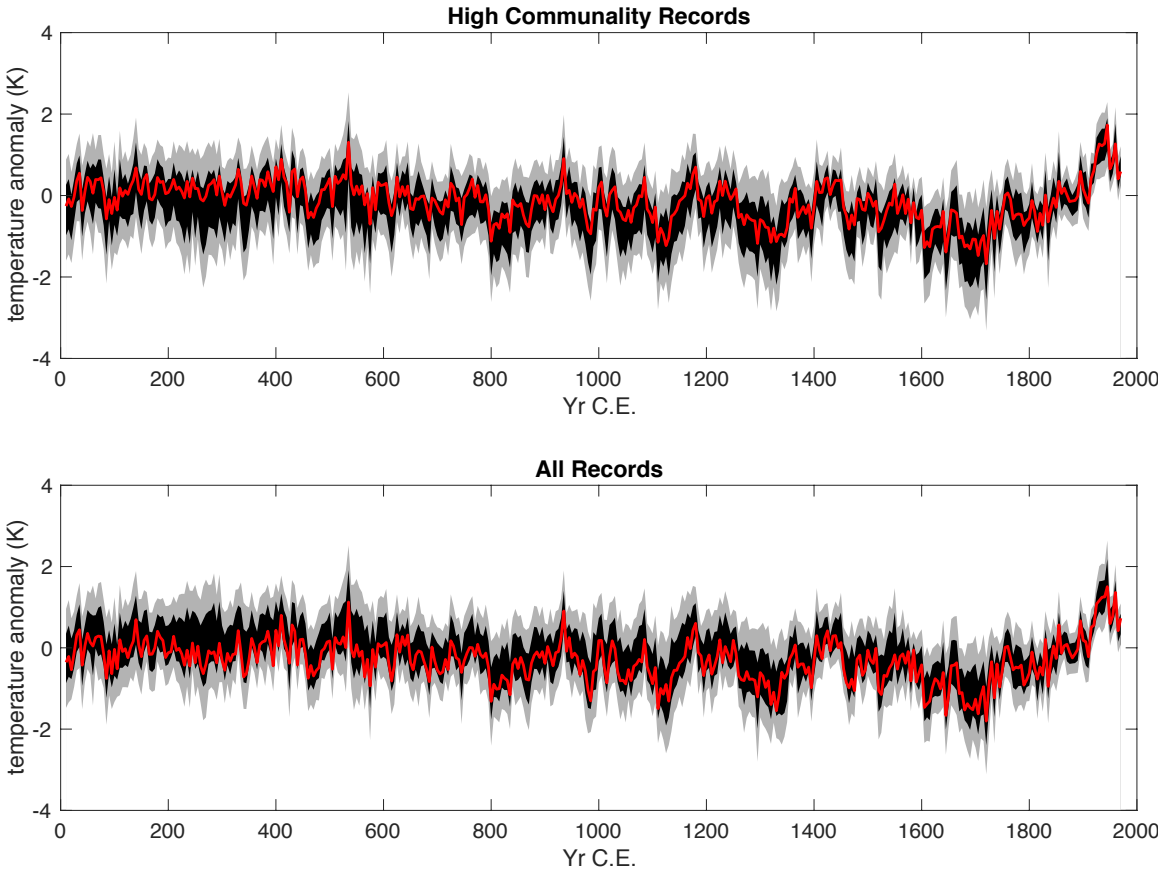

Figure B.4 Comparison of reconstruction using only high communality records (top) and all records (bottom). Red line in top (bottom) figure is all record (high communality) average for reference.

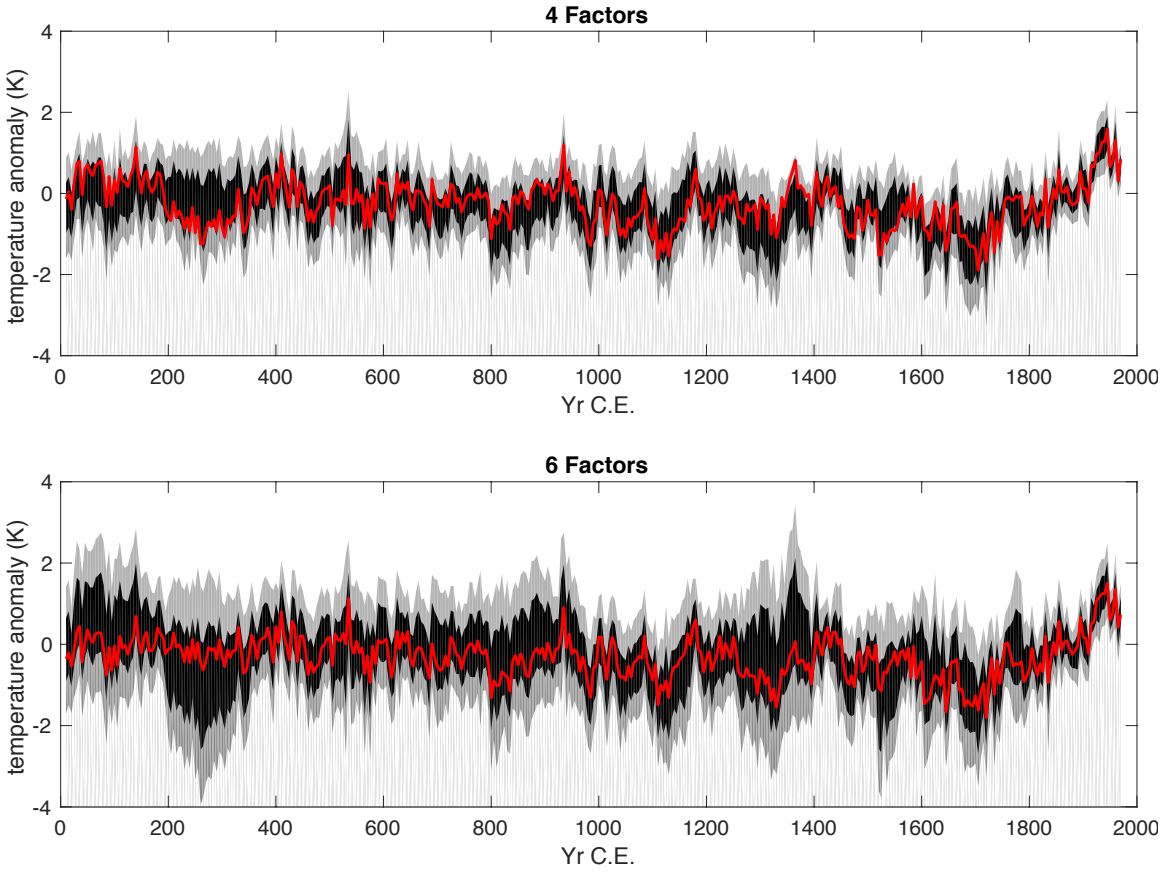

Figure B.5 Comparison of reconstruction using only four proxy factors (top) and six proxy factors (bottom). Red line in top (bottom) figure is six factor (four factor) average for reference.

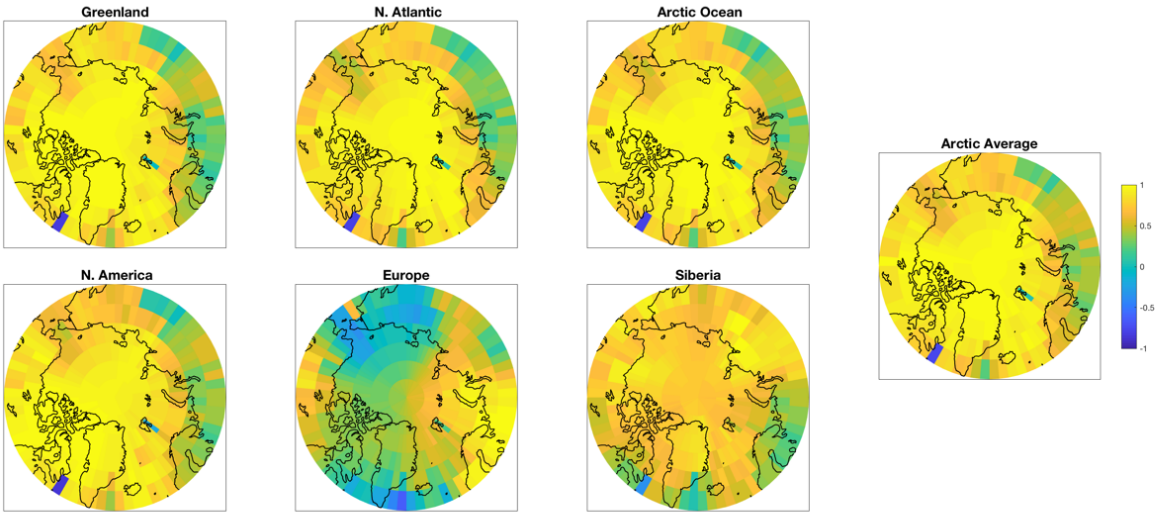

Figure B.6 Pearson's correlation coefficient for each gridcell to the given regional or Arctic average.

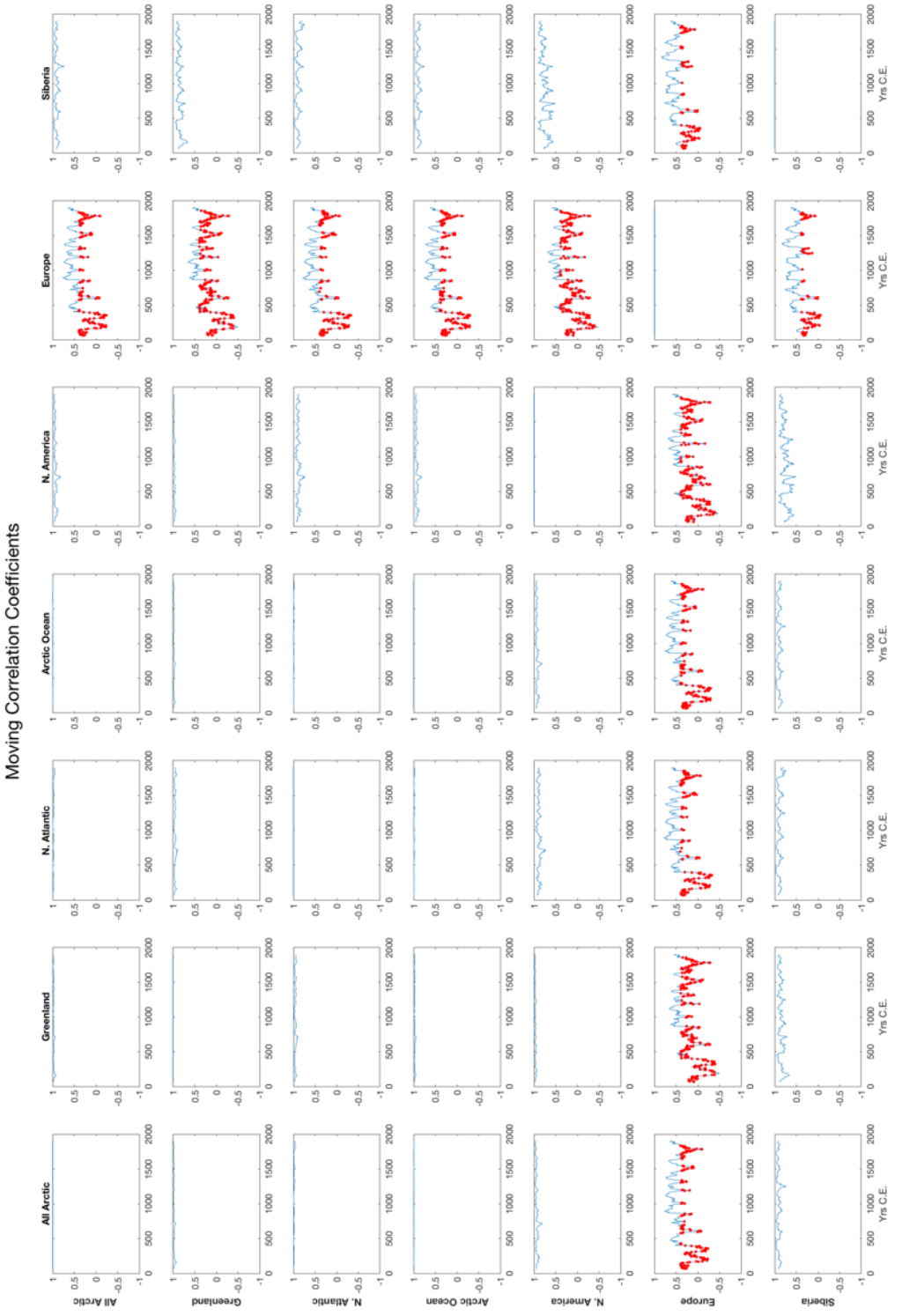

Figure B.7 Moving correlation coefficients between regions. Red dots indicate correlation is not significant at p=0.05.

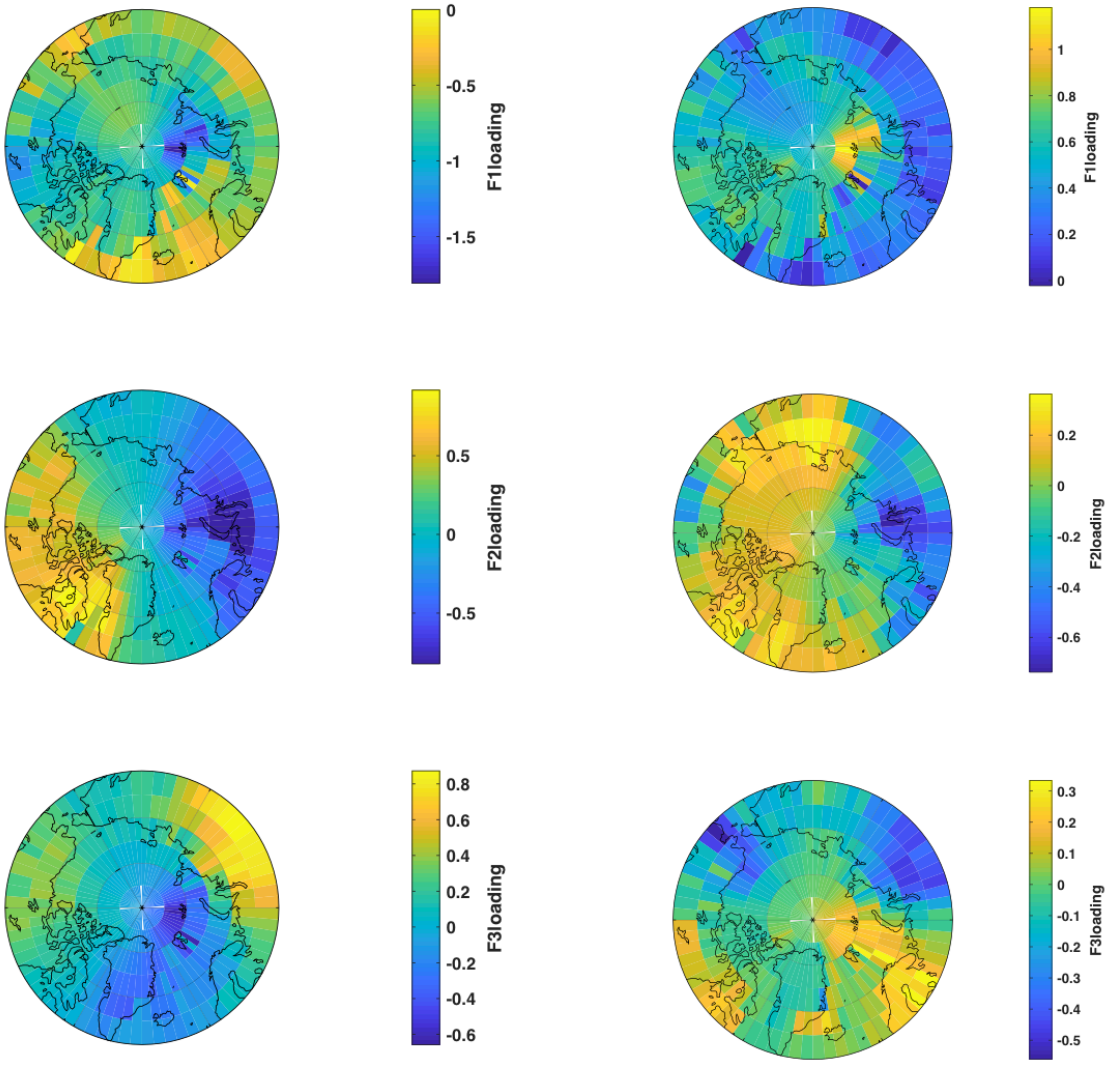

Figure B.8 Loadings of first three factors of R-mode analysis in Hadley reanalysis dataset (left) and last 2ka reconstruction (right).

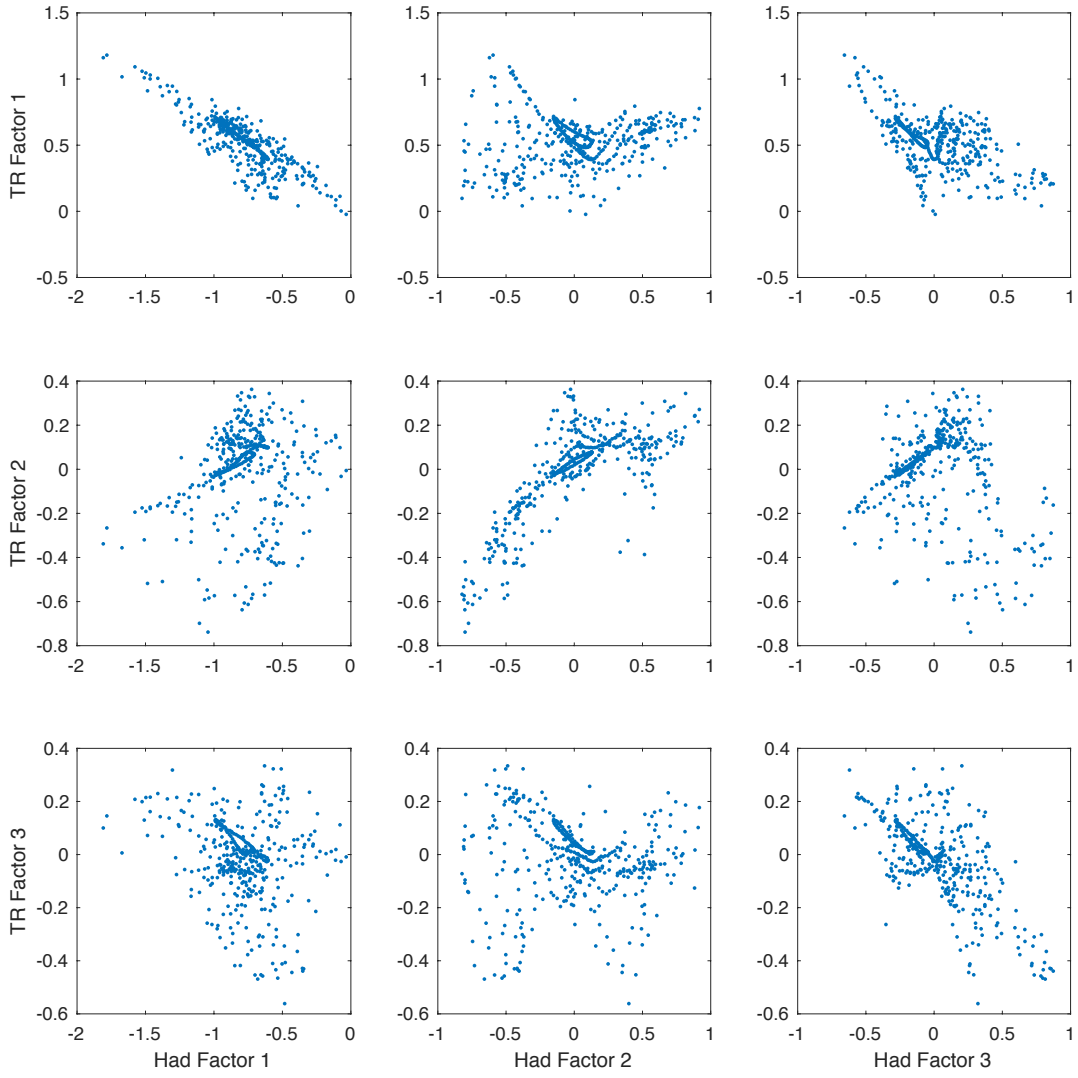

Figure B.9 Correlations between temperature reconstruction factors (Y-axis) and Hadley factors (x-axis).

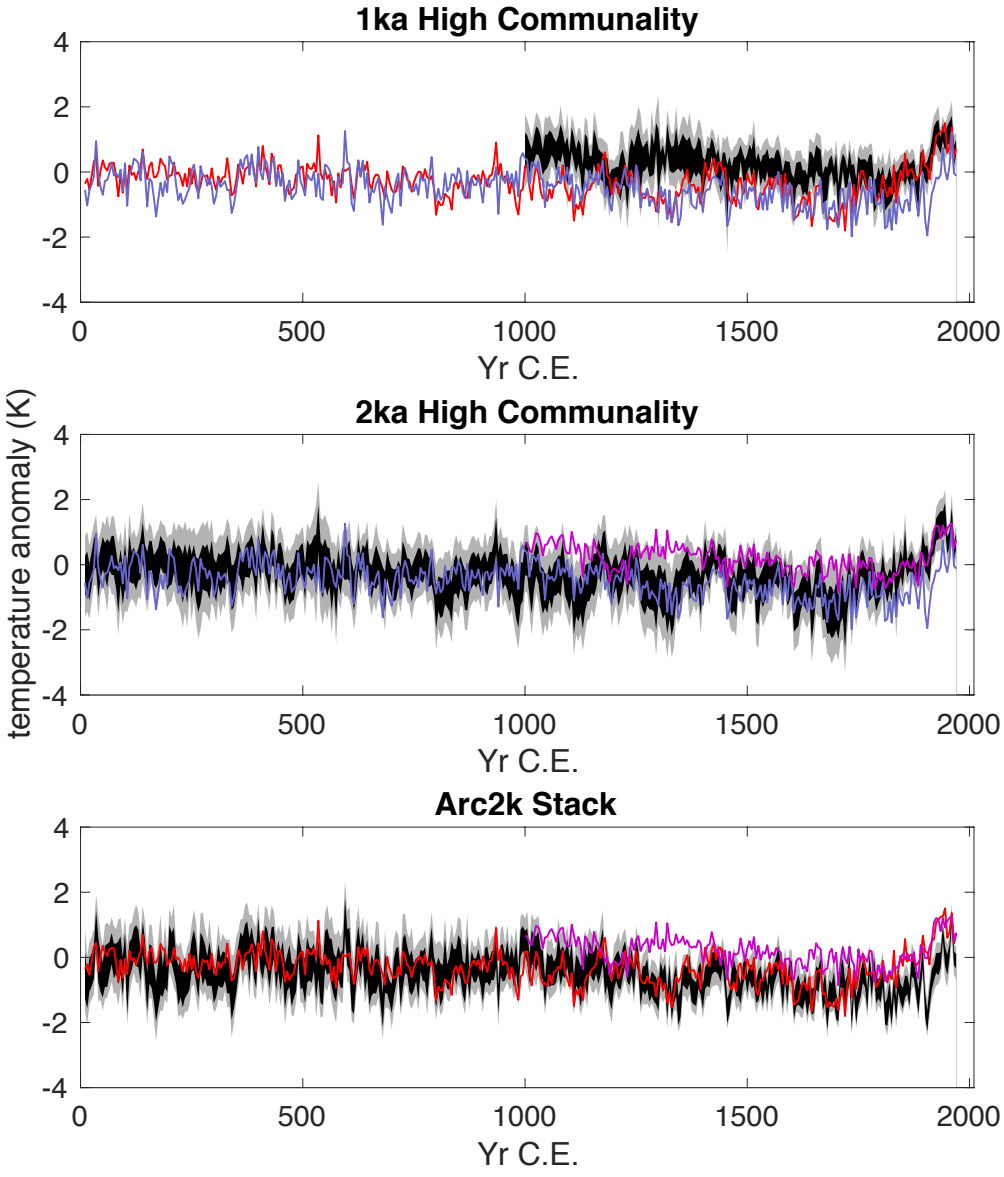

Figure B.10 Comparison of 1ka (top), 2ka (middle) and previously published Arc2k stacks. Top Figure: red line is 2ka high communality average, blue line is Arc2k average. Middle: blue line is Arc2k average, fuchsia line is 1ka average. Bottom: red line is 2ka average, fuchsia line is 1 ka average.

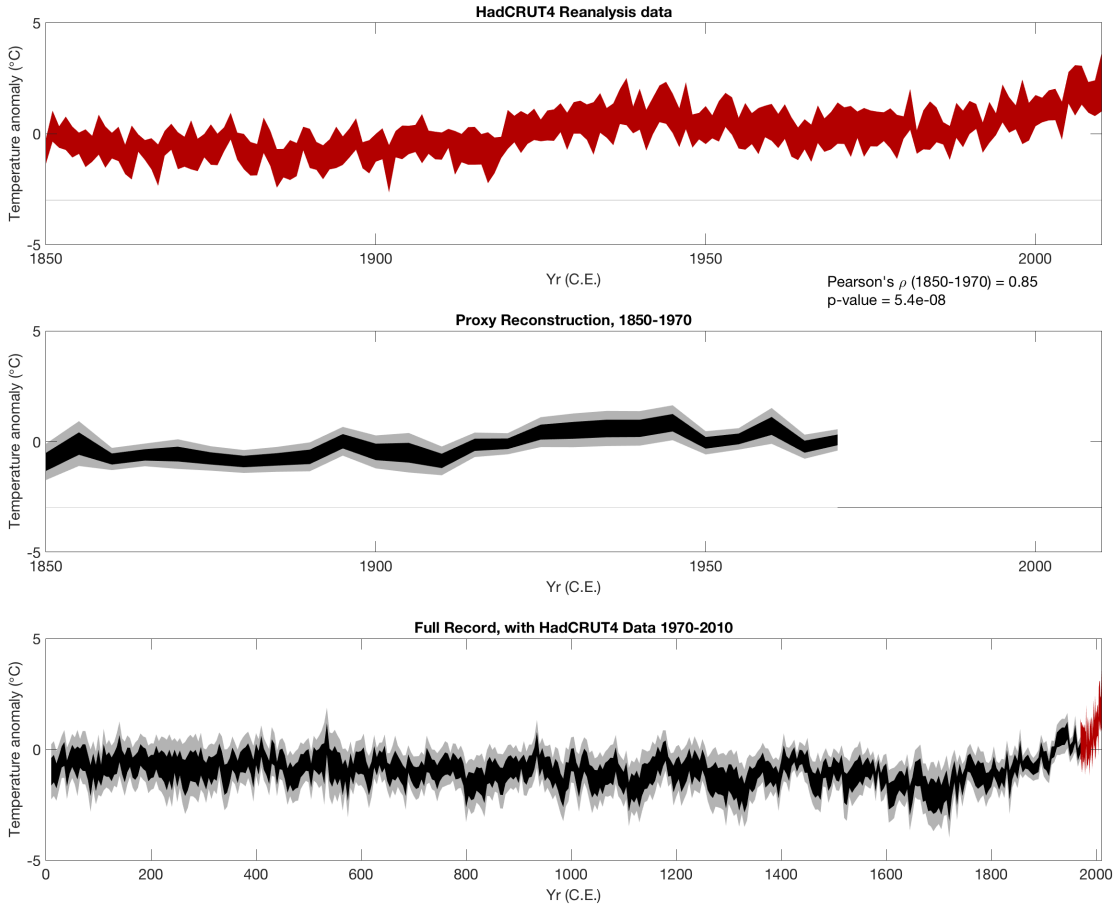

Figure B.11 Comparison of HadCrut4.2 reanalysis data with proxy reconstruction for the period 1850-2010. Top: HadCrut4.2 reanalysis average. Middle: Proxy reconstruction 1850-1970. Bottom: Full common era record, with HadCrut4.2 average 1970-2010.

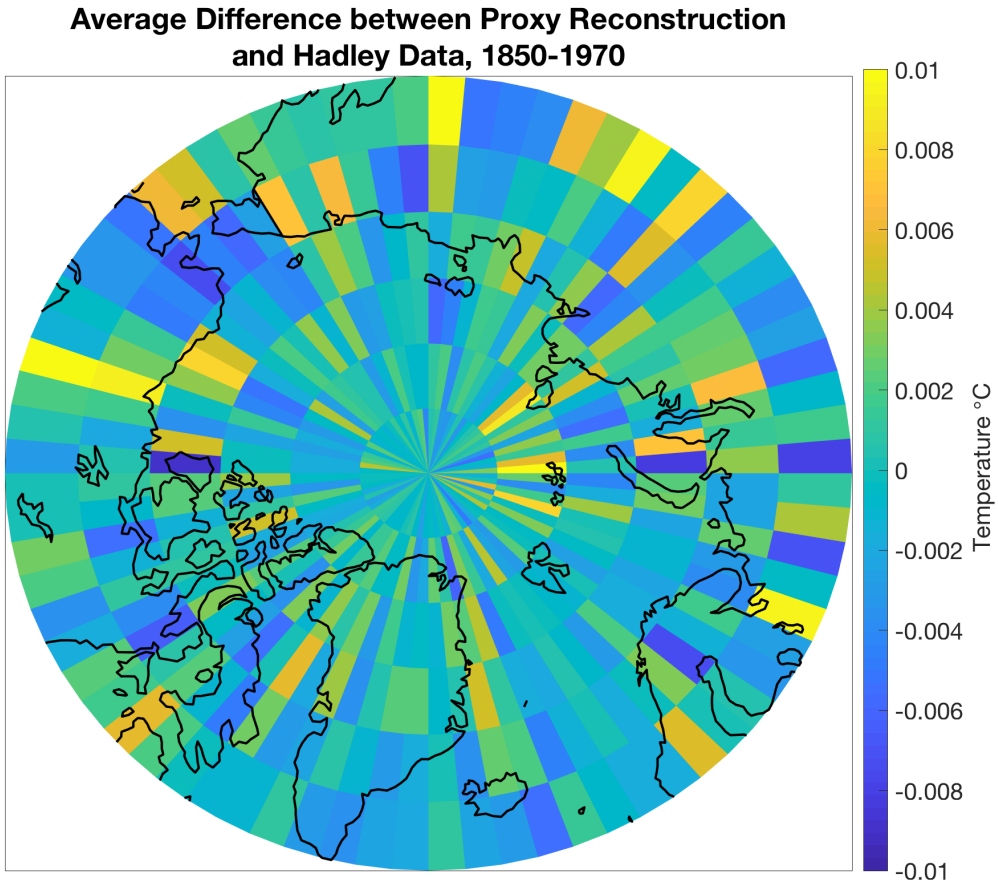

Figure B.12 Average difference between reconstruction and Hadley reanalysis data for the period 1850-1970.

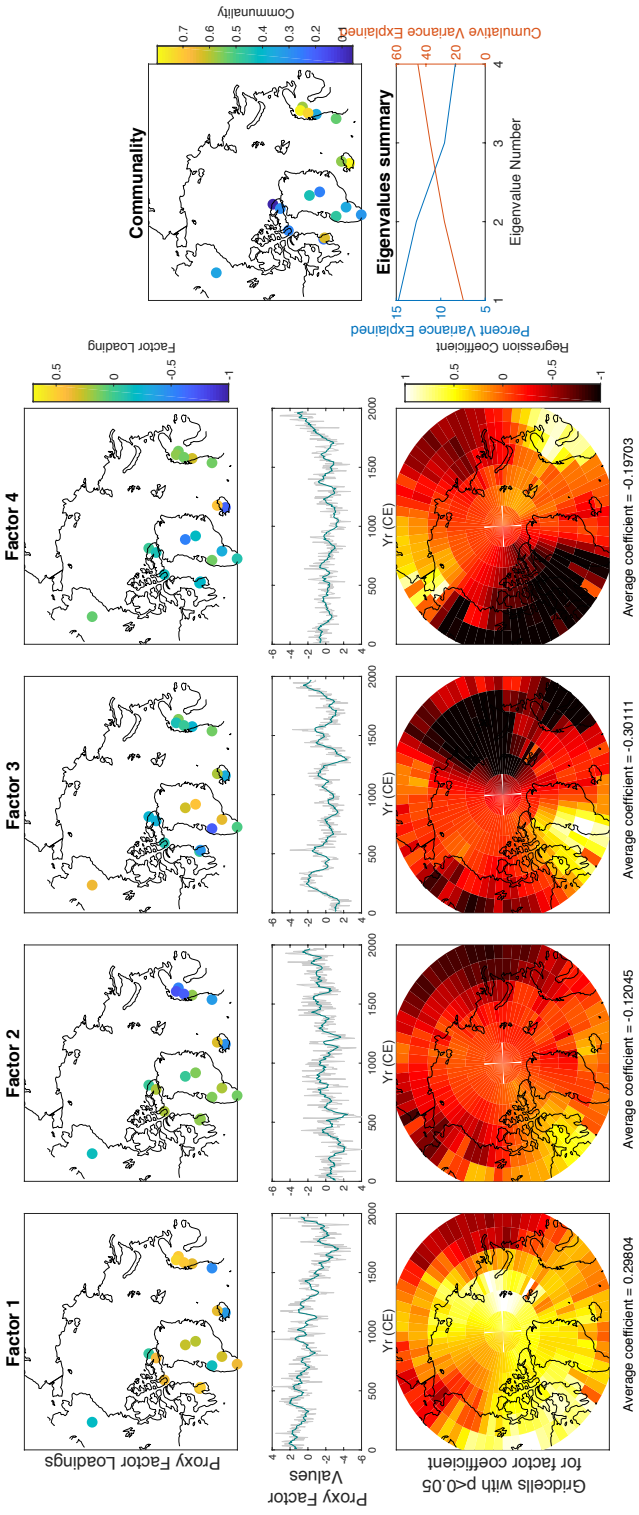

Figure B.14 Summary of proxy factor-reanalysis regressions for winter (DJF) reanalysis data

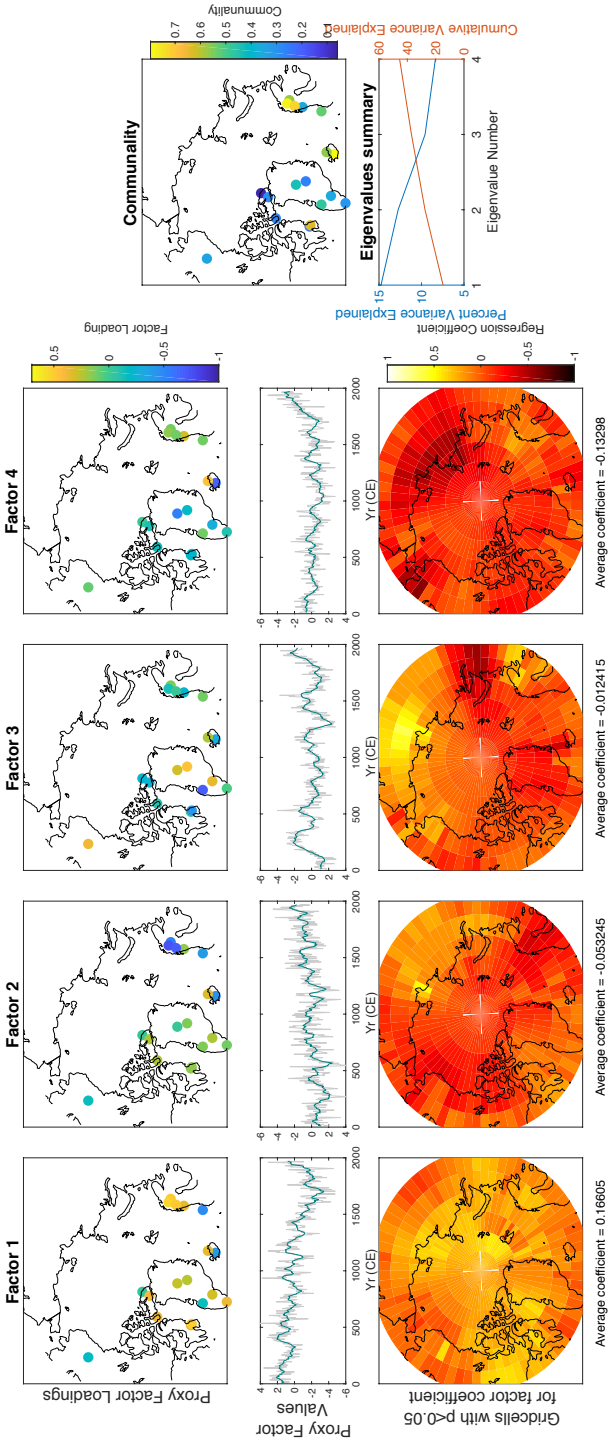

Figure B.14 Summary of proxy factor-reanalysis regressions for summer (JJA) reanalysis data

Table B.1 Summary of Proxies Retained for the Analysis

PAGES 2k ID	Country/Ocean	Site Name	Latitude (°)	Longitude (°)	Elevation (m)	Archive Type	Archive Code	Proxy Type	Archive Start Year (C.E.)	Archive End Year (C.E.)	Resolution (yrs)	Reference
Arc_022	Iceland	Hvítárvatn	64.6	-19.8	422	lake sediment	1	varve thickness	0	2000	1	10.1016/j.quascirev.2011.05.026
Arc_033	Canada	Agassiz	80.7	-73.1	1700	glacier ice	2	d18O	0	1972	1	10.1029/2007JD009143
Arc_035	Greenland	Dye	65.18	-43.83	2480	glacier ice	2	d18O	1	1978	1	10.1016/j.quascirev.2009.11.002
Arc_036	Greenland	GRIP	72.58	-37.64	3238	glacier ice	2	d18O	1	1979	1	10.1016/j.quascirev.2009.11.002
Arc_042	United States of America	Screaming Lynx Lake	66.07	-145.4	223	lake sediment	1	midge	-1067	1988	51	10.1073/pnas.1110913108
Arc_043	Greenland	Braya Sø	67	-50.7	170	lake sediment	1	alkenone	-998	1999	29	10.1073/pnas.1101708108
Arc_044	Canada	Devon Ice Cap	75.33	-82.5	1800	glacier ice	2	d18O	1	1971	5	10.1038/301205a0
Arc_045	Canada	Penny Ice Cap P96	67.25	-66.75	1810	glacier ice	2	d18O	5	1980	25	10.1126/science.279.5351.692
Arc_053	Canada	Penny Ice Cap P96	67.25	-65.75	1810	glacier ice	2	melt	9	1984	25	10.1029/2001JB001707
Arc_062	Sweden	Tornetrask	68.26	19.6	320	tree	3	MXD	-39	2010	1	10.1177/0959683612460791
Arc_10	Central Russia	Polar Urals	66.8	65.8	N/A	tree	3	Maximum density	778	1990	1	10.1126/science.1066208
Arc_15	Scandinavia	Lapland	69.0	25.0	N/A	tree	3	Ring width	0	2005	1	10.1130/B30088.1
Arc_49	Scandinavia	Okshola cave	67.0	15.0	165.0	speleothem	4	Speleothem	-5565	1997	32	10.5194/cp-5-667-2009
Arc_52	North Atlantic	Lake Igaliku	61.0	-45.4	15.0	lake sediment	1	Lake sediment	-7577	2001	58	10.1007/s10933-012-9594-5
Arc_55	North Atlantic	P1003	63.8	5.3	0.0	Marine sediment	5	d18O	-5931	1998	8	10.1016/j.quascirev.2011.07.025
Arc_57	North Atlantic	MD99-2275	66.6	-17.4	0.0	Marine sediment	5	Alkenone	-2549	2001	4	10.1029/2011PA002169

Appendix C. Late Holocene glacier and ice sheet variability in south Greenland

C.1. Site descriptions

C1.1 Nuuk Ice Margin

We collected six boulders from the ice margin near Nuuk from immediately outboard of the latest drift limit (Figure C.1), approximately 100 m from the modern ice margin. Five boulders came from outboard of the ice sheet margin and one from outboard of Narsap Sermia, a marine terminating outlet glacier approximately 3 km south of the first five boulders. This site therefore marks the point when ice was last more advanced than its most recent limit. Chauvenet's criterion identifies the oldest age as an outlier, so we exclude it from the age calculation. The average age of the remaining five boulders is 8.3 ± 0.3 ka, similar to nearby deglacial ages for southwest Greenland (Larsen et al., 2013; Carlson et al. 2014). This indicates that, at least in this location, the advance depositing the latest drift was its most extensive since early in the Holocene.

C.1.2 Naajat Sermiat

The moraines sampled at Naajat Sermiat were deposited by a land-terminating extension of a marine-terminating outlet glacier of the Qassimiut Lobe of the ice Sheet (Naajat Sermiat has subsequently retreated onto land). The landscape shows three distinctive terrains (Figure C.2). The outermost is characterized by substantial soil development, clearly eroded boulders, and a deflated moraine (moraine A). Moraines B-D mark the boundary between this outermost terrain and the intermediate terrain, which has some soil development, and preservation of small erosional features, including extensively polished and striated bedrock. We sampled and processed 17 boulders from moraines B and D; 10 from innermost moraine D and seven from outermost moraine B. The innermost terrain was impossible to directly access and observe, but field and satellite photos indicate it is characterized by bare rock, with little to no soil development or vegetation.

We exclude the oldest age (NQ-13-36) from the calculation of the average age of the outer moraine (moraine B). The remaining six ages have an average age of 600 ± 170 B.P. We use the six youngest ages with overlapping uncertainties from the inner moraine (moraine D) to calculate an average moraine exposure age, at 520 ± 150 B.P. The two moraines have statistically identical ages, suggesting relatively rapid retreat and moraine deposition over no more than several hundred years.

C.1.3 Jespersen Bræ

Jespersen Bræ is a land-terminating outlet glacier of the Julianhåb Ice Cap. The modern drift limit is partially obscured by reworking by outwash streams of both Jespersen Bræ and the adjacent unnamed outlet glacier. However, several small moraines are preserved on the outwash plain from both glaciers (Figure C.3). We targeted a left lateral moraine on the hillside above the modern outwash (Figure C.3). Boulders were 2-3 m high and tended to be more angular than other moraines described here, and there is clear evidence of ongoing erosion around the boulders, possibly exacerbated by several feral sheep occupying the hillside. While the very active erosion and deposition in the outwash plain may have destroyed more recent late-Holocene advances more extensive than the most recent advance, this lateral moraine likely represents the largest late-Holocene advance, as there are no trimlines or moraines above this one.

The three youngest ages from the moraine have overlapping uncertainties and an average age of 3,700 ± 400 B.P. The late Holocene maximum of Jespersen Bræ therefore may have occurred in the earliest Neoglacial.

C.1.4 Sermeq Kangilleq

The land-terminating Sermeq Kangilleq is an outlet glacier of the Julianhåb Ice Cap which shares a trunk with Jespersen Bræ. Like Jespersen Bræ, there is an active outwash plain in front of the glacier, but the outwash stream is more channelized, permitting better moraines. We sampled two boulders from a series of three low moraine ridges approximately 1 km outboard of Sermeq Kangilleq. A further three ridges were approximately 300 m inboard of those we sampled, but these are on the opposite side of

the outwash stream and impossible to access on foot. As with Jespersen Bræ, it is possible that larger late Holocene advances were erased by outwash plain activity. However, there are no clear trimlines above the one which connects directly with the moraines we sampled (Figure C.4).

Unlike the other moraines and boulders sampled here, these moraine ridges are very small, with 2-3 m high crests. The boulders themselves are also much smaller, generally up to 0.5 m high. The Sermeq Kangilleq boulders showed very few signs of post-depositional weathering, and there was no vegetation growth or soil development in the matrix between boulders. We exclude one age based on Chauvenet's criterion, the remaining three ages average to 370 ± 140 B.P. This suggests the maximum late Holocene advance of Sermeq Kangilleq may have been its most recent advance.

C.1.5 Paarlit Sermia

Paarlit Sermia is a marine-terminating outlet glacier draining a small unnamed ice cap in southernmost Greenland. There is a clear recent trimline throughout the fjord at ~300 m above sea level. In addition to this main trimline, satellite imagery indicates a trimline fragment just above the larger trimline, ~3 km in front of the modern glacier front at ~315 m above sea level. The trimline is on a cliff that is actively eroding, however the top of the trimline fragment is a large boulder train with a clear crest separated from the cliffside, so the boulders were likely deposited by ice instead of rockfall from the cliff above (Figure C.5). Boulders from this trimline are sub-angular and 3-4 m high.

We dated six boulders from the trimline. The four youngest have overlapping uncertainties with an average age of 720 ± 120 B.P. Like Naajat Sermiat therefore, Paarlit Sermia experienced a late Holocene maximum sometime before ~1300 CE.

C.1.6 Tupaussat

We collected samples from two moraines adjacent to Tupaussat Lake in southern Greenland. Mosquito Glacier (informal name) is a cirque glacier which at present has no connection with either the Julianhåb Ice Cap or any smaller unnamed ice caps. The outer

moraine, at about 2 km from the modern glacier front, has a crest ~200 m above the valley floor, forming the southern boundary to Tupaussat Lake. It has significant soil and vegetation development; the sides and crests of the moraine are grassy, and boulders were often brittle with ample evidence of active weathering and large lichens covering the boulder (Figure C.6). The boulders themselves were at least 2-3 m high. We dated six boulders from the crest of this outer moraine, after excluding one outlier the remaining five boulders have an average age of 11.5 ± 1 ka.

The inner moraine is significantly smaller, although with similarly large 2-4 m boulders. There is limited soil development on the moraine, which is approximately 1.4 km from the current glacier front. We dated six boulders from the moraine. Three boulders have overlapping uncertainties with an average age of 840 ± 220 B.P. Therefore, like Paarlit Sermia, Jespersen Bræ, and Naajat Sermiat, the Tupaussat glacier reached its late Holocene maximum before the latest Little Ice Age.

C.2. Calculation of previously published ages

We recalculate all published deglacial ages within 5 km of the modern margin near our two deglacial sites using the same methods we used to calculate deglacial ages in this analysis. From south Greenland, we use ages from the highlands north of Narsarsuaq published by Carlson et al. (2014) and Nelson et al. (2014), as these are the only published deglacial ages within 5 km of the modern margin from southernmost Greenland. From west Greenland, we recalculate ages published by Larsen et al. (2013), Levy et al. (2012) and Carlson et al. (2014) near Sermeq glacier, Kangaarsarsuup Sermia, Kangiata Nunaata Sermia, and Insunnguata Sermia (near Kangerlussuaq). All ages are calculated using the Arctic production rate (Young et al. 2013) in the CRONUS online exposure age calculator, version 3 (hess.ess.washington.edu), with the Lal/Stone time-varying scaling scheme. Outliers are identified as those samples that do not overlap within 1-sigma uncertainty. Sample information, recalculated ages, and local averages are reported in Table C.1.

C.3 Description of Lower Nuulussuaq Lake and core analysis

To assess the timing of ice retreat as measured by a threshold lake adjacent to a moraine dated with ^{10}Be ages, we targeted Lower Nuulussuaq Lake (informal name). This lake is positioned adjacent to the outer Naajat Sermiat moraine discussed in the main text. The moraine is at the crest of a bedrock rise, so as soon as ice retreats from the moraine meltwater is diverted away from the lake (Figure C.7).

Lower Nuulussuaq lake is a small, shallow lake, ~2 m deep at its deepest point. In September 2014, we extracted four cores from the lake using a universal coring head and piston corer from Aquatic Research Instruments. Cores LNL1409-A1 and LNL1409-B1 (hereafter A1 and B1) are adjacent cores from the south basin of the lake, and LNL1409-F1 and LNL1409-G1 (hereafter F1 and G1) are from the North lake basin. We subsampled cores A1 and F1 in the field, and archived cores B1 and G1 in the Oregon State University marine geology repository (Table C.2). Cores B1 and G1 were scanned for relative element abundances every 0.5 mm on the Oregon State ITRAX XRF core scanner and photographed for high-resolution optical imagery.

We extracted macrofossils from cores A1 and F1. In core A1, we targeted the prominent silt-gyttja contact 17 cm below the surface. We retrieved one moss sample, two leaves, and a twig from this (see Figure C.8 for examples of macrofossils). Samples were subjected to standard acid-base-acid leaching prior to combustion to generate CO2 for preparation of graphite. Radiocarbon analyses were performed at Australian National University (ANU) at the Single Stage Accelerator Mass Spectrometry (SSAMS) Lab in the Research School of Earth Sciences (Fallon et al., 2010). The silt/gyttja contact in the cores from the north basin at 21 cm is less prominent; we targeted both this contact and several organic horizons within the lower silt unit.

All cores are characterized by an upper organic gyttja unit and a lower silt unit. The contact between these units is accompanied by significant geochemical changes revealed by XRF data in both scanned cores: core B1 is characterized by declining Ba/Ti, Si/Ti, and K/Ti ratios and increasing Br/Ti and Fe/Ti ratios above the contact (Figure C.9). In contrast, core G1 shows several prominent excursions in all values above the

contact, although these may be due to changes in grain size and layers of coarse, sorted fluvial sediment above the contacts.

The two-sigma age range for all ^{14}C ages is 0.7-0.05 ka BP. However, it is likely that cores F1 and G1 contain mostly reworked sediments. The lower sediments in these cores are more heterogenous than from the south basin, with a less distinct silt gyttja contact and several organic horizons. The main inflows and outflows to the lake are in the north basin, and the two layers of coarser sand also suggest this basin may be subject to high-energy events. Its location immediately adjacent to the proglacial delta may also make the north basin susceptible to deposition of reworked sediments. The south basin, by contrast, has a much clearer contact between the silt and gyttja layers, and is isolated from the north basin by a bathymetric rise, these cores therefore more likely record the timing of change from a silt to organic-dominated environment. The 2-sigma age range from this contact is 0.5-0.2 ka BP (Table C.3).

C.4 Outlier calculations using Chauvenet's criterion and 1-sigma overlap

Figures C.10 to C.21 show probability density plots for all sites. If there is only one plot for the site, Chauvenet's criterion excluded the same samples as those that do not overlap within one sigma. Where Chauvenet's criterion excludes different samples, a second PDF is shown for that site with samples excluded using Chauvenet's criterion.

C.5 References

Carlson, A.E., Winsor, K., Ullman, D.J., Brook, E.J., Rood, D.H., Axford, Y., LeGrande, A.N., Anslow, F.S., Sinclair, G., 2014. Earliest Holocene south Greenland ice sheet retreat within its late Holocene extent. *Geophysical Research Letters* 41, 5514-5521

Fallon, S.J., Fifield, L.,K., Chappell, J.M.., 2010. The next chapter in radiocarbon dating at the Australian National University: Status report on the single stage AMS. *Nucl. Instruments Methods Phys. Res. Sect. B Beam Interact. with Mater. Atoms* dx.doi.org/10.1016/j.nimb.2009.10.059.

Larsen, N.K., Funder, S., Kjær, K.H., Kjeldsen, K.K., Knudsen, M.F., Linge, H., 2013. Rapid early Holocene ice retreat in West Greenland. *Quaternary Science Reviews* 92, 310-323

Levy, L.B., Kelly, M.A., Howley, J.A., Virginia, R.A., 2012. Age of the Ørkendalen moraines, Kangerlussuaq, Greenland: constraints on the extent of the southwestern margin of the Greenland Ice Sheet during the Holocene. *Quaternary Science Reviews* 52, 1-5

Young, N.E., Schaefer, J.M., Briner, J.P., Goehring, B.M., 2013. A Be-10 production rate calibration for the Arctic. *Journal of Quaternary Science* 28, 515-526

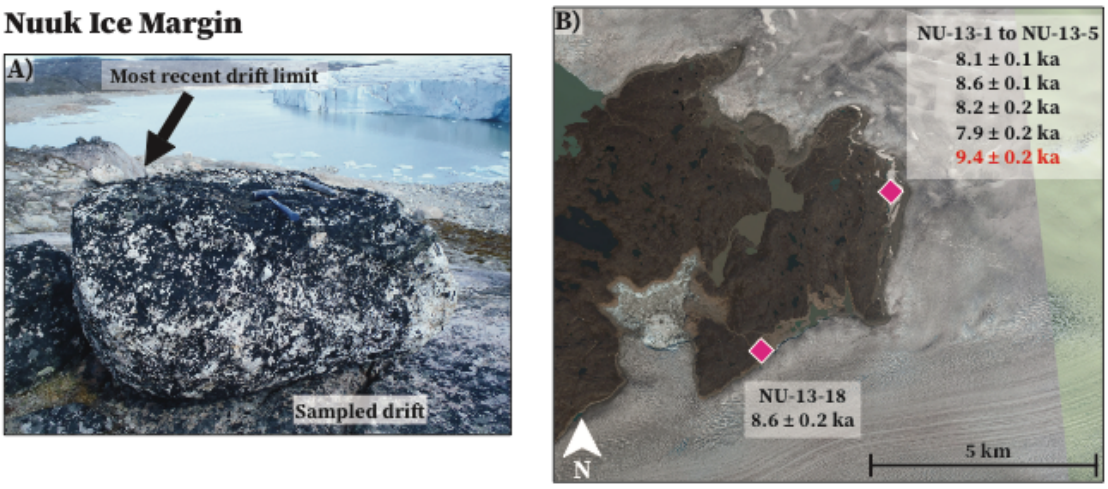

Figure C.1 Site map and photos of Nuuk ice margin samples. (A) Photograph of representative boulder showing the sampled landscape, most recent drift limit, and modern ice margin. (B) Satellite image showing locations and ages of boulders sampled. Ages in red italics are excluded from average calculations as outliers.

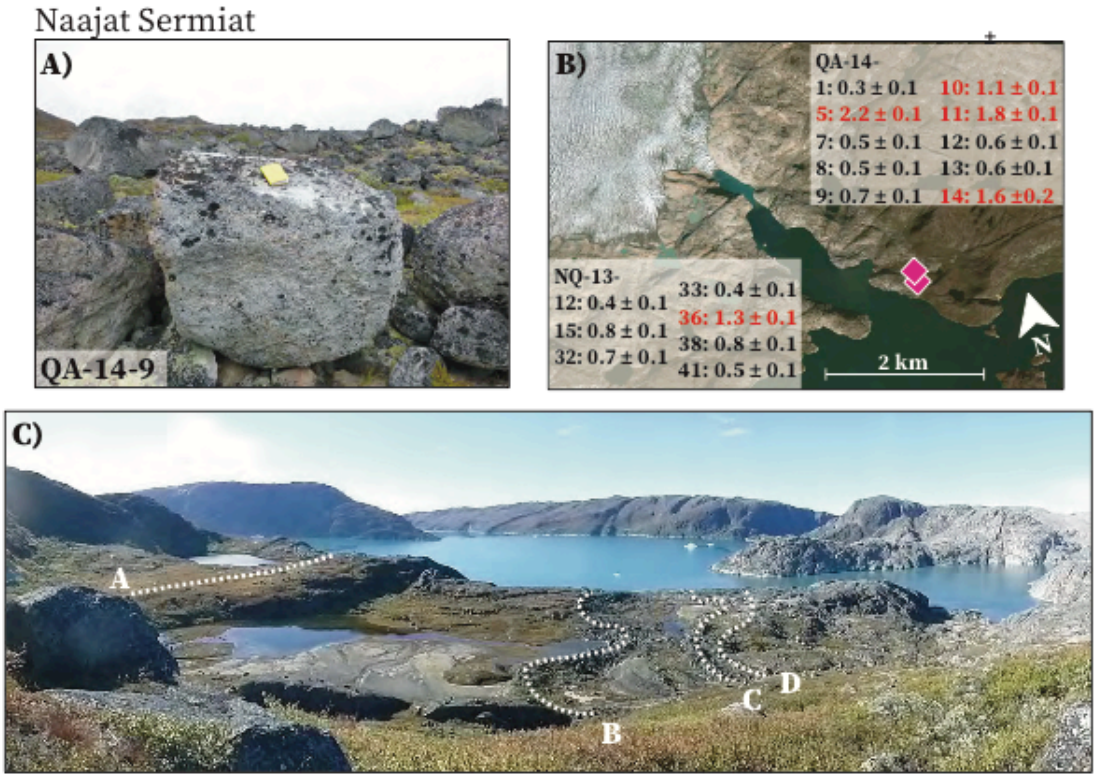

Figure C.2 Photographs and maps of Naajat Sermiat site. (A) representative boulder from moraine D. (B) Satellite image showing locations and ages of boulders sampled. Ages in red italics are excluded from average calculations as outliers. (C) panoramic photograph of moraines. Moraines B-D separate oldest terrain from intermediate terrain. Barren rock on far right is most recently deglaciated terrain.

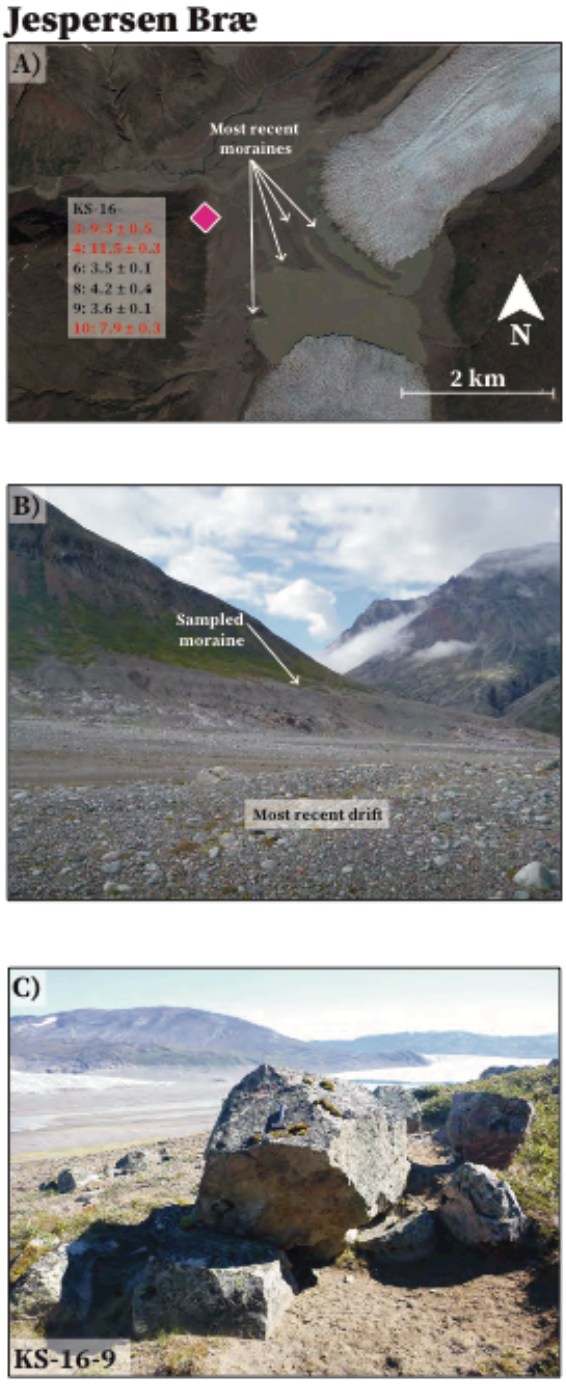

Figure C.3 Photographs and maps of Jespersen Bræ site. (A) Satellite image showing locations and ages of boulders sampled. Ages in red italics are excluded from average calculations as outliers. (B) View of sampled left lateral moraine from outwash plain. (C) Representative boulder from moraine. Jespersen Bræ is visible in background.

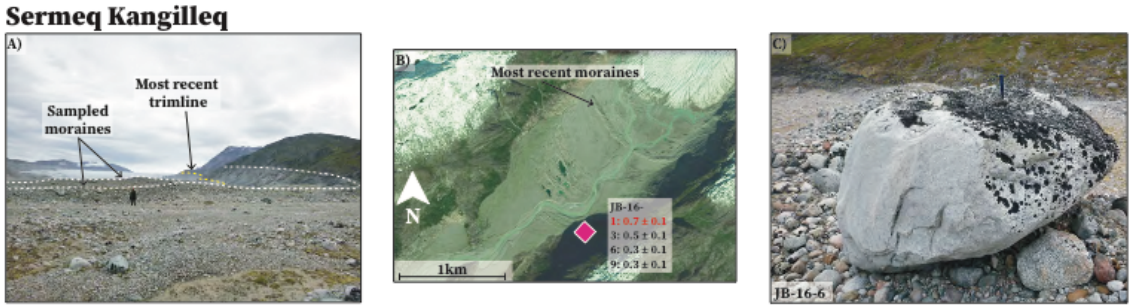

Figure C.4 Photographs and maps of Sermeq Kangilleq site. (A) Photograph of sampled morianes and most recent trimline, from outwash plain. (B) Satellite image showing locations and ages of boulders sampled. Ages in red italics are excluded from average calculations as outliers. (C) Representative boulder from frontal moraine.

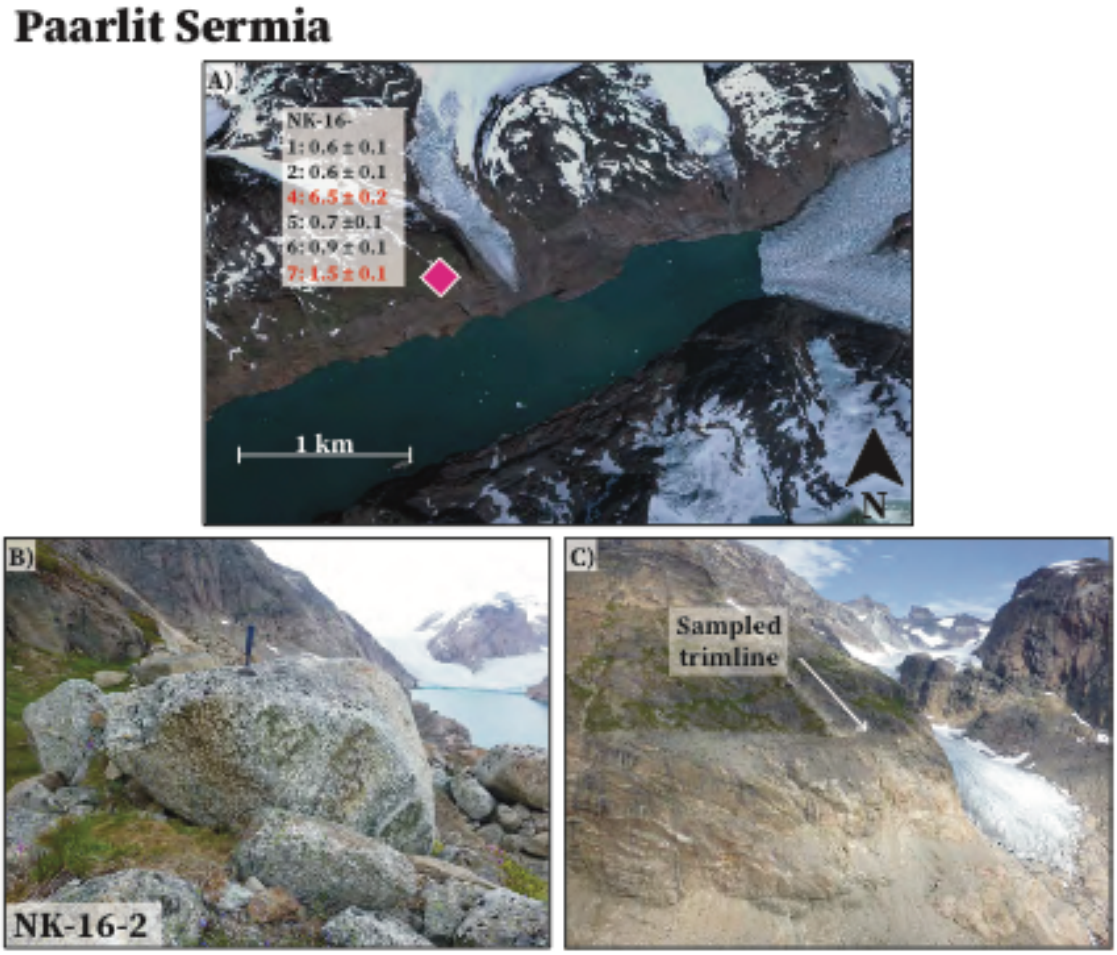

Figure C.5 Photographs and maps of Paarlit Sermia site. (A) Satellite image showing locations and ages of boulders sampled. Ages in red italics are excluded from average calculations as outliers. (B) Photograph of representative boulder. Paarlit Sermia is visible in background. (C) Aeial image of sampled trimline.

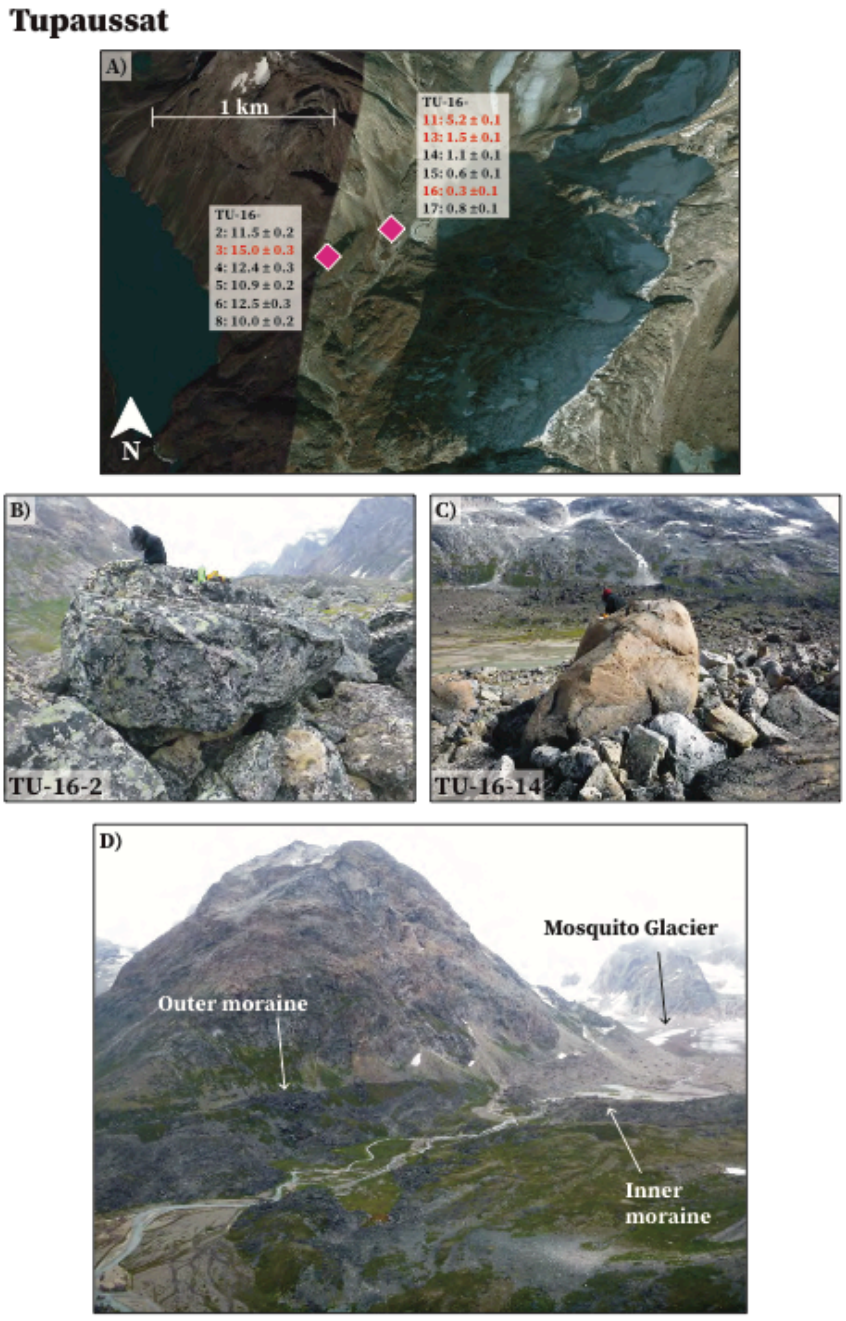

Figure C.6 Maps and photographs of Tupaussat site. (A) Satellite image showing locations and ages of boulders sampled. Ages in red italics are excluded from average calculations as outliers. (B) Representative boulder from outer moraine. (C) Representative boulder from inner moraine. (D) Aerial photograph of moraines, with a view of Mosquito Glacier's modern position.

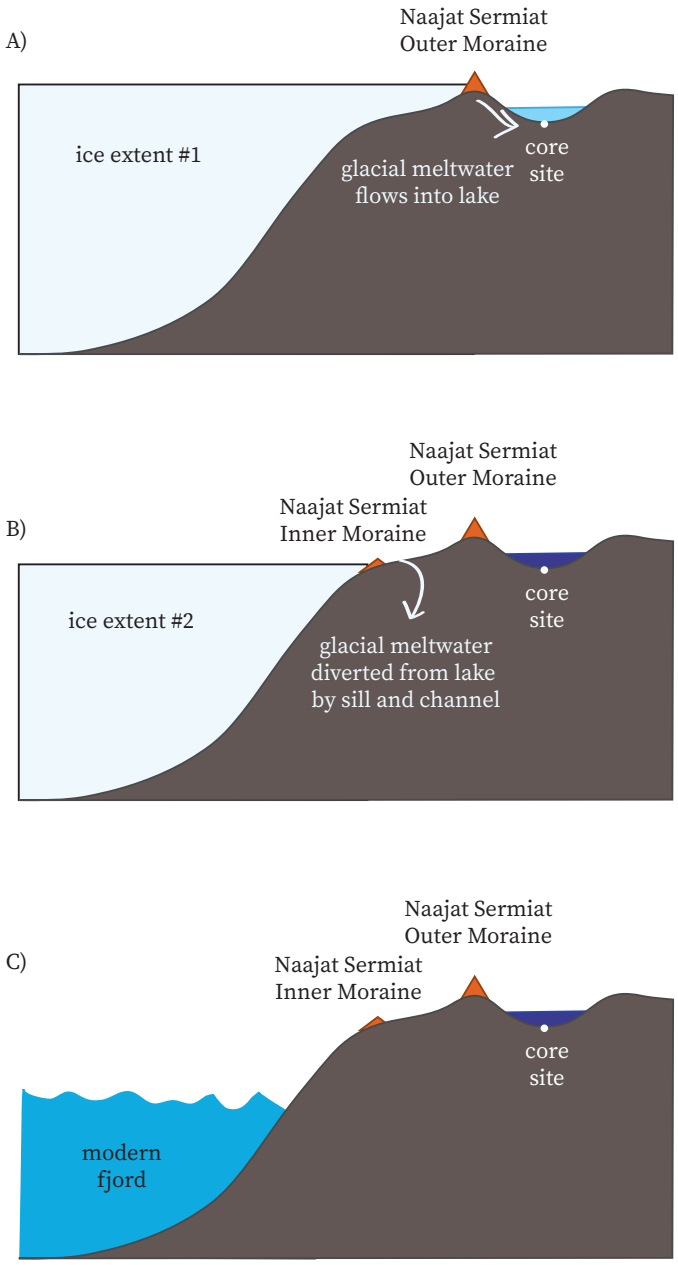

Figure C.7 General diagram of Lower Nuulussuaq Lake Formation. (A) Deposition of outer moraine, initiation of glacial sediment deposition in lake. (B) Retreat from outer moraine, glacial meltwater diverted from lake. (C) Retreat from inner moraine

Figure C.8 Examples of macrofossils

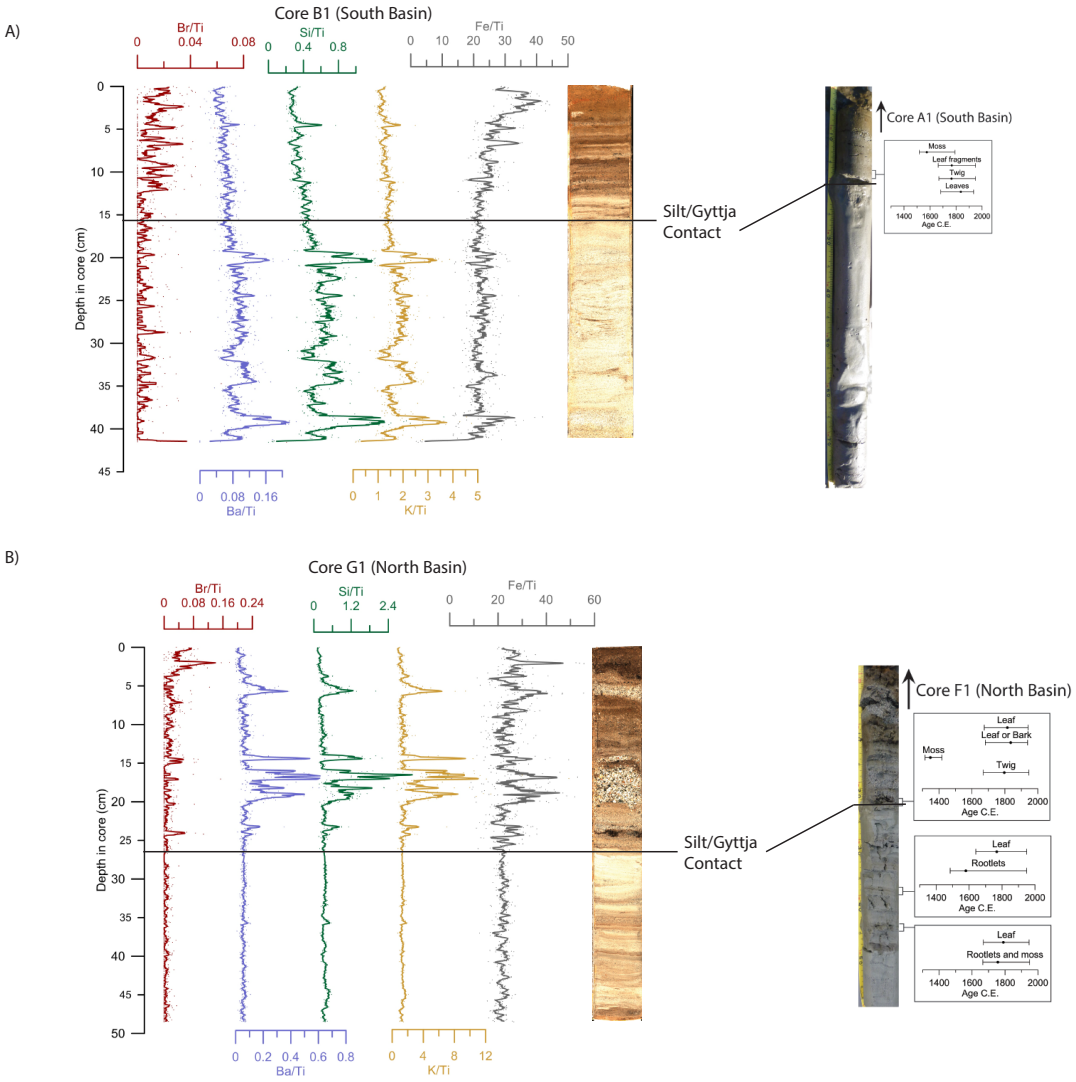

Figure C.9 Summary of geochemical and radiocarbon results from Lower Nuulussuaq Lake cores. (A) South basin cores. Left graph is geochemical results from ITRAX XRF (Core B1). Dots are individual measurements at 0.5 mm resolution, heavy line is 5-pt running mean. Right is photograph of core A1, with 14C ages. Brackets represent total 2-sigma age range calculated in CALIB, points are the median probability. (B) South basin cores. Left graph is geochemical results from ITRAX XRF (Core G1). Dots are individual measurements at 0.5 mm resolution, heavy line is 5-pt running mean. Right is photograph of core F1, with 14C ages. Brackets represent total 2-sigma age range calculated in CALIB, points are the median probability.

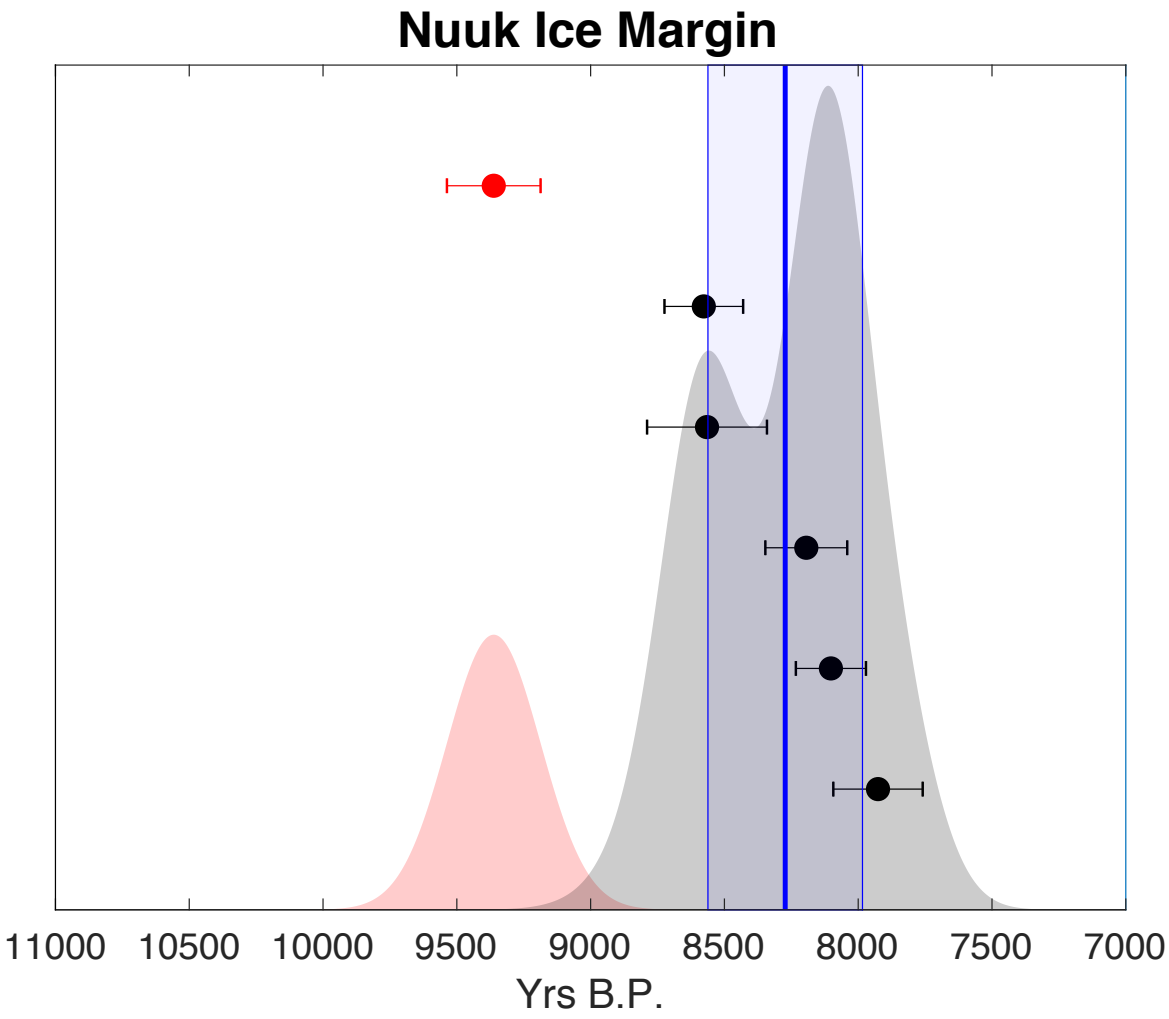

Figure C.10 Nuuk Ice Margin PDF

Average age of samples (outliers excluded): 8273

Standard deviation of samples (outliers excluded): 289

Number of samples (including outliers): 7

Number of outliers excluded: 1

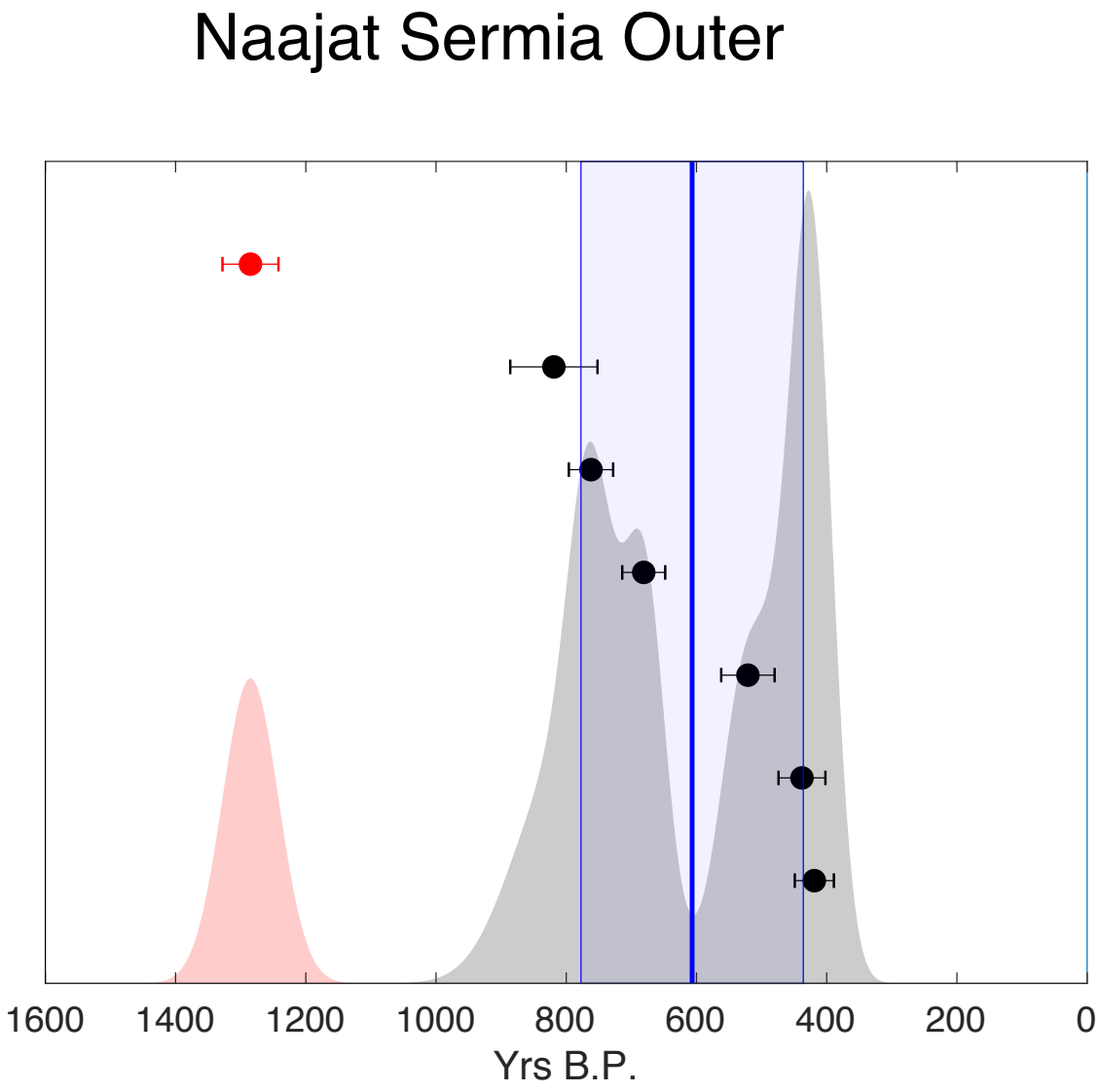

Figure C.11 Nuuk Ice Margin PDF

Average age of samples (outliers excluded): 607

Standard deviation of samples (outliers excluded): 171

Number of samples (including outliers): 7

Number of outliers excluded: 1

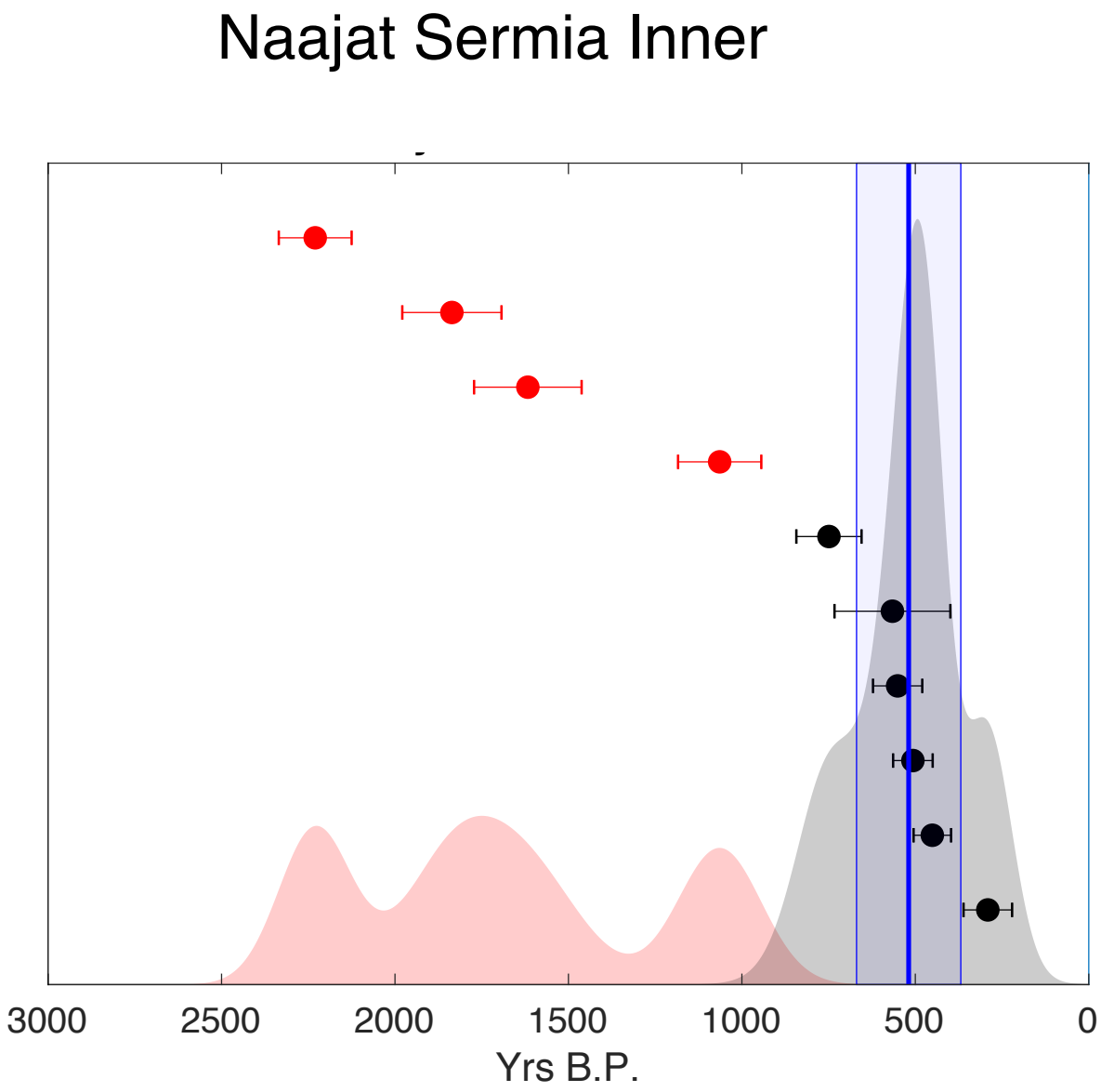

Figure C.12 Naajat Sermia Inner PDF

Average age of samples (outliers excluded): 519

Standard deviation of samples (outliers excluded): 150

Number of samples (including outliers): 10

Number of outliers excluded: 4

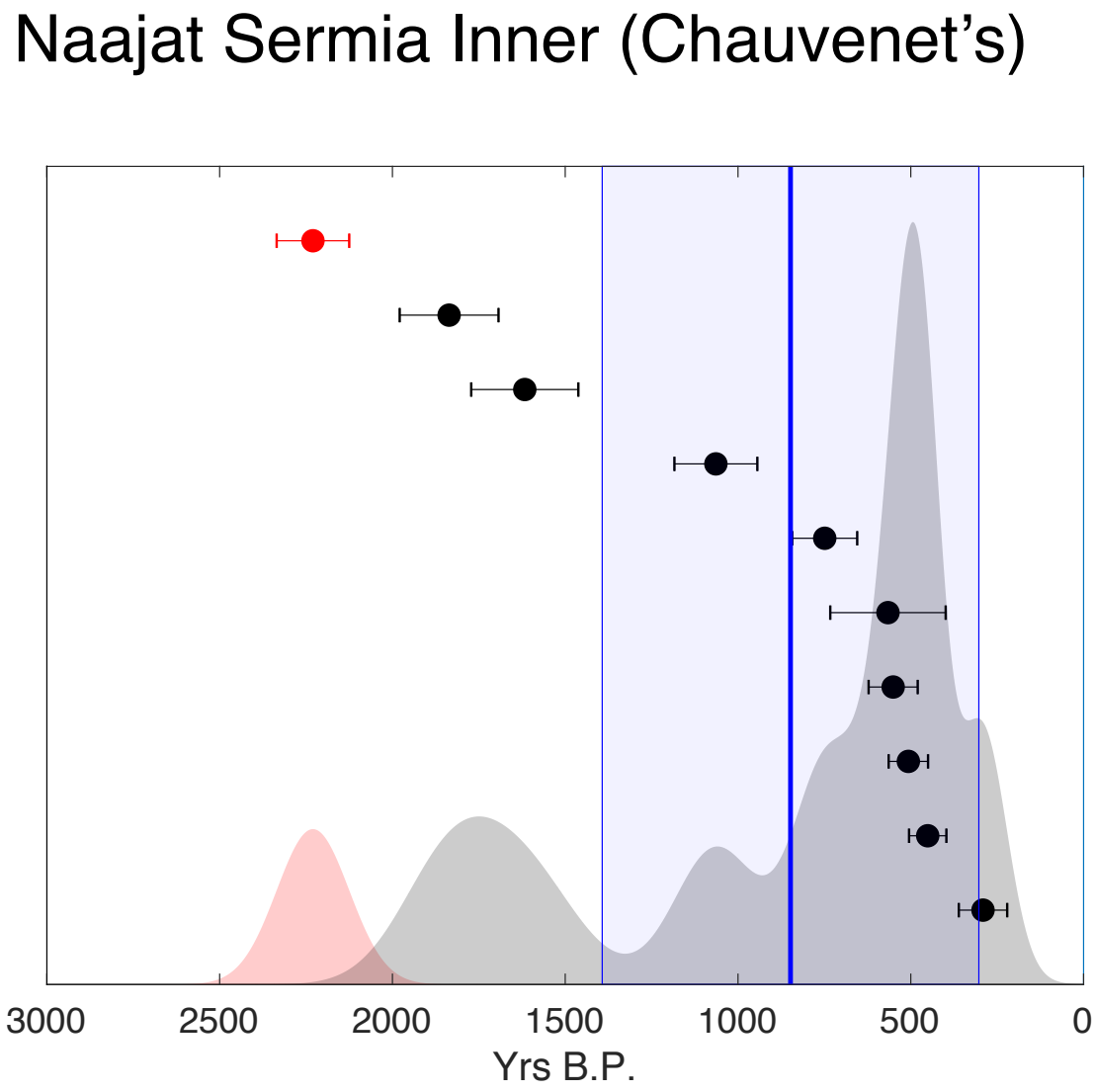

Figure C.13 Naajat Sermia Inner PDF (Chauvenet's)

Average age of samples (outliers excluded): 848

Standard deviation of samples (outliers excluded): 545

Number of samples (including outliers): 10

Number of outliers excluded: 1

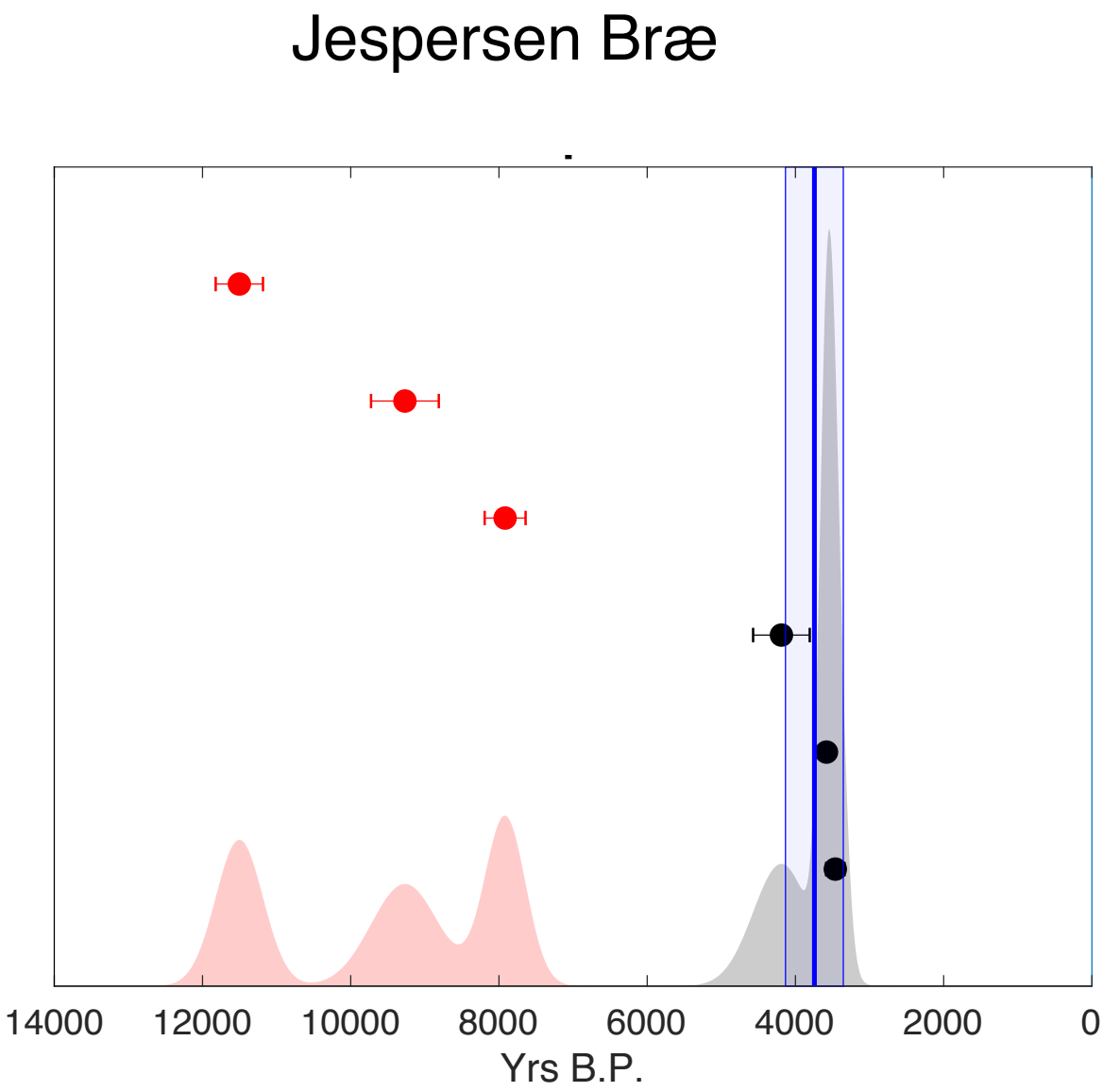

Figure C.14 Jespersen Bræ PDF

Average age of samples (outliers excluded): 3744

Standard deviation of samples (outliers excluded): 390

Number of samples (including outliers): 6

Number of outliers excluded: 3

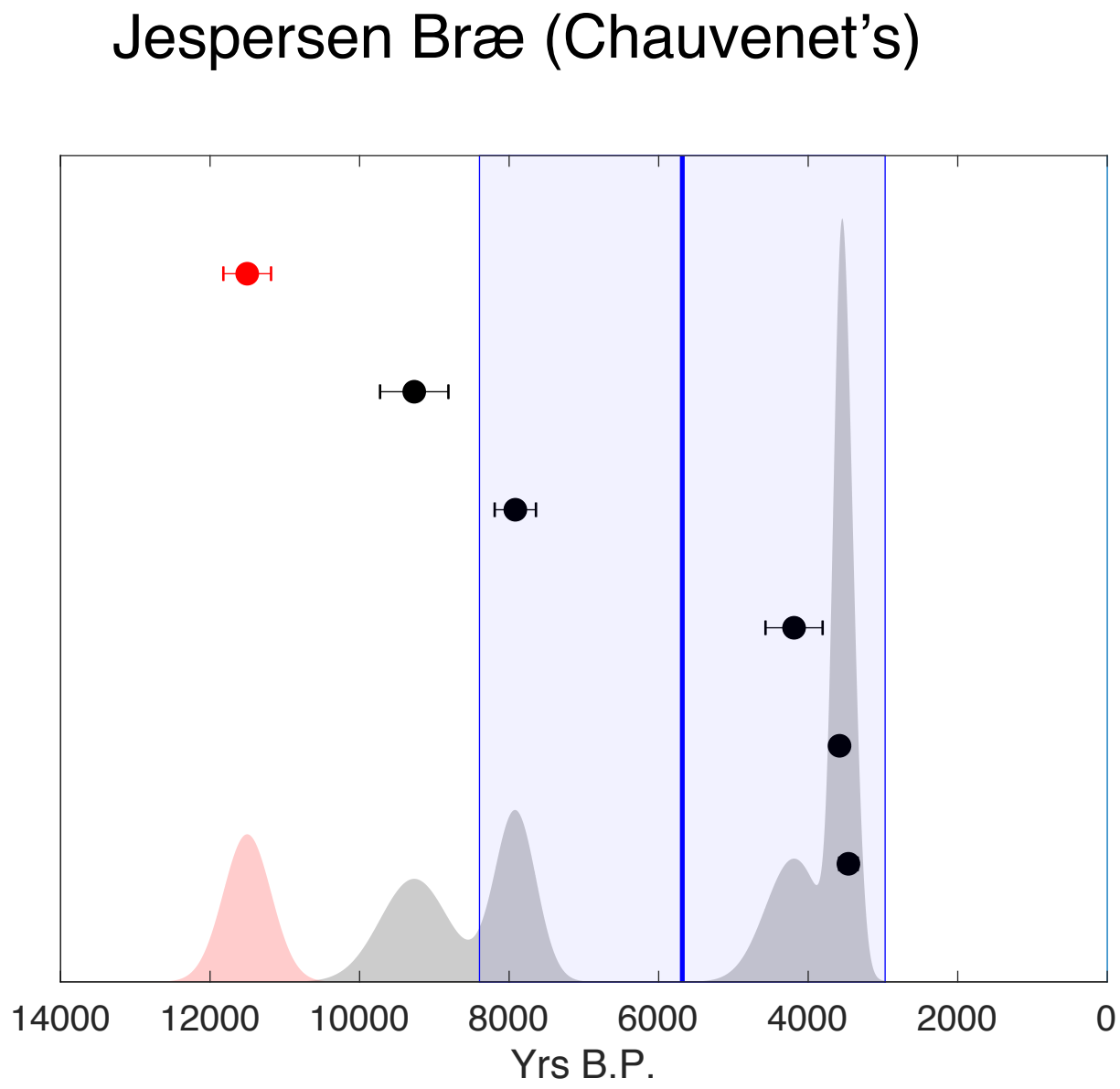

Figure C.15 Jespersen Bræ PDF(Chauvenet's)

Average age of samples (outliers excluded): 5684

Standard deviation of samples (outliers excluded): 2713

Number of samples (including outliers): 6

Number of outliers excluded: 1

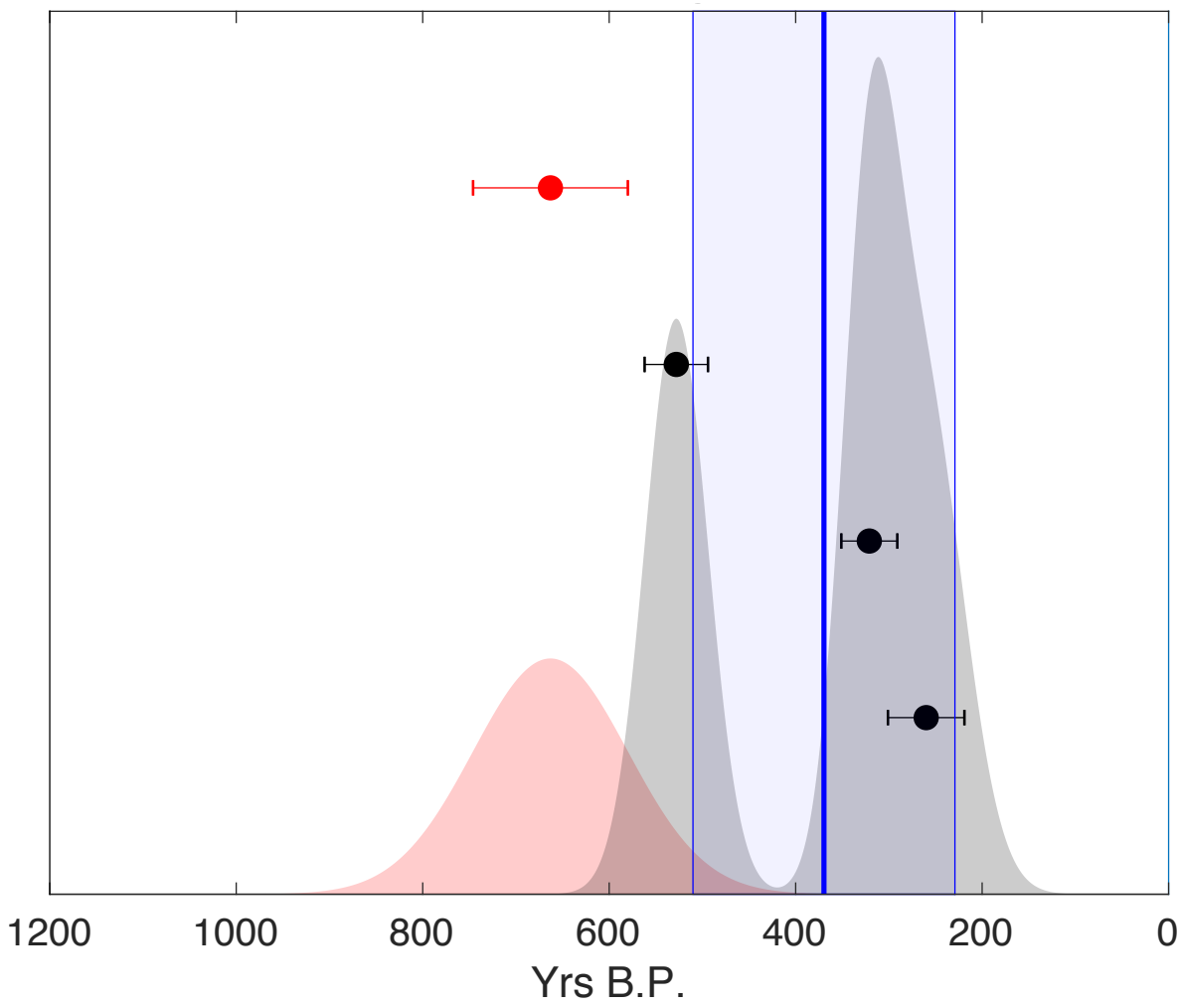

Figure C.16 Sermeq Kangilleq PDF

Average age of samples (outliers excluded): 370

Standard deviation of samples (outliers excluded): 140

Number of samples (including outliers): 4

Number of outliers excluded: 1

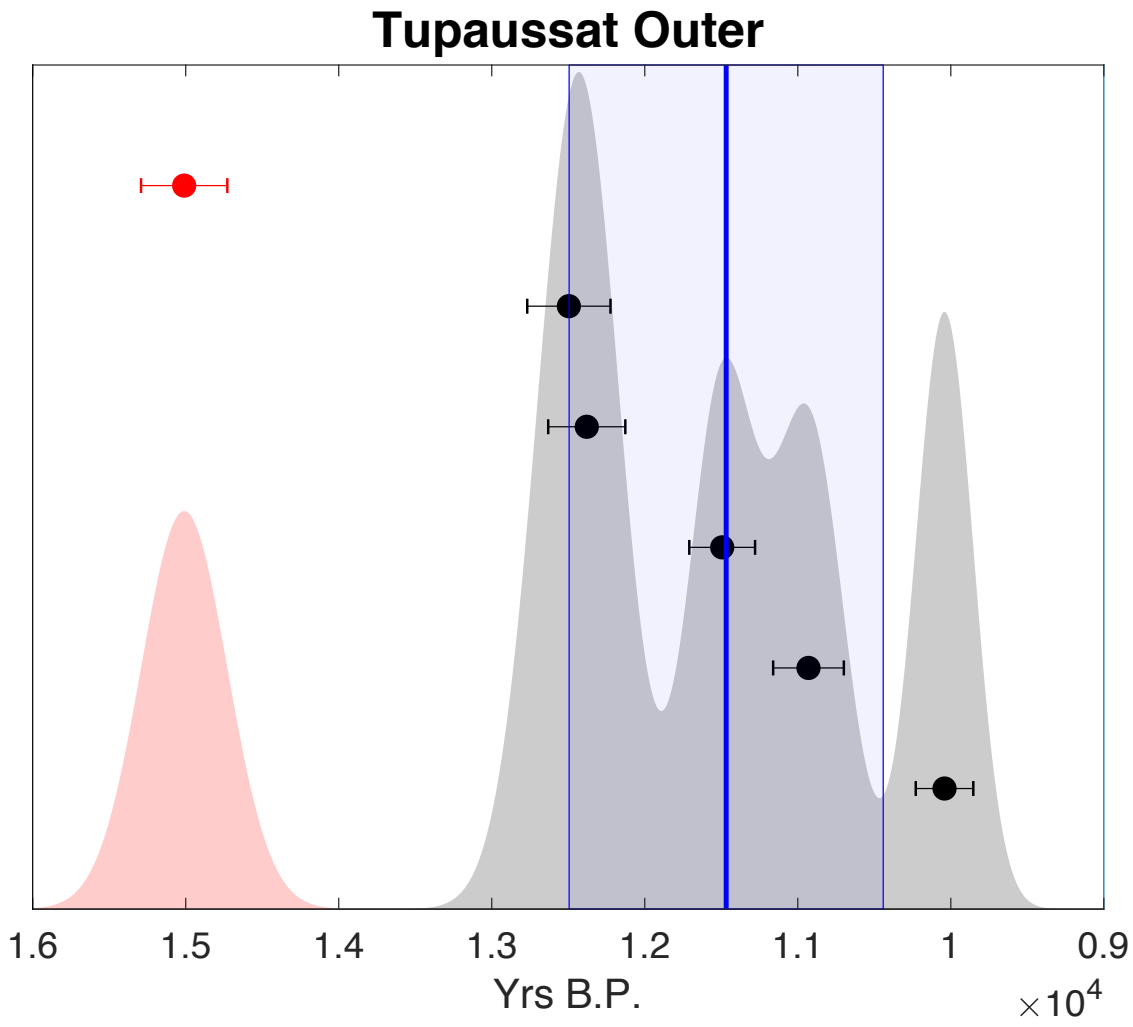

Figure C.17 Tupaussat Outer PDF

Average age of samples (outliers excluded): 11486

Standard deviation of samples (outliers excluded): 1026

Number of samples (including outliers): 6

Number of outliers excluded: 1

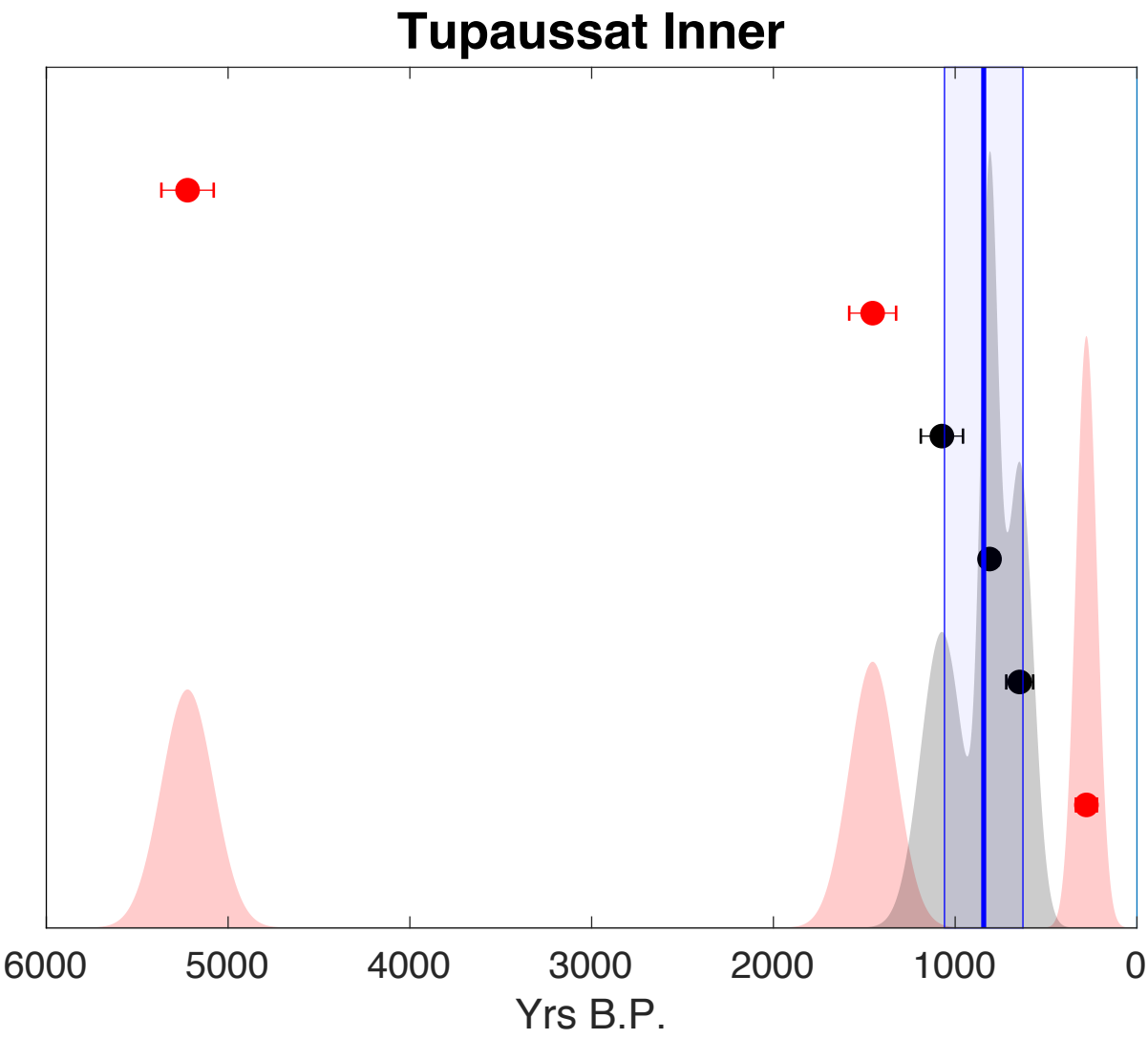

Figure C.18 Tupaussat Inner PDF

Average age of samples (outliers excluded): 843

Standard deviation of samples (outliers excluded): 216

Number of samples (including outliers): 6

Number of outliers excluded: 3

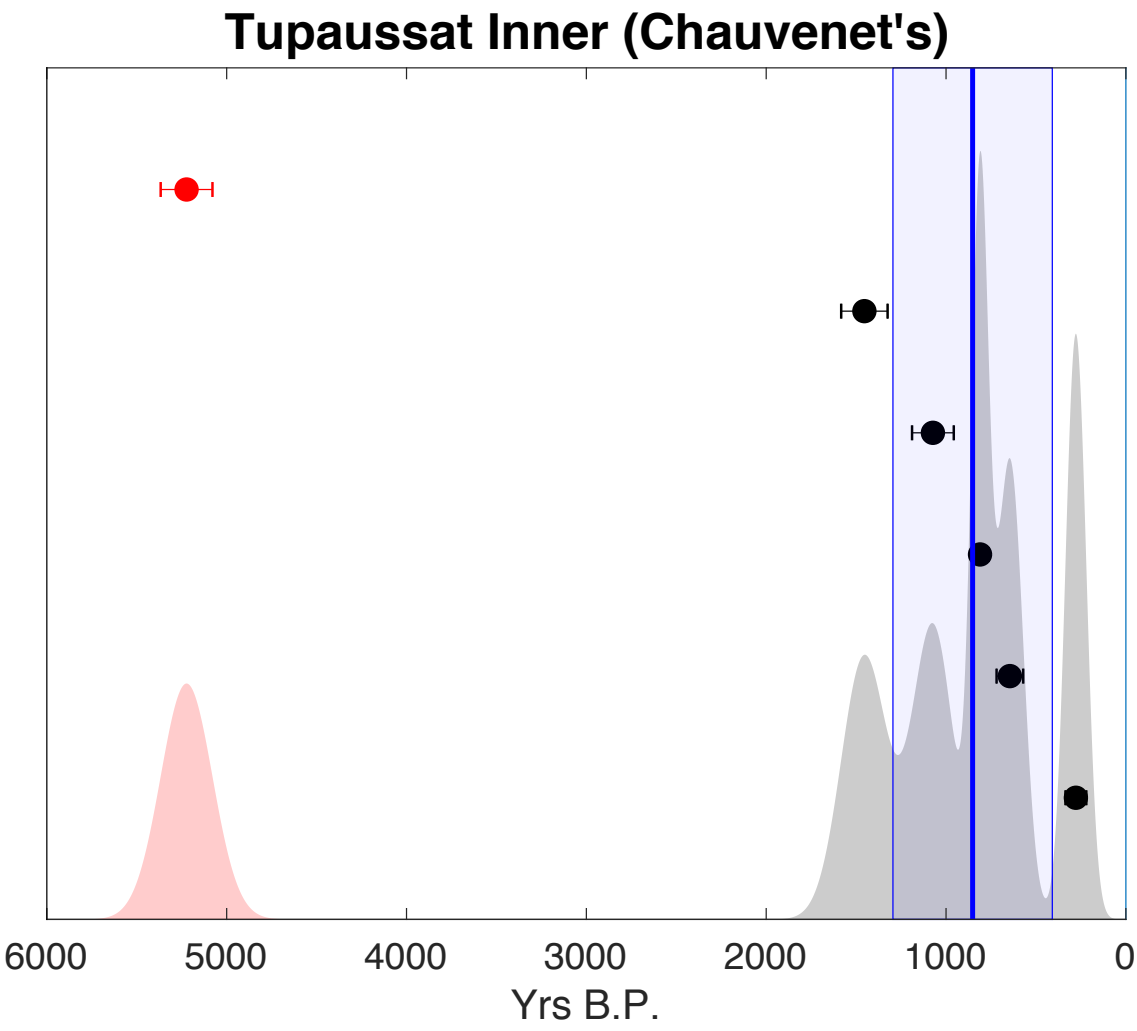

Figure C.19 Tupaussat Inner PDF (Chauvenet's)

Average age of samples (outliers excluded): 852

Standard deviation of samples (outliers excluded): 443

Number of samples (including outliers): 6

Number of outliers excluded: 1

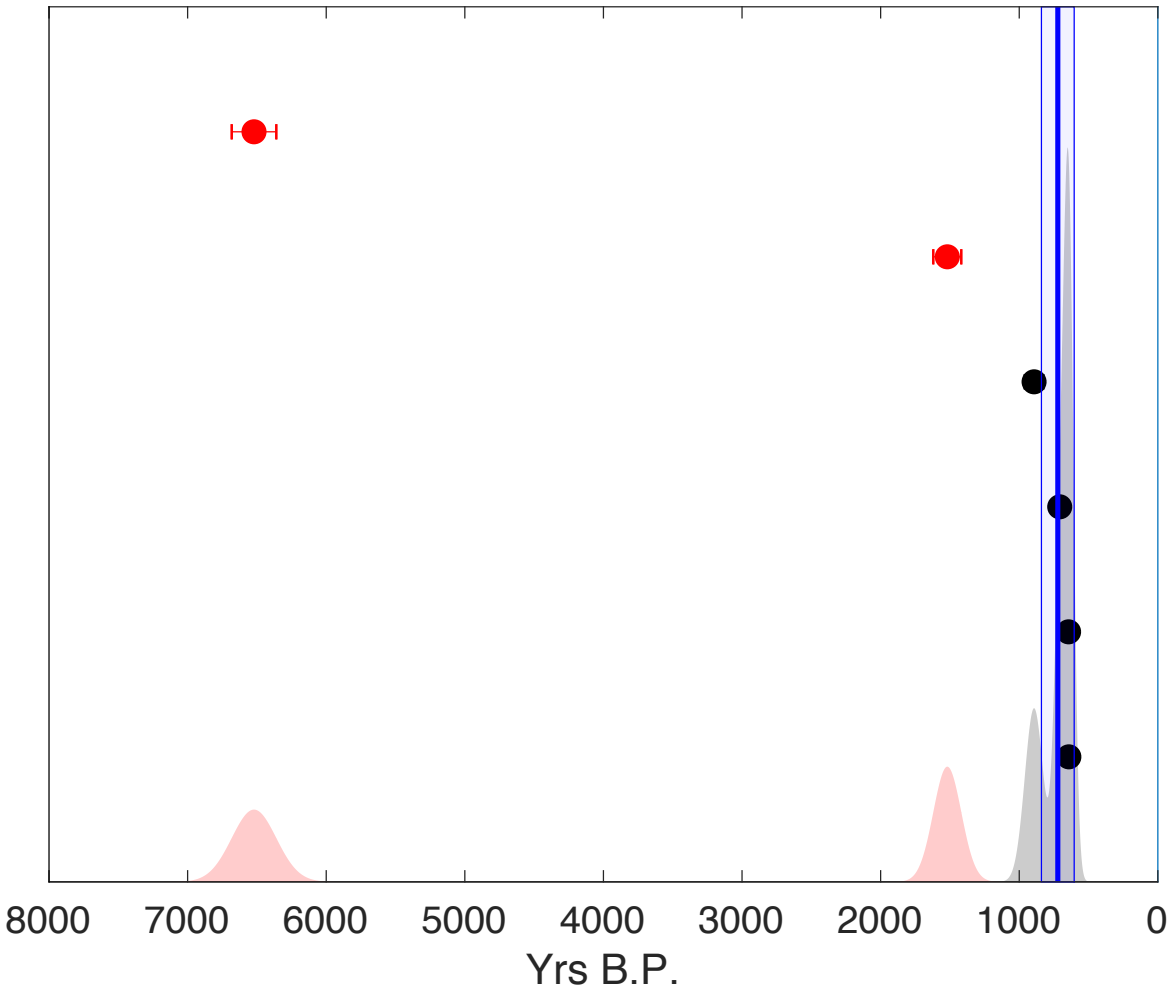

Figure C.20 Paarlit Sermiat PDF

Average age of samples (outliers excluded): 722

Standard deviation of samples (outliers excluded): 118

Number of samples (including outliers): 6

Number of outliers excluded: 2

Paarlit Sermiat (Chauvenet's)

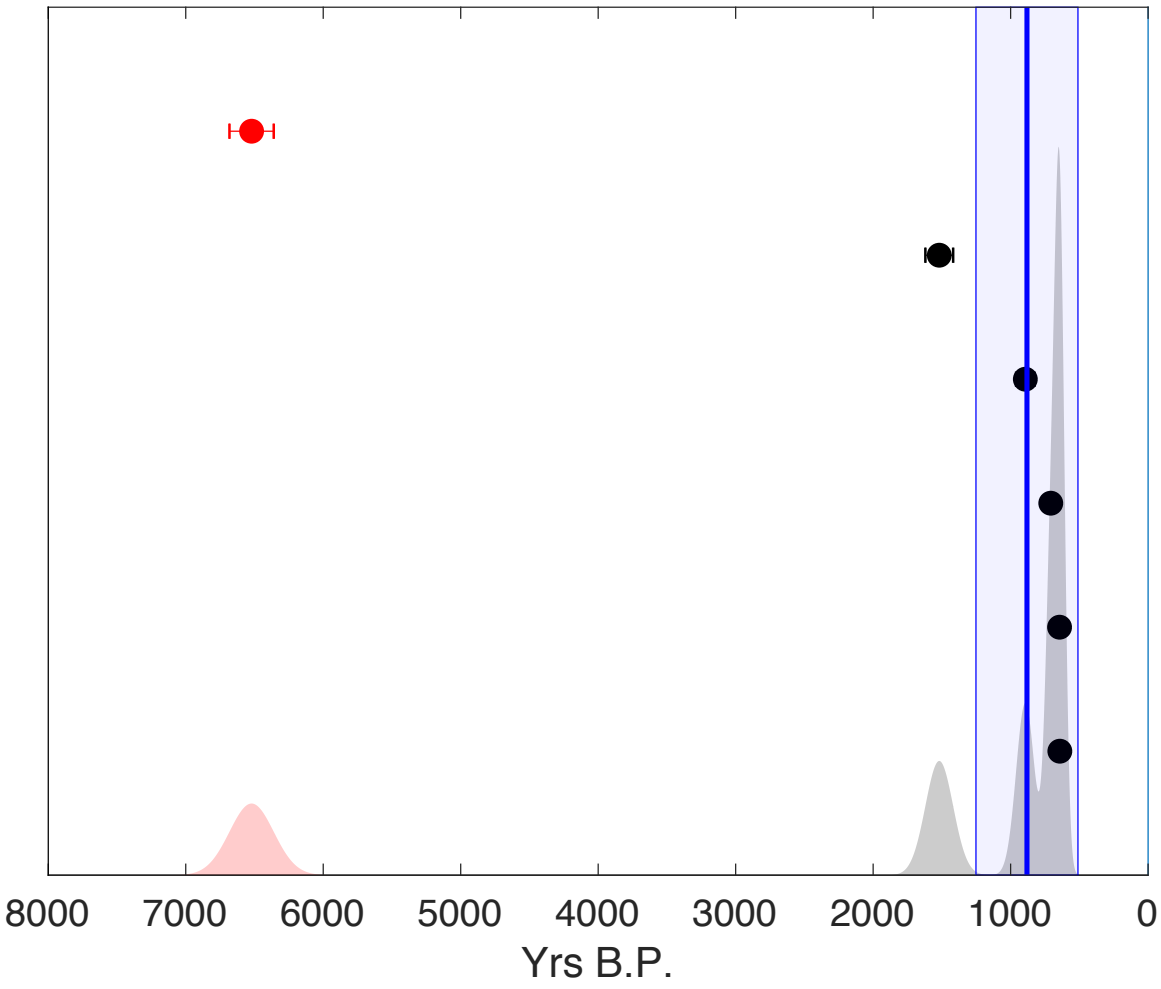

Figure C.21 Paarlit Sermiat PDF (Chauvenet's)

Average age of samples (outliers excluded): 881

Standard deviation of samples (outliers excluded): 370

Number of samples (including outliers): 6

Number of outliers excluded: 1

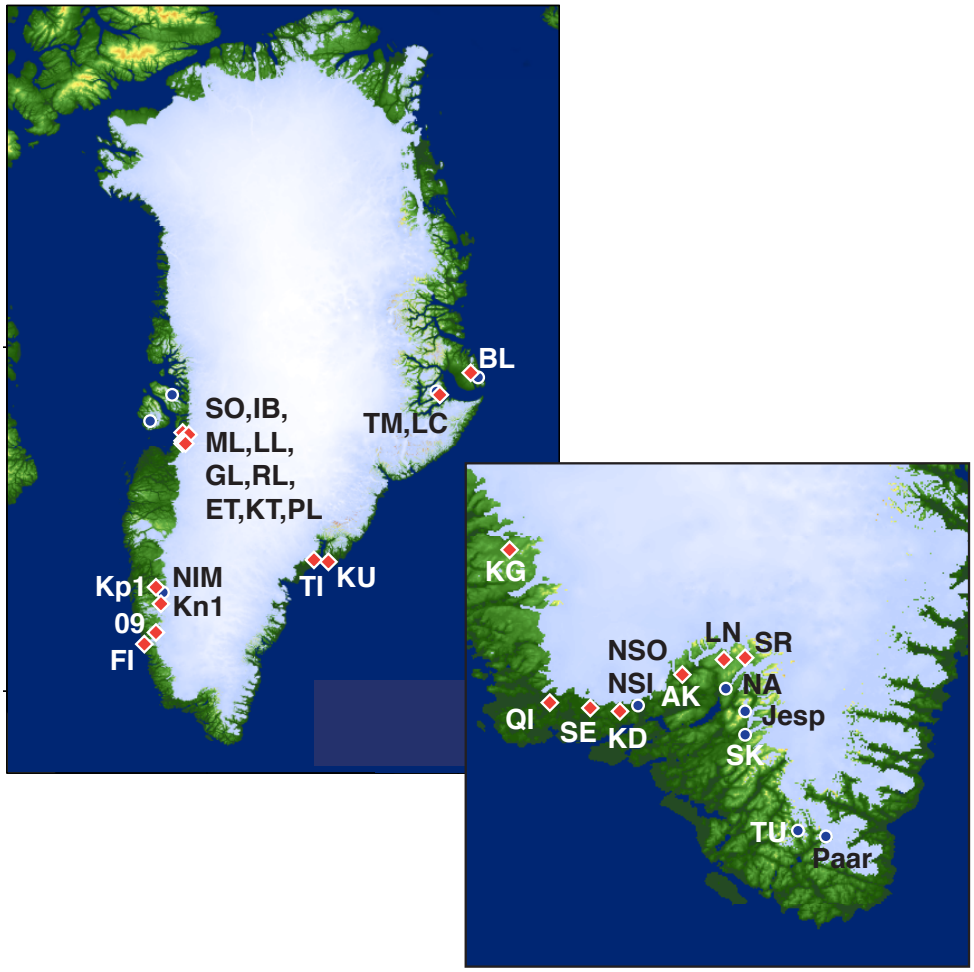

Figure C.22 Map of threshold lakes and cosmogenic sites referred to in text. See table C.6 for explanation of abbreviations

Table C.1 Published Sample Information

Table C.1: Published Sample Information

Sample Name	Publication	Latitude (°N)	Longitude (°E)	Elevation (m asl)	Thickness (cm)	Topographic Shielding Factor	^{10}Be Concentration (atoms g^{-1})	^{10}Be Uncertainty (atoms g^{-1})	Sample Age (yrs B.P.)	Internal Error (yrs)	External Error (yrs)
SOUTH GREENLAND											
Narsarsuaq Highlands								**Average**	11208 ± 421		
NA-19-08	Carlson et al. 2014	61.19696667	-45.3122	496	1.5	0.9996	79408.91612	2097.885322	11464	304	526
NA-20-08	Carlson et al. 2014	61.19691667	-45.31223333	501	1.5	0.9996	78673.36791	3102.522134	11299	447	616
NA-21-08	Carlson et al. 2014	61.19593333	-45.31413333	514	2	0.9996	81638.31738	1709.258529	11638	244	500
NA-22-08	Carlson et al. 2014	61.19593333	-45.31413333	514	1.5	0.9996	74906.21576	1938.152287	10608	275	483
GLX25A	Nelson et al. 2014	61.193	-45.302	556	5	0.9996	81700	2000	11476	282	514
GLX25B	Nelson et al. 2014	61.193	-45.302	554	3	0.9996	77900	1190	10766	165	436
NUUK TO KANGERLUSSUAQ											
Kangaarsuup Sermia								**Average**	10168 ± 100		
BUK0871	*Larsen et al. 2013*	*64.0478*	*-49.5806*	*1212*	*8.0*	*0.9996*	*157453.39*	*11760.91*	*12580*	*943*	*1054*
BUK0873	*Larsen et al. 2013*	*64.0477*	*-49.5820*	*1210*	*10.0*	*0.9996*	*335157.62*	*11729.34*	*27419*	*966*	*1413*
BUK0874	Larsen et al. 2013	64.0456	-49.5783	1179	10.0	0.9996	121765.70	4468.62	10130	373	532
BUK0875	Larsen et al. 2013	64.0456	-49.5783	1179	8.0	0.9996	124632.82	5037.28	10205	413	563
Sermeq								**Average**	9217 ± 100		
BUK0856	*Larsen et al. 2013*	*63.6050*	*-49.8066*	*1130*	*7.0*	*0.9996*	*295524.11*	*6612.84*	*25251*	*569*	*1107*
BUK0857	*Larsen et al. 2013*	*63.6056*	*-49.8079*	*1142*	*1.0*	*0.9996*	*269654.32*	*6755.49*	*21693*	*546*	*981*
BUK0858	*Larsen et al. 2013*	*63.6085*	*-49.7955*	*1232*	*5.0*	*0.9996*	*312610.82*	*9966.19*	*24052*	*771*	*1189*
BUK0862	Larsen et al. 2013	63.6019	-49.8471	900	9.0	0.9996	87454.60	5285.06	9217	558	656
BUK0863	Larsen et al. 2013	63.6019	-49.8471	900	5.0	0.9996	90293.71	3982.98	9216	407	534
BUK0865	*Larsen et al. 2013*	*63.5976*	*-49.8730*	*1005*	*3.0*	*0.9996*	*215558.71*	*9967.83*	*19861*	*923*	*1187*
BUK0866	*Larsen et al. 2013*	*63.5977*	*-49.8756*	*1005*	*5.0*	*0.9996*	*222915.89*	*9352.61*	*20882*	*881*	*1179*
Kangiata Nunaata Sermia								**Average**	9582 ± 1059		
BUK0876	*Larsen et al. 2013*	*64.3560*	*-49.2981*	*1303*	*8.0*	*0.9996*	*235616.52*	*6846.54*	*17470*	*510*	*831*
BUK0879	Larsen et al. 2013	64.3547	-49.2941	1263	6.0	0.9996	127925.53	14106.38	9582	1059	1118
BUK0881	*Larsen et al. 2013*	*64.3244*	*-49.5740*	*760*	*6.0*	*0.9996*	*113230.24*	*14267.97*	*13299*	*1681*	*1754*
Isunnguata Sermia								**Average**	6934 ± 340		
KN-11-08	Carlson et al. 2014	67.0907	-50.241	180	2	0.9996	37654.20807	3692.462567	7377	725	776
KN-12-08	Carlson et al. 2014	67.0907	-50.241	180	1.5	0.9996	34096.25546	1359.937047	6678	267	366
KN-13-08	Carlson et al. 2014	67.0907	-50.241	180	2	0.9996	34404.99231	1819.057986	6765	358	439
KN-14-08	*Carlson et al. 2014*	*67.0897*	*-50.2416*	*168*	*2.5*	*0.9996*	*26466.14264*	*964.5660636*	*5303*	*194*	*277*
KN-15-09	Carlson et al. 2014	67.1532	-50.0551	514	3	0.9996	49511.67434	1452.993799	7124	209	339
KN-16-08	Carlson et al. 2014	67.0962	-50.2439	174	2.5	0.9996	39167.73996	2035.792697	7729	403	496
KN-18-09	Carlson et al. 2014	67.1535	-50.0552	510	2	0.9996	48449.61375	1491.051893	6948	214	337
KN-19-09	Carlson et al. 2014	67.15371667	-50.05485	507	3.5	0.9996	46083.94361	979.681982	6711	143	289
LL0901	Levy et al. 2012	67.105	-50.29	247	1.8	0.9996	3.47E+04	8.17E+02	6386	151	283
LL0902	Levy et al. 2012	67.103	-50.282	241	2.6	0.9996	3.77E+04	1.08E+03	7017	201	331
LL0903	Levy et al. 2012	67.101	-50.283	242	1.8	0.9996	3.78E+04	1.12E+03	6985	207	334
LL0904	Levy et al. 2012	67.092	-50.294	224	2.6	0.9996	3.65E+04	9.74E+02	6909	185	318
LL0906	Levy et al. 2012	67.159	-50.102	432	2	0.9996	4.42E+04	9.73E+02	6824	150	296
LL0907	Levy et al. 2012	67.158	-50.104	434	2.4	0.9996	4.56E+04	1.19E+03	7044	184	322
LL0908	Levy et al. 2012	67.158	-50.105	423	1.5	0.9996	4.72E+04	1.45E+03	7299	225	354
LL0909	Levy et al. 2012	67.161	-50.119	449	1.6	0.9996	4.32E+04	1.35E+03	6545	205	319
LL0911	Levy et al. 2012	67.162	-50.116	458	2.6	0.9996	4.36E+04	1.13E+03	6603	171	301

Table C.2: Description of Cores from Lower Nuulussuaq Lake						
Core Name	**Basin**	**Latitude**	**Longitude**	**Water Depth (m)**	**Core Length (cm)**	**Comments**
LNL1409-A1	South Basin	61.01328	-46.52037	1.6	81	Subsampled in field
LNL1409-B1	South Basin	61.0133	-46.5204	1.6	44	Archived at Oregon State University
LNL1409-F1	North Basin	61.01398	-46.52046	2	57	Subsampled in field
LNL1409-G1	North Basin	61.01398	-46.52046	2	45	Archived at Oregon State University

Table C.2 Description of Cores from Lower Nuulussuaq Lake

Table C.3: Radiocarbon Ages									
Core	**Depth**	**OSU Lab ID**	**Material**	**ANUID**	**Raw14C Age**	**Error**	**2-sigma minimum (yrs B.P.)**	**2-sigma maximum (yrs B.P.)**	**2-sigma median (yrs B.P.)**
Core A1									
LNL1409-A1	16.5	D1	Leaves	13245	110	25	318	65	163
LNL1409-A1	16.5	D2	Twig	13246	155	20	332	51	235
LNL1409-A1	17.5	E1	Leaf frags	13247	170	25	337	50	233
LNL1409-A1	17.5	E2	Moss	13248	280	25	483	209	425
Core F1									
LNL1409-F1	21	A1	Twig	13238	145	20	331	55	203
LNL1409-F1	21	A2	Moss	13239	565	20	685	582	652
LNL1409-F1	21	A3	Leaf or Bark	13240	125	20	319	62	165
LNL1409-F1	21	A4	Leaf	13241	135	25	325	59	185
LNL1409-F1	36.5	B1	Rootlets	13242	280	40	515	50	420
LNL1409-F1	36.5	B2	Leaf	13350	210	35	359	50	232
LNL1409-F1	42.5	C2	Rootlets/mos	13243	175	20	335	50	234
LNL1409-F1	42.5	C3	Leaf	13244	145	25	331	54	200

Table C.3 Radiocarbon ages from Lower Nuulussuaq Lake

Table C.4 Blank Information							
Run	**OSU Sample Name**	**ANSTO Sample Code**	**Carrier Added (ug**	**LE_BeO [A]**	**Be10/Be9**	**sigma**	**sigma[%]**
Dec-17	Blank-16-1	IBlk161	0.869	3.33	2.162E-15	4.24E-16	19.63
Dec-17	Blank-16-3	IBlk163	0.8716	3.95	1.006E-15	1.90E-16	18.92
Dec-17	Blank-16-4	IBlk164	0.848	5.07	1.011E-15	1.69E-16	16.68
Dec-17	Blank-17-1	IBlk171	0.835	2.92	1.257E-15	2.68E-16	21.33
Dec-17	Blank-17-2	IBlk172	0.874	2.97	1.403E-15	3.62E-16	25.83
Dec-17	Blank-17-3	IBlk173	0.87	2.56	1.026E-15	2.36E-16	22.96
Dec-17	Blank-17-4	IBlk174	0.876	1.9	1.287E-15	3.72E-16	28.88
Dec-17	Blank-17-5	IBlk175	0.856	2.97	3.722E-16	1.86E-16	50.01
Dec-17	Blank-17-6	IBlk176	0.872	3.35	8.290E-16	1.86E-16	22.38
May-18	Blank-18-1	Blank-18-1	0.858	4.72E-06	9.911E-16	1.75E-16	17.69
May-18	Blank-18-2	Blank-18-2	0.865	5.19E-06	9.446E-16	1.79E-16	18.91

Table C.4 Blank Information

Sample name	St			Lm			LSDn		
	Age (yr)	Interr (yr)	Exterr (yr)	Age (yr)	Interr (yr)	Exterr (yr)	Age (yr)	Interr (yr)	Exterr (yr)
JB-16-1	685	86	90	685	86	90	663	83	87
JB-16-3	542	35	40	542	35	40	528	34	39
JB-16-6	321	30	32	321	30	32	321	30	33
JB-16-9	254	40	42	254	40	42	260	41	42
KS-16-10	7829	273	398	7831	273	398	7917	276	405
KS-16-3	9138	450	563	9141	451	564	9269	457	574
KS-16-4	11315	314	524	11318	314	524	11503	319	536
KS-16-6	3438	123	177	3439	123	177	3462	124	179
KS-16-6	7464	477	551	7466	477	551	7561	483	560
KS-16-8	4113	375	404	4114	375	405	4189	382	413
KS-16-9	3550	102	166	3551	102	166	3581	103	169
NK-16-1	658	35	42	658	35	42	642	34	41
NK-16-2	660	39	46	660	39	46	644	38	45
NK-16-4	6352	156	282	6359	157	283	6521	161	292
NK-16-5	727	40	48	728	40	48	708	39	47
NK-16-6	908	69	76	910	69	76	893	67	75
NK-16-7	1532	102	116	1535	102	117	1519	101	116
NQ-13-12	447	36	40	447	36	40	438	36	39
NQ-13-15	852	70	76	851	70	76	819	67	74
NQ-13-32	712	34	43	712	34	43	681	33	41
NQ-13-33	427	30	34	427	30	34	419	30	34
NQ-13-36	1323	44	66	1322	44	66	1285	43	65
NQ-13-38	796	35	46	796	35	46	762	34	44
NQ-13-41	540	42	47	540	42	47	521	41	45
NU-13-1	8025	130	324	8029	130	324	8102	131	331
NU-13-18	8443	220	382	8446	220	383	8565	224	391
NU-13-2	8491	145	346	8494	145	346	8577	147	353
NU-13-3	8117	152	337	8120	152	337	8194	153	343
NU-13-4	7850	165	334	7853	165	334	7926	167	341
NU-13-5	9252	173	384	9256	173	384	9362	175	392
QA-14-1	291	70	71	291	70	71	291	70	71
QA-14-10	1097	124	130	1095	124	130	1064	120	127
QA-14-11	1875	146	161	1873	145	161	1836	143	158
QA-14-12	588	174	175	588	174	175	566	167	169
QA-14-13	572	74	77	572	74	76	551	71	74
QA-14-14	1662	159	170	1660	159	170	1617	155	166
QA-14-5	2264	106	135	2262	106	135	2230	105	134
QA-14-7	525	59	62	525	59	62	507	57	60
QA-14-8	462	56	58	462	56	58	451	54	57
QA-14-9	784	99	103	783	99	103	749	94	98
TU-16-11	5075	140	234	5080	140	234	5223	144	243
TU-16-13	1469	130	141	1472	131	142	1454	129	140
TU-16-14	1086	118	124	1088	118	125	1073	116	123
TU-16-15	662	76	80	662	76	80	645	74	78
TU-16-16	272	56	57	272	56	57	278	58	59
TU-16-17	831	50	58	832	50	58	811	48	57
TU-16-2	11246	210	467	11255	211	467	11494	215	481
TU-16-3	14684	276	610	14694	276	611	15010	282	630
TU-16-4	12106	247	512	12116	247	512	12379	252	528
TU-16-5	10696	226	456	10705	226	456	10930	231	470
TU-16-6	12223	266	525	12233	267	526	12496	272	542
TU-16-8	9839	184	408	9849	185	409	10041	188	421

Table C.5 Calculation of ages using different scaling schemes

Table C.6: Map Reference Key		
Abbreviation	**Full Site Name**	**Reference**
	Cosmogenic Surface Exposure Data	
West Greenland		
UigD	Uigordleq (distal moraine)	Young et al. 2015
UigI	Uigordleq (intermediate moraine)	Young et al. 2015
UigP	Uigordleq (proximal moraine)	Young et al. 2015
LmbD	Lyngmarkdsbreen (distal moraine)	Jomelli et al. 2016
LmbI	Lyngmarkdsbreen (intermediate moraine)	Jomelli et al. 2016
LmbP	Lyngmarkdsbreen (proximal moraine)	Jomelli et al. 2016
South Greenland		
NIM	Nuuk Ice Margin	This study
Jesb	Jespersen Bræ	This study
NarD	Narsarsuaq Moraine	Winsor et al. 2014
NarP	Inside Narsarsuaq Moraine	Winsor et al. 2014
TU	Tupaussat inner moraine	This study
Paar	Paarlit Sermiat	This study
NSO	Naajaat Sermia outer moraine	This study
NSI	Naajaat Sermia inner moraine	This study
SqKq	Sermeq Kangilleq	This study
East Greenland		
BIC	Bregne Ice Cap	Levy et al. 2014
IIC	Istorvet Ice Cap	Lowell et al. 2013
	Threshold Lake Data	
West Greenland		
KT	Kuusuup Tasia	Kelley et al. 2012
PL	Pluto Lake	Young et al. 2011
ET	Eqaluit tasserssuat	Briner et al. 2010
ML	Merganser Lake	Briner et al. 2010
SO	South Oval Lake	Briner et al. 2010
IB	Iceboom Lake	Briner et al. 2010
RL	Raven Lake	Briner et al. 2010
GL	Goose Lake	Briner et al. 2010
LL	Loon Lake	Briner et al. 2010
FI	Fredrickshåb Isblink	Larsen et al., 2015 (geology)
09	09370	Larsen et al., 2015 (geology)
Kp1	Kap01	Larsen et al., 2015 (geology)
Kn1	Kan01	Larsen et al., 2015 (geology)
South Greenland		
LN	Lower Nordboso	Larsen et al., 2011
SR	Storeso and Rundeso	Larsen et al., 2015 (nature)
AK	Akuliarusseq	Larsen et al., 2015 (nature)
KD	Kanderdluasiaup Tasia	Larsen et al., 2015 (nature)
KG	Kingitoq	Larsen et al., 2015 (nature)
SE	Sermilik	Larsen et al., 2015 (nature)
KU	Kulusuk	Belascio et al. 2015
East Greenland		
TI	Torqulertivit Imiat	Larsen et al., 2015 (geology)
LC	Last Chance Lake	Levy et al., 2013
TM	Two Move Lake	Levy et al., 2013
BL	Bone Lake	Lowell et al. 2013

Table C.6 Map reference key

Appendix C.6 Cosmogenic Sample Sheets

Nuuk Ice Margin: NU-13-1

^{10}Be age: 8102 ± 131
Latitude: 64.778
Longitude: -49.514
Altitude: 983 m
Boulder Height: 1.1 m
Lithology: Granite, with quartz vein
Shielding: 0.9756

Sampling Date: 6 Aug 2013

Comments: Granite boulder on bedrock, sampled quartz vein

Nuuk Ice Margin: NU-13-2

^{10}Be age: 8577 ± 147
Latitude: 64.778
Longitude: -49.514
Altitude: 980 m
Boulder Height: 1.0 m
Lithology: Granite, with quartz vein
Shielding: 0.9989

Sampling Date: 6 Aug 2013

Comments: Granite boulder on bedrock, sampled quartz vein

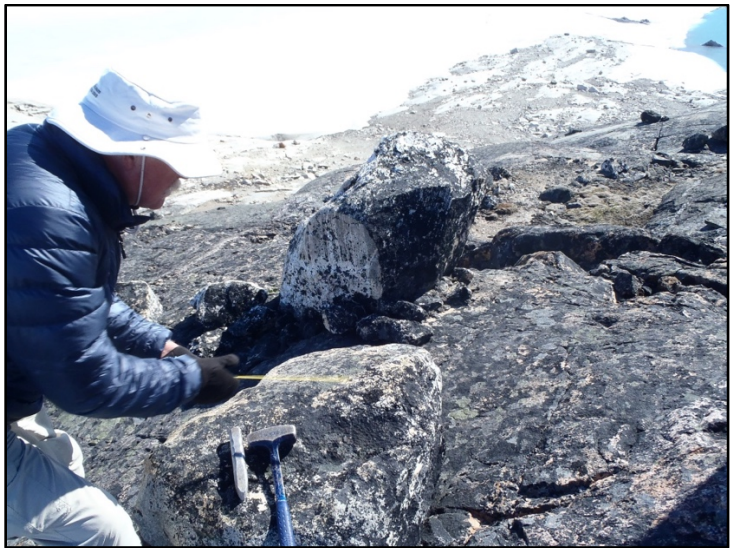

Nuuk Ice Margin: NU-13-3

^{10}Be age: 8194 ± 153
Latitude: 64.778
Longitude: -49.514
Altitude: 980 m
Boulder Height: 0.5 m
Lithology: Granite, with quartz vein
Shielding: 0.9989

Sampling Date: 6 Aug 2013

Comments: Granite boulder on bedrock

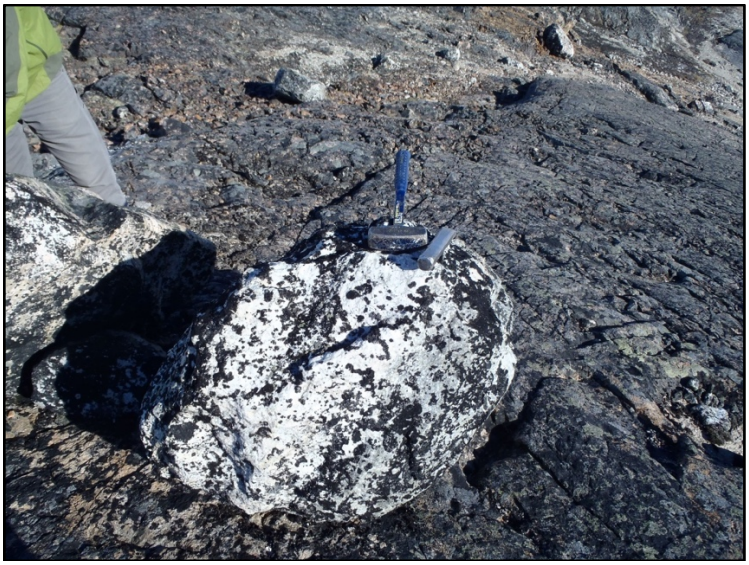

Nuuk Ice Margin: NU-13-4

^{10}Be age: 7926 ± 167
Latitude: 64.778
Longitude: -49.514
Altitude: 986 m
Boulder Height: 1.0 m
Lithology: quartz-rich granite
Shielding: 0.9989

Sampling Date: 6 Aug 2013

Comments: Boulder trundled in field to allow access to NU-13-5

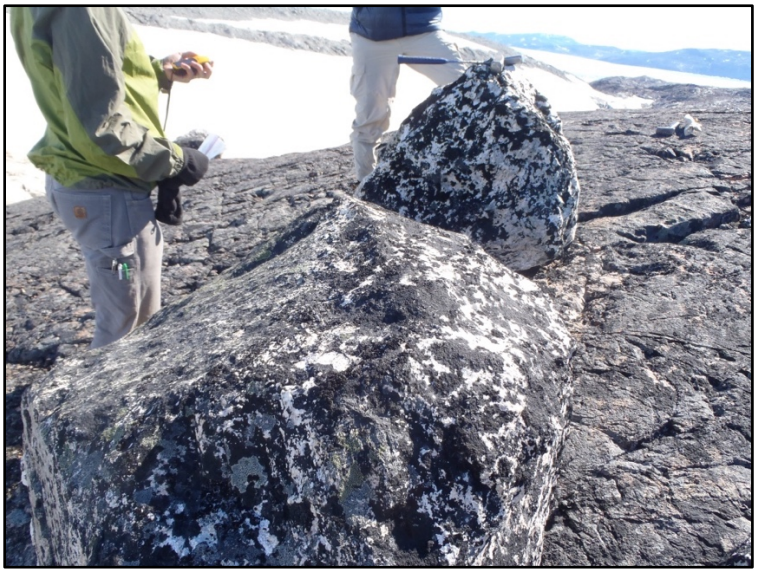

Nuuk Ice Margin: NU-13-5

^{10}Be age: 9362 ± 175
Latitude: 64.778
Longitude: -49.514
Altitude: 980 m
Boulder Height: 1.0 m
Lithology: gneiss
Shielding: 0.9989

Sampling Date: 6 Aug 2013

Comments: Immediately adjacent to NU-13-4

Nuuk Ice Margin: NU-13-18

^{10}Be age: 8565 ± 224
Latitude: 64.742
Longitude: -49.583
Altitude: 735 m
Boulder Height: 0.8 m
Lithology: Granite
Shielding: 1.000

Sampling Date: 7 Aug 2013

Comments:

Naajat Sermiat outer moraine: NQ-13-12

^{10}Be age: 438 ± 36
Latitude: 61.013
Longitude: -46.525
Altitude: 77 m
Boulder Height: 1.4 m
Lithology: Granite
Shielding: 0.9943

Sampling Date: 31 Jul 2013

Comments:

Naajat Sermiat outer moraine: NQ-13-15

^{10}Be age: 819 ± 67
Latitude: 61.013
Longitude: -46.525
Altitude: 77 m
Boulder Height: 2.0 m
Lithology: Granite
Shielding: 0.9943

Sampling Date: 31 Jul 2013

Comments:

Naajat Sermiat outer moraine: NQ-13-32

^{10}Be age: 681 ± 33
Latitude: 61.013
Longitude: -46.528
Altitude: 67 m
Boulder Height: 2.8 m
Lithology: granite
Shielding: 0.9959

Sampling Date: 2 Aug 2013

Comments:

Naajat Sermiat outer moraine: NQ-13-33

^{10}Be age: 419 ± 30
Latitude: 61.013
Longitude: -46.528
Altitude: 67 m
Boulder Height: 2.4 m
Lithology: granite
Shielding: 0.9959

Sampling Date: 2 Aug 2013

Comments:

Naajat Sermiat outer moraine: NQ-13-36

^{10}Be age: 1285 ± 43
Latitude: 61.013
Longitude: -46.528
Altitude: 67 m
Boulder Height: 2.4 m
Lithology: granite
Shielding: 0.9959

Sampling Date: 2 Aug 2013

Comments:

Naajat Sermiat outer moraine: NQ-13-38

^{10}Be age: 762 ± 34
Latitude: 61.013
Longitude: -46.528
Altitude: 62 m
Boulder Height: 1.7 m
Lithology: granite
Shielding: 0.9956

Sampling Date: 2 Aug 2013

Comments:

Naajat Sermiat outer moraine: NQ-13-41

^{10}Be age: 521 ± 41
Latitude: 61.014
Longitude: -46.526
Altitude: 62 m
Boulder Height: 2.2 m
Lithology: granite
Shielding: 0.9955

Sampling Date: 2 Aug 2013

Naajat Sermiat inner moraine: QA-14-1

^{10}Be age: 291 ± 70
Latitude: 61.015
Longitude: -46.525
Altitude: 56 m
Boulder Height: 2.5 m
Lithology: granite
Shielding: 0.9602

Sampling Date: 1 Sep 2014

Comments: Did not photograph

Naajat Sermiat inner moraine: QA-14-5

^{10}Be age: 2230 ± 105
Latitude: 61.015
Longitude: -46.525
Altitude: 59 m
Boulder Height: 2 m
Lithology: granite
Shielding: 0.9897

Sampling Date: 1 Sep 2014

Comments:

Naajat Sermiat inner moraine: QA-14-7

^{10}Be age: 507 ± 57
Latitude: 61.015
Longitude: -46.527
Altitude: 54 m
Boulder Height: 2 m
Lithology: granite
Shielding: 0.9709

Sampling Date: 7 Sep 2014

Comments:

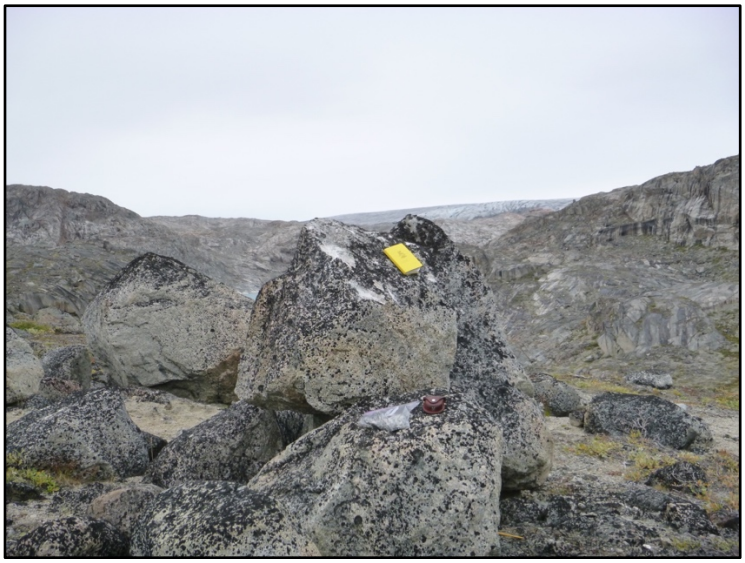

Naajat Sermiat inner moraine: QA-14-8

^{10}Be age: 451± 54
Latitude: 61.014
Longitude: -46.527
Altitude: 65 m
Boulder Height: 1.5 m
Lithology: granite
Shielding: 0.9445

Sampling Date: 7 Sep 2018

Comments: boulder is perched on other boulders of moraine

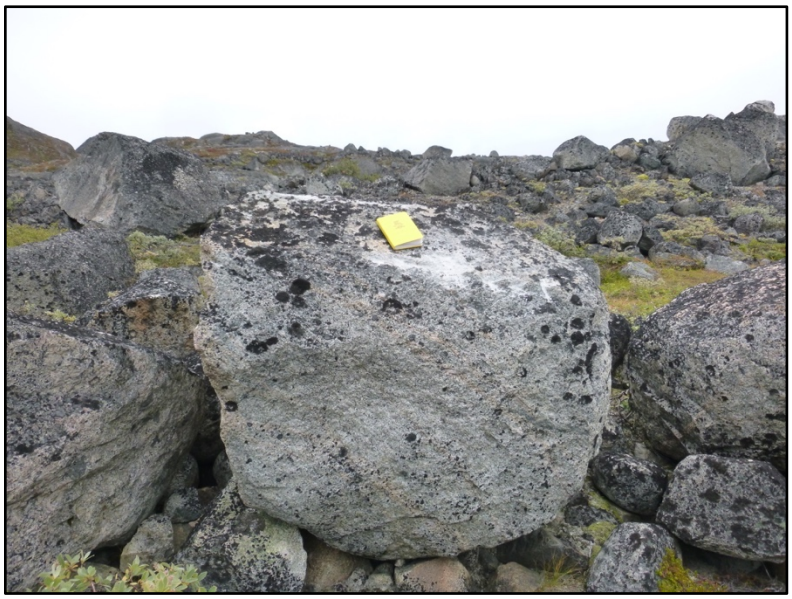

Naajat Sermiat inner moraine: QA-14-9

^{10}Be age: 749 ± 94
Latitude: 61.015
Longitude: -46.526
Altitude: 56 m
Boulder Height: 1.5 m
Lithology: quartz
Shielding: 0.9712

Sampling Date: 7 Sep 2013

Naajat Sermiat inner moraine: QA-14-10

^{10}Be age: 1064 ± 120
Latitude: 61.015
Longitude: -46.525
Altitude: 62 m
Boulder Height: 1.8 m
Lithology: granite
Shielding: 0.9779

Sampling Date: 7 Sep 2013

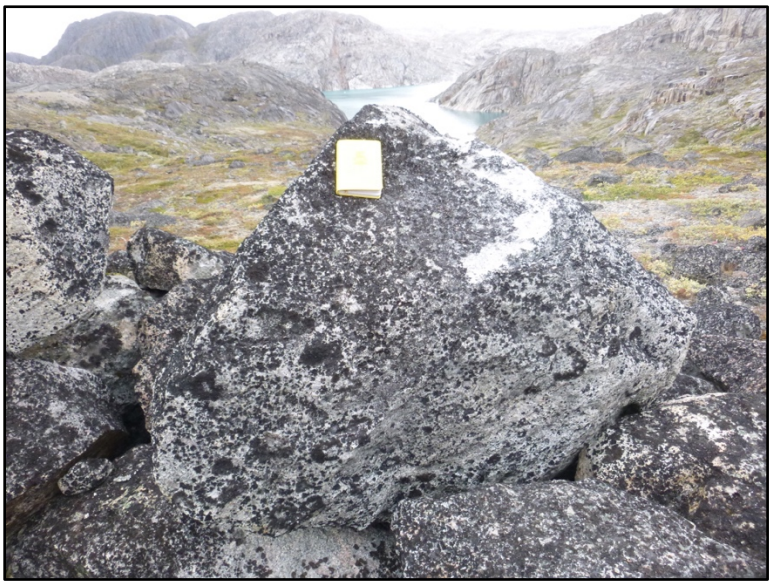

Naajat Sermiat inner moraine: QA-14-11

^{10}Be age: 1836 ± 143
Latitude: 61.015
Longitude: -46.525
Altitude: 63 m
Boulder Height: 1.5 m
Lithology: granite
Shielding: 0.9799

Sampling Date: 7 Sep 2013

Naajat Sermiat inner moraine: QA-14-12

^{10}Be age: 566 ± 167
Latitude: 61.015
Longitude: -46.525
Altitude: 59 m
Boulder Height: 2 m
Lithology: granite
Shielding: 0.9671

Sampling Date: 7 Sep 2013

Naajat Sermiat inner moraine: QA-14-13

^{10}Be age: 551 ± 71
Latitude: 61.015
Longitude: -46.527
Altitude: 59 m
Boulder Height: 2 m
Lithology: granite
Shielding: 0.8782

Sampling Date: 9 Sep 2013

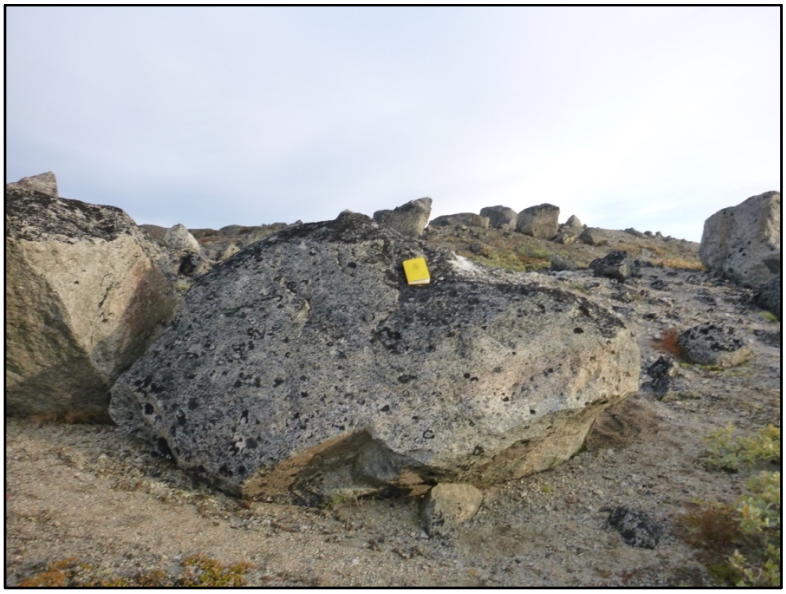

Naajat Sermiat inner moraine: QA-14-14

^{10}Be age: 1617 ± 155
Latitude: 61.015
Longitude: -46.526
Altitude: 57 m
Boulder Height: 1.5 m
Lithology: granite
Shielding: 0.9927

Sampling Date: 9 Sep 2013

Comments: slightly off crest of moraine ridge

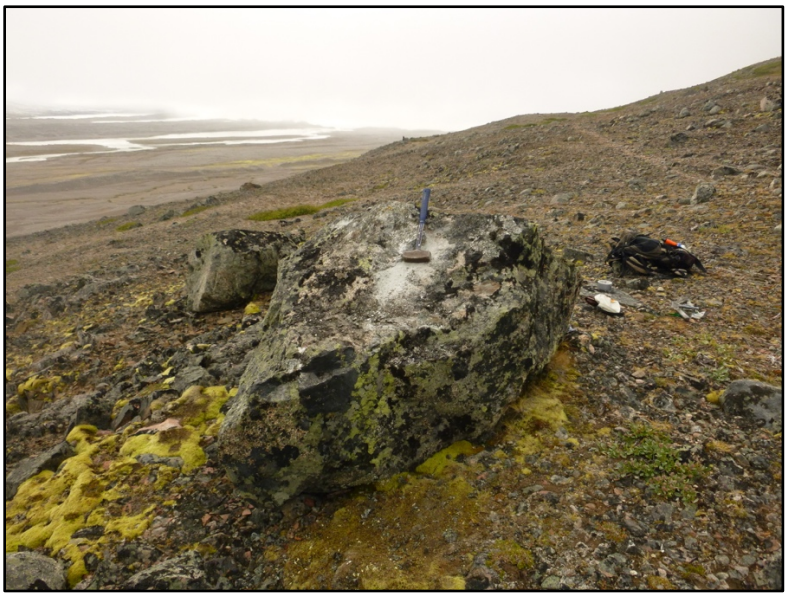

Jespersen Bræ: KS-16-3

^{10}Be age: 9269 ± 457
Latitude: 61.078
Longitude: -45.027
Altitude: 212 m
Boulder Height: 1.5 m
Lithology: granite
Shielding: 0.9515

Sampling Date: 21 Aug 2016

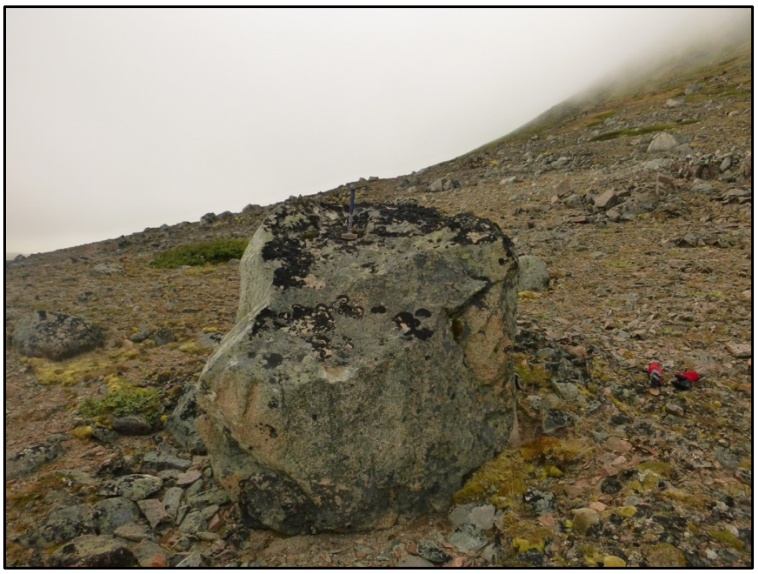

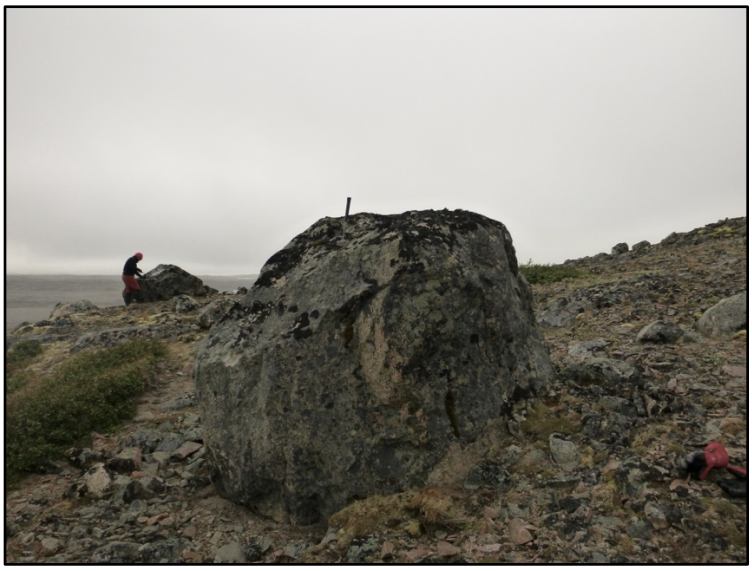

Jespersen Bræ: KS-16-4

^{10}Be age: 11503 ± 319
Latitude: 61.708
Longitude: -45.027
Altitude: 205 m
Boulder Height: 2 m
Lithology: granite
Shielding: 0.9913

Sampling Date: 21 Aug 2016

Comments: samples are from small flakes across face of boulder. Approx. 30m NW of KS-16-3

Jespersen Bræ: KS-16-6

^{10}Be age: 3462 ± 124
Latitude: 61.076
Longitude: -45.026
Altitude: 212 m
Boulder Height: 1 m
Lithology: granite with quartz vein
Shielding: 0.9845

Sampling Date: 21 Aug 2016

Jespersen Bræ: KS-16-8

^{10}Be age: 4189 ± 382
Latitude: 61.074
Longitude: -45.025
Altitude: 213 m
Boulder Height: 2 m
Lithology: granite
Shielding: 0.9180

Sampling Date: 21 Aug 2018

Jespersen Bræ: KS-16-9

^{10}Be age: 3581 ± 103
Latitude: 61.074
Longitude: -45.025
Altitude: 221 m
Boulder Height: 1.5 m
Lithology: granite
Shielding: 0.9966

Sampling Date: 21 Aug 2018

Jespersen Bræ: KS-16-10

^{10}Be age: 7917 ± 276
Latitude: 61.074
Longitude: -45.025
Altitude: 213 m
Boulder Height: 1.2 m
Lithology: granite
Shielding: 0.9694

Sampling Date: 21 Aug 2018

Notes: Did not photograph

Sermeq Kangilleq: JB-16-1

^{10}Be age: 663 ± 83
Latitude: 60.916
Longitude: -45.028
Altitude: 175 m
Boulder Height: 1 m
Lithology: granite
Shielding: 0.9615

Sampling Date: 26 Aug 2016

Sermeq Kangilleq: JB-16-3

^{10}Be age: 528 ± 34
Latitude: 60.917
Longitude: -45.029
Altitude: 175 m
Boulder Height: 0.6 m
Lithology: gneiss
Shielding: 0.9542

Sampling Date: 26 Aug 2016

Sermeq Kangilleq: JB-16-6

^{10}Be age: 321 ± 30
Latitude: 60.916
Longitude: -45.026
Altitude: 169 m
Boulder Height: 2 m
Lithology: granite
Shielding: 0.9858

Sampling Date: 26 Aug 2016

Sermeq Kangilleq: JB-16-9

^{10}Be age: 260 ± 41
Latitude: 60.916
Longitude: -45.024
Altitude: 178 m
Boulder Height: 3 m
Lithology: granite
Shielding: 0.9840

Sampling Date: 26 Aug 2016

Comments: Did not photograph

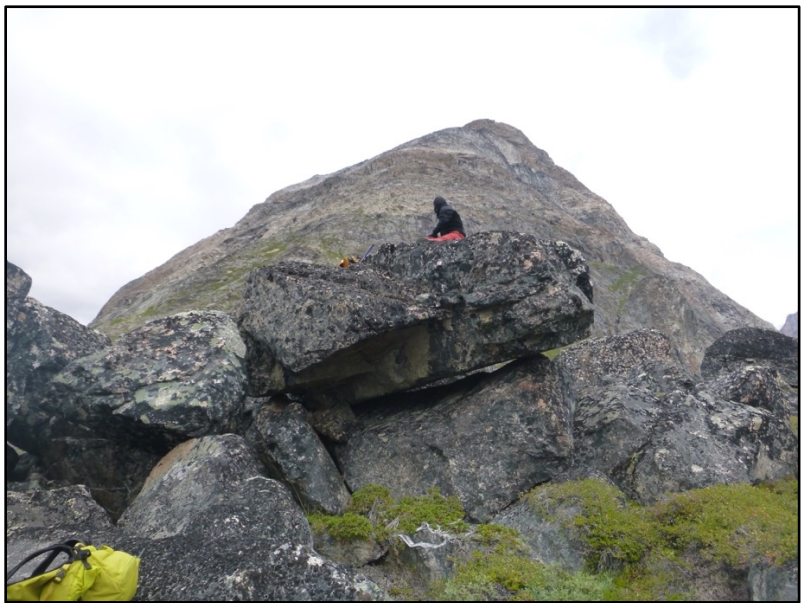

Tupaussat outer moraine: TU-16-2

^{10}Be age: 11494 ± 215
Latitude: 60.381
Longitude: -44.288
Altitude: 276 m
Boulder Height: 2.5 m
Lithology: granite
Shielding: 0.9704

Sampling Date: 2 Aug 2016

Tupaussat outer moraine: TU-16-3

^{10}Be age: 15010 ± 282
Latitude: 60.381
Longitude: -44.288
Altitude: 277 m
Boulder Height: 3 m
Lithology: granite
Shielding: 0.9638

Sampling Date: 2 Aug 2016

Tupaussat outer moraine: TU-16-4

^{10}Be age: 12379 ± 252
Latitude: 60.381
Longitude: -44.287
Altitude: 289 m
Boulder Height: 3.5 m
Lithology: granite
Shielding: 0.9727

Sampling Date: 2 Aug 2016

Tupaussat outer moraine: TU-16-5

^{10}Be age: 10930 ± 231
Latitude: 60.381
Longitude: -44.288
Altitude: 285 m
Boulder Height: 2.5 m
Lithology: granite
Shielding: 0.9721

Sampling Date: 2 Aug 2016

Tupaussat outer moraine: TU-16-6

^{10}Be age: 12496 ± 272
Latitude: 60.388
Longitude: -44.274
Altitude: 305 m
Boulder Height: 3 m
Lithology: granite
Shielding: 0.9238

Sampling Date: 2 Aug 2016

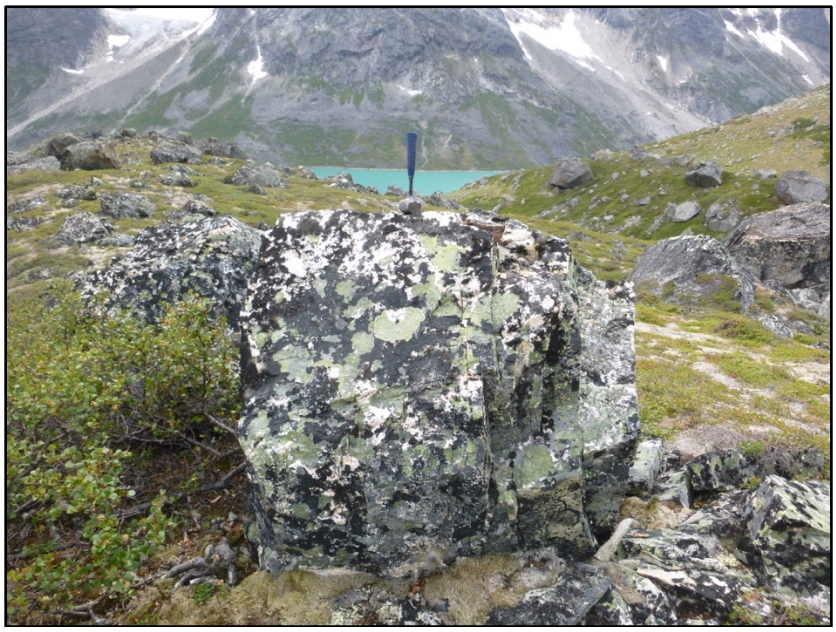

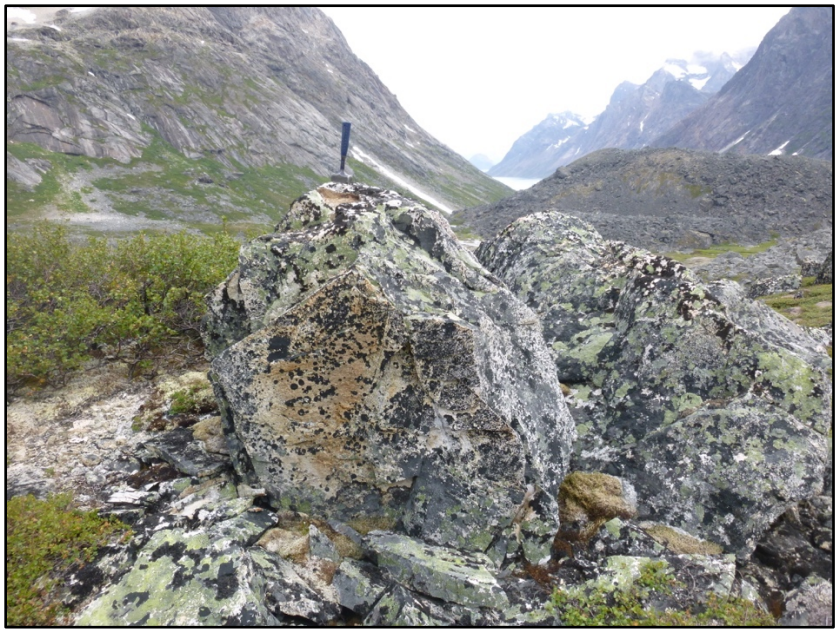

Tupaussat outer moraine: TU-16-8

^{10}Be age: 10041 ± 188
Latitude: 60.382
Longitude: -44.286
Altitude: 297 m
Boulder Height: 1.5 m
Lithology: granite
Shielding: 0.9694

Sampling Date: 2 Aug 2016

Tupaussat inner moraine: TU-16-11

^{10}Be age: 5223 ± 144
Latitude: 60.388
Longitude: -44.274
Altitude: 305 m
Boulder Height: 3 m
Lithology: granite
Shielding: 0.9283

Sampling Date: 3 Aug 2016

Tupaussat inner moraine: TU-16-13

^{10}Be age: 1454 ± 129
Latitude: 60.388
Longitude: -44.274
Altitude: 314 m
Boulder Height: 1.5 m
Lithology: granite
Shielding: 0.9530

Sampling Date: 3 Aug 2016

Tupaussat inner moraine: TU-16-14

^{10}Be age: 1073 ± 116
Latitude: 60.389
Longitude: -44.273
Altitude: 307 m
Boulder Height: 2.5 m
Lithology: granite
Shielding: 0.9549

Sampling Date: 3 Aug 2016

Tupaussat inner moraine: TU-16-15

^{10}Be age: 645 ± 74
Latitude: 60.389
Longitude: -44.273
Altitude: 307 m
Boulder Height: 1.5 m
Lithology: granite
Shielding: 0.9297

Sampling Date: 3 Aug 2016

Tupaussat inner moraine: TU-16-16

^{10}Be age: 278 ± 58
Latitude: 60.389
Longitude: -44.273
Altitude: 319 m
Boulder Height: 1.5 m
Lithology: granite
Shielding: 0.9549

Sampling Date: 3 Aug 2016

Tupaussat inner moraine: TU-16-17

^{10}Be age: 811 ± 48
Latitude: 60.389
Longitude: -44.273
Altitude: 316 m
Boulder Height: 3 m
Lithology: granite
Shielding: 0.9548

Sampling Date: 3 Aug 2016

Paarlit Sermiat: NK-16-1

^{10}Be age: 642 ± 24
Latitude: 60.323
Longitude: -43.932
Altitude: 356 m
Boulder Height: 2 m
Lithology: granite
Shielding: 0.9554

Sampling Date: 4 Aug 2016

Paarlit Sermiat: NK-16-2

^{10}Be age: 644 ± 38
Latitude: 60.323
Longitude: -43.932
Altitude: 351 m
Boulder Height: 1.5 m
Lithology: granite
Shielding: 0.9518

Sampling Date: 4 Aug 2016

Paarlit Sermiat: NK-16-4

^{10}Be age: 6521 ± 161
Latitude: 60.322
Longitude: -43.934
Altitude: 355 m
Boulder Height: 3 m
Lithology: granite
Shielding: 0.7296

Sampling Date: 4 Aug 2016

Paarlit Sermiat: NK-16-5

^{10}Be age: 708 ± 39
Latitude: 60.322
Longitude: -43.933
Altitude: 355 m
Boulder Height: 1.5 m
Lithology: granite
Shielding: 0.8816

Sampling Date: 4 Aug 2016

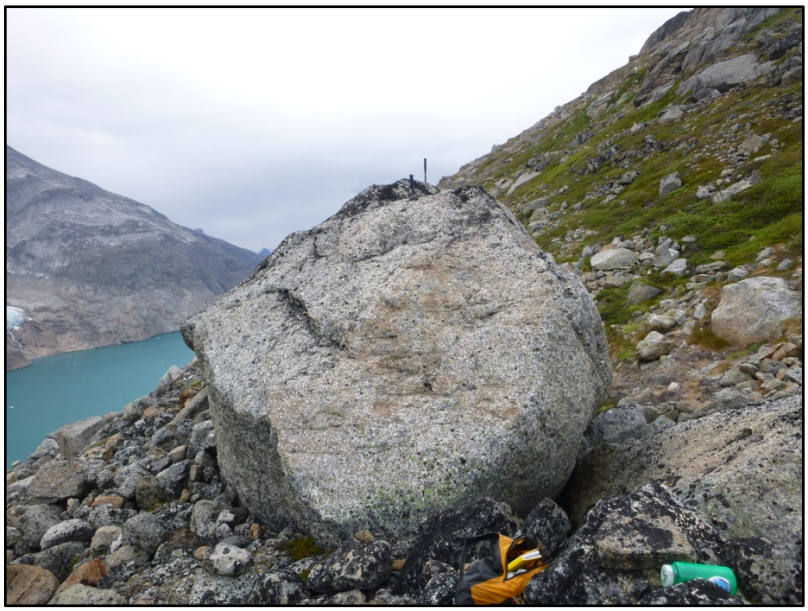

Paarlit Sermiat: NK-16-6

^{10}Be age: 893 ± 67
Latitude: 60.323
Longitude: -43.933
Altitude: 351 m
Boulder Height: 3.5 m
Lithology: granite
Shielding: 0.9545

Sampling Date: 4 Aug 2016

Paarlit Sermiat: NK-16-7

^{10}Be age: 1519 ± 101
Latitude: 60.323
Longitude: -43.933
Altitude: 359 m
Boulder Height: 2.5 m
Lithology: granite
Shielding: 0.9463

Sampling Date: 4 Aug 2016

Bibliography

Alexanderson, H., Håkansson, L., 2014. Coastal glaciers advanced onto Jameson Land, East Greenland during the late glacial-early Holocene Milne Land Stade. *Polar Research,* 33. http://dx.doi.org/10.3402/polar.v33.20313.

Andresen, C.S., Björck, S., Bennike, O., Bond, G., 2004. Holocene climate changes in southern Greenland: evidence from lake sediments. *Journal of Quaternary Science* 19, 783-795

Axford, Y., Losee, S., Briner, J.P., Francis, D.R., Langdon, P.G., Walker, I.R., 2013. Holocene temperature history at the western Greenland Ice Sheet margin reconstructed from lake sediments. *Quaternary Science Reviews* 59, 87-100.

Balco, G., Stone, J.O., Lifton, N.A., Dunai, T.J., 2008. A complete and easily accessible means of calculating surface exposure ages or erosion rates from Be-10 and Al-26 measurements. *Quaternary Geochronology* 3, 174-195.

Balco, G., Briner, J., Finkel, R.C., Rayburn, J.A., Ridge, J.C., Schaefer, J.M., 2009. Regional beryllium-10 production rate calibration for northeastern North America. *Quaternary Geochronology* 4, 93-107.

Bamber J.L., Westaway, R.M., Marzeion, B., Wouters, B., 2018. The land ice contribution to sea level during the satellite era. *Environmental Research Letters*, 13. dx.doi.org:/10.1088/1748-9326/aac2f0

Balco, G., 2011. Contributions and unrealized potential contributions of cosmogenic-nuclide exposure dating to glacier chronology, 1990-2010. *Quaternary Science Reviews* 30, 3-27.

Belascio, N.L., D'Andrea, W.J., Bradley, R.S., 2015. Glacier response to North Atlantic climate variability during the Holocene. *Climate of the Past* 11, 1587-1598

Bennike, O., 2008. An early Holocene Greenland whale from Melville Bugt, Greenland. *Quaternary Research* 69, 72-76.

Bennike, O., Björck, S., 2002. Chronology of the last recession of the Greenland Ice Sheet. *Journal of Quaternary Science* 17, 211-219.

Bennike, O., Sparrrenbom, C.J., 2007. Dating of the Narssarssuaq stade in southern Greenland. Holocene 17, 279-282.

Bennike, O., Björck, S., Lambeck, K., 2002. Estimates of South Greenland late-glacial ice limits from a new relative sea level curve. *Earth and Planetary Science Letters* 197, 171-186.

Bennike, O., Wagner, B., 2012. Deglaciation chronology, sea-level changes and environmental changes from Holocene lake sediments of Germania Havn Sø, Sabine Ø, northeast Greenland. *Quaternary Research* 78, 103-109.

Bennike, O., Wagner, B., Righter, A., 2011. Relative sea level changes during the Holocene in the Sisimiut area, south-western Greenland. *Journal of Quaternary Science,* 26, 353-361.

Berger, A., Loutre, M.F., 1991. Insolation values for the climate of the last 10 million years. *Quaternary Science Reviews* 10, 291-317

Bevis, M., Harig, C., Khan S.A., Brown, A., Simons, F.J., Willis, M., Fettweis, X., van den Broeke, M.R., Madsen, F.B., Kendrick, E., Cacamise, D.J., van Dam, T., Knudsen, P., Nylen, T., 2019. Accelerating changes in ice mass within Greenland, and the ice

sheet's sensitivity to atmospheric forcing. *Proceedings of the National Academy of Sciences* 116, 1934-1939.
Briner, J.P., Håkansson, L., Bennike, O., 2013. The deglaciation and neoglaciation of Upernavik Isstrøm, Greenland. *Quaternary Research* 80, 459-467.

Bierman, P.R., Shakun, J.D., Corbett, L.B., Zimmerman, S.R., Rood, D.H., 2016. A persistent and dynamic East Greenland Ice Sheet over the past 7.5 million years. *Nature* 540, 256-260.

Bindoff, N.L., Stott, P.A., AchutaRao, K.M., Allen, M.R., Gillett, N., Gutzler, D., Hansingo, K., Hegerl, G., Hu, Y., Jain, S., Mokhov, I.I., Overland, J., Perlwitz, J., Sebbari, R., Zhang, X., 2013: Detection and attribution of climate change: From global to regional. In *Climate Change 2013: The Physical Science Basis. Contribution of Working Group I to the Fifth Assessment Report of the Intergovernmental Panel on Climate Change*. T.F. Stocker, D. Qin, G.-K. Plattner, M. Tignor, S.K. Allen, J. Doschung, A. Nauels, Y. Xia, V. Bex, and P.M. Midgley, Eds. Cambridge University Press, pp. 867-952

Bjørk, A.A., et al., 2015. Brief communication: Getting Greenland's glacier names right—a new data set of all official Greenlandic glacier names. *The Cryosphere* 9, 2215-2218.

Bjørk, A.A., Aagaard, S., Lütt, A., Khan, S.A., Box, J.E., Kjeldsen, K.K., Larsen, N.K., Korsgaard, N.J., Cappelen, J., Colgan, W.T., Machguth, H., Andresen, C.S., Peings, Y., Kjær, K.H., 2018. Changes in Greenland's peripheral glaciers linked to the North Atlantic Oscillation. *Nature Climate Change* 8, 48-52.

Briner, J.P., Kaufman, D.S., Bennike, O., Kosnik, M.A., 2014. Amino acid ratios in reworked marine bivalve shells constrain Greenland Ice Sheet history during the Holocene. *Geology*. http://dx.doi.org/10.1130/G34843.1

Briner, J.P., Miller, G.H., Davis, P.T., Finkel, R.C., 2006. Cosmogenic radionuclides from fiord landscapes support differential erosion by overriding ice sheets. *Geological Society of America Bulletin* 118, 406-420.

Briner, J.P., Stewart, H.A.M., Young, N.E., Phillipps, W., Losee, S., 2010 Using proglacial-threshold lakes to constrain fluctuations of the Jakobshavn Isbrae ice margin, western Greenland, during the Holocene. *Quaternary Science Reviews* 29, 3861-3874.

Buizert, C., Gkinis, V., Severinghaus, J.P., He, F., Lecavalier, B.S., Kindler, P., Leuenberger, M., Carlson, A.E., Vinther, B., Masson-Delmotte, V., White, J.W.C., Liu, Z., Otto-Bleisner, B., Brook, E.J., 2014. Greenland temperature responses to climate forcing during the last deglaciation. *Science* 345, 1177-1180.

Caesar, L., Rahmstorf, S., Robinson, A., Feulner, G., Saba, V., 2018. Observed fingerprint of a weakening Atlantic Ocean overturning circulation. *Nature* 556, 191-196.

Carlson, A.E., Clark, P.U., 2012. Ice sheet sources of sea level rise and freshwater discharge during the last deglaciation. *Reviews of Geophysics* 50, RG4007.

Carlson, A.E., Stoner, J.S., Donnelly, J.P., Hillaire-Marcel, C., 2008. Response of the southern Greenland Ice Sheet during the last two deglaciations. *Geology* 36, 359-362.

Carlson, A.E., Winsor, K., Ullman, D.J., Brook, E.J., Rood, D.H., Axford, Y., LeGrande, A.N., Anslow, F.S., Sinclair, G., 2014. Earliest Holocene south Greenland ice sheet retreat within its late Holocene extent. *Geophysical Research Letters* 41, 5514-5521

Chen, X., Zhang, X., Church, J.A., Watson, C.S., King, M.A., Monselesan, D., Legresy, B., Harig, C., 2017. The increasing rate of global mean sea-level rise during 1993-2014. *Nature Climate Change* 7, 492-495.

Church, J.A., Clark, P.U., Cazenave, A., Gregory, J.M., Jevrejeva, S., Levermann, A., Merrifeld, M.A., Milne, G.A., Nerem, R.S., Nunn, P.D., Payne, A.J., Pfeffer, W.T., Stammer, D., Unnikrishnan, A.S., 2013. Sea-Level Change. In: Climate Change 2013: The Physical Science Basis. Contribution of Working Group I to the Fifth Assessment Report of the Intergovernmental Panel on Climate Change [Stocker, T.F., D. Qin, G.-K. Plattner, M. Tignor, S.K. Allen, J. Boschung, A. Nauels, Y. Xia, V. Bex and P.M. Midgley (eds.)]. Cambridge University Press, Cambridge, United Kingdom and New York, NY, USA.

Clark, P.U., Dyke, A.S., Shakun, J.D., Carlson, A.E., Clark, J., Wohlfarth, B., Hostetler, S.W., Mitrovica, J.X., McCabe, A.M., 2009. The Last Glacial Maximum. *Science* 325, 710-714.

Clark, P.U., Shakun, J.D., Baker, P.A., Bartlein, P.J., Brewer, S., Brook, E., Carlson, A.E., Cheng, H., Kaufman, D.S., Liu, Z., Marchitto, T.M., Mix, A.C., Morrill, C., Otto-Bleisner, B.L., Pahnke, K., Russell, J.M., Whitlock, C., Adkins, J.F., Blois, J.L., Clark, J., Colman, S.M., Curry, W.B., Flower, B.P., He, F., Johnson, T.C., Lynch-Stieglitz, J., Markgraf, V., McManus, J., Mitrovica, J.X., Moreno, P.I., Williams, J.W., 2012. Global climate evolution during the last deglaciation. *Proc. Natl. Acad. Sciences* 109, http://dx.doi.org/10.1073/pnas.1116619109.

Clark, P.U., Shakun, J.D., Marcott, S.A., Mix, A.C., Eby, M., Kulp, S., Levermann, A., Milne, G.A., Pfister, P.L., Santer, B.D., Schrag, D.P., Solomon, S., Stocker, T.F., Strauss, B.H., Weaver, A.J., Winkelmann, R., Archer, D., Bard, E., Goldner, A., Lambeck, K., Pierrrehumbert, R.T., Plattner, G., 2016. Consequences of twenty-first-century policy for multi-millenial climate and sea-level change. *Nature Climate Change* 6, 360-369

Cohen, J., Screen, J.A., Furtado, J.C., Barlow, M., Whittleston, D., Coumou, D., Francis, J., Dethloff, K., Entekhabi, D., Overland, J., Jones, J., 2014. Recent Arctic amplification and extreme mid-latitude weather. *Nature Geoscience* 7, 627-637

Colville, E.J., Carlson, A.E., Beard, B.L., Hatfield, R.G., Stoner, J.S., Reyes, A.V., Ullman, D.J., 2011. Sr-Nd-Pb isotope evidence for ice-sheet presence on Southern Greenland during the last interglacial. *Science* 333, 620-623.

Corbett, L.B., Bierman, P.R., Graly, J.A., Neumann, T.A., Rood, D.H. 2013. Constraining landscape history and glacial erosivity using paired cosmogenic nuclides in Upernavik, northwest Greenland. *Geological Society of America Bulletin* 125, 1539-1553.

Corbett, L.B., Young, N.E., Bierman, P.R. Briner, J.P., Neumann, T.A., Rood, D.H., Graly, J.A., 2011. Paired bedrock and boulder ^{10}Be concentrations resulting from early Holocene ice retreat near Jakobshavn Isfjord, western Greenland. *Quaternary Science Reviews* 30, 1739-1747.

Corbett, L.B., Bierman, P.R., Everett Lasher, G., Rood, D.H., 2015. Landscape chronology and glacial history in Thule, northwest Greenland. *Quaternary Science Reviews* 109, 57-67.

Cronauer, S.L., Briner, J.P., Kelley, S.E., Zimmerman, S.R.H., Morlighem, M., 2015. ^{10}Be dating reveals early-middle Holocene age of the Drygalski Moraines in central West Greenland. *Quaternary Science Reviews*, in press.

D'Andrea, W.J., Huang, Y., Fritz, S.C., Anderson, N.J., 2011. Abrupt Holocene climate change as an important factor for human migration in West Greenland. *Proceedings of the National Academy of Sciences,* doi: 10.1073/pnas.1101708108.

Davis, P.T., Briner, J.P., Coulthard, R.D., Finkel, R.W., Miller, G.H., 2006. Preservation of Arctic landscapes overridden by cold-based ice sheets. *Quaternary Research* 65, 156-163.

Diaz, H.F., Trigo, R., Hughes, M.K., Mann, M.E., Xoplaki, E., Barriobedro, D., 2011. Spatial and temporal characteristics of climat in medieval times revisited. *Bulletin of the American Meteorological Society* 92, 1487-1500

Dupont, T.K., Alley, R.B., 2005. Assessment of the importance of ice-shelf buttressing to ice sheet flow. *Geophysical Research Letters*. doi: 10.1029/2004GL022024.

Dyke, A.S., 2004. An outline of North American deglaciation with emphasis on central and northern Canada. In Ehlers, J., and Gibbard, P.L. (eds), *Quaternary Glaciations—Extent and chronology. Part II: North America*. Amsterdam: Elsevier.

Dyke, L.M., Hughes, A.L.C., Murray, T., Heimstra, J.F., Andresen, C.S., Rodés, Á., 2014. Evidence for the asynchronous retreat of large outlet glaciers in southeast Greenland at the end of the last glaciation. *Quaternary Science Reviews* 99, 244-259.

Evans, M.N., Kaplan, A., Cane, M.A., 2002. Pacific se asurface temperature field reconstruction from coral $\delta^{18}O$ data using reduced space objective analysis. *Paleoceanography* 17, dx.doi.org://10.1029/2000PA000590

Evans, M.N., Kaplan, A., Cane, M.A., Villalba, R., 2001. Globality and optimality in climate field reconstructions from proxy data. In Markgraf, V., (ed). *Interhemispheric Climate Linkages*. New York: Cambridge University Press.

Fallon, S.J., Fifield, L.,K., Chappell, J.M.., 2010. The next chapter in radiocarbon dating at the Australian National University: Status report on the single stage AMS. *Nucl.*

Instruments Methods Phys. Res. Sect. B Beam Interact. with Mater. Atoms dx.doi.org/10.1016/j.nimb.2009.10.059.

Farrell, W.E., Clark, J.A., 1976. On postglacial sea level. *Geophysical Journal of the Royal Astronomical Society* 46, 647-667.

Fredskild, B., 1973. Studies in vegetational history of Greenland. *Meddelelser om Grønland Geoscience* 11, 24 pp.

Fritts, H.C., Blasing, T.J., Hayden, B.P., Kutzbach, J.E., 1971. Multivariate techniques for specifying tree-growth and climate relationships and for reconstructing anomalies in paleoclimate. *Journal of Applied Meteorology* 10, 845-864

Funder, S., 1979. The Quaternary geology of the Narssaq area, South Greenland. *Rapport Grønlands Geologiske Undersøgelse* 86, 24 pp.

Funder, S., Kjeldsen, K.K., Kjær, K.H., Ó Cofaigh, C., 2011. The Greenland Ice Sheet during the past 300,000 years: a review. In Ehlers, J., Gibbard, P.L., and Hughes, P.D., eds. *Quaternary Glaciations—extent and chronology*. Amsterdam: Elsevier.

Gardner, A.S., Moholdt, G., Cogley, J.G., Wouters, B., Arendt, A.A., Wahr, J., Berthier, E., Hock, R., Pfeffer, W.T., Kaser, G., Ligtenberg, S.R.M., Bolch, T., Sharp, M.J., Hagen, J.O., van den Broeke, M.R., Paul, F., 2013. A reconciled estimate of glacier contributions to sea level rise: 2003 to 2009. *Science* 340, 852-857

Gibbons, A.B., Megeath, J.D., Pierce, K.L., 1984. Probability of moraine survival in a succession of glacial advances. *Geology* 12, 327-330

Granger, D.E., Lifton, N.A., Willenbring, J.K., 2013. A cosmic trip: 25 years of cosmogenic nuclides in geology. *Geological Society of Americal Bulletin* 125, 1379-1402.

Grömping, U., 2007. Estimators of relative importance in linear regression based on variance decomposition. *The American Statistician* 61, 139-147.

Håkansson, L., Briner, J.P., Aldahan, A., Possnert, G., 2011. ^{10}Be data from meltwater channels suggest that Jameson Land, east Greenland, was ice-covered during the last glacial maximum. *Quaternary Research* 76, 452-459.

Håkansson, L., Briner, J., Alexanderson, H., Aldahan, A., Possnert, G., 2007a. ^{10}Be ages from central east Greenland constrain the extent of the Greenland ice sheet during the Last Glacial Maximum. *Quaternary Science Reviews* 26, 2316-2321.

Håkansson, L., Briner, J.P., Andresen, C.S., Thomas, E.K., Bennike, O., 2014. Slow retreat of a land based sector of the West Greenland Ice Sheet during the Holocene Thermal Maximum: evidence from threshold lakes at Paakitsoq. *Quaternary Science Reviews* 98, 74-83.

Håkansson, L., Graf, A., Strasky, S., Ivy-Ochs, S., Kubik, P.W., Hjort, C., Schlüchter, C., 2007b. Cosmogenic ^{10}Be-ages from the Store Koldewey Island, NE Greenland. *Geografiska Annaler* 89, 195-202.

Håkansson, L., Hjort, H., Möller, P., Briner, J.P., Aldahan, A., Possnert, G. 2009. Late Pleistocene glacial history of Jameson Land, central East Greenland, derived from cosmogenic ^{10}Be and ^{26}Al exposure dating. *Boreas* 38, 244-260.

Hakim, G.J., Emile-Geay, J., Steig, E.J., Noone, D., Anderson, D.M., Tardif, R., Steiger, N., Perkins, W.A., 2016. The last millennium climate reanalysis project: framework and first results. *Journal of Geophysical Research: Atmospheres* 121, 6745-6764

Hansen, J., Ruedy, R., Sato, M., Lo, K., 2010. Global surface temperature change. *Reviews of Geophysics* 48. Dx.doi.org:// 10.1029/2010RG000345

Helama, S., Meriläinen, J., Tuomenvirta, H., 2009. Multicentennial megadrought in northern Europe coincided with a global El Niño-Southern Oscillation drought pattern during the Medieval Climate Anomaly. *Geology* 37, 175-178.

Hogan, K.A., Ó Cofaigh, C., Jennings, A.E., Dowdeswell, J.A., Heimstra, J.F., 2016. Deglaciation of a major palaeo-ice stream in Disko Trough, West Greenland. *Quaternary Science Reviews,* in press. http://dx.doi.org/ 10.1016/j.quascirev.2016.01.018.

Howat, I. M., Joughin, I., Tulaczyk, S. Gogineni, S. 2005. Rapid retreat and acceleration of Helheim Glacier, east Greenland. *Geophysical Research Letters* 32, L22502, doi:10.1029/2005GL024737.

Hughes, A.L.C., Rainsley, E., Murray, T., Fogwill, C.J., Schnabel, C., Xu, S., 2012. Rapid response of Helheim Glacier, southeast Greenland, to early Holocene climate warming. *Geology* 40, 427-430.

Hutter, K., 1983. *Theoretical Glaciology: Material science of ice and the mechanics of glaciers and ice sheets*. Norwell, MA: Kluwer Academic.

Huybrechts, P., 2002. Sea-level changes at the LGM from ice-dynamic reconstructions of the Greenland and Antarctic ice sheets during the glacial cycles. *Quaternary Science Reviews* 21, 203-231.

Imbrie, J., and Kipp, N.G., 1971. A new micropaleontological method for quantitative paleoclimatology: application to a late Pleistocene Caribbean core. In Turekian, K.K., ed. *The Late Cenozoic Glacial Ages*. New Haven: Yale University Press

Imbrie, J., and van Andel, T.H., 1964. Vector analysis of heavy-mineral data. *Geological Soceity of America Bulletin* 75, 1131-1156.

Indermühle, A., Stocker, T.F., Joos, F., Fischer, H., Smith, H.J., Wahlen, M., Deck, B., Mastroianni, D., Tschumi, J., Blunier, T., Meyer, R., Stauffer, B., 1999. Holocene carbon-cycle dynamics based on CO_2 trapped in ice at Taylor Dome, Antarctica. *Nature* 298, 121-126

Jamieson, S.R., Vieli, A., Livingstone, S.J., Ó Cofaigh, C., Stokes, C., Hillenbrand, C.-D., Dowdeswell J.A., 2012; Ice-stream stability on a reverse bed slope. *Nature Geoscience* 5, 799-802

Jennings, A., Andrews, J., Wilson, L., 2011. Holocene environmental evolution of the SE Greenland Shelf North and South of the Denmark Strait: Irminger and East Greenland current interactions. *Quaternary Science Reviews* 30, 980-998.

Jennings, A.E., Hald, M., Smith, M., Andrews, J.T., 2006. Freshwater forcing from the Greenland Ice Sheet during the Younger Dryas: evidence from southeastern Greenland shelf cores. *Quaternary Science Reviews* 25, 282-298.

Jennings, A.E., Walton, M.E., Ó Cofaigh, C., Kilfeather A., Andrews, J.T., Ortiz, J.D., De Vernal, A., Dowdeswell, J.A., 2014. Paleoenvironments during the Younger Dryas-Early Holocene retreat of the Greenland Ice Sheet from outer Disko Trough, central west Greenland. *Journal of Quaternary Science* 29, 27-40.

Jiang, H., Eiriksson, J., Schulz, M., Knudsen, K.-L., Seidenkrantz, M.-S., 2005. Evidence for solar forcing of sea-surface temperature on the North Icelandic Shelf during the late Holocene. *Geology* 33, 73-76.

Jomelli, V., Lane, T., Favier, V., Masson-Delmotte, V., Swingedouw, D., Rinterknect, V., Schimmelpfennig, I., Brunstein, D., Verfaillie, D., Adamson, K., Leanni, L., Mokadem, F., ASTER Team, 2016. Paradoxical cold conditions during the medieval climate anomaly in the Western Arctic. *Nature Scientific Reports* 6, dx.doi.org://10.1038/srep32984

Jones, P.D., Lister, D.H., Osborn, T.J., Harpham, C., Salmon, M., Morice, C.P., 2012. Hemispheric and large-scale land-surface air temperature variations: An extensive revision and update to 2010. *Journal of Geophysical Research: Atmopsheres* 117. dx.doi.org://10.1029/2011JD017139

Joughin, I., Abdalati, W., Fahnestock, M., 2004, Large fluctuations in speed on Greenland's Jakobshavn Isbrae Glacier. *Nature* 432, 608 – 610.

Kaufman, D.S., Schneider, D.P., McKay, N.P., Ammann, C.M., Bradley, R.S., Briffa, K.R., Miller, G.F., Otto-Bleisner, B.L., Overpeck, J.T., Vinther, B.M., Arctic Lakes 2k Project Members, 2009. Recent warming reverses long-term Arctic cooling. *Science* 325, 1236-1239

Kelley, S.E., Briner, J.P., Young, N.E., 2013. Rapid ice retreat in Disko Bugt supported by ^{10}Be dating of the last recession of the western Greenland Ice Sheet. *Quaternary Science Reviews* 82, 13-22.

Kelley, S.E., Briner, J.P., Young, N.E., Babonis, G.S., Csatho, B., 2012. Maximum late Holocene extent of the western Greenland Ice Sheet during the late 20th Century. *Quaternary Science Reviews* 56, 89-98.

Kelley, S.E., Briner, J.P. and Zimmerman, S., 2015. The influence of ice marginal setting on early Holocene retreat rates in central West Greenland. Journal of Quaternary Science, v. 30, p. 271-280

Kelly, M.A., Lowell, T.V., Hall, B.L., Schaefer, J.M., Finkel, R.C., Goehring, B.M., Alley, R.B., Denton, G.H., 2008. A ^{10}Be chronology of late glacial and Holocene mountain glaciation in the Scoresby Sund region, east Greenland: implications for seasonality during lateglacial time. *Quaternary Science Reviews* 27, 2273-2282.
Kelly, M., 1974. The marine limit in Julianhab district, south Greenland, and its isostatic implications. In Blundel, D.J., ed: *Crustal Structure of the Gardar Rift, South Greenland: Report on Fieldwork 1973*. Lancaster: Department of Environmental Sciences

Kelly, M., 1975 A note on the implications of two radiocarbon dated samples from Qaleraglit ima, South Greenland. *Bulletin of the Geological Society of Denmark* 24, 21-26

Khan, S.A, Aschwanden, A., Bjørk, A.A., Wahr, J., Kjeldsen, K.K., Kjær, K.H., 2015. Greenland ice sheet mass balance: a review. *Reports on Progress in Physics* 79, dx.doi.org://10.1088/0034-4885/78/046801

Kirkbride, M.P., Warren, C.R., 1997. Calving processes at a grounded ice cliff. *Annals of Glaciology* 24, 116-121.

Kopp, R.E., Kemp, A.C., Bittermann, K., Horton, B.P., Donnelly, J.P., Roland Gehrels, W., Hay, C.C., Mitrovica, J.X., Morrow, E.D., Rahmstorf, S., 2016. Temperature-driven global sea-level variability in the Common Era. *Proceedings of the National Academy of Sciences* 113. dx.doi.org://10.1073/pnas.1517056113

Koppes, M.N., and Montgomery, D.R., 2009. The relative efficacy of fluvial and glacial erosion over modern to orogenic timescales. *Nature Geoscience* 2, 644-647.

Kuijpers, A., Troelstra, S.R., Prins, M.A., Linthout, K., Akhmetzhanov, A., Bouryak, S., Bachmann, M.F., Lassen, S., Rasmussen, S., Jensen, J.B., 2003. Late Quaternary sedimentary processes and ocean circulation changes at the Southeast Greenland margin. *Marine Geology* 195, 109-129.

Lane, T.P., Roberts, D.H., Rea, B.R., Ó Cofaigh, C., Vieli, A., Rodés, A., 2013. Controls upon the Last Glacial Maximum deglaciation of the northern Uummannaq Ice Stream System, West Greenland. *Quaternary Science Reviews* 92, 324-344.

Larsen, D.J., Miller, G.H., Geirsdóttir, Á, 2011. A 3000-year varved record of glacier activity and climate change from the proglacial lake Hvítárvatn, Iceland. *Quaternary Science Reviews* 30, 2715-2731.

Larsen, N.K., Funder, S., Kjær, K.H., Kjeldsen, K.K., Knudsen, M.F., Linge, H., 2013. Rapid early Holocene ice retreat in West Greenland. *Quaternary Science Reviews* 92, 310-323.

Larsen, N.K., Funder, S., Linge, H., Möller, P., Schomacker, A., Fabel, D., Xu, S., Kjær, K.H., 2016. A Younger Dryas re-advance of local glaciers in north Greenland. *Quaternary Science Reviews,* doi: 10.1016/j.quascirev.2015.10.036.

Larsen, N.K., Kjær, K.H., Lecavalier, B., Bjørk, A.A., Colding, S., Huybrechts, P., Jakobsen, K.E., Kjeldsen, K.K., Knudsen, K.-L., Odgaard, B.V., Olsen, J., 2015. The response of the southern Greenland ice sheet to the Holocene thermal maximum. Geology, doi: 10.1130/G36476.1.

Larsen, N.K., Kjær, K.H., Olsen, J., Funder, S., Kjeldsen, K.K., Nørgaard-Pedersen, N., 2011. Restricted impact of Holocene climate variations on the southern Greenland Ice Sheet. *Quaternary Science Reviews* 3171-3180

Lasher, G.E., Axford, Y., 2019. Medieval warmth confirmed at the Norse Eastern Settlement in Greenland. *Geology* 47, 267-270.

Lecavalier, B.S., Milne, G.A.. Simpson, M.J.R., Wake, L., Huybrechts, P., Tarasov, L., Kjeldsen, K.K., Funder, S., Long, A.J., Woodroffe, S., Dyke, A.S., Larsen, N.K., 2014 A model of Greenland Ice Sheet Deglaciation Constrained by Observations of Relative Sea Level and Ice Extent. *Quaternary Science Reviews* 102, 54-84

Levy, L.B., Kelly, M.A., Howley, J.A., Virginia, R.A., 2012. Age of the Ørkendalen moraines, Kangerlussuaq, Greenland: constraints on the extent of the southwestern margin of the Greenland Ice Sheet during the Holocene. *Quaternary Science Reviews* 52, 1-5.

Levy, L.B., Kelly, M.A., Lowell, T.V., Hall, B.L., Hempel, L.A., Honsaker, W.M., Lusas, A.R., Howley, J.A., Axford, Y.L., 2014. Holocene fluctuations of Bregne ice cap, Scoresby Sund, east Greenland: a proxy for climate along the Greenland Ice Sheet margin. *Quaternary Science Reviews* 92, 356-368.

Levy, L.B., Kelly, M.A., Lowell, T.V., Hall, B.L., Howley, J.A., Smith, C.A., 2016. Coeval fluctuations of the Greenland ice sheet and a local glacier, central East Greenland, during late glacial and early Holocene time. *Geophysical Research Letters* 43, 1623-1631.

Licciardi, J.M., 2000. Alpine glacier and pluvial lake records of late Pleistocene climate variability in the western United States (Ph.D. thesis). Corvallis, Oregon State University, 155p

Lindeman, R.H., Merenda, P.F., Gold, R.Z., 1980. *Introduction to Bivariate and Multivariate Analysis*. Glenview IL: Scott, Foresman and Company.

Ljungqvist, F.C., 2010. A new reconstruction of temperature variability in the extra-tropical northern hemisphere during the last two millenia. *Geografiska Annaler* 92, 339-351.

Lloyd, J.M., Park, L.A., Kuijpers, A., Moros, M., 2005. Early Holocene palaeoceanography and detailed chronology of Disko Bugt, West Greenland. *Quaternary Science Reviews* 24, 1741-1755.

Lloyd, J., M. Moros, K. Perner, R. J. Telford, A. Kuijpers, E. Jansen, McCarthy, D., 2011. A 100 yr record of ocean temperature control on the stability of Jakobshavn Isbrae, West Greenland. *Geology* 39, 867–870.

Long, A.J., Roberts, D.H., Simpson, M.J.R., Dawson, S., Milne, G.A., Huybrechts, P., 2008. Late Weichselian relative sea-level changes and ice sheet history in southeast Greenland. *Earth and Planetary Science Letters* 272, 8-18.

Long, A.J., Woodroffe, S.A., Dawson, S., Roberts, D.H., Bryant, C.L., 2009. Late Holocene relative sea level rise and the Neoglacial history of the Greenland ice sheet. *Journal of Quaternary Science* 24, 345-359.

Lowell, T.V., Hall, B.L., Kelly, M.A., Bennike, O., Lusas, A.R., Honsaker, W., Smith, C.A., Levy, L.B., Travis, S., Denton, G.H., 2013. Late Holocene expansion of Istorvet ice cap, Liverpool Land, east Greenland. *Quaternary Science Reviews* 63, 128-140.

Mann, M.E., Bradley, R.S., Hughes, M.K., 1998. Global-scale temperature patterns and climate forcing over the past six centuries. *Nature* 392, 779-787

Mann, M.E., Zhang, Z., Rutherford, S., Bradley, R.S., Hughes, M.K., Shindell, D., Ammann, C., Faluvegi, G., Ni, F., 2009. Global signatures and dynamical origins of the Little Ice Age and Medieval Climate Anomaly. *Science* 326, 1256-1260

Mann, M.E., Zhang, Z., Hughes, M.K., Bradley, R.S., Miller, S.K., Rutherford, S., Ni, F., 2008. Proxy-based reconstructions of hemispheric and global surface temperature variations over the past two millenia. *Proceedings of the National Academy of Sciences* 105, 13252-13257.

Marcott, S.A., 2011. Late Pleistocene and Holocene glacier and climate change (Ph.D. thesis). Corvallis, Oregon State University, 260 p.

Marcott, S.A., Clark, P.U., Padman, L., Klinkhammer, G.P., Springer, S., Liu, Z., Otto-Bliesner, B.L., Carlson, A.E., Ungerer, A., Padman, J., He, F., Cheng, J., Schmittner, A., 2011. Ice-shelf collapse from subsurface warming as a trigger for Heinrich events. *Proceedings of the National Academy of Sciences*, doi: 10.1073/pnas.1104772108.

Marcott, S.A., Shakun, J.D., Clark, P.U., Mix, A.C., 2013. A reconstruction of regional and global temperature for the past 11,300 years. *Science* 339, 1198-1201

Marzeion, B., Cogley, J.G., Richter, K., Parkes, D., 2014. Attribution of global glacier mass loss to anthropogenic and natural causes. *Science* 345, 919-921

Massa, C., Perren, B.B., Gauthier, É, Bichet, V., Petit, C., Richard, H., 2012. A multiproxy evaluation of Holocene environmental change from Lake Igaliku, South Greenland. *Journal of Paleolimnology* 48, 241-258.

McKay, N.P., Kaufman, D.S., 2014. An extended Arctic proxy temperature database for the past 2,000 years. *Nature Scientific Data* 1, https://doi.org/10.1038/sdata.2014.26

Milne, G.A., Shennan, I., 2013. Isostasy: glaciation induced sea-level change. *Encyclopedia of Quaternary Science* 3, 452-459.

Mix, A.C., et al., 1999. Foraminiferal faunal estimates of paleotemperature: Circumventing the no-analog problem yields cool ice age tropics. *Paleoceanography* 14, 350-359

Morice, C.P., Kennedy, J.J., Rayner, N.A., Jones, P.D., 2012. Quantifying uncertainties in global and regional temperature change using an ensemble of observational estimates: The HadCRUT4 data set. *Journal of Geophysical Research: Atmospheres* 117, dx.doi.org://10.1029/2011JD017187

Möller, P., Larsen, N.K., Kjær, K.H., Funder, S., Schomacker, A., Linge, H., Fabel, D., 2010. Early to middle Holocene valley glaciations on northernmost Greenland. *Quaternary Science Reviews* 29, 3379-3398.

Nelson, A., Bierman, P.R., Shakun, J.D., Rood, D.H., 2014. Using *in situ* cosmogenic ^{10}Be to identify the source of sediment leaving Greenland. *Earth Surface Processes and Landforms*. 39, 1087-1100.

Nøgaard-Pedersen, N., and Mikkelsen, N., 2009. 8000 year marine record of climate variability and fjord dynamics from Southern Greenland. *Marine Geology* 264, 177-189.

Ó Cofaigh, C., Dowdeswell, J.A., Jennings, A.E., Hogan, K.A., Kilfeather, A., Heimstra, J.F., Noormets, R., Evans, J., McCarthy, D.J., Andrews, J.T., Lloyd, J.M., Moros, M., An extensive and dynamic ice sheet on the West Greenland shelf during the last glacial cycle. *Geology*. http://dx.doi.org/10.1130/G33759.1

Ogi, M., Barber, D.G., Rysgaard, S., 2016. The relationship between summer sea ice extent in Hudson Bay and the Arctic Ocean via the atmospheric circulation. *Atmospheric Science Letters* 17, 603-609.

Olsen, J., Kjær, K.H., Funder, S., Larsen, N.K., Ludikova, A., 2011. High-Arctic climate conditions for the last 7000 years inferred from multi-proxy analysis of the Bliss Lake record, North Greenland. *Journal of Quaternary Science*. http://dx.doi.org/10.1002/jqs.1548

Overland, J.E., Wang, M., Walsh, J.E., Stroeve, J.C., 2013. Future Arctic climate changes: Adaptation and mitigation time scales. *Earth's Future* 2, 68-74.

PAGES 2k Consortium, 2017. A global multiproxy database for temperature reconstructions of the Common Era. *Nature Scientific Data* 4, https://doi.org/10.1038/sdata.2017.88

Perkins, W.A., and Hakim, G.J., 2017. Reconstructing paleoclimate fields using online data assimilation with a linear inverse model. *Climate of the Past* 13, 421-436.
Pisias, N.G., 1978. Paleoceanography of the Santa Barbara Basin during the last 8000 years. *Quaternary Research* 10, 366-384

Perner, K., Moros, M., Jennings, A., Lloyd, J.M., Knudsen, K.L., 2013. Holocene palaeoceanographic evolution off West Greenland. *The Holocene* 23, 374-387.

Pisias, N.G., Murray, R.W., Scudder, R.P., 2013. Multivariate statistical analysis and partitioning of sedimentary geochemical data sets : General principles and specific MATLAB scripts. *Geochemistry Geophysics Geosystems* 14, 4015-4020

Pollard, D., DeConto, R., Alley, R.B., 2015. Potential Antarctic Ice Sheet retreat driven by hydrofracturing and ice cliff failure. *Earth and Planetary Science Letters* 412, 112-121.

Praetorious, S.K., Mix, A.C., Jensen, B.J.L., Froese, D.G., Milne, G., Wolhowe, M.D., Addison, J., Prahl, F., 2016. Interaction between climate, volcanism, and isostatic rebound in Southeast Alaska during the last deglaciation. *Earth and Planetary Science Letters* 452, 79-89.

Putkonen, J., Swanson, T., 2003. Accuracy of cosmogenic ages for moraines. *Quaternary Research* 59, http://dx.doi.org/10.1016/S0033-5894(03)00006-1.

Reimer, P.J., Bard, E., Bayliss, A., Beck, J.W., Blackwell, P.G., Ramsey, C.B., Buck, C.E., Haflidason, H., Hajdas, I., Hatté, C., Heaton, T.J., Hoffmann, D.L., Hogg, A.G., Hughen, K.A., Kaiser, K.F., Kromer, B., Manning, S.W., Niu, M., Reimer, R.W., Richards, D.A., Scott, E.M., Southon, J.R., Staff, R.A., Turney, C.S.M., van der Plicht, J., 2013. IntCal13 and Marine13 radiocarbon age calibration curves 0-50,000 BP. Radiocarbon 55, 1869-1887.

Reusche, M., Marcott, S., Ceperley, E., Barth, A., Brook, E., Mix, A., Caffe, M., 2018. Early to late Holocene surface exposure ages from two marine-terminating outlet glaciers in northwest Greenland. *Geophysical Research Letters*, dx.doi.org/10.1029/2018GL078266

Rignot, E., Kanagaratnam, P., 2006. Changes in the velocity structure of the Greenland Ice Sheet. *Science*, 311 986 – 990.

Rignot, E., Koppes, M., Velicogna, I., 2010. Rapid submarine melting of the calving faces of West Greenland glaciers. *Nature Geoscience* 3, 187-191.
Cheng, H., Edwards, R.L., Friedrich, M., Grootes, P.M., Guilderson, T.P.,

Rigor, I.G., Wallace, J.M., Colony, R.L., 2002. Response of sea ice to the Arctic Oscillation. *Journal of Climate* 15, 2648-2663

Rinterknecht, V., Gorokhovich, Y., Schaefer, J., Caffee, M., 2009. Preliminary ^{10}Be chronology for the last deglaciation of the western margin of the Greenland Ice Sheet. *Journal of Quaternary Science* 24, 270-278.

Rinterknecht, V., Jomelli, V., Brunstein, D., Favier, V., Masson-Delmotte, V., Bourlès, D., Leanni, L., Schläppy, R., 2014. Unstable ice stream in Greenland during the Younger Dryas cold event. *Geology,* http://dx.doi.org/10.1130/G35929.1.

Roberts, D.H., Long, A.J., Schnabel, C., Davies, B.J., Xu, S., Simpson, M.J.R., Huybrechts, P., 2009. Ice sheet extent and early deglacial history of the southwestern sector of the Greenland Ice Sheet. *Quaternary Science Reviews* 28, 2760-2773.

Roberts, D.H., Long, A.J., Schnabel, C., Freeman, S., Simpson, M.J.R., 2008. The deglacial history of southeast sector of the Greenland Ice Sheet during the Last Glacial Maximum. *Quaternary Science Reviews* 27, 1505-1516.

Roberts, D.H., Rea, B.R., Lane, T.P., Schnabel, C., Rodès, A., 2013. New constraints on Greenland ice sheet dynamics during the last glacial cycle: evidence from the Uummannaq ice stream system. *Journal of Geophysical Research: Earth Surface* 118, 1-23.

Roe, G.H., Baker, M.B., Herla, F., 2017. Centennial glacier retreat as categorical evidence of regional climate change. *Nature Geoscience* 10, 95-99

Roe, G.H., and O'Neal, M.A., 2009. The response of glaciers to intrinsic climate variability: Observations and models of late-Holocene variations in the Pacific Northwest: *Journal of Glaciology* 55, 839-854.

Scambos, T.A., Bohlander, J.A., Shuman, C.A., Skvarca, P., 2004. Glacier acceleration and thinning after ice shelf collapse in the Larsen B embayment, Antarctica. *Geophysical Research Letters* 31, http://dx.doi.org/10.1029/2004GL020670.

Schaefer, J.M., Finkel, R.C., Balco, G., Alley, R.B., Caffee, M.W., Briner, J.P., Young, N.E., Gow, A.J., Schwartz, R., 2016. Greenland was nearly ice-free for extended periods during the Pleistocene. *Nature* 540, 252-255.

Schimmelpfennig, I., Schaefer, J.M., Akçar, N., Koffman, T., Ivy-Ochs, S., Schwartz, R., Finkel, R.C., Zimmerman, S., Schlüchter, C., 2014. A chronology of Holocene and Little Ice Age glacier culminations of the Steingletscher, Central Alps, Switzerland, based on high-sensitivity beryllium-10 moraine dating. *Earth and Planetary Science Letters* 393, 220-230

Schoof, C., 2005. The effect of cavitation on glacier sliding, *Proceedings of the Royal Society of London Series A* 461, 609-627

Schoof, C., 2007. Ice sheet grounding line dynamics: Steady states, stability, and hysteresis, *Journal of Geophysical Research*, 112, F03S28, doi:10.1029/ 2006JF000664.

Shakun, J., Carlson, A.E., 2010. A global perspective on Last Glacial Maximum to Holocene climate change. *Quaternary Science Reviews* 29, 1801-1816.

Serreze, M.C., and Barry, R.G., 2011. Processes and impacts of Arctic amplification: A research synthesis. *Global and Planetary Change* 77, 85-96

Shakun, J.D., Clark, P.U., He, F., Marcott, S.A., Mix, A.C., Liu, Z., Otto-Bliesner, B., Schmittner, A., Bard, E., 2012. Global warming preceded by increasing carbon dioxide concentrations during the last deglaciation. *Nature* 484, 49-53.

Shannon, S.R., Payne, A.J., Bartholomew, I.D., van den Broeke, M.R., Edwards, T.L., Fettweis, X., Gagliardini, O., Gillet-Chaulet, F., Goelzer, H., Hoffman, M.J., Huybrechts, P., Mair, D.W.F., Nienow, P.W., Perego, M., Price, S.F., Smeets, C.J.P.P., Sole, A.J., van de Wal, R.S.W., Zwinger, T., 2013. Enhanced basal lubrication and the contribution of the Greenland ice sheet to future sea-level rise. *Proceedings of the National Academy of Sciences* 110, 14156-14161.

Sheldon, C., Jennings, A., Andrews, J.T., Ó Cofaigh, C., Hogan, K., Dowdeswell, J.A., Seidenkrantz, M.-S., 2016. Ice stream retreat following the LGM and onset of the west Greenland current in Uummannaq Trough, west Greenland. *Quaternary Science Reviews,* in press. http://dx.doi.org /10.1016/j.quascirev.2016.01.019.

Shepherd, A., Ivins, E.R., A, G., Barletta, V.R., Bentley, M.J., Bettadpur, S., Briggs, K.H., Bromwich, D.H., Forsberg, R., Galin, N., Horwath, M., Jacobs, S., Joughin, I., King, M.A., Lenaerts, J.T.M., Li, J., Lightenberg, S.R.M., Luckman, A., Luthcke, S.B., McMillan, M., Meister, R. Milne, G., Mouginot, J., Muir, A., Nicolas, J.P., Paden, J, Payne, A.J., Pritchard, H.,

Shepherd, A., Wingham, D., Rignot, E., 2004. Warm ocean is eroding West Antarctic Ice Sheet. *Geophysical Research Letters* 31, http://dx.doi.org/10.1029/2004GL021106.

Simpson, M.J.R., Milne, G.A., Huybrechts, P., Long, A.J., 2009. Calibrating a glaciological model of the Greenland ice sheet from the Last Glacial Maximum to present-day using field observations of relative sea level and ice extent. *Quaternary Science Reviews* 29, 1631-1657.

Sinclair, G., Carlson, A.E., Mix, A.C., Lecavalier, B.S., Milne, G.A., Mathias, A., Buizert, C., DeConto, R.M. Diachronous retreat of the Greenland ice sheet during the last deglaciation. *Quaternary Science Reviews* 145, 243-258

Solignac, S., de Vernal, A., Hillaire-Marcel, C., 2004. Holocene sea-surface conditions in the North Atlantic—contrasting trends and regimes in the western and eastern sectors (Labrador Sea vs. Iceland Basin). *Quaternary Science Reviews* 23, 319-334.

Solomina, O.N., Bradley, R.S., Hodgson, D.A., Ivy-Ochs, S., Jomelli, V., Mackintosh, A.N., Nesje, A., Owen, L.A., Wanner, H., Wiles, G.C., Young, N.E., 2015. Holocene glacier fluctuations. *Quaternary Science Reviews* 111, 9-34.

Sparrenbom, C.J., Bennike, O., Björck, Lambeck, K., 2006a. Holocene relative sea-level changes in the Qaqortoq area, southern Greenland. *Boreas* 35, 171-187

Sparrenbom, C.J., Bennike, O., Björck, Lambeck, K., 2006b. Relative sea-level changes since 15000 cal. Yr BP in the Nanortalik area, southern Greenland. *Journal of Quaternary Science* 21, 29-48.

Sparrenbom, C.J., Bennike, O., Fredh, D., Randsalu-Wendrup, L., Zwartz, D., Ljung, K., Björck, S., Lambeck, K., 2013. Holocene relative sea-level changes in the inner Bredefjord area, southern Greenland, *Quaternary Science Reviews*, 69, 107-124.

Stenchikov, G., Robock, A., Ramaswamy, V., Schwarzkopf, M.D., Hamilton, K., Ramachandran, S., 2002. Arctic Oscillation response to the 1991 Mount Pinatubo eruption: Effects of volcanic aerosols and ozone depletion. *Journal of Geophysical Research* 107, dx.doi.org://10.1029/2002JD002090

Storms, J.E.A., de Winter, I.L., Overeem, I., Drijkoningen, G.G., Lykke-Andersen, H., 2012. The Holocene sedimentary history of the Kangerlussuaq Fjord-valley fill, West Greenland. *Quaternary Science Reviews* 35, 29-50

Stroeven, A.P., Fabel, D., Hättestrand, C., Harbor, J., 2002. A relict landscape in the centre of Fennoscandian glaciation: cosmogenic radionuclide evidence of tors preserved through multiple glacial cycles. *Geomorphology* 44, 145-154.

Tarasov, L., Dyke, A.S., Neal, R.M., Peltier, W.R., 2012. A data-calibrated distribution of deglacial chronologies for the North American ice complex from glaciological modeling. *Earth and Planetary Science Letters* 315-316, 30-40.

Tarasov, L., Peltier, W.R., 2002. Greenland glacial history and local geodynamic consequences. *Geophysics Journal International* 150, 198-229.

Thomas, R. H., W. Abdalati, E. Frederick, W. B. Krabill, S. Manizade, and K. Steffen (2003), Investigation of surface melting and dynamic thinning on Jakobshavn Isbrae, Greenland, J. Glaciol., 49(165), 231 – 239, doi:10.3189/172756503781830764.

Van der Veen, C.J., 2002. Calving glaciers. *Progress in Physical Geography* 26, 96-122.
Vaughan, D.G., J.C. Comiso, I. Allison, J. Carrasco, G. Kaser, R. Kwok, P. Mote, T. Murray, F. Paul, J. Ren, E. Rignot, O. Solomina, K. Steffen and T. Zhang, 2013: Observations: Cryosphere. In: Climate Change 2013: The Physical Science Basis. Contribution of Working Group I to the Fifth Assessment Report of the Intergovernmental Panel on Climate Change [Stocker, T.F., D. Qin, G.-K. Plattner, M. Tignor, S.K. Allen, J. Boschung, A. Nauels, Y. Xia, V. Bex and P.M. Midgley (eds.)]. Cambridge University Press, Cambridge, United Kingdom and New York, NY, USA.

Vose, R.S., Arndt, D., Banzon, V.F., Easterling, D.R., Gleason, B., Huang, B., Kearns, E., Lawrimore, J.H., Menne, M.J., Peterson, T.C., Reynolds, R.W., Smith, T.M.,

Williams, C.N., Wuertz, D.B., 2012. NOAA's merged land-ocean surface temperature analysis. 2012. *Bulletin of the American Metorological Society* 93, 1677-1685

Wang T., Surge, D., Mithen., S., 2012. Seasonal temperature variability of the Neoglacial (3300-2500 B.P.), and Roman Warm Period (2500-1600 B.P.) reconstructed from oxygen isotope ratios of limpet shells (*Patella vulgata*), Northwest Scotland. *Palaeogeography, Palaeoclimatology, Palaeoecology* 317-318, 104-113.

Warrick, R., Oerlemans, J., Beaumont, P., Braithwaite, R.J., Drewery, D.J., Gornitz, V., Grove, J.M., Haeberli, W., Higashi, A., Leiva, J.C., Lingle, C.S., Lorius, C., Raper, S.C.B., Wold, B., Woodworth, P.L., 1991. 9. Sea Level Rise. In Houghton, J.T., Jenkins, G.J., Ephraums, J.J., 1991. *Climate Change: The IPCC Scientific Assessment*.

Waters, C.N., Zalasiewicz, J., Summerhayes, C., Barnosky, A.D., Poirier, C., Gałuszka, A., 2016. The Anthropocene is functionally and stratigraphically distinct from the Holocene. *Science* 351, dx.doi.org:// 10.1126/science.aad2622

Weidick, A., 1959. Glacial variations in West Greenland in historical time, part 1. *Meddelelser om Grønland*, 158, 4

Weidick, A., 1975. Holocene shorelines and glacial stages in Greenland—an attempt at correlation. Rapp. Grønl. Geol. Unders. 41, 39.

Weidick, A., Kelly, M., Bennike, O., 2004. Late Quaternary development of the southern sector of the Greenland Ice Sheet, with particular reference to the Qassimiut lobe. Boreas 33, 284-299

Williams, K.M., 1993. Ice sheet and ocean interactions, margin of the East Greenland Ice Sheet (14 ka to present): diatom evidence. *Paleoceanography* 8, 69-83.

Winsor, K., Carlson, A.E., Klinkhammer, G.P., Stoner, J.S., Hatfield, R.G., 2012. Evolution of the northeast Labrador Sea during the last interglaciation. *Geochemistry, Geophysics, Geosystems* 13, http://dx.doi.org/10.1029/2012GC004263.

Winsor, K., Carlson, A.E., Rood, D.H., 2014. ^{10}Be dating of the Narsarsuaq moraine in southernmost Greenland: evidence for a late-Holocene ice advance exceeding the Little Ice Age maximum. *Quaternary Science Reviews* 98, 135-143.

Winsor, K., Carlson, A.E., Caffee, M., Rood, D.H., 2015a. Rapid last-deglacial thinning and retreat of the marine-terminating southwestern Greenland ice sheet. *Earth and Planetary Science Letters* 426, 1-12.

Winsor, K., Carlson, A.E., Welke, B., Reilly, B., 2015b. Early deglacial onset of southwestern Greenland ice-sheet retreat on the continental shelf. *Quaternary Science Reviews* 128, 117-126.

Wunderlich, F., Mitchell, D.M., 2017. Revisiting the observed surface climate response to volcanic eruptions. *Atmospheric Chemistry and Physics* 17, 485-499.

Young, N.E., Briner, J.P., 2015. Holocene evolution of the western Greenland Ice Sheet: assessing geophysical ice-sheet models with geological reconstructions of ice-margin change. *Quaternary Science Reviews* 114, 1-17.

Young, N.E., Briner, J.P., Stewart, H.A.M., Axford, Y., Csatho, B., Rood, D.H., Finkel, R.C., 2011a. Response of Jakobshavn Isbrae, Greenland, to Holocene climate change. *Geology* 39, 131-134.

Young, N.E., Briner, J.P., Axford, Y., Csatho, B., Babonis, G.S., Rood, D.H., Finkel, R.C., 2011b. Response of a marine-terminating Greenland outlet glacier to abrupt cooling

8200 and 9300 years ago. *Geophysical Research Letters* 38, http://dx.doi.org/10.1029/2011GL049639.

Young, N.E., Schaefer, J.M., Briner, J.P., Goehring, B.M., 2013a. A Be-10 production rate calibration for the Arctic. *Journal of Quaternary Science* 28, 515-526.

Young, N.E., Briner, J.P., Rood, D.H., Finkel, R.C., Corbett, L.B., Bierman, P.R., 2013b. Age of the Fjord Stade moraines in the Disko Bugt region, western Greenland, and the 9.3 and 8.2 ka cooling events. *Quaternary Science Reviews* 60, 76-90.

Young, N.E., Schweinsberg, A.D., Briner, J.P., Schaefer, J.M., 2015. Glacier maxima in Baffin Bay during the Medieval Warm Period coeval with Norse settlement. *Sci. Adv.*, e1500806.

Zweck, C., Huybrechts, P., 2005. Modeling of the northern hemisphere ice sheets during the last glacial cycle and glaciological sensitivity. *Journal of Geophysical Research: Atmospheres* 110. http://dx.doi.org/10.1029/2004JD005489.

Zwally, H.J., Abdalati, W., Herring, T., Larson, K., Saba, J., Steffen., K., 2002. Surface melt-induced acceleration of Greenland Ice-Sheet flow. *Science* 12, 218-222.

Zwally, H.J., Li, J., Brenner, A.C., Beckley, M., Cornejo, H.G., DiMarzio, J., Giovinetto, M.B., Neumann, T.A., Robbins, J., Saba, J.L., Yi, D., Wang, W., 2011. Greenland ice sheet mass balance: distribution of increased mass loss with climate warming; 2003-07 versus 1992-2002., *Journal of Glaciology* 25, 88-102